GLYCOPEPTIDE ANTIBIOTIC BIOSYNTHESIS AND RESISTANCE

IN *Streptomyces toyocaensis* NRRL 15009

GLYCOPEPTIDE ANTIBIOTIC BIOSYNTHESIS AND RESISTANCE IN

Streptomyces toyocaensis NRRL 15009

By

CHRISTOPHER GARY MARSHALL, B.Sc.

A Thesis

Submitted to the School of Graduate Studies

In Partial Fulfilment of the Requirements

for the Degree

Doctor of Philosophy

McMaster University

DOCTOR OF PHILOSOPHY (1999)
(Biochemistry)

McMaster University
Hamilton, Ontario

TITLE: Glycopeptide Antibiotic Biosynthesis and Resistance in
Streptomyces toyocaensis NRRL 15009

AUTHOR: Christopher Gary Marshall, B.Sc. (McMaster University)

SUPERVISOR: Professor G.D. Wright

NUMBER OF PAGES: xxi, 290

Abstract

Genetic and biochemical studies were conducted on *S. toyocaensis* NRRL 15009, a gram-positive sporulating filamentous bacterium, and producer of the glycopeptide antibiotic A47934. This compound is structurally similar to the clinically important antibiotic vancomycin, and the recent spread of vancomycin-resistant enterococci (VRE) in North American hospitals has driven the need for new glycopeptides with enhanced activities. Studies were aimed at developing an understanding of the mechanism of A47934 biosynthesis in *S. toyocaensis* NRRL 15009, as well as the mechanism of resistance employed by this organism. Two cosmid clones, containing a partial A47934 biosynthesis gene cluster on a total of 65 kilobases of *S. toyocaensis* NRRL 15009 chromosomal DNA, were isolated for study. Preliminary sequencing indicates the presence of several genes predicted in glycopeptide assembly, such as peptide synthetases and glycosyltransferases. Furthermore, using a oligonucleotide probe designed to identify D-alanine-D-alanine ligases, an 8.1 kilobase chromosomal fragment was isolated from *S. toyocaensis* NRRL 15009 and found to contain genes very similar to VRE *vanH*, *vanA* and *vanX*. Phylogenetic analysis of the predicted products of these genes showed them to be more similar to the VRE enzymes than any other in each enzyme class. These genes were also found in the vancomycin producer *A. orientalis* C329.2 and several other glycopeptide antibiotic producing organisms. Not only does this imply that these organisms employ a mechanism of resistance similar to clinical VRE, it also suggests that these organisms may have been the source of the VRE genes. The enzymes VanHst and DdlN were studied in some detail and found to have biochemical properties similar to

their corresponding VRE enzymes VanH and VanA, respectively. Given that the latter group of enzymes has physical properties that have impeded detailed analysis of enzyme mechanism, these new enzymes could find use as model systems in drug development programs.

Dedication

This thesis and all of the work contained within it is dedicated to my

Grandmother, Maisie Lydia Marshall, who took me to the Ontario Science Centre more

times than I can remember.

Acknowledgements

I would like to thank my Ph.D. supervisor, Professor Gerry Wright, for immeasurable support and guidance throughout the duration of my training. I would also like to thank him for his infectious enthusiasm and devotion to the study of nature.

I would also like to thank the members of my committee, Prof. J. Capone, Prof. P. Harrison, and Prof. H. Schellhorn, whose insights have kept me on track all these years.

I would like to thank the Department of Biochemistry, which has provided an excellent program in which students may flourish. I would especially like to thank Lisa Kush and Dale Tomlinson, who have been exceptionally helpful to myself and those I worked with.

I would like to thank the other members of Prof. Wright's research group for their countless suggestions and support in trying times.

I would like to thank Prof. Brenda Leskiw of the University of Alberta, who took me in as one of her own students and taught me invaluable techniques in *Streptomyces* molecular genetics. I would also like to thank Dr. Astrid Petrich for sharing her expertise in this area.

I would like to thank my wife, Karyn, for all her patience, love and support while I spend many late evenings collecting this data.

Finally, I would like to thank NSERC, for providing funds to this project and to MRC for the Studentship which paid my salary for three years. It is my hope that these agencies continue to thrive and ensure quality Canadian research for years to come.

Table of Contents

Chapter 5. Identification of *van*A/B-like Genes in *S. toyocaensis* NRRL 15009 and other GPA-producing Organisms

Chapter 6. Identification and Purification of D-alanyl-D-alanine Ligases from S. toyocaensis NRRL 15009

Chapter 7. Purification and Characterisation of the D-Alanyl-D-Lactate Ligase DdlN from A. orientalis C329.2

Chapter 10. Recent Developments and General Conclusions

Abbreviations

Ala	Alanine
βHT	β-hydroxytyrosine
6-MSA	6-methylsalicylic Acid
ACP	Acyl Carrier Protein
ARO	Aromatase
AS	Ammonium Sulphate
AT	Acyl Transfer
ATCC	American Tissue Type Collection
ATP	Adenosine 5'-triphosphate
BLAST	Basic Local Alignment Search Tool
BOB	Benzyloxybenzaldehyde
bp	Base pairs
bP-450s	Bacterial P-450s
BPx	Bromoperoxidase
BSA	Bovine Serum Albumin
C	Cytosine
CAPS	3-(cyclohexylamino)-1-propanesulfonic acid
CHT	Chloro-hydroxytyrosine
CIAP	Calf Intestinal Alkaline Phosphatase
cl-eremomycin	Chloro-eremomycin
CLF	Chain Length Factor
CoA	Coenzyme A
contig	Contiguous DNA sequence
CoP	Cofactor Packet
cos	Cohesive End Sequence
CPO	Chloroperoxidase (*Caldariomyces fumago*)
CPx	Chloroperoxidase (*S. toyocaensis* NRRL 15009)
CYC	Cyclase
dATP	deoxy-Adenosine 5'-triphosphate
DCD	Dichlorodimedone
Ddl	D-Ala-D-Ala Ligase
deg	Degenerate
DEAE	Diethylaminoethyl
DH	Dehydratase
D-Hbut	D-hydroxybutyric Acid
DHPA	D-hydroxyphenylacetic Acid
DHPG	D-hydroxyphenylglycine
D-Hval	D-hydroxyvaleric Acid
D-lact	D-lactate
D-LDH	D-lactate Dehydrogenase
DMSO	Dimethylsulfoxide

DNA	Deoxyribonucleic Acid
DTT	Dithiothreitol
EDTA	Ethylene-diamine-tetraacetic acid
ER	Enoylreductase
ES-MS	Electrospray-Mass Spectrometry
Ery	Erythromycin
FAD	Flavin Adenine Dinucleotide
FASs	Fatty Acid Synthases
FMN	Flavin Mononucleotide
for	forward
G	Guanosine
GPAs	Glycopeptide Antibiotics
GPS	Genome Priming System
HEPES	N-2-hydroxyethylpiperazine-N'-2-ethanesulfonic acid
HPLC	High Performance Liquid Chromatography
IPTG	Isopropyl-β-D-thiogalactopyranoside
IRs	Inverted Repeats
kb	Kilobase Pairs
k_{cat}	Catalytic Rate Constant
K_{ii}	Intercept Inhibition Binding Constant
k_{inact}	Inactivation Rate Constant
K_{is}	Slope Inhibition Binding Constant
K_m	Michaelis Menten Constant
k_{obsd}	Observed Rate of Inactivation Constant
KR	Ketoreductase
k_{regain}	Regain of Activity Rate Constant
KS	Ketosynthase
K_s	Substrate Dissociation Constant
LB	Luria Broth
LDH	Lactate Dehydrogenase
MBP	Maltose Binding Protein
MCD	Monochlorodimedone
MCS	Multiple Cloning Site
MIC	Minimal Inhibitory Concentration
MRSA	Methicillin Resistant *Staphylococcus aureus*
NADH	Nicotinamide Adenine Dinucleotide (reduced)
NADPH	Nicotinamide Adenine Dinucleotide Phosphate (reduced)
NaOAc	Sodium Acetate
NEB	New England Biolabs
NMR	Nuclear Magnetic Resonance
NOE	Nuclear Overhauser Effect
ORF	Open Reading Frame
PAB	Penassay Broth
PCR	Polymerase Chain Reaction

PEG	Polyethyleneglycol
PEP	Phosphoenolpyruvate
PFGE	Pulsed Field Gel Electrophoresis
PG	Peptidoglycan
pHPG	*p*-hydroxyphenylglycine
PK	Pyruvate Kinase
PKSs	Polyketide Synthases
PMSF	Phenylmethylsulfonyl flouride
PNK	Polynucleotide Kinase
pPant	Phosphopantethiene
PVDF	Polyvinyledene Fluoride
rev	Reverse
RFLP	Restriction Fragment Length Polymorphism
RNA	Ribonucleic Acid
RT	Room Temperature
SAM	Streptomycete Antibiotic Activity Medium
SDS-PAGE	Sodium Dodecyl Sulphate-Polyacrylamide Gel Electrophoresis
SFM	Soygrit Fermentation Medium
SVM	Soygrit Vegetative Medium
TAE	Tris-Acetate-EDTA
TBE	Tris-Boric Acid-EDTA
Tcm	Tetracenomycin
TE	Thioesterase
TFA	Trifluoroacetic Acid
TLC	Thin Layer Chromatography
Tris	Tris(hydroxymethyl)aminomethane
tRNA	transfer RNA
tyr-tyr-tyr	Tri-L-tyrosine
U	Units
UDP	Uridine Diphosphate
UDPGlcNAc	UDP-*N*-acetylglucosamine
UDPMurNAc	UDP-*N*-acetylmuramic acid
UMP	Uridine Monophosphate
V_e	Elution Volume
V_o	Void Volume
VRE	Vancomycin Resistant Enterococci
VRSA	Vancomycin Resistant *Staphylococcus aureus*
X-gal	5-bromo-4-chloro-3-indolyl-β-D-galactopyranoside
YEME	Yeast Extract-Maltose Extract

List of Figures

List of Tables

Personal Publications

1. **Marshall, G. C., and G. D. Wright.** 1996. Purification and characterization of two haloperoxidases from the glycopeptide antibiotic producer Streptomyces toyocaensis NRRL 15009. Biochem Biophys Res Commun. **219**(2):580-3

2. **Marshall, C. G., G. Broadhead, B. K. Leskiw, and G. D. Wright.** 1997. D-Ala-D-Ala ligases from glycopeptide antibiotic-producing organisms are highly homologous to the enterococcal vancomycin-resistance ligases VanA and VanB. Proc Natl Acad Sci U S A. **94**(12):6480-3.

3. **Marshall, C. G., and G. D. Wright.** 1997. The glycopeptide antibiotic producer Streptomyces toyocaensis NRRL 15009 has both D-alanyl-D-alanine and D-alanyl-D-lactate ligases. FEMS Microbiol Lett. **157**(2):295-9

4. **Marshall, C. G., I. A. Lessard, I. Park, and G. D. Wright.** 1998. Glycopeptide antibiotic resistance genes in glycopeptide-producing organisms. Antimicrob Agents Chemother. **42**(9):2215-20.

5. **Marshall, C. G., and G. D. Wright.** 1998. DdlN from vancomycin-producing Amycolatopsis orientalis C329.2 is a VanA homologue with D-alanyl-D-lactate ligase activity. J Bacteriol. **180**(21):5792-5.

6. **Marshall, C. G., M. Zolli, and G. D. Wright.** 1999. Molecular mechanism of VanHst, an alpha-ketoacid dehydrogenase required for glycopeptide antibiotic resistance from a glycopeptide producing organism. Biochemistry. **38**(26):8485-91.

Chapter 1

Introduction

1.1 Antibiotics

In her book, "The Coming Plague", Laurie Garrett describes what life was like for North Americans in the early part of this century by giving a specific account of her Uncle Bernard's experiences with microbial disease (15). Bernard was 7 years old when the influenza pandemic of 1918 hit, killing over 20 million people. Shortly thereafter, his father nearly died from typhoid fever and his grandfather died of tuberculosis. When he met his wife in 1939, she was deaf in one ear due to a childhood bacterial infection, a complication of which resulted in her right leg falling short of the left by an inch. Bernard then suffered through bacterial pneumonia, which carried a 40% mortality rate in those days. The impact that microbes had on Bernard's life was not atypical. Viral and bacterial infections were an intrinsic part of existence, and affected social, cultural and economic aspects of society.

It is therefore difficult to underestimate the contribution that antibiotics have made to the quality of life enjoyed by our society today. The early antibiotics such as the sulfonamides and the penicillins quickly eradicated many of the disease-causing microbes from the general population. Several new classes have been introduced since then, including quinalones, tetracyclines, cephalosporins, macrolides, aminoglycosides, and glycopeptides. While the medical revolution ushered in by these drugs is recent enough that a few remember the pre-antibiotic era, the majority of people today were born into a world not threatened by microbial infection. In 1969, the Surgeon General of the United States declared that we may "close the book on infectious diseases", which

seemed a reasonable prognosis given the potent combination of antibiotic and vaccine therapies (34). However, it was not long after that that various forms of antibiotic resistance, a phenomenon prophesized by microbiologists and geneticists from the onset of antibiotic use, developed in sufficient populations to warrant "re-opening the book". Today, resistance threatens the use of every class of clinically used antibiotic in every hospital across North America. There is an urgent need for the development of new strategies to combat resistance if we are to extend this golden period of microbial immunity.

1.2   Use and Importance of Glycopeptide Antibiotics

Glycopeptide antibiotics occupy an important niche in the current arsenal against microbial pathogens in that they are the most effective treatment of gram positive, hospital acquired (or nosocomial) infections, such as urinary tract and surgical infections. These types of infections are particularly problematic in elderly and immuno-compromised patients and have become more of a concern as these groups increase in numbers in hospital populations. In 1994, about 5% of all patients admitted suffered some kind of nosocomial infection (63).

Urinary tract infections are by far the most common nosocomial disease, followed by an approximately equal prevalence of surgical and respiratory infections (Figure 1.1) (9). While the gram-negative (and intrinsically glycopeptide resistant) *Escherichia coli* are the predominant causative agent of urinary tract infections, the gram-positive enterococci and streptococci are a close second and are the leading cause of surgical
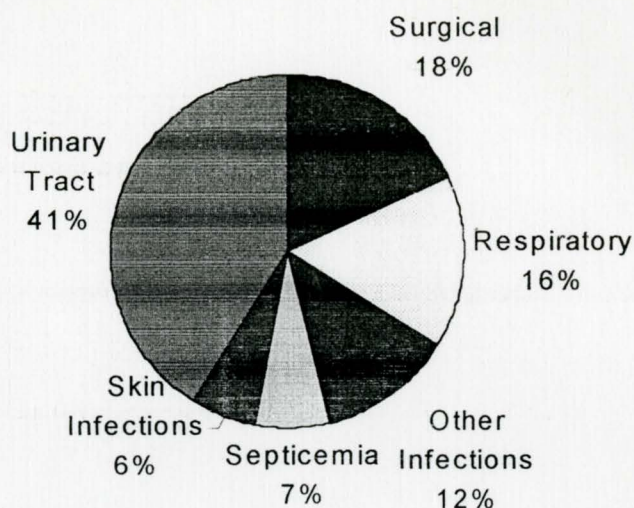
Figure 1.1. Incidence of Nosocomial Infection. The source for this
data can be found in Ref. 9.

infections. Also gram-positive is the notorious *Staphylococcus aureus*, a highly

aggressive microbe prevalent in surgical infection. From annual statistics collected by

various surveillance systems, it is apparent that gram-positive organisms are increasingly

the cause of hospital infections, and that they will continue to be so in the future (45).

In the 1950s, gram-positive nosocomial infections due to *S. aureus*, a major cause

of surgical sepsis, septicaemia and bacteraemia, were successfully treated with β-lactams

or aminoglycoside antibiotics. In the early 1960s, however, outbreaks of methicillin

resistant *S. aureus* (MRSA) developed and other classes of antibiotics (chloramphenicols,

tetracyclines, and aminoglycosides) were required to keep this pathogen in check.

Today, MRSA has acquired resistance to all of these classes of antibiotics as well as to

the cephalosporins, erythromycins and sulfonamides (44). Glycopeptide antibiotics, in

particular vancomycin and teicoplanin, are the only forms of treatment remaining for many cases of MRSA infection.

While enterococci are not as aggressive a pathogen as *S. aureus,* their prevalence in nosocomial infection maintains their status as a clinically important microbe. Although enterococci are part of the normal flora of the intestinal and genital tract, they often develop into infections in individuals whose health has been compromised. The two species most commonly associated with infection – *Enterococcus faecalis* and *Enterococcus faecium* - have, until recently, been held in check with a combination therapy of β-lactam/aminoglycoside antibiotics (35). What has brought the enterococci to the attention of the medical community (apart from their ubiquity in the hospital environment) is their ability to acquire and spread multi-drug resistance phenotypes. Enterococci have intrinsic low-level β-lactam resistance that has been enhanced in many strains by the acquisition of a plasmid borne β-lactamase (43). Aminoglycoside resistance first appeared in the 1970s and was widespread by the mid-1980s (40). Furthermore, the use of broad-spectrum antibiotics such as cephalosporins, carbapenems, and fluoroquinalones has increased the prevalence of enterococcal infections by virtue of the fact that these drugs have limited activity against them (42). Currently, glycopeptide antibiotics and a combination of β-lactam/β-lactamase therapy are the only effective treatments left. The very recent development of acquired glycopeptide resistance in both *E. faecalis* and *E. faecium* (64) poses a serious threat as a) an untreatable affliction and b)

a potential donor of resistance to MRSA and the creation of an aggressive and unstoppable pathogen.

In addition to the control of nosocomial infections due to *Staphylococcus aureus*, *Streptococcus spp.* and *Enterococcus spp.*, glycopeptide antibiotics are used orally against *Clostridium difficile*, a pathogen that causes pseudomembraneous colitis (27).

The importance of glycopeptide antibiotics is reflected in reports of their annual usage (28). Currently only vancomycin and teicoplanin are approved for clinical use in humans, with world-wide demand for the former far outweighing the latter. The use of vancomycin in the United States has risen from 2,000 kg/year in 1984 to over 11,000 kg/year in 1996. Vancomycin consumption in the U.S. is greater than that of France, Germany, Italy, and the U.K. combined.

Despite its importance in treating serious infection, several problems have been associated with vancomycin use (14). Many of the unpleasant side effects experienced with vancomycin administration when it was first introduced into the clinic (such as deafness) were alleviated by improving the level of purity of the drug in clinical preparations, however some of the difficulties are intrinsic to the antibiotic itself. Vancomycin is not absorbed orally and intramuscular injection causes severe pain at the site of administration. It can only be delivered by intravenous drip over a lengthy period of time (60 minutes) as more rapid delivery can result in anaphylactic shock. Its half-life is relatively short, varying from 3 to 13 hours depending on the patient, and patients require several daily doses (up to four). In addition, vancomycin is considered to be potentially nephrotoxic. Teicoplanin has much better pharmacokinetics and is less toxic,

however it has reduced activity against some strains of staphylococci, and remains less popular than vancomycin with clinicians. The fact that vancomycin is still widely used despite these technical difficulties is a testament its importance in the clinic.

Other glycopeptide antibiotics that have found use include ristocetin and avoparcin. Ristocetin was initially a candidate for the treatment of disease in humans. However it was abandoned as such upon the discovery that it causes aggregation of blood platelets (25). This has been put to use in the diagnosis of von Willebrand's disease, an affliction resulting in the lack of a plasma protein required for ristocetin-induced agglutination. Avoparcin has until very recently been used in massive quantities in Europe as an animal feed additive. Several studies indicated a geographic correlation between avoparcin use on farms and the percentage of the population colonized by glycopeptide resistant enteric bacteria (5, 29). As a result, avoparcin was discontinued in this function in many European countries.

1.3 Structure and Activity of Glycopeptide Antibiotics

Although vancomycin and teicoplanin are the only two approved for clinical use, the structures of over 100 glycopeptide antibiotics (GPAs) are currently known. Vancomycin was the first GPA discovered in an extract from soil samples taken from the jungles of Borneo in the early 1950s (38). It was eventually developed by the American pharmaceutical company Eli Lilly and Co. and used for the first time in the clinic in 1959. It was not until 1982 that the complete structure of vancomycin was solved, using a combination of X-ray studies and proton NMR (57, 67). By making use of the nuclear

Overhauser effect (NOE), a relatively new NMR technique at the time, Dudley H.

Williams was the principle contributor in the structure determination. Figure 1.2

illustrates the accepted structure of vancomycin. It is a linear heptapeptide rich in

hydrophobic and aromatic amino acids. From N-terminus to C-terminus, vancomycin
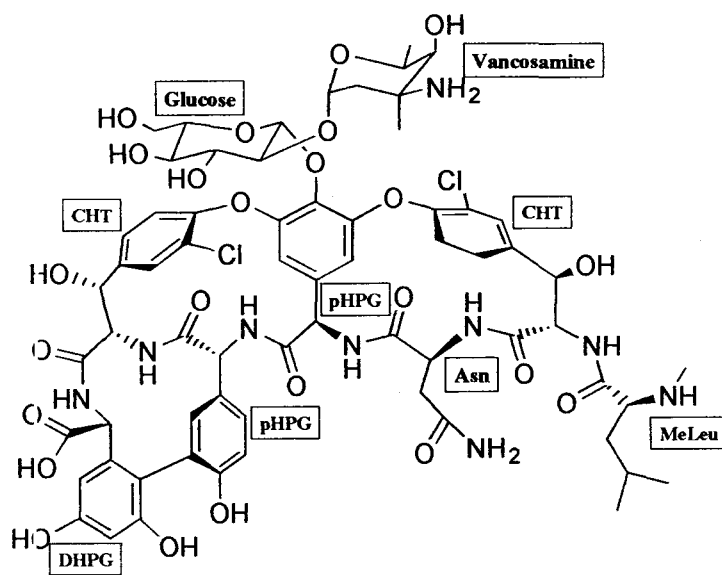
Figure 1.2 Chemical Structure of the GPA Vancomycin.

consists of N-methyl leucine, m-chloro-β-hydroxytyrosine (CHT), asparagine, p-

hydroxyphenylglycine (pHPG), pHPG, CHT and 2,4-dihydroxyphenylglycine (DHPG).

The stereochemistries of these unusual amino acids are all R with the exception of

residues 6 and 7, corresponding to the incorporation of D-amino acids at positions 1

through 5. The peptide core of vancomycin is highly cross-linked, with phenolic coupling

of the aromatic rings of residues 2, 4, and 6, as well as direct carbon-carbon coupling of

the aromatic rings of residues 5 and 7. This gives the structure a highly rigid and ordered

form, a characteristic reflected in the compound's stability in the presence of peptidases.

A common feature in GPAs is the attachment of 6-membered sugar rings, of which

vancomycin has two -- glucose is attached to the phenyl hydroxyl of residue 4 and

vancosamine is attached to glucose by a α-1,2' glucosidic link. The structure

determinations of other GPAs, some of which are shown in Figure 1.3, made apparent

certain conserved features of this antibiotic class. All GPAs contain seven amino acids

linked in a linear head-to-tail fashion. Residues 2, 4 and 6 are always conserved and

always linked together to form the triphenylether system observed in vancomycin.
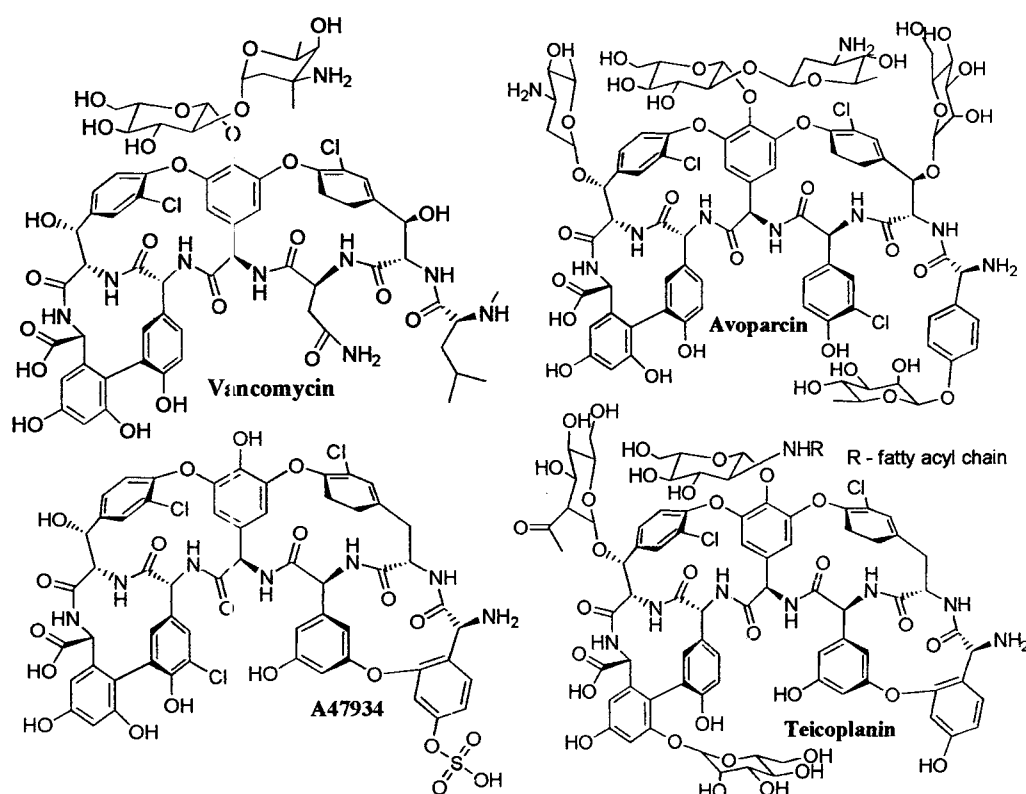
Figure 1.3. Various Glycopeptide Antibiotics.

Residues 5 and 7 are also conserved and are always linked via a carbon-carbon bond to

give the biphenyl. Sugar residues are often, but not always, attached to the peptide core,

giving rise to the preference of some researchers to refer to this class as dalbaheptides

rather than glycopeptides (46, 73), which admittedly makes more sense. Sugars vary in

structure, quantity and site of substitution, although residue 4 is almost always glycosylated.

GPAs have been classified into four major groups, based primarily on the type of amino acids found at positions 1 and 3 (71). Group I GPAs have aliphatic amino acids in these positions, and include vancomycin and eremomycin. Those that belong in group II have aromatic residues at positions 1 and 3 and include avoparcin. Ristocetin and A47934 are two of the members of group III, which also have aromatics at these positions but differ in that the two residues are joined by ether linkage. Group IV is as group III however the sugar constituent attached to residue 4 is acylated with a fatty acid. GPAs in this group include teicoplanin, ardacin and kibdelin. Most of the GPAs fall into the broad categories defined by these groups, however at least one – synmonicin, with an aromatic at position 1 and aliphatic at position 3 -- does not. Small variations in the antimicrobial potency of GPAs across the various groups suggest that residues 1 and 3 are not the primary determinants of activity (Table 1.1) (46). There is evidence, however, that sugar residues and fatty acyl chains contribute significantly to antibiotic activity.

Table 1.1. Activity of Various Glycopeptide Antibiotics

Glycopeptide Antibiotic	Group	*E. faecium* MIC (ug/mL)
Vancomycin	I	1
Eremomycin	I	1
Orienticin A	I	1
Avoparcin	II	2
Actinoidin	II	8
Ristocetin	III	2
Actaplanin	III	1
Teicoplanin	IV	0.06

1.4 Mode of Action of Glycopeptide Antibiotics

The rigid cup-like configuration predicted by the structure of GPAs and the fact that they are only active against gram-positive bacteria indicated early on that these molecules may function in the inhibition of cell wall synthesis. Unlike a small molecule which evolves to fit into the active site of an enzyme, GPAs are large and have evolved a structured pocket, suitable for the binding of small molecules themselves. The cell wall of bacteria is composed of a large polymer of peptidoglycan (PG), however each monomeric unit has short, flexible peptides ideal for binding into such a pocket. Early studies by Nieto, Perkins and Reynolds established an affinity of GPAs for PG and narrowed down the target to the carboxyl terminus of the peptide component (48, 51). In 1980, Dudley Williams determined the solution structure of the GPA ristocetin in a complex with an analogue of the PG peptide (26), providing solid evidence for this predicted binding, and for a role for GPAs in inhibition of the late stages of cell wall biosynthesis.

PG is a polymer consisting of repeated units of the disaccharide N-acetylmuramic acid – N-acetylglucosamine. To the former is attached the pentapeptide L-alanyl-γ-D-glutaryl -L-lysyl-D-alanyl-D-alanine (in Gram-positive bacteria, while in Gram-negative bacteria L-lysine is usually replaced by *meso*-diaminopimelate). Several layers of the repeating disaccharide envelop the cell, with the peptides facing inward and outward. To provide mechanical strength to these concentric sheaths, the final structure has covalent bridges linking the peptides of adjacent layers. This link is formed by a peptide bond

between the L-lysine (or *meso*-diaminopimelate) of one strand and the penultimate D-

alanine of another (Figure 1.4). A thorough analysis of the biosynthesis of the bacterial

cell wall has established that three distinct stages can be classified (Figure 1.5) (11).

**N-acetyl N-acetyl
glucosamine muramic acid**

**Penta-
peptide**
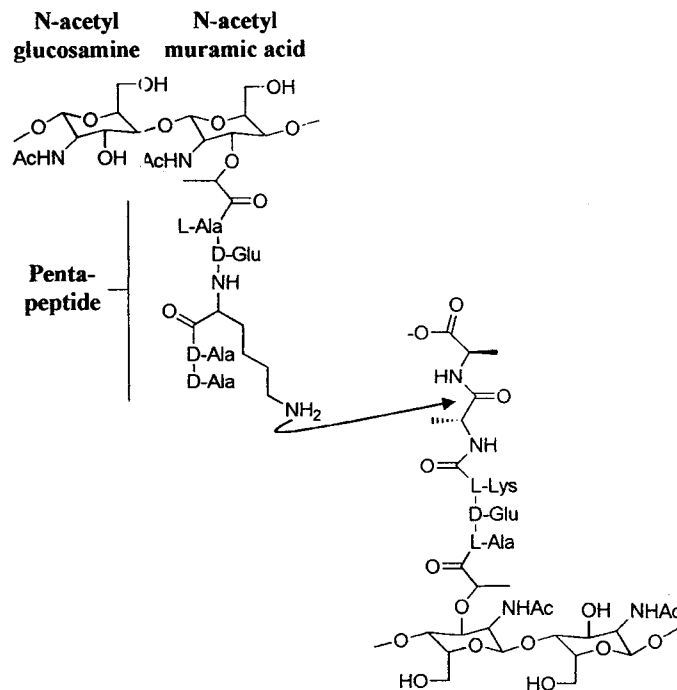
Figure 1.4. Cross-Linking of the Peptide Component of Peptidoglycan.

Stage I involves the intracellular synthesis of the two sugars and of the D-amino

acids required for building PG. UDP-N-acetylmuramic (UDPMurNAc) acid is

synthesized by the enzymes MurA and MurB from UDP-N-acetylglucosamine

(UDPGlcNAc), which is in turn manufactured from the primary metabolite fructose-6-

phosphate. D-alanine is synthesized by a racemase from the L-isomer. D-glutamate is

formed similarly in some bacteria, while in others it is the transamination product of α-

ketoglutarate.

A UDPMurNAc-pentapeptide is the final product of stage II, in which ATP-

dependent ligases extend the peptide chain from its carboxy-terminus. MurC, MurD and

MurE attach L-alanine, D-glutamine, L-lysine, respectively, to form the UDPMurNAc-

tripeptide. D-ala-D-ala is synthesized by a D-alanyl-D-alanine ligase (Ddl) and added as

a dipeptide by MurF.
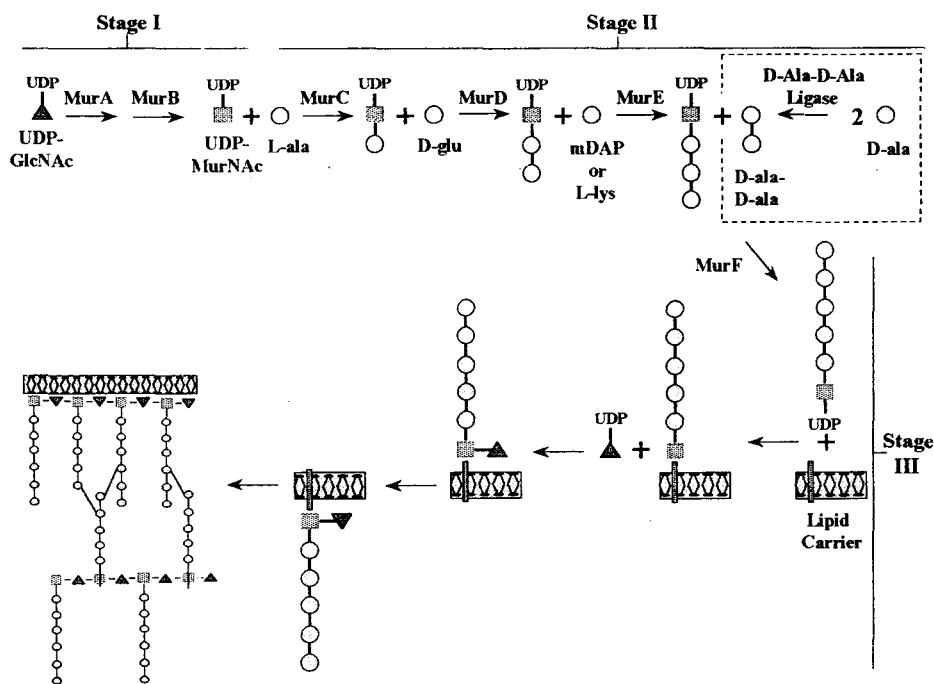
Figure 1.5. Stages of Peptidoglycan Assembly.

In stage III UDPMurNAc-pentapeptide is attached to an undecaprenyl lipid carrier

(releasing UMP), joined with UDP-GlcNAc (again releasing UMP), and shuttled across

the membrane. Here it is joined with the growing peptidoglycan by transglycosylases,

releasing the lipid carrier, and is subject to covalent crosslinking by transpeptidases.

Nucleophilic attack of L-lysine on the penultimate D-alanine releases the terminal D-

alanine into solution.

Each stage of biosynthesis has at least one class of antibiotics that is dedicated to its inhibition (Table 1.2). Stage I enzymes that bind D-alanine are inhibited by the structural analogue cycloserine, while formation of UDP-MurNAc is inhibited by fosfomycin. Bacitracin binds to the membrane bound lipid carrier after release of it payload and prevents it from re-entering the cycle, thus blocking the synthesis in Stage II. The most famous group of all antibiotics - the β-lactam family - inhibit Stage III, by binding to and covalently modifying any enzyme that metabolizes a D-D peptide bond. This includes transpeptidases, carboxypeptidases and endopeptidases, and there are several in every bacterium (7 known in *E. coli*).

Table 1.2. Inhibition of PG Synthesis

Stage of PG Synthesis	Antibiotic	Enzyme Inhibited
I	D-Cycloserine	Alanine Racemase Ddl
	Fosfomycin	Phosphoenolpyruvate: UDP-GlcNAc-3-enolpyruvyltransferase
II	Bacitracin	Undecaprenyl-pyrophosphate phosphatase
III	Glycopeptide Antibiotics	Transglycosylase Transpeptidase
	β-Lactam Antibiotics	Transpeptidase carboxypeptidase endopeptidase

GPAs are also inhibitors of Stage III PG synthesis. The structure of vancomycin complexed with N-acetyl-D-alanyl-D-alanine (also solved by D. Williams) clearly demonstrates the mechanism of antibiotic activity (Figure 1.6) (68). The rigid peptide backbone of the heptapeptide forms 5 hydrogen bonds with the 2 terminal D-alanine residues. None of the GPAs' side chains (R groups) participate in the hydrogen bonds,

however they clearly have a role in providing the appropriate geometry to the molecule

as they are extensively involved in cross-linking. Three of the five hydrogen bonds are
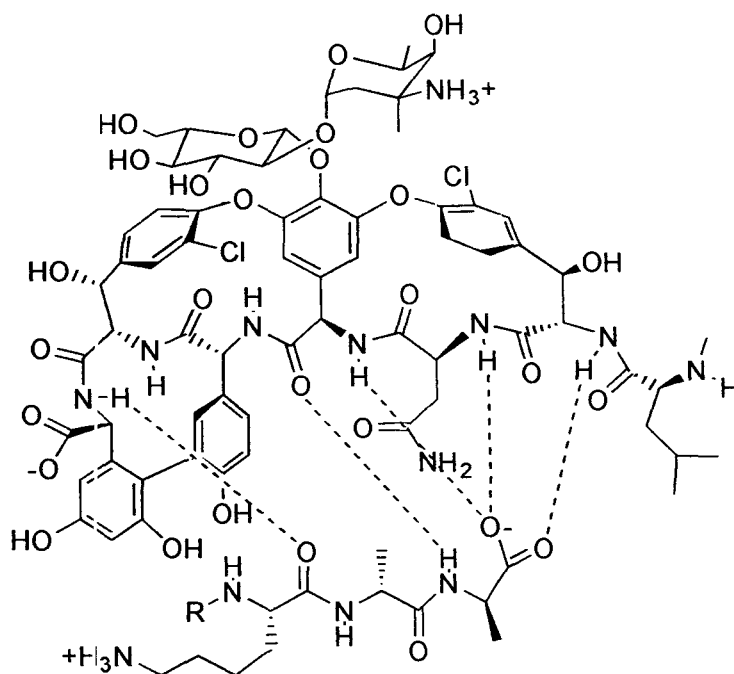
Figure 1.6. Vancomycin Complex with Lysyl-D-Alanyl-D-Alanine. Figure adapted from Ref. 66.

made to the terminal carboxyl of the second D-alanine molecule, highlighting this group

as the pivotal determinant in GPA binding. GPAs inhibit stage III of PG synthesis,

therefore, by binding PG intermediates containing the terminal tri-peptide L-lysyl-D-

alanyl-D-alanine and sterically interfering with transglycosylation and transpeptidation

reactions. Without the reinforcement and rigidity of intact PG, the cells are easily lysed

by mechanical forces and osmotic pressures.

The sugar residues of GPAs also play a role in inhibition, assisting in the back-to-

back dimerization of two GPA molecules bound to PG. GPA dimerization was

discovered in 1989 and has since been well characterized (39). The solution structure of

dimerized ristocetin (Figure 1.7) illustrates that the dimer is held together by 6 hydrogen

bonds. Four of these involve functional groups solely from the peptide backbones of the

GPAs, none of which are involved in interacting with the peptidoglycan terminus. The
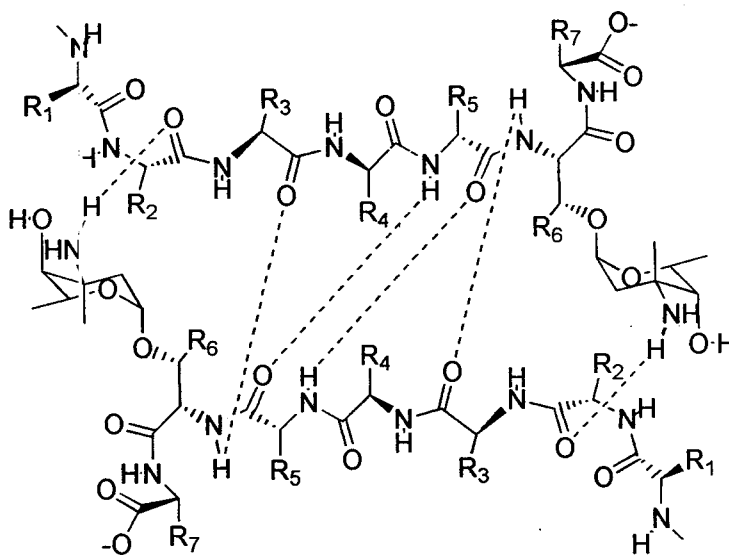
Figure 1.7. Glycopeptide Dimer. Figure adapted from Ref. 66.

other two hydrogen bonds involve groups from both the peptide backbone and the

ristosamine sugar group (attached to residue 6). This latter interaction appears to

function additionally in assisting the amide hydrogens of residues 1 and 2 in their

hydrogen bonds with the carboxylate of D-alanine. This dimerization is believed to

enhance activity in at least two ways. Once a dimerized GPA is bound to PG at one face,

the binding of the other face to a PG constituent is essentially an intramolecular event

rather than an bimolecular event, reducing the entropic barrier to binding. Secondly,

dimerization is believed to stabilize the interaction of each GPA with their PG target,

particularly through the hydrogen bonds involving the sugar amines. Thus GPAs with

sugar residues that enhance dimerization should be more potent antibiotics. This function is well supported by studies that show a distinct correlation between the dimerization constant of a given GPA and its ability to bind a) soluble cell wall analogues such as N-acetyl-L-lysyl-D-alanyl-D-alanine and b) said cell wall analogues inserted into detergent micelles in a fashion mimicking the cell wall (66). In addition, GPAs that dimerized well were more resistant to soluble cell wall analogues when their inhibitory activity was challenged in competition assays (Figure 1.8).

In the case of Group IV antibiotics such as teicoplanin, no dimerization is observed, however resistance to soluble cell wall analogues in competition assays is unusually high (Figure 1.8). This resistance is ablated by the removal of the fatty acyl chain, which is believed to act as a membrane anchor. This anchor serves the same purpose as dimerization in that, once inserted into the cell membrane, binding of PG becomes an intramolecular event. However, Figure 1.8 shows that teicoplanin's resistance to soluble cell wall analogues is well below those GPAs that dimerize strongly, emphasising the important contribution of dimerization on stabilizing the hydrogen bonds to the D-alanine carboxylate.

In addition to facilitating dimerization, there is recent evidence that the glycosyl moieties of GPAs function as inhibitors on their own (16), perhaps by mimicking the PG disaccharide and inhibiting transglycosylases. This would be a clever trick to increase their effective concentration and decrease the entropy of binding by using the peptide core to localize themselves near these enzymes.
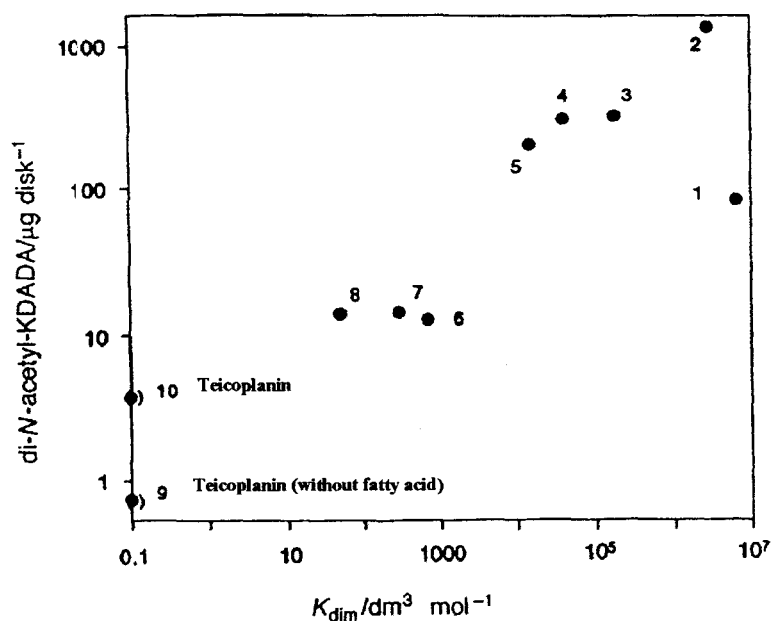
Figure 1.8. Relationship of GPA Dimerization and Antimicrobial Activity. Activity was assessed as the amount of cell wall analogue required to ablate growth inhibition zones around a cotton disk containing GPA. Figure adapted from Ref. 66.

1.5 Biosynthesis of Glycopeptide Antibiotics

Almost nothing is known about the biosynthesis of GPAs. A logical scheme of synthesis involves four stages I) Synthesis of the unusual amino acids and sugars from available cellular metabolites II) Assembly of the linear peptide III) Crosslinking of the peptide and IV) Attachment of sugars, acyl chains or any other functionalities (73). Stages III and IV may not be distinct, however, and certain modifications such as hydroxylation or halogenation could occur before or after peptide assembly.

Some of the precursor molecules of vancomycin have been identified through *in vivo* incorporation studies done by D.H. Williams and colleagues using isotopically-labelled metabolites (19). Approximately 5 fold enrichment of the ^{13}C NMR signal

corresponding to CHT α-carbons was observed when antibiotic producing cultures were

fed with ^{13}C-tyrosine, suggesting a tyrosine origin for these residues (Figure 1.9). Similar

(S)-tyrosine   **β-hydroxy-(S)-tyrosine**

m-chloro-β -hydroxy-
tyrosine (CHT)   **(R)-β-hydroxy-(R,S)-**
tyrosine (β -HT)
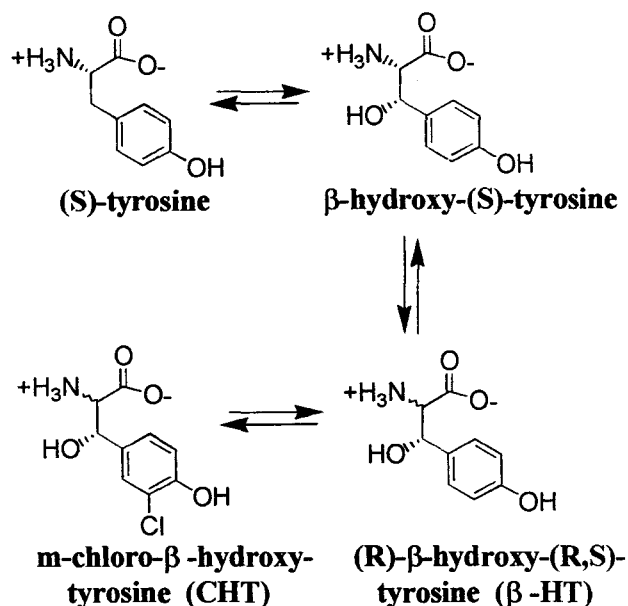
Figure 1.9 CHT Biosynthesis Scheme.

enrichment experiments implicate tyrosine in pHPG synthesis, and a pathway with a p-

hydroxymandelate intermediate is predicted (Figure 1.10). Interestingly, acetate is well

incorporated into DHPG, suggesting a polyketide pathway for this residue (Figure 1.11).

All of these predicted activities occur in Stage I of GPA biosynthesis. There is no

biochemical data available to support predicted activities in Stage II or Stage III events.

Assembly of peptides containing unusual amino acids had been characterized in other

systems, however, and may serve as a general model for Stage II.

The enzyme that attaches glucose onto the peptide core of vancomycin (Stage IV)

is the only biosynthetic enzyme to be detected and purified from cell-free extracts of a

GPA-producing organism (72). It is a 44kDa soluble protein and will use TDP-galactose

as well as TDP-glucose with optimum activity at a pH between 9 and 10 and a

temperature of $37^{O}C$.
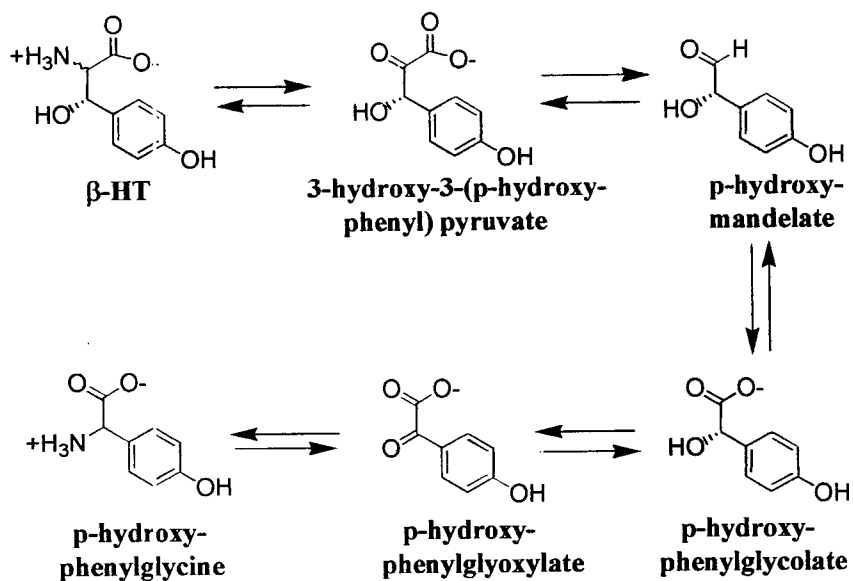
Figure 1.10. pHPG Biosynthesis Scheme.
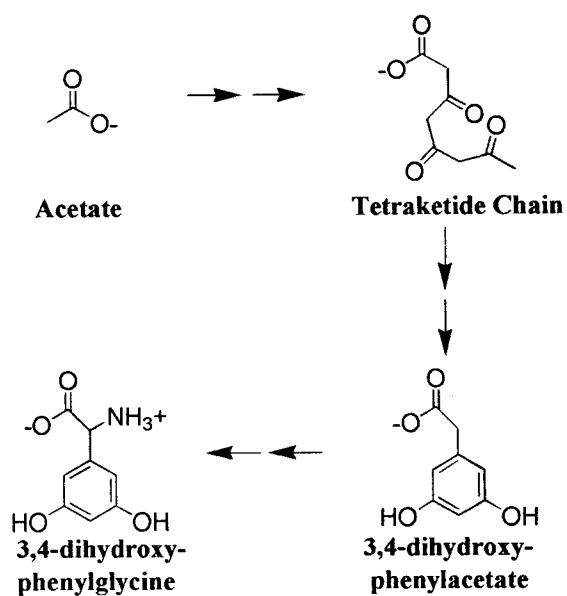
Figure 1.11. DHPG Biosynthesis Scheme.

1.6 Biosynthesis of Peptide Antibiotics

GPAs are all linear peptides composed of unusual amino acids that have been extensively modified in the final product. A group of metabolites that share these traits are the peptide antibiotics - such as gramicidin S, surfactin and enniatin B (Figure 1.12). The systems that make these peptides have been extensively studied and serve as a model for the likely mode of peptide assembly of GPAs (Stage II).

$$D\text{-Phe} \rightarrow Pro \rightarrow Val \rightarrow Orn \rightarrow Leu$$
$$\uparrow \qquad\qquad\qquad\qquad \downarrow \quad \textit{Gramicidin S}$$
$$Leu \leftarrow Orn \leftarrow Val \leftarrow Pro \leftarrow D\text{-Phe}$$

$$C_{10\text{-}12}\text{-CH-CH}_2\text{-CO} \rightarrow Glu \rightarrow Leu \rightarrow D\text{-Leu}$$
$$| \qquad\qquad\qquad\qquad\qquad \downarrow \quad \textit{Surfactin}$$
$$O \text{------} Leu \leftarrow D\text{-Leu} \leftarrow Asp \leftarrow Val$$

$$D\text{-HIV} \rightarrow MeVal \rightarrow D\text{-HIV}$$
$$\uparrow \qquad\qquad\qquad \downarrow \quad \textit{Enniatin B}$$
$$MeVal \leftarrow D\text{-HIV} \leftarrow MeVal$$
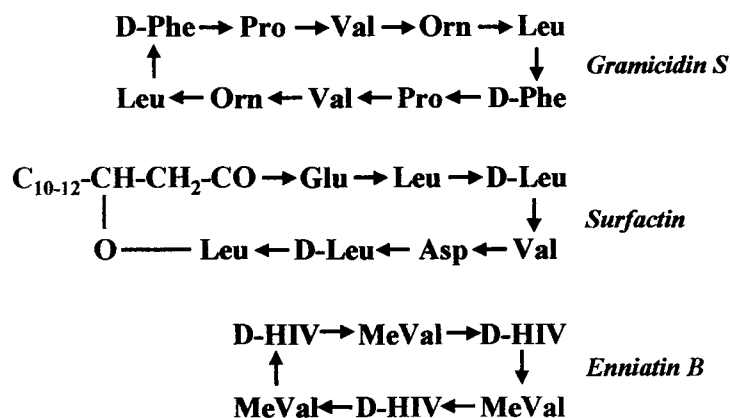
Figure 1.12. Composition of Various Peptide Antibiotics.

A few peptide antibiotics are synthesized on ribosomes and therefore are made from only protein amino acids (41). They usually undergo a variety of post-translational modifications including dehydration, epimerization, thioesterification, and proteolytic cleavage to generate the final active product. Examples include subtilin (*B. subtilis*) (49), microcin B-17 (*E. coli*) (55), and ancovenin (*Streptomyces* sp.) (65).

Peptides composed of non-proteinaceous amino acids must be linked in a non-ribosomal manner. These reactions are carried out on large, multi-domain enzymes in what has been termed a "thio-template mechanism" (31). Similar to ribosomal synthesis,

the peptide is grown from its carboxyl-terminus, but all of the information encoding the

sequence of assembly is found in the assembling enzyme. While the molecular details of

this system have not yet been fully elucidated, the current body of data generally supports

the following model.

Each amino acid in the peptide has a corresponding module in the assembling

enzyme. Each module has a minimum of two essential domains, but 6 different domains

have been identified (6, 36, 60). The adenylation domain uses ATP to adenylate the

amino acid carboxyl group, activating it for nucleophilic attack. The amino acid is then

thioesterified to a 4'-phosphopantetheinyl (pPant) cofactor which is covalently attached

to the thiolation domain located just adjacent to the adenylation domain (Figure 1 13).
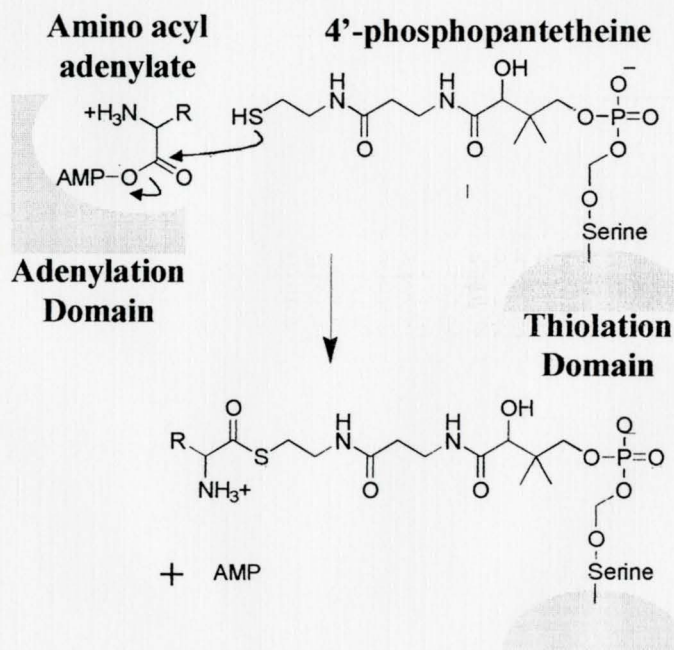
Figure 1.13. Formation of Acyl-Thiolation Domain Intermediate.
Figure adapted from Ref. 36.

The pPant cofactor is long and flexible, and is free to move about the enzyme within its range of motion. The covalently bound amino acid of module 1 is thus transported to the condensation domain of the next module in the enzyme, where it is attacked by the pPant-amino-acid (the "extender unit") prepared by that module. The resulting dipeptide is now attached to the thiolation domain of the second module and the process of transportation/condensation is continued along the surface of the enzyme until the full peptide is generated, at which time release is catalyzed by a thioesterase (TE) domain.

The adenylation and the thiolation domains in each module are the core enzymatic domains in that they are found in every module in the enzyme, however other domains may be present as needed. The condensation domain, which catalyzes the attack of the extender unit amino group on the activated carbonyl of the growing chain, is fundamental to peptide growth and as such is found in every module except (occasionally) the first. There is some evidence that it also has a role in elongation proof-reading in that it has specificity requirements for the R group of the extender unit (6). Two other domains function to modify the residues of the growing peptide. Epimerization domains alter the stereochemistry of the α-carbon as necessary, and N-methylation domains methylate amides in the peptide backbone. These domains are located in close proximity to the two core domains, as expected given the tethered nature of the acyl chain. In addition, the last module usually contains a TE domain to release the completed chain. Release may be mediated by some external nucleophile (usually water) or by a nucleophile in the assembled peptide, releasing either a linear or a cyclic product, respectively.

The modular nature of these enzymes is reflected in their genetic organization

(Figure 1 14). The genes encoding the modules of the assembly enzyme are colinear with

the sequence of the peptide product. The thiolation domain is always immediately 3' to
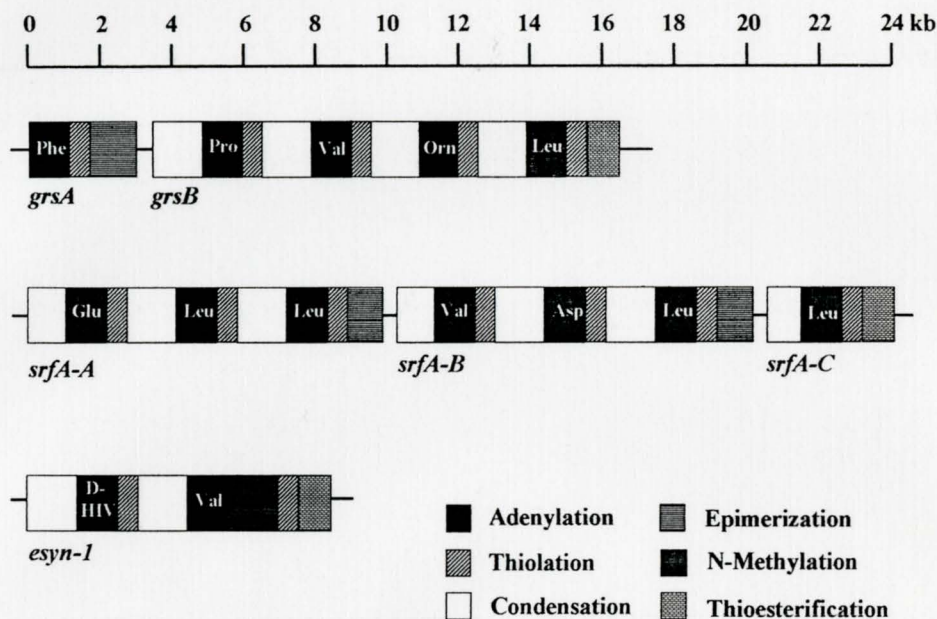
Figure 1.14. Genetic Arrangement of Peptide Synthetases.

the adenylation domain, except when a N-methyltransferase domain is required. When

present, condensation domains are 5' to the adenylation domains and epimerization

domains are always 3' to thiolation domains. TE domains are 3' to the thiolation domain

of the last module, or are sometimes a separate polypeptide. These modules are capable

of functioning entirely independently of one another, however they must function

together in a template capacity to achieve specific peptide elongation (60, 61). Genes

range in size from just under 2 kb for a single module containing only an adenylation and

thiolation domain to nearly 47 kb for the giant 11 module cyclosporin synthase.

Bacterial assembly systems (gramicidin S, surfactin) appear to be broken up into separate enzymes which associate with each other non-covalently, whereas fungal enzymes keep all of the modules on a single gene product (enniatin B, cyclosporin). In the case of gramicidin S, since the decapeptide is made from 2 identical pentapeptides, only 5 modules are required.

The advantage to non-ribosomal peptide synthesis is the many degrees of freedom that exist in the composition of the peptide chain. In addition to non-proteinaceous amino acids, hydroxy acids can be incorporated to form hybrid peptide-depsipeptides. Epimerization and N-methylation further add diversity to the structure, as do the various mechanisms of release which can produce cyclic peptides or lactones. The disadvantage is the huge cost of synthesis due to the need for modular enzymes. As a result of this limitation, most polymers made this way consist of only 7 residues, whereas ribosomally synthesized chains can be much longer.

It has been pointed out that the modular assembly of peptides by the thio-template mechanism bears much similarity to the assembly of certain polyketides (30). Acetates, propionates and carboxylates are sequentially added via their carboxylated coenzyme A-thioesters on a multi-domained enzyme. The growing chain is shuttled from one catalytic site to another using a pPant cofactor and after each round of condensation, a variety of modification domains are present to make necessary adjustments to the newly added member (discussed further in Chapter 3). Release is by thioesterification and post-translational modifications are usually extensive. The genes encoding these polyketide synthases (PKSs) are clustered and the domains that condense and modify the

carboxylate units are co-linear with their sequence in the final product. Similar to the case with non-ribosomal peptides, polyketides made this way are usually much shorter than their fatty acid cousins, which are made from similar precursors but are synthesized on systems that perform iterative rounds of identical chemistry. Thus it appears these two systems, non-ribosomal peptide synthetases and polyketide synthases, requiring similar chemistry have evolved similar biochemistry to complete the task.

An additional mechanism of assembling peptides non-ribosomally exists in which acyl-phosphates are generated to promote peptide bond formation. Intermediates are not covalently bound to the assembly enzymes, which bear no homology to the modules of the thio-template based enzymes. Short peptides such as glutathione and D-alanyl-D-alanine are manufactured in this fashion, although the lengthy mycobacillin (13 amino acids - all proteinaceous) is also believed to be made this way (17, 56).

1.7 Resistance to Glycopeptide Antibiotics

Clinical resistance to GPAs first emerged in 1986, more than 30 years after vancomycin had entered into the clinic, in the form of vancomycin resistant enterococci (VRE) (33). Distinct phenotypes were observed and labelled VanA and VanB. Today that has been extended to VanC and VanD. All of the vancomycin resistant phenotypes utilise a similar molecular mechanism, but differ from each other in the level of resistance, spectrum of resistance and in the ability of resistance to be transferred from one cell to the next (Table 1.3) (32). The VanA phenotype is found in several strains, confers high level resistance to both vancomycin and teicoplanin, and as the resistance

genes are located on a plasmid, this phenotype is readily transferable. VanB, observed in

E. faecalis and *E. faecium,* denotes high level resistance to vancomycin but cells are

susceptible to teicoplanin. Although the genetic elements required for resistance are

encoded in the chromosome, transfer of resistance is observed in some strains (52). Both

VanA and VanB phenotypes are inducible forms of resistance, in that drug must be

present for the requisite genes to be expressed. In the case of the VanB phenotype, the

inability of teicoplanin to induce this expression is the basis for the lack of resistance

observed. The VanC class, corresponding to clinically rare species of enterococci,

possess low-level resistance to vancomycin, are susceptible to teicoplanin and are not

capable of transferring resistance. These organisms are considered intrinsically resistant

to vancomycin as every strain examined possesses the VanC phenotype, however both

inducible and constitutive forms of this phenotype have been observed (54). VanD is the

most recently reported phenotype, displaying medium-level vancomycin resistance and

low-level resistance to teicoplanin. Resistance is constitutive and is not transferable.

Table 1.3. Phenotypes of Glycopeptide Resistant Enterococci

Phenotype	Sample Species	MIC (mg/L)		Transferable Resistance	Induction
		Vancomycin	Teicoplanin		
VanA	*E. faecium* *E. faecalis* *E. avium* *E.gallinarum*	64 -> 1,000	16 – 512	Yes	Yes
VanB	*E. faecium* *E. faecalis*	4 – 1,024	0.25 – 2	Yes	Yes
VanC	*E. gallinarum* *E. casseliflavus*	2 – 32	0.12 – 2	No	Some
VanD	*E. faecium* *E. faecalis*	16 – 64	2 – 4	No	No

The mechanism of resistance in the VanA phenotype is the most studied and sets

a general theme that is followed in all the other phenotypes. The 7 genes associated with

high-level vancomycin resistance were originally isolated on the transposon *Tn1546* by

Patrice Courvalin's group of the Pasteur Institute (Figure 1.15) (22). *vanR* and *vanS*

IR$_L$ ORF1 ORF2 *vanR* *vanS*   *vanH* *vanA* *vanX*   *vanY* *vanZ* IR$_R$
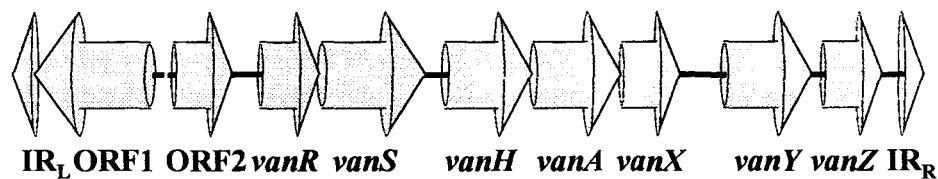
Figure 1.15. Arrangement of *vanA* Resistance Genes on Transposon *Tn1546*.

constitute a two-component signal transduction pathway that initiates expression of the

gene cluster in the following proposed mechanism (2). *vanS* encodes a membrane-bound

receptor histidine kinase which functions to activate the product of the *vanR* gene, a

transcriptional activator, by phosphorylating a critical aspartate. VanS itself becomes

activated by an unidentified extracellular signal indicating the presence of vancomycin

(69). In its phosphorylated form, VanR upregulates expression of itself as well as *vanH*,

vanA and *vanX* - the three genes necessary and sufficient for vancomycin resistance

(Figure 1.16). VanA is the pivotal enzyme, a ddl that preferentially catalyses the

formation of the depsipeptide D-alanyl-D-lactate (10). VanH is a dehydrogenase that

supplies VanA with D-lactate generated from pyruvate (12). VanX is a dipeptidase with

exquisite specificity, degrading endogenous pools of D-alanyl-D-alanine while leaving

depsipeptides intact (70). The result is a large increase in the cellular ratio of D-alanyl-

D-lactate:D-alanyl-D-alanine and the subsequent incorporation by MurF of the

depsipeptide into PG precursor, specifically UDPMurNAc-pentapeptide. The resulting

incorporation of D-alanyl-D-lactate into mature peptidoglycan leaves vancomycin one

less amide nitrogen to hydrogen bond with and a concomitant 1000-fold decrease in
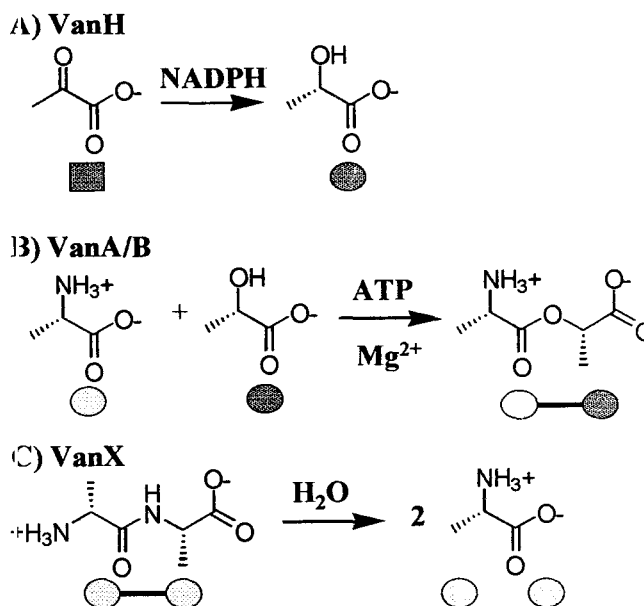
Figure 1.16. Enzymatic Activities of _van_ Gene Products.

binding affinity (12). Thus, rather than modify the antibiotic so that it can no longer bind

its target, as is the case in many resistance mechanisms, vancomycin resistant enterococci

have altered the target, rendering the drug clinically useless (Figure 1.17). This is one of

the most complex and elegant examples of evolved bacterial resistance to an antibiotic.

The other genes found on the Tn1546 chromosome are _vanY_ and _vanZ_, and are

not necessary for vancomycin resistance, but serve auxiliary functions that enhance the

phenotype. VanY is a carboxypeptidase that cleaves off terminal D-alanine from PG

precursors (21), and VanZ confers teicoplanin resistance by an unknown mechanism (3).

A. Susceptible B. Resistant

N-Acetylmuramic Acid (▣)
N-Acetylglucosamine (▲)
L-Ala-D-Glu-mDAP-
  D-Ala-D-Ala (o-o-o-o-o-o)

L-Ala-D-Glu-mDAP-
  D-Ala-D-X (o-o-o-o-o-●)

X = D-Ser or D-Lact
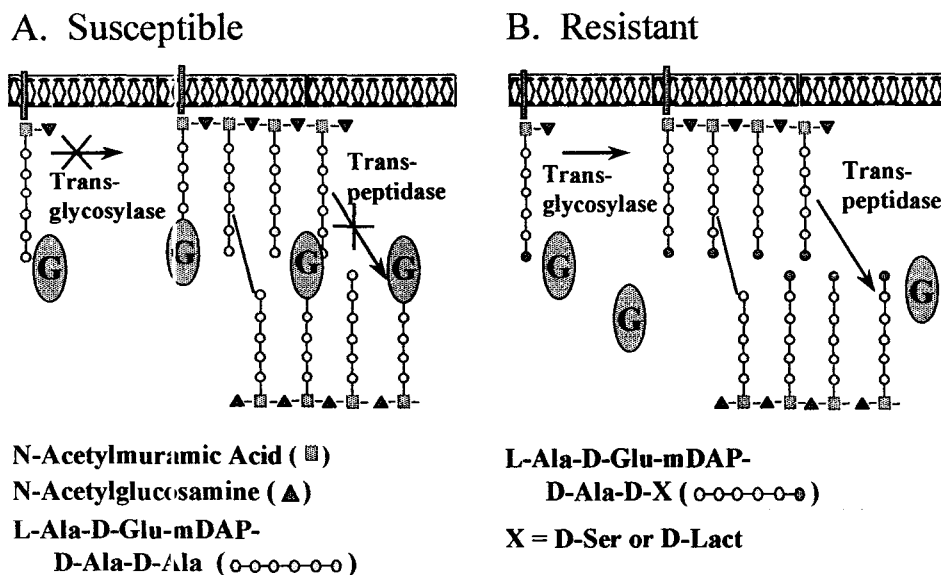
Figure 1.17. Mechanism of Glycopeptide Resistance. Figure designed by Dr. G.D. Wright.

The molecular mechanism for the VanB phenotype is identical, although the genetic elements are distinct (52) (Figure 1.18). These isolates have their own versions of the van gene cluster - *vanRB, vanSB, vanHB, vanB, vanXB* and *vanYB* that function to alter PG. *vanZ* is not present, however, and an additional gene *vanW*, of unknown function, is.

For strains expressing the VanC phenotype, organisms employ a regular ddl as well as one which prefers to make D-alanyl-D-serine (53). PG containing this dipeptide still possess the amide hydrogen of the peptide bond which GPAs use for binding, however the all important carboxyl has been pushed out of the GPA's pocket and no longer interacts favourably. A portion of the gene cluster from *E. gallinarum* BM 4147 has been published (1). Downstream of the *vanC* ligase gene is *vanXY$_c$*, which encodes a

bi-functional VanX/VanY, and also *vanT*, encoding a racemase that synthesizes D-serine.

There has been no report of any VanR or VanS homologues in VanC organisms.
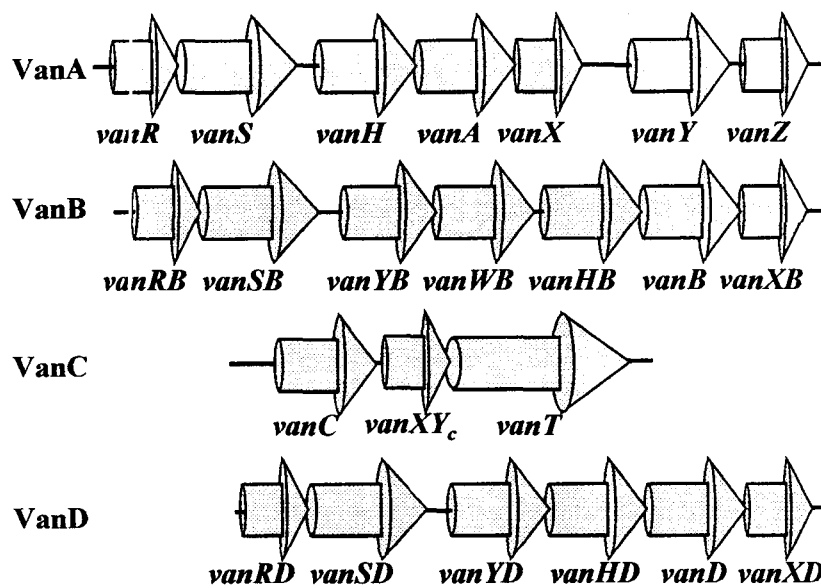
Figure 1.13. Genetic Organisation of the Van Phenotypes.

In the VanD phenotype, strains possess the VanD ddl which has high primary

sequence homology to the VanA and VanB enzymes (50), and as such are presumably

manufacturing depsipeptides. The gene cluster includes a *vanH*, *vanX*, *vanY* as well as a

vanR and *vanS*. It is not known why the VanR and VanS enzymes are not functioning in

their usual manner to confer inducible expression of the gene cluster.

Although not clinically relevant, intrinsic vancomycin resistance has been

observed in some lactic acid bacteria such as the leuconostocs, pediococci and the

lactobacilli (7). These organisms have ddls that constitutively make depsipeptide from

pools of naturally abundant D-lactate. Phylogenetic analysis indicates that these genes

are most likely not the source of clinical resistance genes (Figure 1.19).

DdlSynechocystis   Bacillus
DdlEhirae
Haemophilus
DdlEfaecalis
DdlB
Mycobacterium
Buchnera
DdlA
Aquifex
VanC-1
VanC-2
Helicobacter
VanC-3
Borrelia
VanD
Leuconostoc VanB2 VanA
mesenteroides   VanB
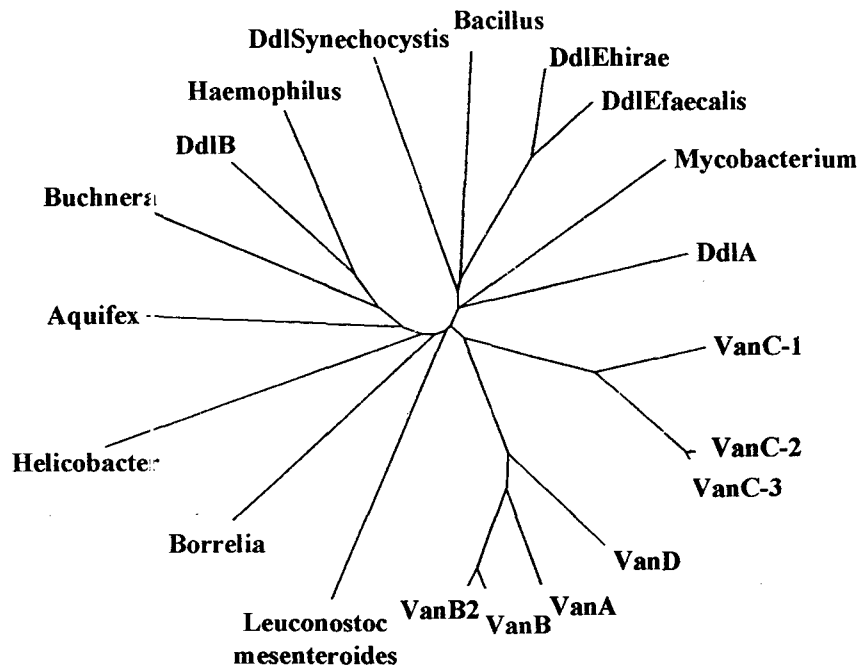
Figure 1.19. Genetic Relationship of D-alanyl-D-alanine Ligases.
Figure produced using Clustal W and TreeDraw.

High-level GPA resistance in laboratory mutants of *S. aureus* has been created by successive passage of susceptible strains in media containing increasing amounts of GPA (58). These vancomycin-resistant *S. aureus* (VRSA) mutants have thickened cell walls with significantly decreased cross-linking in their PG. The mechanism of resistance is not understood, however it appears to be distinct from the VRE mechanism as oligonucleotide probes for *vanA/B* resistance genes do not hybridise to DNA from these organisms. It has been proposed that by binding to terminal D-alanyl-D-alanine in PG that is not actively being synthesised decreases the effective concentration of the GPA (20). Thus cells with thick walls, rich with intact D-ala-D-ala, soak up the bulk of the GPA and actively growing PG is free to polymerize and transpeptidate.

As GPA-producing bacteria are gram-positive and must therefore protect themselves from their own toxic metabolite, it has been suggested that they may be the source of the clinical resistance cluster found in the VanA and VanB phenotypes. Prior to the work contained in this thesis, only a teicoplanin resistance-conferring element has been cloned from its producing strain, and the primary sequence encoded by the Open Reading Frame (ORF) responsible for resistance does not match any of the sequences contained in the protein databank (59).

Clinical vancomycin resistance is a serious threat to health care for a number of reasons: 1) Resistance often occurs in the subset of enterococci that are resistant to β-lactams, resulting in infections that are extremely difficult to treat. 2) Transfer of vancomycin resistance to *S. aureus* or *S. pneumoniae* will result in the creation of truly "killer" microbes. 3) The ubiquitous nature of enterococci allows for multiple reservoirs of resistant strains and makes it extremely difficult to prevent dissemination. 4) The use of GPAs in animal feed, a common practice until very recently, has been correlated with the occurrence of VRE and has resulted in increased prevalence in certain populations. Vancomycin use in the clinic has continued to increase despite the danger of selecting for VRE for the simple reason that there is no alternative currently available.

1.8 Strategies to Combat Glycopeptide Antibiotic Resistance

Given the serious consequences of widespread vancomycin resistance, it is apparent that every available strategy to overcome this problem should be explored. The three logical avenues to pursue are 1) Study the enzymes involved in vancomycin

resistance and develop molecules capable of inhibiting them. 2) Design novel glycopeptide antibiotics with increased potency against resistant organisms. 3) Screen for novel antibiotics which act on a different target than that of the GPAs.

1.8.1 Inhibition of Resistance

Each of the five gene products required for inducible vancomycin resistance are potential targets for inhibitor design. The most accessible is VanS, which possesses an extracellular domain that responds to some aspect of vancomycin presence. Direct binding of GPAs by VanS is unlikely as other inhibitors of cell wall synthesis with varied chemical structures also induce GPA resistance (4), suggesting a response to the inhibition of PG synthesis itself. Only antibiotics that inhibit a specific step of synthesis (transglycosylation) induce GPA resistance, indicating that a specific PG intermediate may be the VanS ligand. An observation that argues against this model is that GPAs with little or no antimicrobial activity can induce the resistance phenotype (18), suggesting that alternative pathways may exist. Once the ligand of VanS is defined, an analogue that saturates the binding site but does not trigger signal transduction could serve as a potent inhibitor.

VanR is a response regulator, of which there are many in a bacterial cell. It binds DNA and is not expressed at high levels until activated. No clinically available therapeutic functions by targeting a bacterial transcriptional activator, and generally there is little precedent for this mode of inhibition. However, signal transduction in prokaryotes is coming under greater scrutiny and is among the favourites for new bacterial targets.

VanH reduces pyruvate, a ubiquitous member of fundamental metabolic pathways. It may not be a good target as inhibitors may be toxic to the host. However, primary sequence alignments indicate that there is sufficient differentiation between bacterial and mammalian dehydrogenases that an inhibitor could be VanH specific.

The most likely target of the pathway is undoubtedly VanA. This enzyme is pivotal to the resistance mechanism and catalyses a very "un-mammalian" reaction. It is the sole source of altered PG termini and must be expressed well or operate with excellent efficiency if the cells are to live. Its substrate D-alanine is small and there is precedent for inhibition of D-alanine binding enzymes (D-alanine racemase by cycloserine, transpeptidases, carboxypeptidases and endopeptidases by β-lactams).

Another good target is VanX. It too plays a key role as knockouts of this gene lose their resistance phenotype. Its substrate is uniquely bacterial and there is good precedent for inhibitor design of peptidases. Work has been done to try and inhibit VanX at Abbott Laboratories, however inhibitor design was prohibited by the extremely small active site evolved by the enzyme (13).

The van enzymes of enterococci have all been cloned and studied to a limited extent, however development of inhibitors with pharmaceutical potential has been problematic. An obstacle has been the difficulty working with these enzymes, whose physical properties limit their study. VanA is poorly soluble and will not form crystals for X-ray analysis, and VanH will only form crystals when fused to thioredoxin (62). The lack of a suitable pool of homologues has prevented the study of alternative systems which could serve as models for the clinical enzymes.

1.8.2 Design of Novel Glycopeptides

At present, only vancomycin and teicoplanin are used clinically despite the fact

that there are over a hundred known glycopeptides. The reason for this is that none of

the other GPAs tested have any significantly improved activity or pharmacokinetics, and

all of them have basically the same mechanism of action (and are thus rendered

ineffective by altered PG). Some promising results have been obtained using chemically

modified GPAs whose added functional groups greatly increase dimerization and

interaction with the cell membrane (Figure 1.20) (23, 47). This added stability is
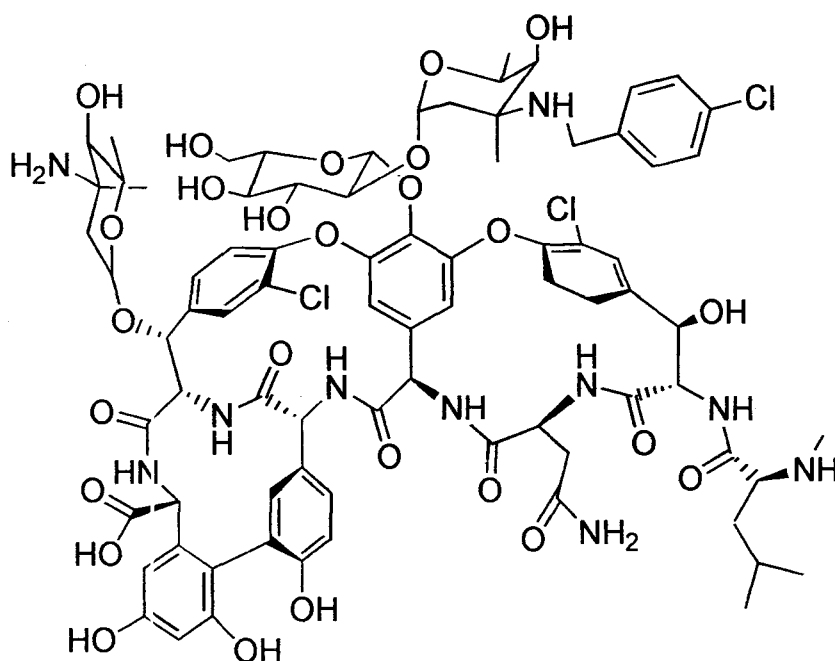
Figure 1.20 The GPA LY191145.

believed to compensate for the loss of the peptide bond hydrogen, allowing sufficient

binding of PG terminating in depsipeptide. These GPA derivatives were discovered by

random chemical modification and high-throughput screening, an efficient and successful

way of developing new antibiotics. This technique is limited, however, in that the core

molecule remains unaltered, and thus the basic mechanism of action remains the same.

Rational modifications of the peptide core have not yet been attempted as virtually

nothing is known about the biosynthesis of glycopeptide antibiotics.

1.8.3 Identification of Antibiotics that Act at Different Targets

Only a few of the processes essential to a bacterium's existence are targeted by

the host of antibiotics available today. Many classes of antibiotics target the same

process, with protein translation, DNA replication and cell wall synthesis among the

most popular pathways to inhibit. Resistance developed to one class of antibiotic by

changing the nature of the target can effect resistance to other classes, and potentially un-

treatable infections. Therefore, there is much potentially gained by increasing the

variability in pathways inhibited by therapeutic agents and this is an area of active

research in many laboratories. Unfortunately, this approach is more labour-intensive and

exploratory as both target and inhibitor are undefined parameters. Given the urgent need

for inhibitors of GPA-resistant organisms, this approach must be used in conjunction with

other methods that develop existing mechanisms of inhibition.

1.9 Project Goals and Strategy

Understanding the mechanism of glycopeptide biosynthesis is an appealing goal

for a variety of reasons. 1) It should lay the foundation for the rational design of novel

GPA antibiotics. 2) GPAs are complex molecules requiring several steps to synthesise.

Determining the order of these steps will provide insights into the way the producing

organism meets the evolutionary demands for co-ordination and efficiency in the completion of a complex task. 3) Several steps predict unusual chemistry. Enzymes with novel mechanisms could be discovered. 4) Should GPAs be made the same way as peptide antibiotics, new modules will be available for study and increase the pool of modules available for combinatorial biosynthesis. This technique involves the random assembly of modules capable of different chemistry, and the subsequent screening of host organisms for novel products with some useful activity. 5) GPA biosynthesis may entail a novel mechanism of peptide assembly. It was therefore the primary goal of my studies to investigate the mechanism of glycopeptide biosynthesis in a glycopeptide-producing organism.

A secondary goal of my studies was to determine the mode of glycopeptide resistance in producing organisms, for the following reasons. 1) The resistance mechanism may provide clues as to the origin of clinical glycopeptide resistance. 2) The resistance enzymes could serve as alternative templates for the design of inhibitors of clinical resistance enzymes. 3) A novel resistance mechanism could be uncovered. 4) Identification of the resistance genes could facilitate discovery of the biosynthesis genes, as these gene clusters are often proximal in the chromosome.

My initial strategy employed what is known as the reverse genetics approach. My plan was to identify an enzyme involved in glycopeptide biosynthesis or resistance in a producing organism and purify it to homogeneity. Proteolysis and peptide sequencing would allow the design of oligonucleotide probes to screen a genomic library made from large tracts of chromosomal DNA. As the genes employed in antibiotic biosynthesis and

resistance are frequently clustered, this should yield a large number of the genes of interest. These would be cloned into protein expression systems and the enzymes obtained in sufficient quantity for detailed study. This technique has been successfully employed in several library-screening experiments for a variety of different gene products.

Several enzyme activities are implicated in the biogenesis of a GPA, however a successful screen of cell-free extract prepared from a GPA-producer requires that the activity be pathway specific. The hydroxylation of tyrosine to the β-hydroxy form is predicted to be a fundamental early step in the synthesis of 4 of the 5 conserved residues in GPA biosynthesis and is not a primary metabolic event. This activity was the primary candidate for my reverse genetic approach.

Although no information was available on the type of enzyme activities employed in mediating resistance in producing organisms, a D-alanyl-D-alanine ligase of altered specificity was almost certainly involved. Several well-developed enzyme assays were available for screening for this enzyme in cell-free extracts. Upon its purification, I could use the reverse genetics approach to identify the corresponding gene and any relevant genes in the flanking regions.

1.10 Streptomyces toyocaensis as a Model System of Study

The enzymes for which I planned to screen are expected to be present in any glycopeptide-producing organism, which includes species from the genera *Streptomyces*, *Actinoplanes*, *Nocardia*, *Amycolatopsis*, *Kibdelosporangia* and *Pseudonocardia*.

Streptomyces toyocaensis NRRL 15009, the producer of the aglycone GPA A47934 was chosen for several reasons: 1) The organism is a strong and reliable producer of the GPA A47934, and its fermentation characteristics are well documented (8). 2) There exists clear biochemical evidence that the organism uses the same pathways used in vancomycin biosynthesis, and therefore the same predicted enzyme activities (74). 3) *Streptomyces* have been well studied and several aspects of growth, genetic manipulation and assay of crude cell extract have been developed and documented (24).

4) A gene cloning system in *S. toyocaensis* NRRL 15009 has been developed by Eli Lilly (37). 5) As an aglycone, A47934 is relatively devoid of functionality and can serve as a scaffold in GPA engineering experiments. 6) A47934 is sufficiently different from vancomycin in its composition that should other groups perform studies on the latter, our studies would still contribute significantly to the understanding of GPA biosynthesis. 7) Finally, and most importantly at the inception of the project, *S. toyocaensis* NRRL 15009 was available for study, whereas *Amycolatopsis orientalis* C329.2, the producer of vancomycin, was not. For these reasons, *S. toyocaensis* NRRL 15009 was selected as the model system for studying GPA biosynthesis and resistance.

1.11 References

1. **Arias, C. A., M. Martin-Martinez, T. L. Blundell, M. Arthur, P. Courvalin, and P. E. Reynolds.** 1999. Characterization and modelling of VanT: a novel, membrane-bound, serine racemase from vancomycin-resistant *Enterococcus gallinarum* BM4174. Mol Microbiol. **31**(6):1653-64.

2. **Arthur, M., F. Depardieu, G. Gerbaud, M. Galimand, R. Leclercq, and P. Courvalin.** 1997. The VanS sensor negatively controls VanR-mediated transcriptional activation of glycopeptide resistance genes of *Tn1546* and related elements in the absence of induction. J Bacteriol. **179**(1):97-106.

3. **Arthur, M., F. Depardieu, C. Molinas, P. Reynolds, and P. Courvalin.** 1995. The vanZ gene of Tn1546 from *Enterococcus faecium* BM4147 confers resistance to teicoplanin. Gene. **154**(1):87-92.

4. **Baptista, M., F. Depardieu, P. Courvalin, and M. Arthur.** 1996. Specificity of induction of glycopeptide resistance genes in *Enterococcus faecalis*. Antimicrob Agents Chemother. **40**(10):2291-5.

5. **Bates, J., J. Z. Jordens, and D. T. Griffiths.** 1994. Farm animals as a putative reservoir for vancomycin-resistant enterococcal infection in man [see comments]. J Antimicrob Chemother. **34**(4):507-14.

6. **Belshaw, P. J., C. T. Walsh, and T. Stachelhaus.** 1999. Aminoacyl-CoAs as probes of condensation domain selectivity in nonribosomal peptide synthesis. Science. **284**(5413):486-9.

7. **Billot-Klein, D., L. Gutmann, S. Sable, E. Guittet, and J. van Heijenoort.** 1994. Modification of peptidoglycan precursors is a common feature of the low-level vancomycin-resistant VANB-type *Enterococcus* D366 and of the naturally glycopeptide-resistant species *Lactobacillus casei, Pediococcus pentosaceus, Leuconostoc mesenteroides*, and *Enterococcus gallinarum*. J Bacteriol. **176**(8):2398-405.

8. **Boeck, L. D., and F. P. Mertz.** 1986. A47934, a novel glycopeptide-aglycone antibiotic produced by a strain of *Streptomyces toyocaensis* taxonomy and fermentation studies. J Antibiot (Tokyo). **39**(11):1533-40.

9. **Brock, T. D., M. T. Madigan, J. M. Martinko, and J. Parker.** 1994. Biology of Microorganisms, p. 517-519. Prentice Hall, Englewood Cliffs, NJ.

10. **Bugg, T. D., S. Dutka-Malen, M. Arthur, P. Courvalin, and C. T. Walsh.** 1991. Identification of vancomycin resistance protein VanA as a D-alanine:D-alanine ligase of altered substrate specificity. Biochemistry. **30**(8):2017-21.

11. **Bugg, T. D., and C. T. Walsh.** 1992. Intracellular steps of bacterial cell wall peptidoglycan biosynthesis: enzymology, antibiotics, and antibiotic resistance. Nat Prod Rep. **9**(3):199-215.

12. **Bugg, T. D., G. D. Wright, S. Dutka-Malen, M. Arthur, P. Courvalin, and C. T. Walsh.** 1991. Molecular basis for vancomycin resistance in *Enterococcus faecium* BM4147: biosynthesis of a depsipeptide peptidoglycan precursor by vancomycin resistance proteins VanH and VanA. Biochemistry. **30**(43):10408-15.

13. **Bussiere, D. E., S. D. Pratt, L. Katz, J. M. Severin, T. Holzman, and C. H. Park.** 1998. The structure of VanX reveals a novel amino-dipeptidase involved in mediating transposon-based vancomycin resistance. Mol Cell. **2**(1):75-84.

14. **Felmingham, D.** 1993. Towards the ideal glycopeptide. J Antimicrob Chemother. **32**(5):663-6.

15. **Garret, L.** 1994. The Coming Plague: Newly Emerging Diseases in a World Out of Balance. Farrar, Straus, and Giroux, New York.

16. **Ge, M., Z. Chen, H. R. Onishi, J. Kohler, L. L. Silver, R. Kerns, S. Fukuzawa, C. Thompson, and D. Kahne.** 1999. Vancomycin Derivatives that Inhibit Peptidoglycan Biosynthesis without Binding D-Ala-D-Ala. Science. **284**:507-511.

17. **Ghosh, S. K., S. Majumder, N. K. Mukhopadhyay, and S. K. Bose.** 1985. Functional characterization of constituent enzyme fractions of mycobacillin synthetase. Biochem J. **230**(3):785-9.

18. **Grissom-Arnold, J., W. E. Alborn, Jr., T. I. Nicas, and S. R. Jaskunas.** 1997. Induction of VanA vancomycin resistance genes in *Enterococcus faecalis*: use of a promoter fusion to evaluate glycopeptide and nonglycopeptide induction signals. Microb Drug Resist. **3**(1):53-64.

19. **Hammond, D. J., M. P. Williamson, D. H. Williams, L. D. Boeck, and G. G. Marconi.** 1982. On the biosynthesis of vancomycin. J Chem Soc (Chem Comm):344-346.

20. **Hanaki, H., H. Labischinski, Y. Inaba, N. Kondo, H. Murakami, and K. Hiramatsu.** 1998. Increase in glutamine-non-amidated muropeptides in the peptidoglycan of vancomycin-resistant *Staphylococcus aureus* strain Mu50. J Antimicrob Chemother. **42**(3):315-20.

21. **Handwerger, S.** 1994. Alterations in peptidoglycan precursors and vancomycin susceptibility in Tn917 insertion mutants of *Enterococcus faecalis* 221. Antimicrob Agents Chemother. **38**(3):473-5.

22. **Handwerger, S., and J. Skoble.** 1995. Identification of chromosomal mobile element conferring high-level vancomycin resistance in *Enterococcus faecium*. Antimicrob Agents Chemother. **39**(11):2446-53.

23. **Hermann, R., F. Ripamonti, G. Romano, E. Restelli, P. Ferrari, B. P. Goldstein, M. Berti, and R. Ciabatti.** 1996. Synthesis and antibacterial activity of derivatives of the glycopeptide antibiotic A-40926 and its aglycone. J Antibiot (Tokyo). **49**(12):1236-48.

24. **Hopwood, D. A., M. J. Bibb, K. F. Chater, T. Keiser, C. J. Bruton, H. M. Keiser, D. J. Lydiate, C. P. Smithe, and J. M. Ward.** 1985. Genetic Manipulations of *Streptomyces*. John Innes Foundation, Norwich.

25. **Howard, M. A., and B. G. Firkin.** 1971. Ristocetin--a new tool in the investigation of platelet aggregation. Thromb Diath Haemorrh. **26**(2):362-9.

26. **Kalman, J. R., and D. H. Williams.** 1980. An NMR Study of the Structure of the Antibiotic Ristocetin A: The Negative Nuclear Overhauser Effect in Structure Elucidation. J Am Chem Soc. **102**:897-.

27. **Keighley, M. R., D. W. Burdon, Y. Arabi, J. A. Williams, H. Thompson, D. Youngs, M. Johnson, S. Bentley, R. H. George, and G. A. Mogg.** 1978. Randomised controlled trial of vancomycin for pseudomembranous colitis and postoperative diarrhoea. Br Med J. **2**(6153):1667-9.

28. **Kirst, H. A., D. G. Thompson, and T. I. Nicas.** 1998. Historical yearly usage of vancomycin [letter]. Antimicrob Agents Chemother. **42**(5):1303-4.

29. **Klare, I., H. Heier, and H. Claus.** 1995. *Enterococcus faecium* strains with *vanA*-mediated high-level glycopeptide resistance isolated from animal foodstuffs and fecal samples of humans in the community. Microbial Drug Resistance. **1**:265-272.

30. **Kleinkauf, H., and H. von Dohren.** 1995. Linking peptide and polyketide biosynthesis. J Antibiot (Tokyo). **48**(7):563-7.

31. **Kleinkauf, H., and H. von Dohren.** 1990. Nonribosomal biosynthesis of peptide antibiotics. Eur J Biochem. **192**(1):1-15.

32. **Leclercq, R., and P. Courvalin.** 1997. Resistance to glycopeptides in *enterococci*. Clin Infect Dis. **24**(4):545-54; quiz 555-6.

33. **Leclercq, R., E. Derlot, J. Duval, and P. Courvalin.** 1988. Plasmid-mediated resistance to vancomycin and teicoplanin in *Enterococcus faecium*. N Engl J Med. **319**(3):157-61.

34. **Levy, S. B.** 1992. The Antibiotic Paradox. Plenum Press, New York and London.

35. **Low, D. E., B. M. Willey, S. Betschel, and B. Kreiswirth.** 1994. *Enterococcis*: pathogens of the 90s. Eur J Surg Suppl. **573**:19-24.

36. **Marahiel, M. A.** 1997. Protein templates for the biosynthesis of peptide antibiotics. Chem Biol. **4**(8):561-7.

37. **Matsushima, P., and R. H. Baltz.** 1996. A gene cloning system for *'Streptomyces toyocaensis'*. Microbiology. **142**(Pt 2):261-7.

38. **McCormick, M. K., W. M. Stark, G. E. Pittenger, R. C. Pittenger, and G. M. McGuire.** 1955. Antibiot. Annu. .

39. **Mckay, J. P., U. Gerhard, D. A. Beauregard, R. A. Maplestone, and D. H. Williams.** 1994. Dissection of the Contributions toward Dimerization of Glycopeptide Antibiotics. J Am Chem Soc. **116**:4573.

40. **Mederski-Samoraj, B. D., and B. E. Murray.** 1983. High-level resistance to gentamicin in clinical isolates of *enterococci*. J Infect Dis. **147**(4):751-7.

41. **Miyashiro, S., and S. Udaka.** 1982. Screening and some properties of new macromolecular peptide antibiotics. J Antibiot (Tokyo). **35**(10):1319-25.

42. **Murray, B. E.** 1997. Vancomycin-resistant *enterococci*. Am J Med. **102**(3):284-93.

43. **Murray, B. E., K. V. Singh, S. M. Markowitz, H. A. Lopardo, J. E. Patterson, M. J. Zervos, E. Rubeglio, G. M. Eliopoulos, L. B. Rice, F. W. Goldstein, and**

et al. 1991. Evidence for clonal spread of a single strain of beta-lactamase-producing *Enterococcus* (*Streptococcus*) *faecalis* to six hospitals in five states. J Infect Dis. 163(4):780-5.

44. **Neu, H. C.** 1992. The crisis in antibiotic resistance [see comments]. Science. 257(5073):1064-73.

45. **Nicas, T.** 1998. Glycopeptide Resistance.

46. **Nicas, T. I., and R. D. G. Cooper.** 1997. Vancomycin and Other Glycopeptides, p. 363-392. *In* W. R. Strohl (ed.), The Biotechnology of Antibiotics. M. Dekker, New York.

47. **Nicas, T. I., D. L. Mullen, J. E. Flokowitsch, D. A. Preston, N. J. Snyder, R. E. Stratford, and R. D. Cooper.** 1995. Activities of the semisynthetic glycopeptide LY191145 against vancomycin-resistant *enterococci* and other gram-positive bacteria [published erratum appears in Antimicrob Agents Chemother 1996 May;40(5):1330]. Antimicrob Agents Chemother. 39(11):2585-7.

48. **Nieto, M., H. R. Perkins, and P. E. Reynolds.** 1972. Reversal by a specific peptide (diacetyl-alpha gamma-L-diaminobutyryl-D- alanyl-D-alanine) of vancomycin inhibition in intact bacteria and cell- free preparations. Biochem J. 126(1):139-49.

49. **Nishio, C., S. Komura, and K. Kurahashi.** 1983. Peptide antibiotic subtilin is synthesized via precursor proteins. Biochem Biophys Res Commun. 116(2):751-8.

50. **Perichon, B., P. Reynolds, and P. Courvalin.** 1997. VanD-type glycopeptide-resistant *Enterococcus faecium* BM4339. Antimicrob Agents Chemother. 41(9):2016-8.

51. **Perkins, H. R., and M. Nieto.** 1970. The preparation of iodinated vancomycin and its distribution in bacteria treated with the antibiotic. Biochem J. 116(1):83-92.

52. **Quintiliani, R., Jr., and P. Courvalin.** 1996. Characterization of Tn1547, a composite transposon flanked by the IS16 and IS256-like elements, that confers vancomycin resistance in *Enterococcus faecalis* BM4281. Gene. 172(1):1-8.

53.   **Reynolds, P. E., H. A. Snaith, A. J. Maguire, S. Dutka-Malen, and P. Courvalin.** 1994. Analysis of peptidoglycan precursors in vancomycin-resistant *Enterococcus gallinarum* BM4174. Biochem J. **301**(Pt 1):5-8.

54.   **Sahm, D. F., L. Free, and S. Handwerger.** 1995. Inducible and constitutive expression of vanC-1-encoded resistance to vancomycin in *Enterococcus gallinarum*. Antimicrob Agents Chemother. **39**(7):1480-4.

55.   **San Millan, J. L., R. Kolter, and F. Moreno.** 1985. Plasmid genes required for microcin B17 production. J Bacteriol. **163**(3):1016-20.

56.   **Sengupta, S., and S. K. Bose.** 1972. Peptides from a mycobacillin-synthesizing cell-free system. Biochem J. **128**(1):47-52.

57.   **Sheldrick, G. M., P. G. Jones, O. Kennard, D. H. Williams, and G. A. Smith.** 1978. Structure of vancomycin and its complex with acetyl-D-alanyl-D-alanine. Nature. **271**(5642):223-5.

58.   **Sieradzki, K., and A. Tomasz.** 1996. A highly vancomycin-resistant laboratory mutant of *Staphylococcus aureus*. FEMS Microbiol Lett. **142**(2-3):161-6.

59.   **Sosio, M., R. Lorenzetti, F. Robbiati, and M. Denaro.** 1991. Nucleotide sequence to a teicoplanin resistance gene from *Actinoplanes teichomyceticus*. Biochim Biophys Acta. **1089**(3):401-3.

60.   **Stachelhaus, T., A. Huser, and M. A. Marahiel.** 1996. Biochemical characterization of peptidyl carrier protein (PCP), the thiolation domain of multifunctional peptide synthetases. Chem Biol. **3**(11):913-21.

61.   **Stachelhaus, T., A. Schneider, and M. A. Marahiel.** 1995. Rational design of peptide antibiotics by targeted replacement of bacterial and fungal domains. Science. **269**(5220):69-72.

62.   **Stoll, V. S., A. V. Manohar, W. Gillon, E. L. MacFarlane, R. C. Hynes, and E. F. Pai.** 1998. A thioredoxin fusion protein of VanH, a D-lactate dehydrogenase from *Enterococcus faecium*: cloning, expression, purification, kinetic analysis, and crystallization. Protein Sci. **7**(5):1147-55.

63.   **Swartz, M. N.** 1994. Hospital-acquired infections: diseases with increasingly limited therapies. Proc Natl Acad Sci U S A. **91**(7):2420-7.

64. **Uttley, A. H., C. H. Collins, J. Naidoo, and R. C. George.** 1988. Vancomycin-resistant *enterococci* [letter]. Lancet. **1**(8575-6):57-8.

65. **Wakamiya, T., Y. Veki, T. Shiba, Y. Kido, and Y. Motoki.** 1985. The structure of ancovenin, a new peptide inhibitor of angiotensin I converting enzyme. Tetrahedron Lett. **26**:665-668.

66. **Williams, D. H.** 1996. The glycopeptide story--how to kill the deadly 'superbugs' Nat Prod Rep. **13**(6):469-77

67 **Williams, D. H., and J. Kalman.** 1977 Structural and mode of action studies on the antibiotic vancomycin. Evidence from 270-MHz proton magnetic resonance. J Am Chem Soc. **99**(8):2768-74.

68. **Williams, D. H., M. P. Williamson, D. W. Butcher, and S. J. Hammond.** 1983. Detailed Binding Sites of the Antibiotics Vancomycin and Ristocetin A. Determination of Intermolecular Distances in Antibiotic/Substrate Complexes by Use of the Time-Dependent NOE. J Am Chem Soc. **105**:1332.

69 **Wright, G. D., T. R. Holman, and C. T. Walsh.** 1993. Purification and characterization of VanR and the cytosolic domain of VanS: a two-component regulatory system required for vancomycin resistance in *Enterococcus faecium* BM4147 Biochemistry **32**(19):5057-63.

70. **Wu, Z., G. D. Wright, and C. T. Walsh.** 1995. Overexpression, purification, and characterization of VanX, a D-, D- dipeptidase which is essential for vancomycin resistance in *Enterococcus faecium* BM4147 Biochemistry **34**(8):2455-63.

71 **Yao, R. C., and L. W. Crandall.** 1994. Glycopeptides: Classification, occurrence, and discovery, p. 1-24. *In* r. Nagarajan (ed.), Glycopeptide Antibiotics. Marcel Dekker, New York.

72. **Zmijewski jr., M. A., and B. Briggs.** 1989. Biosynthesis of vancomycin: Identification of TDP-glucose aglycosyl-vancomycin glycosyltransferase from *Amycolatopsis orientalis*. FEMS Microbiol Lett. **59**:129-133.

73. **Zmijewski jr., M. A., and J. T. Fayerman.** 1994. Glycopeptide Antibiotics, p. 71-83. *In* L. C. Vining and C. Stuttard (ed.), Genetics and Biochemistry of Antibiotic Production. Butterworth-Heineman, Boston.

74. **Zmijewski jr., M. J., B. Briggs, R. Logan, and L. D. Boeck.** 1987 Biosynthetic studies on antibiotic A47934. Antimicrob Agents Chemother. **31**(10):1497-501

Chapter 2

Fermentation of *S. toyocaensis* NRRL 15009:
Development of Conditions Favouring A47934 Production

2.1 Introduction

The genus *Streptomyces* falls under the class of filamentous actinomycetes, a very large grouping of gram-positive bacteria to which an entire volume of *Bergey's Manual* is dedicated (10). Filamentous actinomycetes is divided into eight groups, including *Mycobacteria, Actinoplanes* and *Nocardia* as well as *Streptomyces*. Despite significant morphological differences, they are all closely related genetically and their genetic material is particularly rich in guanosines and cytosines, in the 60s to 70s mole percent. All actinomycetes are generally non-motile and most are spore forming.

Streptomyces is a large genus with more than five hundred species. They are characterised by 1) G+C mole fraction of genetic material between 69 and 73 percent, 2) mycelial filaments are 0.5-1.0 μm in diameter and usually lack cross-walls, 3) A complex life cycle involving production of spores, and 4) A propensity to synthesise antibiotics. Hundreds of different antibiotics, about half of all known microbial antibiotics, are made by *Streptomyces*, by far the most prolific genus in this regard (8). A number of these have proven important clinically, including streptomycin (an aminoglycoside), tetracycline (a polyketide), chloramphenicol, and vancomycin (a glycopeptide).

Very few *Streptomyces* naturally occur in aqueous environments, preferring the solid support provided by a soil environment. They are so abundant in this environment that the odor that most people associate with earth is in fact due to terpenes which they secrete, called geosmins. They prefer an alkaline or neutral medium, and grow optimally

in well-drained areas that provide a semi-dry environment. Not surprising given their

ecology, optimal growth occurs at 25 ^{O}C, and they are capable of surviving on a wide

variety of carbon sources such as sugars, alcohols, organic acids, amino acids, and

aromatic compounds. Extracellular hydrolytic enzymes allow for the metabolism of

polysaccharides (starch, cellulose), proteins, fats, and in some cases hydrocarbons, lignin,

tannin and even rubber (4).

The *Streptomyces* life cycle involves a series of morphological changes beginning

with germination and outgrowth from a free spore (Figure 2.1) (6). Growth occurs at the
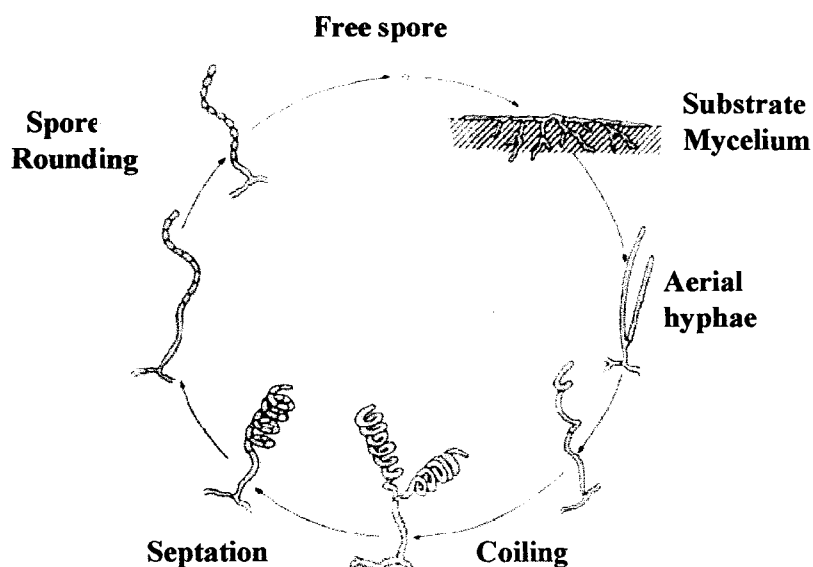
Figure 2.1. *Streptomyces* Life Cycle. Reproduced from Ref. 6 with permission.

tip of the extending filaments, and branching occurs often, producing a tightly woven mat

of cells. The lack of cellular division upon growth results in the presence of several

copies of the chromosome in each filament. The end of the vegetative phase, in which

this matrix of multi-nucleoid mycelia (termed substrate mycelia) develop along the

surface of the growth medium, is marked by the development of aerial hyphae, called sporophores. These grow upward from the colony, cannibalizing the substrate mycelia below and replicating the chromosome for packaging into spores called conidia. The forming of cross-walls, or septation, segregates nucleoids into discreet compartments and is usually accompanied by the coiling of the aerial filaments, producing tight clusters of loosely tethered spores. Some chance mechanical disturbance disrupts and distributes free spores to a distant location where they can germinate and colonise the surrounding area.

The production of secondary metabolites such as pigments, antibiotics and signaling molecules coincides with the development of aerial hyphae and sporulation. Production of these molecules is conditional, however, on the conditions of growth, and can be influenced by temperature, pH, aridity, the composition and concentration of ions, nitrogen sources, and other components of the growth media. The mechanisms that regulate these processes are largely unknown, however in some well-studied systems like *S. coelicolor* a variety of factors have been implicated in controlling gene expression (2). Several distinct pathways appear to be present, triggered by various signals (nutrient depletion, cell density, etc), that result in cascades ultimately affecting both global and specific gene expression. It is not known if these pathways work in concert or have overlapping functions, as little of the details have been elucidated. Most *Streptomyces* fermentations are optimised by trial and error methodologies. Generally, conditions that favour sporulation, such as a more alkaline and dry environment, tend to favour the

production of secondary metabolites, consistent with the observation that these two processes are genetically linked (5).

Streptomyces cultures grown in liquid media will also produce secondary metabolites, in spite of the fact that they do not sporulate under these conditions. Spores are germinated in a vegetative medium and then are transferred to a fermentation medium to promote antibiotic production. Larger quantities of antibiotic can be obtained by growth in liquid media than by growth on agar plates due to the sheer number of mycelia that are generated. Generally, the same conditions that favour growth and drug production on a solid surface apply when fermenting cultures. As *Streptomyces* are aerobic, a high degree of aeration is required for growth and often for drug production (9). The presence of baffles in culture flasks 1) increases the amount of dissolved oxygen in culture and 2) disrupts filamentous growths, increasing the surface area of cells exposed to oxygen.

Fermentation studies on *S. toyocaensis* NRRL 15009 done by The Lilly Research Laboratories have identified suitable conditions for its growth and for the production of the antibiotic A47934 (3). The media was of complex organic composition, including soybean grits and corn steep liquor. Microscopy studies revealed highly filamentous, branched mycelia that formed short, openly spiralled aerial hyphae. Conidia were decorated with thistle-like protrusions giving a spiny fascia to the sporophores. Colonies produced a light olive gray pigment in good abundance.

Growth in liquid culture entered stationary phase after 48 hours after a 1% vol/vol inoculum from saturated culture. A47934, which is secreted from the cell, began to be

produced at around hour 40 and production was linear until hour 120, at which point it rapidly declined. Culture pH was observed to decrease from 7.1 to 6.6 during growth and recover to 7.1 during the course of antibiotic production. Antibiotic yields were approximately 0.8 mg/mL, and were found to be highly associated with the biomass. Glucose, dextrin and corn starch were found to be the best carbon sources for drug production while soybean byproducts, cotton-seed meal or casein hydrolates were the best sources of nitrogen. Tyrosine was found to reduce A47934 yields by almost 25%, while pHPG increased it nearly 50%.

In order to identify activities predicted in A47934 biosynthesis in cell-free extracts of *S. toyocaensis* NRRL 15009, it was necessary to obtain mycelia that are actively synthesising and secreting antibiotic. Therefore the early goals of the project were to 1) develop protocols to successfully grow *S. toyocaensis* NRRL 15009 on solid media as well as in liquid culture. 2) Develop methods to identify pure culture of *S. toyocaensis* NRRL 15009 and recognise contamination. The need for these methods was emphasised by the rich composition of the culture media, the lack of selection in this media and the relatively slow growth rate of the organism. 3) Develop assays for the detection of A47934 in complex mixtures extracted from fermenting culture. 4) Reproduce the fermentation conditions that resulted in robust production of A47934. 5) Create viable culture stocks for storage and propagation. These seemed like relatively straightforward objectives that could be easily met, however they would prove to be more difficult to accomplish than anticipated.

2.2 Materials

Media reagents and ninhydrin were obtained from BDH. Corn steep liquor was obtained from Sigma. Soybean grits (soygrits) was a gift from the Archer Daniels Midland Co.. Potato starch was purchased from a local food supply store. Gram stain reagents were purchased from Beckton Dickinson. 3-(cyclohexylamino)-1-propanesulfonic acid (CAPS) and fluorescamine were purchased from Sigma. Silica Thin-Layer Chromatography Sheets were purchased from Merck. HPLC column was a CSC Spherisorb ODS2. Purified A47934 (100 mg) was a gift from Eli Lilly. Plastic baffles were made in the McMaster Health Science Centre Biomedical workshop. Stainless steel springs used as culture baffles were purchased from Western Spring and Wire. *Streptomyces toyocaensis* NRRL15009 was obtained from the United States Agricultural Research Service Patent Culture Collection.

2.3 Methods

2.3.1 Culture Media

All media were sterilised by autoclaving at 121 ^{O}C, 15 psi for 20 min, unless indicated otherwise. Solid media were formed by the addition of agar to 1.5 percent, unless indicated otherwise, and typically dried for 24 hours at room temperature (RT) before use or storage at 4 ^{O}C.

Bennet Agar

5g Potato Starch
1g Casaminoacids
0.9g Yeast Extract
7.5g Agar
1 mL Czapek mineral mix (500 X)
ddH$_2$O to 500 mL

Soytone Vegetative Medium (SVM)

1.5 g glucose
2.0 g potato starch
1.5 g soytone
1.0 g yeast extract
0.2 g CaCO$_3$
1.0 mL Corn steep liquor
ddH$_2$O to 100 mL
pH to 6.5

Soygrit Vegetative Medium

1.5 g glucose
2.0 g potato starch
1.5 g soygrits
1.0 g yeast extract
0.2 g CaCO$_3$
1.0 mL Corn steep liquor
ddH$_2$O to 100 mL
pH to 6.5

Czapek Mineral Mix (500 X)

10g KCl
10 g MgSO$_4$•7H$_2$O
12g NaNO$_3$
0.4g FeSO$_4$•7H$_2$O
200 μL conc HCl
ddH$_2$O to 100 mL

Fermentation Medium

2.5g glucose
3.0g potato starch
1.5g nitrogen source
0.5g casaminoacids
0.25g CaCO$_3$
0.2 mL Czapek Mineral Mix
ddH$_2$O to 100 mL
pH to 6.8-7.0

Soygrit Fermentation Medium (SFM)

2.5g glucose
3.0g potato starch
1.5g soygrits (ground to a fine powder)
0.5g casaminoacids
0.25g CaCO$_3$
0.2 mL Czapek Mineral Mix
ddH$_2$O to 100 mL
pH to 6.8-7.0

Streptomyces Antibiotic Activity Medium (SAM)

15.0 g d-glucose
15.0 g soytone
5.0 g NaCl
1.0 g yeast extract
1.0 g CaCO$_3$
2.5 mL glycerol

2.3.2 Inoculation

Lyophilised spores were used as the original inoculum and were germinated in Soytone Vegetative Medium. Subsequent inoculations of Vegetative Media were made with 0.5% vol/vol of thawed spore suspensions. Fermentation media were inoculated with 1% vol/vol of saturated Vegetative Medium using a wide-bore pipette tip. The non-homogeneous consistency of cultures grown in Vegetative Media required that the flask be swirled constantly during the drawing of the inoculum.

2.3.3 Growth Conditions

All liquid cultures were grown at 30 $^{\circ}$C, 250 rpm in Erlenmeyer flasks capable of holding five times the volume of the culture being grown. Plastic baffled cultures contained rectangular shaped baffles of width 25 mm, thickness 7 mm and of variable length with holes of diameter 12 mm. Spring baffled cultures contained a stainless steel spring made from 0.038 inch wire formed into coils with a 4 mm repeat distance. These were wrapped around the inside perimeter of the base of the flask. Cultures grown in Vegetative Media were saturated 48 hours after inoculation by spore suspension and subsequently used to inoculate Fermentation Media.

Cultures grown on solid media were streaked or plated on media contained in disposable plastic petri dishes and then incubated 5 to 7 days at 30 $^{\circ}$C. Incubators contained a shallow plate of ddH$_2$O to prevent excessive drying during growth.

2.3.4 Assays for Growth and Purity

Monitoring growth by measuring the optical density of liquid culture at 600 nm was not feasible due to the heterogeneity of culture broths. Heterogeneity was a result of

both the *Streptomyces* mycelium, which grows as large insoluble aggregates, as well as

insoluble components in the media, such as starch and soybean grits.

Two techniques were used to monitor growth of *S. toyocaensis* NRRL 15009 in

liquid media. 1) Samples (1-5 mL) of growing cultures were taken using a wide bore

pipette while swirling the culture flask and centrifuged at 5000 x g for 5-10 min or until

supernatant was cleared. The mass of the pellet was recorded and plotted against the

time the culture was grown. 2) Light microscopy on gram-stained samples of cultures

was used as a qualitative assay for the degree of growth. Gram staining was by the

following procedure:

1. Using a sterile flame loop dab bacterial cells from a liquid culture or colony into a drop of sterile water on a glass slide. Swirl loop to mix and spread cells evenly in a diameter of about 1 cm. Air dry slide (can use a hair dryer)
2. Fix cells to the slide by passing 1-2 times through a flame. Label with marker.
3. Immerse cells in crystal violet solution for 1 min. Wash with a gentle stream of water.
4. Immerse cells in iodine solution for 1 min. Wash as before.
5. Immerse cells in ethanol solution and agitate for 10 seconds. Wash.
6. Immerse cells in saffranin solution for 10 seconds. Wash.
7. Dab dry with a kimwipe. Relabel if necessary. Visualise cells under low magnification with a light microscope and find a patch of suitable density. Increase magnification to appropriate levels.

Culture purity was assayed by light microscopy of gram-stained samples as above

and by streaking out cultures onto solid media and checking colony morphology.

2.3.5   Assays for A47934

Pure A47934 was used to develop screens for fermentation broths which might be

producing the drug. Three were developed - a biological assay (bioassay), thin-layer

chromatography (TLC) and high-pressure liquid chromatography (HPLC).

In the bioassay, A47934 was spotted onto sterile cotton disks placed onto a lawn of *Bacillus subtilis*. The zone of inhibition around the disks after 16 hours of growth at 37 ^{O}C was recorded:

1. Dilute a saturated culture of *B. subtilis* 2-fold with fresh media.
2. Plate out 100 uL on a petri plate of solid media lacking antibiotic.
3. On the back of the plate divide the area up into regions no smaller than 2 cm^2. Label each region with the name of the sample that will be applied.
4. Using ethanol-sterilized tweezers, aseptically place sterile filter disks down on the agar surface in the center of each region.
5. Apply 10 uL of drug-containing sample to each region. Incubate plates face up at 37 ^{O}C overnight. Record diameter of the zone of inhibition around disk.

A47934 applied to silica TLC sheets was eluted with a solvent system of acetonitrile:methanol:water (8:1:1). Plates (10 cm) were run to near completion, dried and A47934 was visualized by UV-fluorescence, ninhydrin or fluorescamine.

A47934 was also resolved by HPLC on a silica-C18 reverse phase column (5 μM, 25 x 0.46cm) using an isocratic elution system of 25% acetonitrile in 0.2% ammonium acetate. Injections (100 μL) were eluted at 0.4 mL/min and eluant was monitored at 254 nm. To generate a standard curve, various concentrations (0.125-0.5 mg/mL) of A47934 were injected in duplicate and peak heights integrated.

2.3.6 *Fermentation of S. toyocaensis NRRL 15009 to Produce A47934*

Spores were germinated in a vegetative medium until they were observed by gram stain to be saturated (usually 48 hours). Fermentation media were inoculated with 1% vol/vol of the same vegetative medium and grown at 30 ^{O}C, 250 rpm for several days.

The fermentations varied in nitrogen content, volume and aeration (presence or absence

of baffles).

In each case, antibiotic had to be extracted from the biomass by buffered alkalisation.

High levels of A47934 secretion results in biomass saturation and considerable A47934

levels in solution, thus to measure total antibiotic both the culture broth and biomass-

extractions were assayed. The extraction protocol was as follows:

1. Pre-weigh a microcentrifuge tube and label along with age of culture.
2. Swirl culture to mix mycelia and remove a 0.5 mL sample. Spin 1 min and transfer
   supernatant to a tube marked S1. Remove all supernatant and mass pellet. Record
   mass and culture age.
3. Add 100 µL 1.0M CAPS pH11 and resuspend by pipetting. Spin 1 min and collect
   supernatant.
4. Neutralize supernatant with 100 µL 1.0M phosphate buffer pH6. Label this S2.
   Assay both S1 and S2 for the presence of antibiotic.

2.3.7 Culture Preservation

Densely sporulating cultures grown on plates of solid media were placed in

plastic bags with their openings well sealed to prevent excessive moisture loss. Plates

were stored at 4 °C for months.

Mycelial stocks were made from liquid cultures grown to mid to late logarithmic

phase. Sterile glycerol was added to 20% final concentration and aliquots were stored at

-70 °C for years. Subsequent inoculation was from frozen scrapings of these stocks.

The most durable form of *Streptomyces* culture stock is frozen spore suspensions.

These can tolerate multiple rounds of freezing and thawing and remain viable for many

years. Due to the tendency of these cultures to become contaminated, it is prudent to

perform the entire procedure in the most sterile environment available, such as a laminar

flow hood. The following was adapted from the *Streptomyces* Laboratory Manual

published by the John Innes Institute (7):

1. Using a sterilized spoonula, gently scrape the surface of an agar plate containing a **densely** sporulated culture. Carefully transfer spores to a Universal bottle containing 9 mL water/plate.
2. Vortex scrapings as vigorously as possible for 1 min, or sonicate for two minutes in a bath sonicator.
3. Transfer to a filter tube (see Figure 2.2), and allow to filter by gravity. Solution should be turbid with spores.
4. Transfer filtrate to a falcon tube and spin @ 3000 rpm for 10 min. Decant supernatant **as soon as the centrifuge stops**. Resuspend spores in the drop remaining by vortexing.
5. Add 1 mL of 20% glycerol / plate scraped. Transfer to labelled cyrovials for storage @ -80 $^{\circ}$C. Add 200 µL sterile water or media to the empty falcon tube and streak out on an appropriate medium to assay for contamination.

Falcon Tube

Gauze

Non-absorbent cotton

Test tube
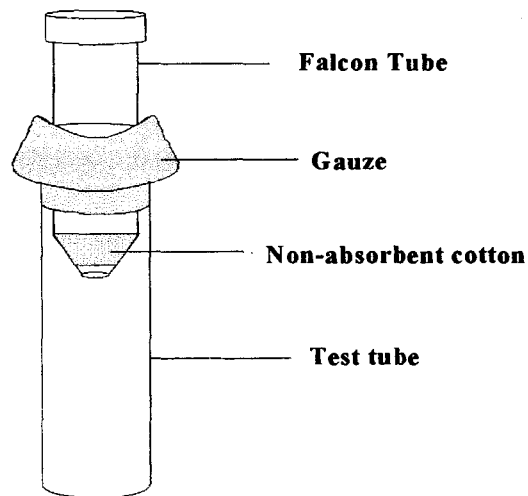
Figure 2.2. Spore Suspension Filter Tube.

2.4 Results and Discussion

2.4.1 Growth and Morphology of S. toyocaensis NRRL 15009

Extensive studies on the media preferences of *S. toyocaensis* NRRL 15009 were not carried out as the overall objective of the study was simply to obtain culture that was producing A47934 in good yield. A logical beginning was to use the same media and culture conditions used by the Lilly Research Laboratories in their fermentation studies. In liquid media, glucose was the carbon source and was easily obtained. The nitrogen source, however, was soybean grits which is not commercially available and furthermore is largely insoluble, complicating mycelial processing after growth. Soytone (papain digested peptone from soymeal) used as a substitute resulted in good spore germination in vegetative media, as determined by light microscopy. Soytone was also used as a substitute in fermentation media, as was sodium nitrate, tryptone, and casaminoacids in separate fermentation experiments. Table 2.1 shows that soytone-containing fermentation broth yielded by far the most mycelia after 96 hours of growth, with 14.7 grams resulting from a 100 mL culture. Tryptone and casaminoacids were similar, at 5.5 and 3.5 g, while sodium nitrate gave the poorest growth at 1.4g. Growth of *S. toyocaensis* NRRL 15009 in liquid media was problematic as the richness of the media and the slow growth rate of the organism resulted in frequent contamination. Pure *S. toyocaensis* NRRL 15009 cultures formed spherical aggregates 2 to 7 mm in diameter that settled to the bottom of the flask without increasing solution turbidity.

The importance of recognising *Streptomyces* morphology was highlighted by unrecognised contamination problems at the outset of the project. Light microscopy of

gram-stains of pure *S. toyocaensis* NRRL 15009 cultures revealed morphology described by the Lilly Research Labs. Mycelia appeared as tangled mats of long filamentous cells that stained dark purple with crystal violet. They were easily distinguishable from the small red rods of *E. coli* or the short, relatively thick purple rods of *Bacillus*. *S. toyocaensis* NRRL 15009 mycelia were best described as long, fine, hair-like filaments that branched and interwove.

Table 2.1. Effect of Nitrogen Source on Growth and A47934 Production

Nitrogen Source	Mycelial Mass (g)	Culture pH	A47934 Produced (mg)
Sodium nitrate	1.4	7.0	No
Casamino Acids	3.5	5.2	No
Tryptone	5.5	5.7	No
Soytone	14.7	6.7	No

On solid media, *S. toyocaensis* NRRL 15009 colonies had a distinct morphology as well. Colonies were perfectly round but had irregular edges and a wrinkled surface that appeared somewhat dry, unlike the glistening colonies of *E. coli*. Colonies also appeared to have depth, and if sporulation occurred, developed a fuzzy texture and a greenish-gray colour.

Scanning electron micrographs of *S. toyocaensis* NRRL 15009 colonies grown on agar provided the most detailed information on mycelial morphology (Figure 2.3). The sample sectioned for the micrograph was in the process of sporulating and the aerial hyphae are clearly coiled and septated. Spiny protrusions can just be made out on their surface. Micrographs of cultures that had not developed aerial hyphae revealed the

smooth, glossy texture of substrate mycelia. Thus, as expected, the images taken match those of The Lilly Research group very closely
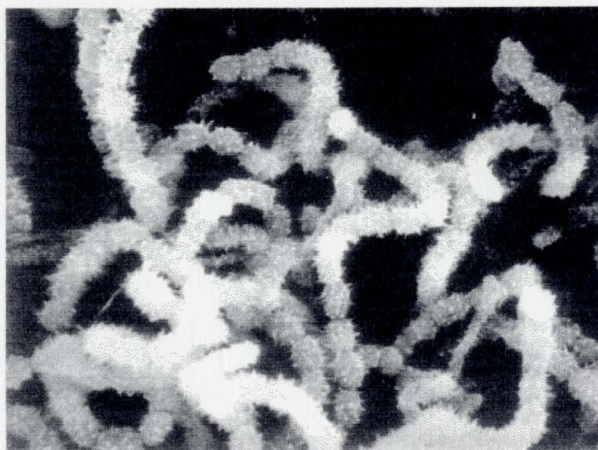
Figure 2.3. Electron micrograph of *S. toyocaensis* NRRL 15009 Aerial Mycelia on Agar.

2.4.2 Assays for A47934

The biological assay was a convenient assay and was the only assay that actually demonstrated antimicrobial activity, but it was a poor quantitative assay Figure 2.4 shows that the radius of the zone of inhibition is only moderately affected by large changes in the amount of antibiotic applied. The major advantages of the bioassay were sensitivity and high throughput capability

In TLC assays, pure A47934 had a Rf value of 0.5 using the solvent system described, varying somewhat from previous reports of 0.7 in this same system. A47934 was visible by UV, but was barely visible by ninhydrin treatment and did not appear with fluorescamine at all. The poor sensitivity of this assay did not make it a good candidate for screening *S. toyocaensis* NRRL 15009 fermentations.
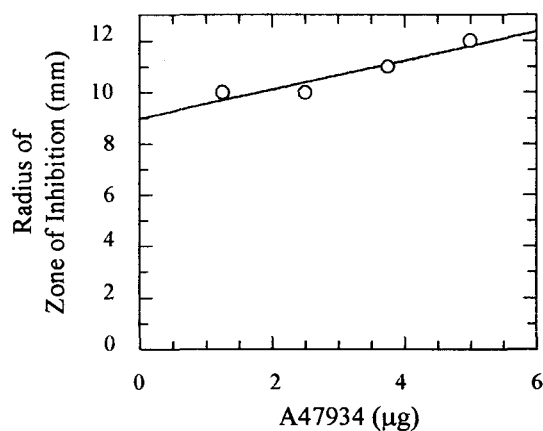
Figure 2.4. Effect of A47934 on Inhibition of _B._
subtilis. Cotton disk diameter was 7 mm.

A47934 eluted from the HPLC C18 column as a sharp peak at 10.5 min under the

conditions used. The peak was fully reproducible and in standard curve experiments the

plot of peak area versus A47934 injected was fit to a linear equation with a correlation

coefficient of 0.99 (Figure 2.5). While the HPLC assay was both sensitive and

quantitative, it was the most laborious.
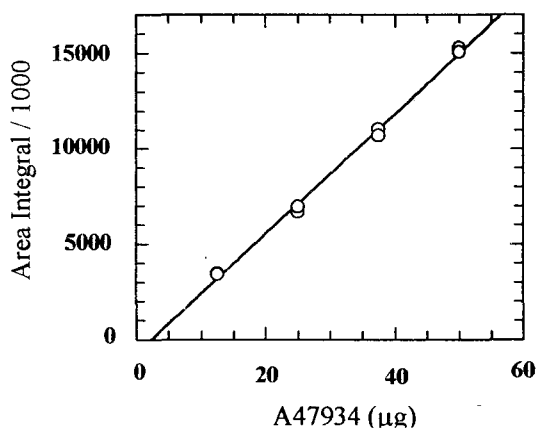
Figure 2.5. HPLC Standard Curve.

2.4.3 A47934 Production by S. toyocaensis NRRL 15009

Fermentation broths containing nitrogen sources alternative to soygrits were

initially assayed for the presence of A47934 using the bioassay against *Bacillus subtilis*.

While reasonable amounts of mycelia were grown, Table 2.1 shows that none of these

fermentations resulted in any production of antibiotic. Soygrits were obtained from

Archer Daniels Midland and used to make Soygrit Vegetative Medium and Soygrit

Fermentation Medium (SFM). *S. toyocaensis* NRRL 15009 grown in this way produced

good quantities of A47934 as determined by bioassay. Preliminary attempts to generate a

time course by removing samples from a single growing culture were unsuccessful for

two reasons. 1) The insolubility of the soygrits and the mycelia themselves made it

impossible to sample representative aliquots of the biomass. 2) Fermentation was

sensitive to changes in culture volume incurred by removing samples. A time course was

therefore generated using several individual 25 mL cultures given the same inoculum and

grown to specific time points. HPLC was used to accurately measure the amount of

A47934 associated with the biomass and released into the fermentation broth (Table 2.2).

The profile generated resembled that of the Lilly Research group (Figure 2.6). Drug

production began after hour 40 and peaked near hour 140, with active drug synthesis

clearly occurring around hour 95. Growth appeared to continue until hour 140,

considerably longer than the Lilly study, however mycelial mass was difficult to measure

due to the presence of insoluble soygrits. The total yield of drug was nearly identical at

0.77 mg/mL.

Table 2.2. Time Course of Growth and A47934 Production in SFM

Time (hours)	Fraction	A47934 present (mg)	Radius of Inhibition(mm)	Total A47934 present (mg)	Mycelial Mass (g)
0	soluble	0	0	0	0
	biomass	0	0		
45	soluble	0	0	0	3.5
	biomass	0	6.0		
95	soluble	2.4	5.0	5.3	3.5
	biomass	2.9	10.5		
135	soluble	12.4	8.0	19.2	5.6
	biomass	6.8	12.0		
184	soluble	7.6	9.5	14.7	4.8
	biomass	7.1	10.5		

A47934 (mg) determined by HPLC assay. Radius of inhibition (mm) determined by bioassay. Mycelial mass reported was from 25 mL cultures grown in SFM (mass of soygrits has been subtracted).
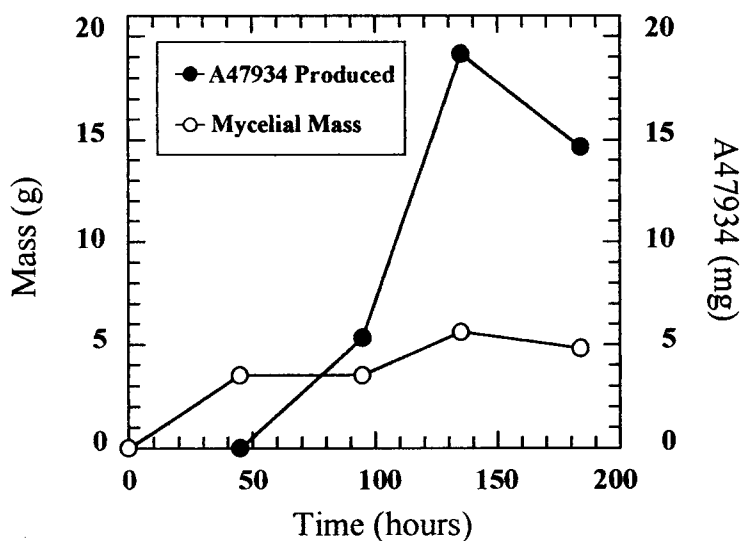
Figure 2.6. A47934 Production by *S. toyocaensis* NRRL 15009 grown in SFM.

Technical difficulties in working with the largely particulate soygrits were somewhat alleviated by grinding to a fine powder before addition to media. A more serious problem was the lack of A47934 production in cultures greater than 50 mL in volume. Proteins involved in secondary metabolite production tend to be poorly

expressed in their natural host and large quantities of cells are required to facilitate their purification – a key component of the reverse genetics approach. This problem was partially solved by growing liquid culture in the presence of plastic baffles, which served to break up the mycelia and allow for cultures up to 100 mL to produce antibiotic in moderate yield (as determined by bioassay). Plastic baffles were later replaced with spring baffles which disrupted the mycelia more thoroughly, although A47934 production was not detectably affected. The best yields of drug production were always obtained from 50 mL cultures grown in Soygrit Fermentation Medium (ground soygrits) in 250 mL baffled Erlenmeyer flasks.

Later in the course of studies, SAM media was discovered in The Handbook of Microbiological Media (1), and *S. toyocaensis* NRRL 15009 was observed to grow in SAM as well as it did in Soygrit Fermentation Medium. A47934 production was nearly equivalent as determined by bioassay. The major advantage of SAM media was the general solubility of its components and therefore the ease of processing harvested mycelia.

Despite the use of soygrit fermentation media and SAM, A47934 production by *S. toyocaensis* NRRL 15009 was inconsistent. The cause of this was unknown, however some evidence indicated that small fluctuations in growth conditions such as temperature, shaking or inoculum size may have been responsible (data not shown). In addition to *S. toyocaensis* NRRL 15009 cultures not producing antibiotic when they were expected to, the opposite also occurred. A47934 production was observed to occur on several occasions in soytone-containing media, despite the fact that repeated experiments

indicated that it would not produce drug in this environment. It was therefore clearly

necessary to 1) maintain absolute consistency in every possible variable when fermenting

S. toyocaensis NRRL 15009, regardless of whether the variable has been established as

an important factor in drug production (eg. light exposure, humidity, autoclave time). 2)

Assay for antibiotic production every time cell-free extract is prepared to screen for

A47934 biosynthetic enzymes.

2.4.4 Stock Preservation and Viability

Densely sporulating plates of *S. toyocaensis* NRRL 15009 stored at 4 $^{\circ}$C maintain

spore viability for several months. Frozen mycelia stocks were viable for years but were

not routinely used for inoculation due to the heterogeneity of the inoculum, and the

difficulty in obtaining a robust inoculum. Spore suspensions made from *S. toyocaensis*

NRRL 15009 serve as an excellent source for inoculation and are easily made as plates of

S. toyocaensis NRRL 15009 sporulate densely and are hardy. These spore suspensions

remained viable for years despite repeated rounds of freezing and thawing.

2.5 Conclusions

S. toyocaensis NRRL 15009 grew in a variety of media, however clearly preferred to

grow in the presence of soy extracts. *S. toyocaensis* NRRL 15009 grown in these media

possessed morphology very similar to that described by the Eli Lilly Group. The

biological assay for A47934 was by far the most convenient, the TLC assay was not very

useful and the HPLC assay was cumbersome but most quantitative. Fermentation

conditions resulting in robust A47934 production required that mycelia be grown in

soygrits, and by grinding up the soygrits and using spring baffles these fermentation

conditions were made suitable for the production of large quantities of mycelia. The

kinetics of drug production were characterised and 96 hours of growth was defined as the

optimal time point to screen for A47934 biosynthetic enzyme activities in cell-free

extracts.

2.6 References

1   **Atlas, R. M.** 1993. Handbook of Microbiological Media. CRC Press Inc, Boca
        Raton.

2.   **Bibb, M.** 1996. 1995 Colworth Prize Lecture. The regulation of antibiotic
        production in *Streptomyces coelicolor* A3(2). Microbiology **142**(Pt 6)**:**1335-44.

3.   **Boeck, L. D., and F. P. Mertz.** 1986. A47934, a novel glycopeptide-aglycone
        antibiotic produced by a strain of *Streptomyces toyocaensis*: taxonomy and
        fermentation studies. J Antibiot (Tokyo). **39**(11)**:**1533-40.

4.   **Brock, T. D., M. T. Madigan, J. M. Martinko, and J. Parker.** 1994. Biology of
        Microorganisms, p. 517-519. Prentice Hall, Englewood Cliffs, NJ.

5.   **Champness, W. C., and K. F. Chater.** 1994. Regulation and integration of
        antibiotic production and morphological differentiation in *Streptomyces* spp. *In* P
        J Piggot, C. P Morgan Jr, and P Youngman (ed.), Regulation of Bacterial
        Differentiation. American Society for Microbiology, Washington D.C.

6.   **Gusek, T. W., and J. E. Kinsella.** 1992. Review of the *Streptomyces
        lividans*/vector pIJ702 system for gene cloning. Crit Rev Microbiol. **18**(4)**:**247-60.

7   **Hopwood, D. A., M. J. Bibb, K. F. Chater, T. Keiser, C. J. Bruton, H. M.
        Keiser, D. J. Lydiate, C. P. Smithe, and J. M. Ward.** 1985. Genetic
        Manipulations of *Streptomyces*. John Innes Foundation, Norwich.

8.   **Miyadoh, S.** 1993. Research on antibiotic screening in Japan over the last decade:
        a producing microorganisms approach. Actinomycetologica. **7:**100-106.

9   **Porter, J. N.** 1975. Cultural conditions for antibiotic-producing microorganisms. Methods Enzymol. **43:**3-23.

10.   **Williams, S. T. (ed.).** 1989. Bergey's Manual. Volume 4, vol. 4. Williams and Wilkins, Baltimore.

Chapter 3

Identification of Activities Predicted in A47934 Biosynthesis in
Cell-free Extracts of *S. toyocaensis* NRRL 15009

3.1 Introduction

3.1.1 Enzyme Activities Associated with A47934 Biosynthesis and Resistance

The GPA A47934 is similar to vancomycin in several respects (Figure 3.1). The sequence of residues in A47934, from its amino-terminus to its terminal carboxylate is

pHPG → *m*-chloro-tyrosine → DHPG → pHPG → *m*-chloro-pHPG → CHT →DHPG.
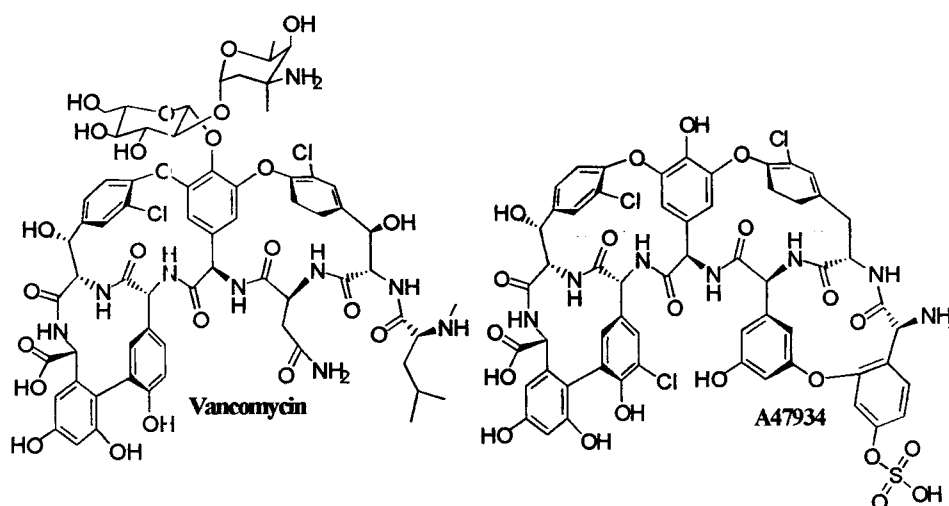
Figure 3.1. Comparison of the GPAs Vancomycin and A47934.

Thus the key residues CHT, pHPG and DHPG are conserved and the pathways predicted for their synthesis through ^{13}C-enrichment experiments in vancomycin-producing *A. orientalis* should also apply in *S. toyocaensis* NRRL 15009. This is supported by studies in which [^{14}C]-labelled precursors were added to fermentations of *S. toyocaensis* NRRL 15009 and the amount of label incorporated into A47934 was measured (23). Addition of [^{14}C]-*p*-HPG and [^{14}C]-tyrosine to cultures resulted in A47934 acquiring 14 and 10 percent of the total radioactivity added, respectively. [^{14}C]-acetate was incorporated at lower levels of 0.5%, however the flux through the acetate pathway is much greater, as

evidenced by the low levels of unincorporated material left in the fermentation broth. It is therefore very likely that the biosynthetic pathways leading to the synthesis of the GPA amino acids in *S. toyocaensis* NRRL 15009 are the same as in *A.orientalis*. As is the case for all GPAs, the manner in which these unique amino acids are assembled into the linear heptapeptide and then cross-linked to give the rigid peptide core is unknown, although it is likely that the former event occurs by the action of a peptide synthetase.

In the previous chapter, conditions that resulted in robust antibiotic production and the window in which A47934 biosynthetic enzymes operate were defined. This chapter describes the search for some of these biosynthetic activities, as well as activities associated with antibiotic resistance, in cell free extracts of *S. toyocaensis* NRRL 15009. Using a reverse genetics approach, the corresponding genes can be identified in the genome with the intention of finding all or many of the genes required for A47934 biosynthesis. While several activities are predicted in drug assembly, those which are critical to the pathway (early steps or repeatedly required steps), those which are specific to the pathway, and those which utilise substrates which are commercially available are ideal candidates for screening cell-free extracts. Also important is the difficulty in establishing the assay itself as well as performing it with acceptable reproducibility and throughput capacity. β- hydroxylation of tyrosine, assembly of acetate/malonate into a tetraketide, and adenylation of amino acid residues for thioesterification to peptide synthetases meet these criteria to varying degrees and are considered in turn. In addition, D-alanyl-D-alanine ligase activity with altered substrate specificity, as the predicted mode of resistance, is also considered.

Three of the hydroxyphenyl rings in A47934 and two of the hydroxyphenyl rings in vancomycin are *meta*-chlorinated. Chloroperoxidation, of free residues or of residues incorporated into heptapeptide, is therefore also predicted to occur in the biosynthesis of GPAs. The screening and detection of chloroperoxidases, however, is not covered in this chapter as it is discussed separately in Chapter 4.

The only reported case of the *in vitro* detection of an enzyme involved in GPA biosynthesis was a report describing the attachment of glucose onto the peptide core of vancomycin (22). TDP-glucose:aglycosyl-vancomycin glycosyltransferase was detected in cell-free extracts of *A. orientalis* C329.2 using [14C]TDP-glucose and vancomycin aglycone as substrates and HPLC/mass spectrometry to analyse reaction products. This activity is not suitable for screening in the *S. toyocaensis* NRRL 15009 system as A47934 is an aglycone GPA.

3.1.2 β-hydroxylation of Tyrosine

The hydroxylation of (D,L)-tyrosine at its β-carbon (Figure 3.2) is predicted to occur in the synthesis of 4 of the 7 residues in A47934, and is not predicted to occur in other pathways in *S. toyocaensis* NRRL 15009. Furthermore, screening is facilitated as the reaction substrate [14C]-tyrosine is readily available and the predicted reaction product, β-hydroxytyrosine (βHT), can be synthesised with available reagents in only a few steps. It was therefore the primary target for identification of an A47934 biosynthesis activity in cell-free extracts. This type of reaction is predicted to be
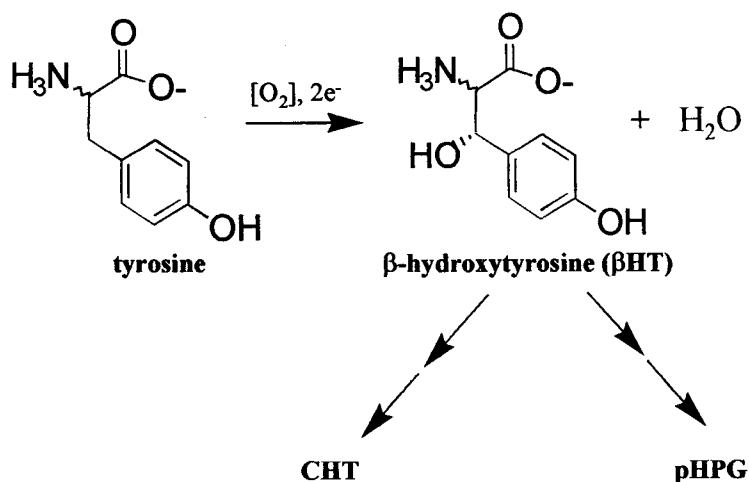
Figure 3.2. β-hydroxylation of Tyrosine.

catalysed by a monooxygenase (also called mixed-function oxygenases or hydroxylases).

The general reaction equation is:

$$AH + BH_2 + O—O \rightarrow A—OH + B + H_2O$$

in which AH is the main substrate, often an alkyl chain or aromatic ring, and BH_2 is the

co-substrate, and by necessity has a high negative reduction potential. Molecular di-

oxygen is reduced by four reducing equivalents to water, at the expense of 2 reducing

equivalents from the co-substrate and two from the main substrate. The energy to initiate

the reduction of oxygen comes from the co-substrate, which is usually a reduced

nicotinamide, but can also be ascorbate or α-ketoglutarate (6, 10). As the direct

interaction of oxygen and carbon in organic compounds is spin-forbidden, all oxygenases

require a cofactor, either a transition metal (iron, copper), or an organic group capable of

functioning as an electron sink (flavin, pterin) (5). Iron is used much more often than any

other transition metal. Flavins are more commonly used in bacteria and eucaryotic

microorganisms, while pterins are found primarily in animal cells (21). Further

classification of monooxygenases is based on the type of main substrate, either aromatic

ring or alkyl chain.

The family of monooxygenases which have been best characterised are the

cytochrome P-450s, which use heme-iron to shuttle electrons from NAD(P)H to di-

oxygen. Bacterial P-450s (bP-450s) are b-type cytochromes, containing protoporphyrin

IX as their heme cofactor. Almost all of them are soluble, and based on sequence

comparisons they can be divided into 2 distinct families (13). Class I bP-450s are similar

to mitochondrial forms of the enzyme, and utilise a 2-component electron transport chain

to obtain their electrons (Figure 3.3). Electrons are abstracted from NAD(P)H by a FAD-

containing reductase (called a P-450 reductase flavoprotein), which then feeds them one

NAD(P)+   **Reduced**   **Oxidized**   **Reduced**   **RH**

                Cytochrome   **Iron-sulfur**   **Cytochrome**   **O₂**
2e⁻ **P-450 reductase** 1e⁻ **ferrodoxin** 1e⁻   **P-450**
                flavoprotein   **H₂O**

                Oxidized   **Reduced**   **Oxidized**   **ROH**
NAD(P)H
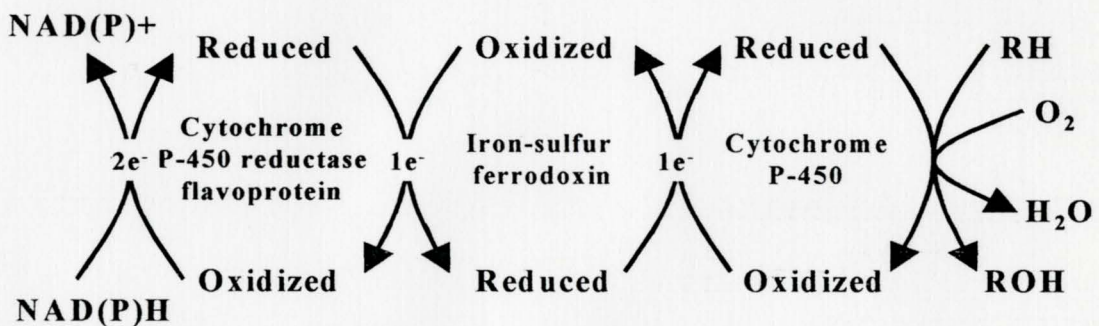
Figure 3.3. Type I Cytochrome P-450 Electron Transport Chain.

at a time to the bP-450 via an iron-sulfur protein (iron-sulfur ferrodoxin). This class

encompasses all but one bacterial enzyme, that from *B. megeterium* BM-3 which mimics

the hepatic-type P-450s (14, 15). These enzymes contain two distinct domains, one that

binds heme and possesses P-450 activity, and another that binds FAD and FMN and

possesses NADPH-dependent reductase ability Thus the BM-3 system is

mechanistically similar to the Class I systems but does not employ an iron-sulfur electron

shuttle. In either case, heme-bound ferric (Fe^{3+}) iron in the cytochrome P-450 receives

electrons one at a time. The catalytic cycle, with all proposed intermediates, is depicted

in Figure 3.4 (13). Spectroscopic studies have been used to characterise reaction

intermediates, however most are difficult to describe in formal redox terms (ie.
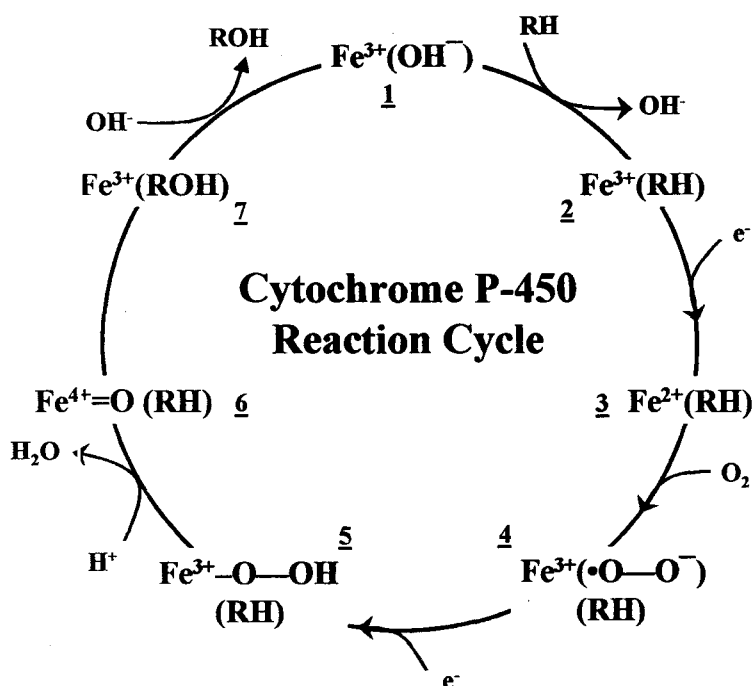
Figure 3.4. Cytochrome P-450 Reaction Cycle. Adapted from Ref.13.

transferred electron density is rarely fully localised to one atom), and some are very

short-lived. Substrate displacement of the hydroxy anion ligand to form **2** changes the

spin state of ferric iron and facilitates 1 electron reduction to generate the ferrous (Fe^{2+})

intermediate **3**. Binding of molecular oxygen results in what is best described as ferric

iron bound to superoxide anion (**4**). One electron reduction of the iron atom allows

further reduction to peroxide to give **5** (this intermediate is also described as ferrous iron

bound to superoxide, and is probably somewhere in between). Acid catalysis facilitates the heterolysis of the remaining dioxygen bond to produce free water and the ferryl iron-oxy intermediate (6). The formal oxidation state of the iron is 5+, however an electron is donated from the porphyrin ring to form a ferryl-porphyrin radical cation. This activated complex serves in substrate hydroxylation to give the hydroxylated product liganded to ferric heme (7), which is displaced by water to restore the resting state of the enzyme (1).

Assays for a P-450 monooxygenase therefore require NAD(P)H and the main substrate. An electron transport system, if necessary, would be present in cell-free extract but would have to be added in exogenously during the course of P-450 purification. Supplementing extracts with ferric iron ensure the maximal activity of any potentially required ferrodoxin.

The best characterised copper-containing monooxygenase is dopamine β-hydroxylase, which converts dopamine to the neurotransmitter norepinephrine in a reaction very similar to that predicted in βHT synthesis (Figure 3.5) (19). This mammalian enzyme has two Cu^{2+} atoms at distinct sites with distinct functions. The copper in the electron transfer site binds ascorbate and extracts from it two electrons to produce dehydroascorbate (Figure 3.6). This step reduces both bound Cu^{2+} to Cu^+, however only one of these copper sites is involved in oxygen activation (18). The reduced copper in the substrate hydroxylation site binds to oxygen and reduces it by two equivalents to the peroxide. Unlike the iron atom in P-450s, the copper atom is not thought to be able to tolerate the level of oxidation incurred upon full reduction of
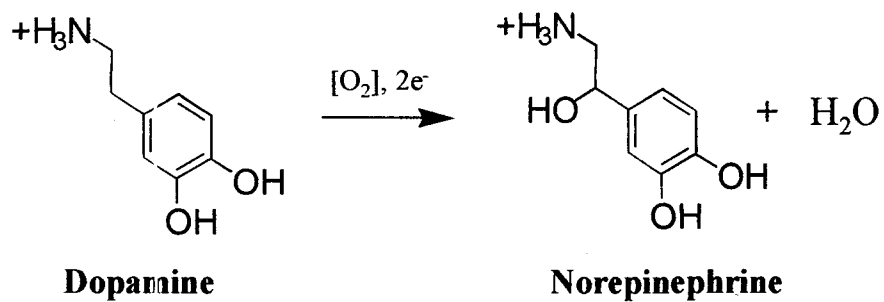
Figure 3.5 Dopamine β-hydroxylase Reaction.
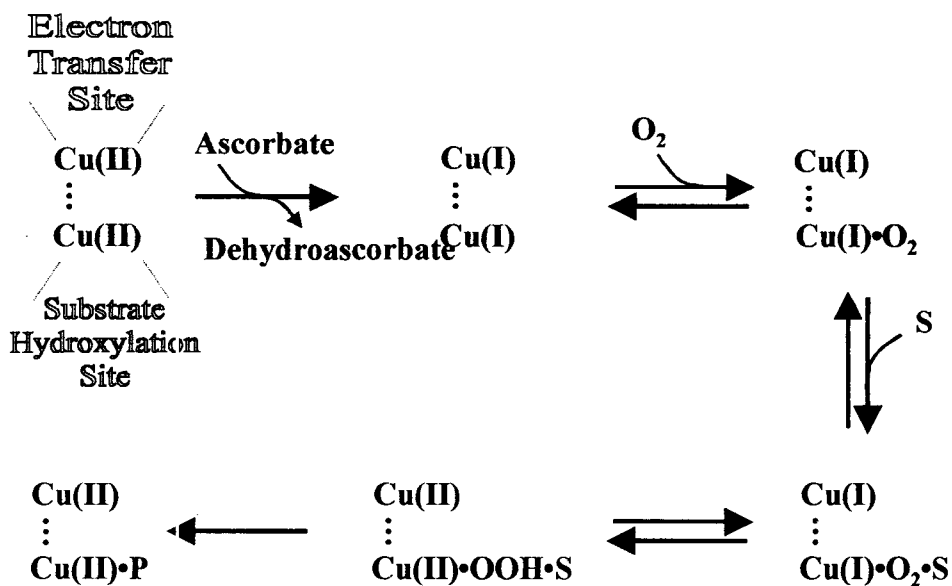
Figure 3.6. Dopamine β-hydroxylase Catalytic Cycle. Adapted from Ref. 18.

oxygen to water. In the currently proposed model, the remaining oxygen-spanning bond

is disrupted by a radical mechanism, in which an active site tyrosine provides a single

electron to allow scission of the peroxide bond and generation a Cu^{2+}-oxy radical (Figure

3.7) (20). The tyrosine radical is transferred to the carbon atom that is to be the site of

hydroxylation in the main substrate, and bond formation occurs to give the hydroxylated

product liganded to copper. Active site water displaces the product and it is released.

Activity screens for copper-containing monooxygenases like dopamine β-hydroxylase

require copper, ascorbate, and the main substrate.
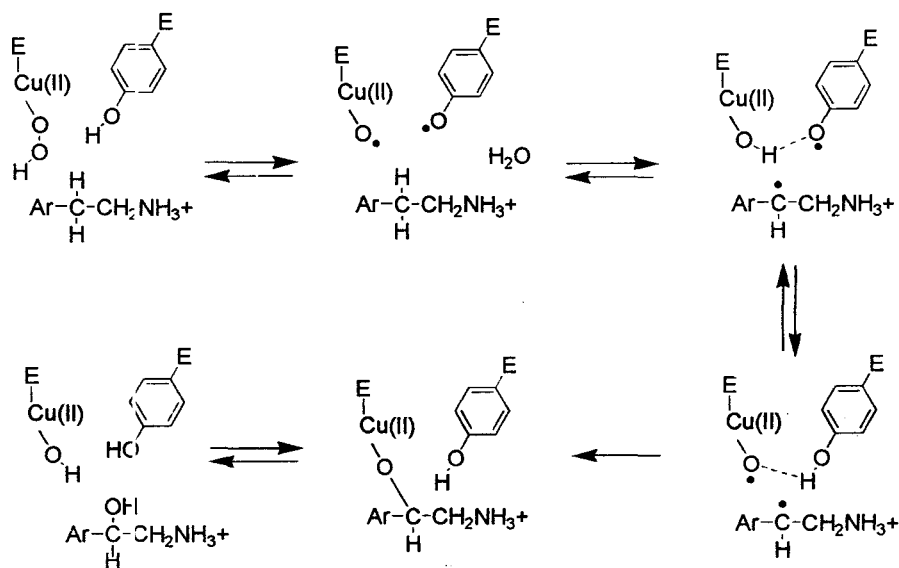
Figure 3.7. Proposed Dopamine β-hydroxylase Hydroxylation Mechanism.
Adapted from Ref. 18.

Flavin-containing monooxygenases (*p*-hydroxybenzoate hydroxylase, salicylate

hydroxylase) and pterin-containing monooxygenases (phenylalanine hydroxylase,

tyrosine hydroxylase, tryptophan hydroxylase) work by similar mechanisms, which is not

surprising given the structural similarity of the bound cofactors (Figure 3.8). Both use

NAD(P)H for reducing equivalents, however flavoproteins are directly reduced while

pterin-containing enzymes require an additional enzyme, dihydropteridine reductase (21).
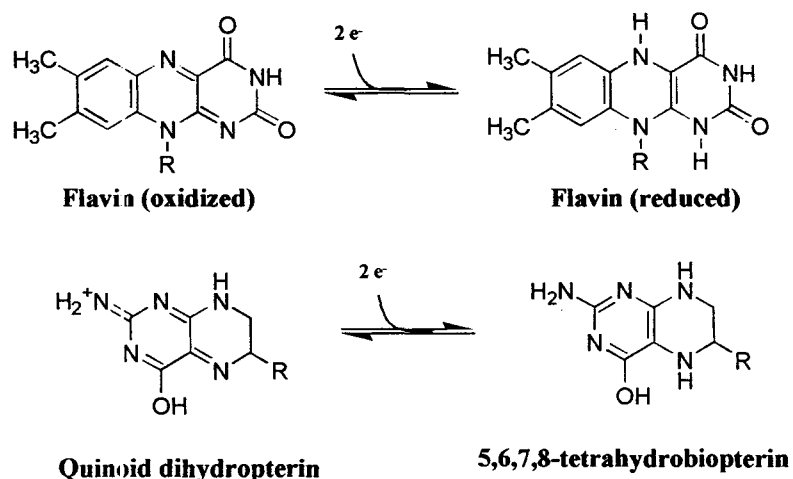
Figure 3.8. Flavin and Pterin Cofactors Used by Monoxygenases.
The reduced cofactors act as electron sinks, and are capable of reducing molecular

dioxygen to a covalently-bound peroxide form. This intermediate hydroxylates the main

substrate to regenerate the oxidised cofactor (5). Importantly, both these classes of

monooxygenase utilise a specific type of main substrate, hydroxylating only aromatic

rings (and usually only activated ones). Given their substrate limitations these types of

hydroxylases are unlikely candidates in βHT synthesis.

As tyrosine β-hydroxylation is very similar to dopamine hydroxylation and since

the reaction is carried out in a bacterial setting, assays were designed that screened for

primarily the copper-containing and the type I cytochrome P-450 type monooxygenases.

A third type of screen was utilised in which flavins were present in assay mixtures to

address the possibility of type II P-450-mediated hydroxylation. Additionally, a fourth

screen included all of the cofactors used in the other three screens.

To recognise formation of the reaction product βHT it is beneficial to chemically

synthesise some for use as a standard in TLC or HPLC separation assays. The synthesis

of hydroxyphenylserines has been described previously (1) and is readily accomplished

by reacting glycine with p-benzyloxybenzaldehyde under sufficiently basic conditions to

deprotonate the glycine α-carbon (Figure 3.9). The resulting β-p-benzyloxyphenylserine
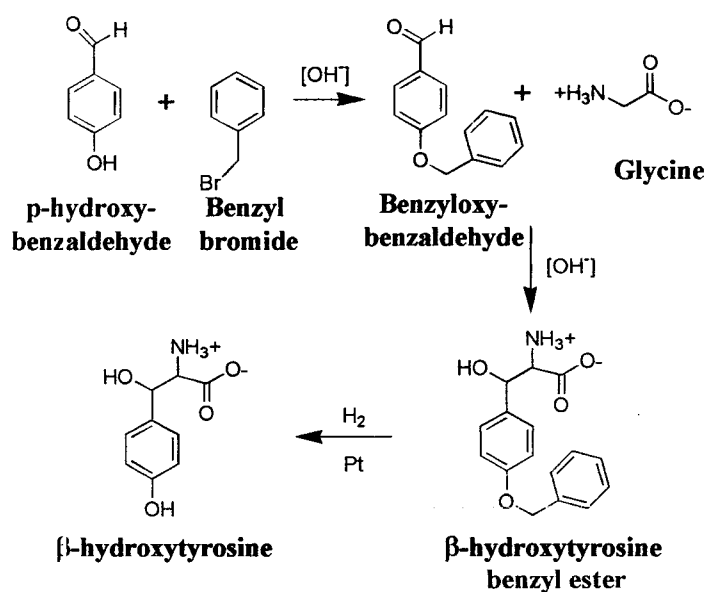
Figure 3.9. β-hydroxytyrosine Synthesis Scheme.

is hydrogenated to give β-p-hydroxyphenylserine, or βHT, in all four possible

diasteromeric combinations. Only the (2S,3R)-βHT is incorporated into A47934,

however both the C2 and C3 stereochemistry is lost in the formation of pHPG and it is

possible that any of the four are made. It was therefore my objective to synthesise βHT

using this procedure and then characterize the properties of the mixture of diastereomers.

This would facilitate the detection of a putative monooxygenase involved in A47934 biosynthesis.

3.1.3 Tetraketide Assembly

There are two DHPG residues in A47934, proposed to originate from the repetitive condensation of malonate units onto an acetate starter unit in a polyketide assembly mechanism (Figure 3.10). Polyketide synthases (PKSs) perform chemistry
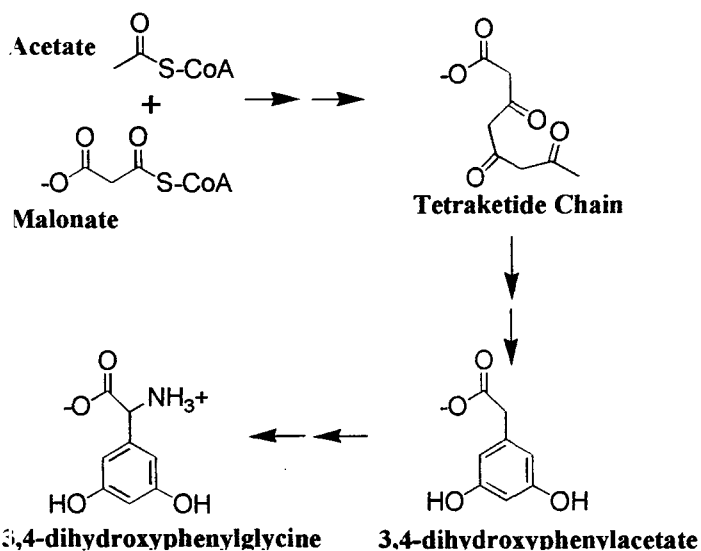
Figure 3.10 Tetraketide Assembly in A47934 Biosynthesis

similar to fatty acyl synthases (FASs), in which a thioesterified acyl chain is grown two carbon units per cycle by repeated rounds of Claisen condensation (Figure 3.11) (10). The extender unit, malonyl-CoA is thioesterified to a 4'-phosphopantetheine group (pPant) on the acyl carrier protein (ACP) of the FAS. The starter unit (or the growing acyl chain, depending on whether the cycle has begun or not), is thioesterified to a cysteine residue of the FAS ketosynthase domain (KS). When the extender unit is

brought in proximity to the starter unit, decarboxylative condensation results in the

extension of the acyl chain by two carbon units and its simultaneous transfer to the ACP.

The keto group of the previous extension reaction is then subject to ketoreduction by a

ketoreductase domain (KR), dehydration by a dehydratase domain (DH), enoyl reduction

by an enoyl reductase domain (ER), and then transfer back to the ketosynthase domain
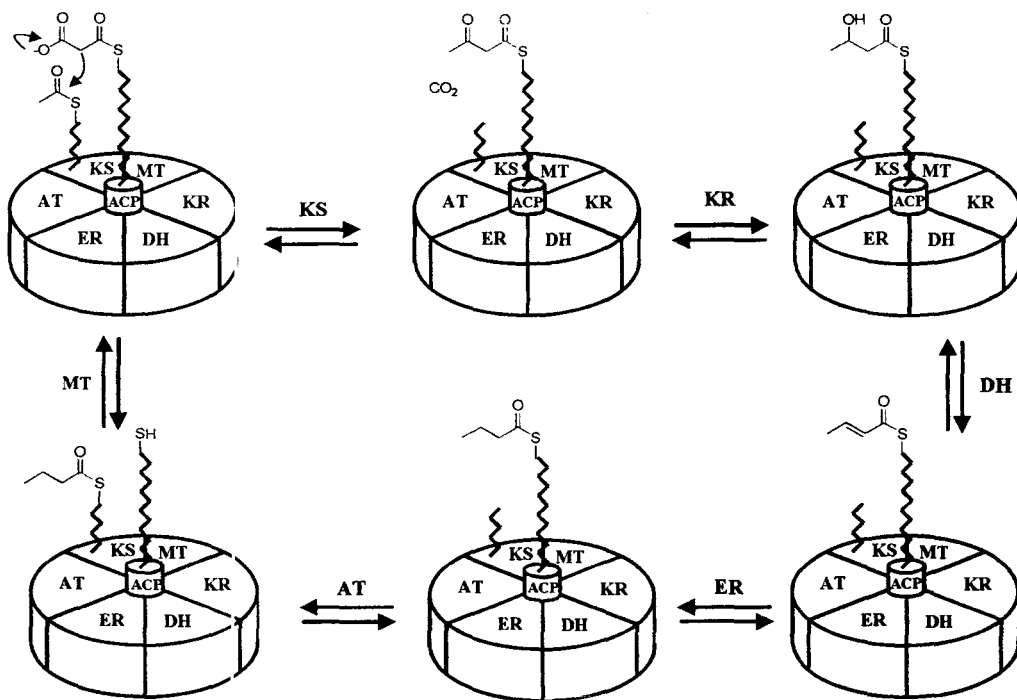
Figure 3.11. Model for the Mechanism of FAS. Adapted from Ref. 10.

catalysed by the acyl-ACP transacetylase domain (AT). The ACP is charged with

another malonyl-CoA by the malonyl-CoA-ACP transferase and the cycle can begin

again. When the chain is fully extended, release is by hydration of the thioester,

catalysed by a thioesterase domain (TE). In PKSs, the events are identical, however

considerable degrees of freedom are added. 1) The starter and extender units can vary in

length and be linear or branched. 2) The extent of processing of the keto group can vary, from fully oxidised to reduced or anywhere in between 3) Product release can occur in several ways resulting in cyclic products including lactones and lactams. 4) The released product is highly functionalised and can undergo additional chemical modification, such as glycosylation, acylation, etc. PKSs are predicted to be structurally similar to FASs as they also possess distinct domains that perform specialised functions. However PKSs do differ from FASs in that they may contain additional domains to help them incorporate the added levels of programming required in making a polyketide. Additionally, some PKSs lack the domains that perform chemistry not required in their polyketide product (Figure 3.12). The amount of variation from FASs depends on the type of PKS.
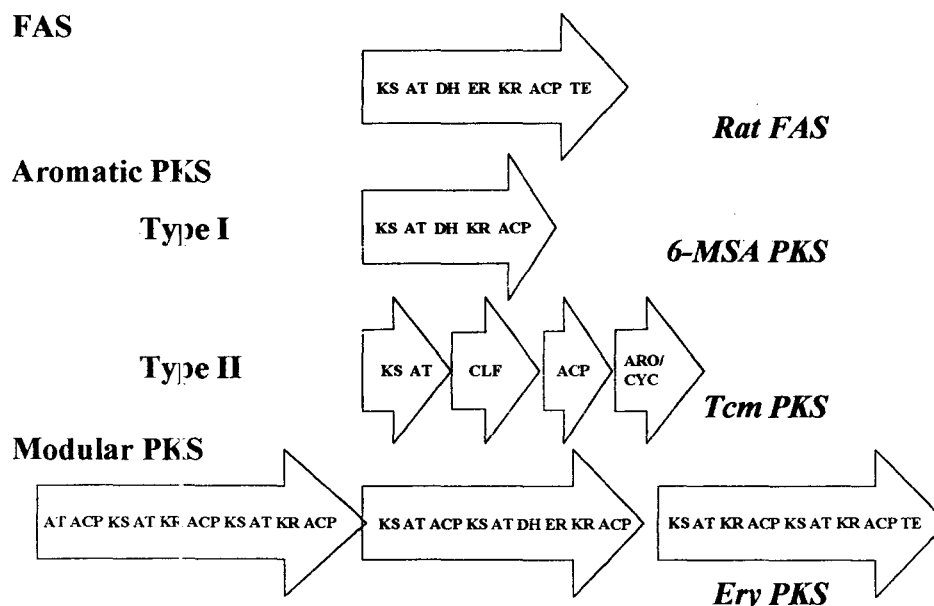
Figure 3.12. Architecture of Aromatic and Modular PKSs. Not drawn to scale.

PKSs are divided into two classes based on the type of chemistry they perform

(7). In polyketide products in which the amount of keto processing is identical or nearly

identical each cycle, the aromatic PKS, like FAS, uses the same active sites for iterative

rounds of condensation and keto processing. Unlike FAS, however, aromatic PKSs

usually keep their keto groups intact, and therefore do not employ KR, DH and ER

activities. Aromatic PKSs therefore require few domains to synthesise their polyketide

product. Aromatic PKSs are further divided into type I, in which the various activities

are contained on a single polypeptide, and type II in which individual proteins are

responsible for each activity. Type II PKSs contain additional activities such as chain

length factor (CLF), cyclase (CYC) and aromatase (ARO) activities (12). The aromatic

polyketide 6-methylsalicylic acid (6-MSA) is elaborated by a type I PKS, while

actinorhodin (Act) and tetracenomycin (Tcm) are manufactured by type II aromatic PKSs

Tetracenomycin C   **6-methylsalicylic acid**

Erythromycin   **Tylosin**
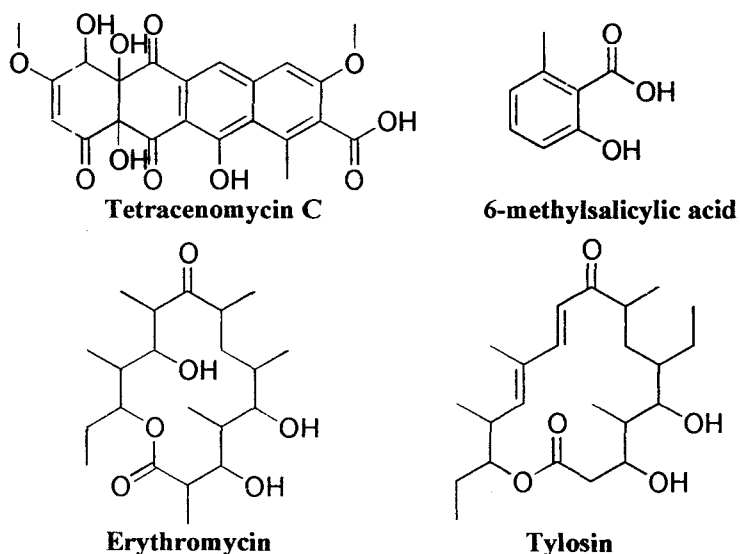
Figure 3.13. Polyketides Elaborated by Aromatic and Modular PKSs.

(Figure 3.13). The other class of PKS, known as modular PKSs, use unique domains for each round of condensation and processing (8). For every extender unit there are distinct modules that possess all of the domains required for its attachment and processing. In this regard, modular PKSs more closely resemble peptide synthetases than they do FASs, growing to massive sizes when the final product contains several extender units. Modular PKSs are more variable in the type of extender units incorporated, using three and even 4 carbon chains, and there can be considerable variation in the degree of keto reduction. Domains not required in processing a given extender unit are not found in that unit's module. The best studied modular PKS product is certainly erythromycin (Ery).

As the tetraketide predicted to form in DHPG biosynthesis is a product of two carbon extender units and the keto groups are all completely unreduced, an aromatic PKS is predicted to perform the assembly. Despite the fact that tetraketide assembly is predicted to be a core process in A47934 biosynthesis and that the substrates for the reaction – acetyl-CoA and malonyl-CoA are readily available in radiolabelled form, a major disadvantage of screening this activity is the lack of specificity of these substrates for this pathway. Several primary metabolic pathways utilise either one of these substrates, and fatty acid synthesis utilises both. However, as peak A47934 production occurs when cells are entering into stationary phase, many of these primary metabolic pathways should be in reduced states of flux, allowing for tetraketide formation to compete for substrates at a reasonable level. The tetraketide is predicted to spontaneously cyclize and aromatize in an aqueous environment, so the expect product from *in vitro* assays will be the dihydroxyphenylacetate (DHPA) intermediate (Figure

3.10). It would be convenient to have some of this product to use as a standard for TLC

and HPLC identification, however none was available. I therefore looked for differences

in acetate-derived product profiles in extracts of *S. toyocaensis* NRRL 15009 obtained

from cultures 1) in growth phase (primary metabolism) and 2) in stationary phase

(secondary metabolism, including A47934 production). If preliminary evidence

indicated novel products were being formed in drug-producing cultures, chemical

synthesis of DHPA would be warranted.

3.1.4   Amino Acid Adenylation

While there is no biochemical evidence to support the action of a peptide

synthetase in A47934 peptide assembly, the precedent in the assembly of peptide

antibiotics and the unusual nature of the amino acids in A47934 strongly suggest a role

for this class of enzyme. As discussed in the Introduction, amino acids are activated by

ATP-dependent adenylation for their thioesterification to a pPant cofactor (Figure 3.14).
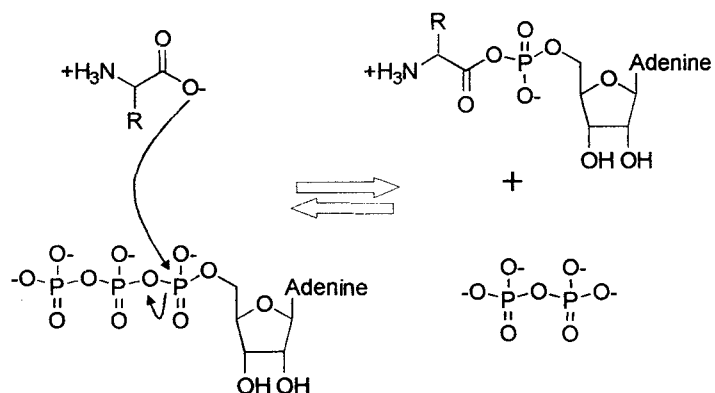
Figure 3.14. Adenylation Reaction of Peptide Synthetases.

This reaction is reminiscent of amino acyl adenylation utilised by amino-acyl-tRNA synthetases to facilitate their attachment to transfer RNA molecules. Fortunately, the latter group of enzymes will not use 2'-deoxyadenosine triphosphate (dATP) (9), nor will many of the other ATP-utilising enzymes of the prokaryotic cell. This allows for a relatively specific assay using the amino acid and dATP as substrate. A common technique for ATP-utilising reactions operating near equilibrium is to measure the rate of microscopic exchange, in which the rate of incorporation of ^{32}P from pyrophosphate to ATP is measured (17). As reaction products develop, the rate of the back-reaction (ie. to form the substrates) increases until equilibrium is met and reaction occurs at an equal rate in both directions. The back reaction is measured because ATP binds to glass filter paper whereas pyrophosphate does not, allowing for thorough separation of reactant from product and detection of even miniscule amounts of labelled ATP. This technique has been successfully used to assay several different peptide synthetases, and provided that the amino acid substrate is readily available, it is an ideal assay as it is both fundamental to and specific for the pathway in question. I therefore planned to assay for peptide synthetase adenylation activity in extracts of *S. toyocaensis* NRRL 15009 using tyrosine, pHPG and βHT (once it is made) as substrates.

It is worth mentioning that limitations associated with screening for either a polyketide synthase or a peptide synthetase lie in downstream events in the reverse genetics approach. For the ultimate goal of designing an oligonucleotide probe useful in screening a genomic library of *S. toyocaensis* NRRL 15009, it is necessary to purify sufficient levels of the biosynthetic enzyme that an amino-terminal sequence can be

determined (by Edman degradation). Very large enzymes, such as PKSs and PSs, are typically expressed at low levels and have poor *in vitro* stability, losing activity during the course of purification. Thus, even though screening for tyrosine β-hydroxylation required the synthesis of a standard for its purification, it remained a better candidate for the reverse genetics approach, as monooxygenases are smaller, hardier proteins.

3.1.5   D-alanyl-D-alanine Ligation

While not a biosynthetic enzyme, D-alanyl-D-alanine ligase (Ddl), which ligates two molecules of D-alanine in an ATP dependent fashion (Figure 3.15), was a good enzyme to screen for in *S. toyocaensis* NRRL 15009 for several reasons. 1) Resistance genes are often clustered with biosynthetic genes in the chromosome (11). 2) At that time, every case of glycopeptide resistance has been due to a Ddl of altered specificity
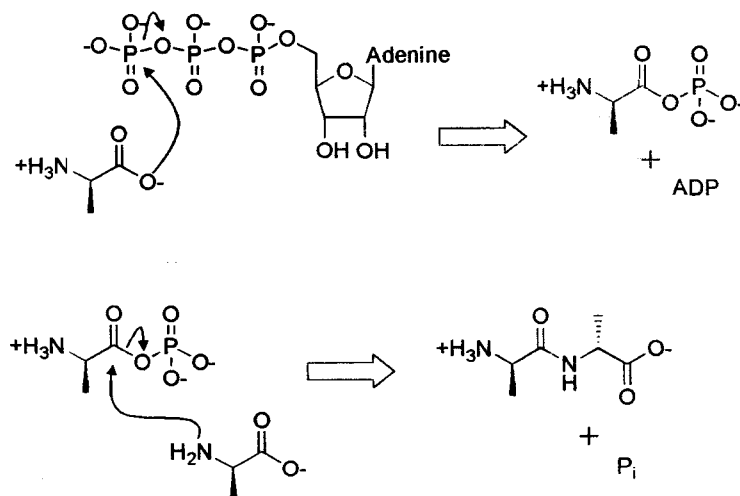
Figure 3.15. **D-Alanyl-D-Alanine Ligase Reaction.**

(16). 3) D-alanine is rarely used for anything other than cell-wall synthesis pathways. 4) D-alanine is readily available in radiolabelled form. 5) D-alanyl-D-alanine is commercially available. 6) Ddl assays are already developed and are easily performed (3).

Assuming the mode of resistance in *S. toyocaensis* NRRL 15009 does employ a Ddl of altered specificity, at least two scenarios can be envisioned. Either the Ddl is employed in all stages of growth in a constitutive manner, or it is induced upon the onset of A47934 production, in which case another Ddl serves the cell during the growth phase. As other bacteria synthesise non-D-alanine terminating PG constitutively with no apparent disadvantage, it seemed that it would make more sense for an GPA producer to do the same. To address either possibility, however, cells should be harvested in late log phase when some growth still occurs but A47934 production has begun.

While the identity of the alternative substrate (should there be one) is unknown, Ddls of altered specificity will make D-alanyl-D-alanine in the presence of excess D-alanine. Thus a Ddl can readily be identified and then subsequently assayed for the preferential usage of an alternative substrate that would constitute resistance to A47934. Amino acids seemed like a good group to test since they are naturally abundant, the chemistry of the reaction is conserved and there is precedent for the use of an amino acid in GPA resistance. I therefore planned to screen *S. toyocaensis* NRRL 15009 for D-alanine-D-alanine formation using [^{14}C]-D-alanine and ATP, and then test a variety of amino acids for preferential incorporation. Reaction products would be analysed by TLC.

This chapter describes the synthesis of the predicted A47934 intermediate βHT, and the screening of cell-free extracts of *S. toyocaensis* NRRL 15009 for activities corresponding to tyrosine-β-hydroxlase, polyketide synthase, peptide synthetase, and D-ala-D-ala ligase.

3.2 Materials

p-hydroxybenzaldehyde and benzyl bromide were purchased from Aldrich. Glycine was obtained from BDH. Silica and Cellulose TLC sheets were made by Merck. UV-Visible spectroscopy was performed on a Varian Cary 3E Spectrophotometer. NMR was done on a 300 MHz Bruker spectrometer. HPLC was done using a CSC Spherisorb ODS2.

N-2-hydroxyethylpiperazine-*N'*-2-ethanesulfonic acid (HEPES) and dithiothreitol (DTT) were obtained from Bioshop. Tris(hydroxymethyl)aminomethane (Tris), phenylmethylsulfonyl fluoride (PMSF), adenosine 5'-triphosphate (ATP), flavin adenine dinucleotide (FAD), flavin mononucleotide (FMN), nicotinamide adenine dinucleotide (NAD), nicotinamide adenine dinucleotide phosphate (NADP) and acetyl coenzyme A (acetyl CoA) were from Boehringer Mannheim. Ascorbate and ethylene-diamine-tetraacetic acid (EDTA) were purchased from BDH. Cupric acetate, ferric sulfate, malonyl coenzyme A (malonyl CoA) and tyrosine were obtained from Sigma. [^{14}C]-malonyl CoA, [^{14}C]-tyrosine, and [^{32}P]-pyrophosphate sodium salt were from Dupont. [^{14}C]-D-alanine was purchased from ICN Biomedicals. Sodium pyrophosphate was

obtained from Aldrich. ATP binding assays were performed with Whatman P-81

phosphocellulose paper and scintillation counting was performed in a Beckman LS 3801.

3.3 Methods

3.3.1 Synthesis and Characterization of βHT

All reaction products in the course of the synthesis were analysed for identity and

purity by both silica TLC (hexane:ethyl acetate, 1:1) and proton NMR. For NMR, sample

(4 mg) was dissolved in 1 mL of a suitable solvent, either deuterated water, DMSO or

deuterated chloroform containing trimethylsilane as a reference compound.

Benzyoxybenzaldehyde (BOB). Potassium hydroxide (1 g) was dissolved into 20 mL

MeOH and used to solublise *p*-hydroxybenzaldehyde (2 g). 1.1 molar equivalent of

benzyl bromide was added dropwise with stirring and the mixture was heated at reflux

gently for 4 hours. A potassium bromide precipitate formed and was removed by

filtration. Silica TLC indicated BOB in the precipitate, which was subsequently

extracted with 5 mL ethyl acetate and filtered. Both filtrates were pooled, incubated at −

20 $^{\circ}$C for 2 hours to precipitate BOB and filtered. Precipitate was dissolved in hot

methanol and left at −20 $^{\circ}$C to recrystallize. Crystals were filtered and washed with cold

MeOH. R_f (*n*-butanol:acetic acid:water 6:3:1) 0.81; ^{1}H NMR (CDCl$_3$) δ 9.9 (s, 1H), 7.83

(d, 2H, J = 9 Hz), 7.41 (m, 5H), 7.08 (d, 2H, J = 9 Hz), 5.15 (s, 2H).

βHT-O-benzyl (synthesized by Gerry Wright). *βHT-O-benzyl* was synthesised as

described previously (1). To a solution of potassium hydroxide (2.8 g, 50 mmol) in

absolute ethanol (37 mL), glycine (1.85 g, 25 mmol) was added and mixed until

dissolved. To this a solution of BOB (10.5 g, 50 mmol) in 12 mL ethanol was added and

warmed with gentle mixing until clear. The solution was allowed to stand at RT

overnight and a brown oil was recovered by decanting. The oil was dissolved in 2N HCl

(50 mL) and extracted twice with ethyl acetate and the aqueous solution dried under

vacuum in the presence of silica. This was washed twice with hexane:ethyl acetate (5:1)

and *βHT-O-benzyl* eluted with methanol. After neutralisation with HCl and an overnight

incubation at -20 $^{\circ}$C, a solid was recovered and recrystallised from methanol. R_f (*n*-

butanol:acetic acid:water 6:3:1) 0.46; ^{1}H NMR (D$_2$O/NaOD) δ 7.06 (d, 2H, J = 8 Hz),

6.34 (m, 5H), 6.02 (d, 2H, J = 8 Hz), 4.54 (d, 1H, J = 4.0), 4.14 (s, 2H), 3.21 (d, 1H, J =

6.0).

βHT. The benzylated hydroxy acid (1.5g) was dissolved in 10 mL of ethanol and

approximately a gram of palladium on charcoal added. The mixture was stirred under

hydrogen gas overnight at atmospheric pressure. The reaction was filtered and

deprotection determined to be nearly 100% complete by silica TLC. βHT was

concentrated by evaporating the solvent, and then recrystallised from methanol in pure

form. R_f (*n*-butanol:acetic acid:water 6:3:1) 0.38; ^{1}H NMR (D$_2$O/NaOD) δ 6.89 (d, 2H, J

= 8.0), 6.39 (d, 2H, J = 8.0), 4.50 (d, 1H, J = 3.8), 3.19 (d, 1H, J = 5.8).

Wavelength scans of βHT and tyrosine were performed on 1 mM of sample in 10

mM Tris-Cl, buffered to either pH 7.5 or pH 10, at a scan rate of 60 nM/min in a Varian

Cary 3 Spectrophotometer. TLC was on Cellulose F using *n*-butanol:acetic acid:water at

either a 6:3:1 or 12:3:5 mixture ratio. Compounds were visualised by illumination under

UV light and treatment with ninhydrin. HPLC was on a silica-C18 reverse phase column

(5 μM, 25 x 0.46cm) using an isocratic elution system of either 10 or 20% acetonitrile in

0.1% trifluoroacetic acid (TFA). Injections (20 μL, 10 μg) were applied at 0.5 mL/min

and elution products monitored at 280 nM.

3.3.2   Growth and Lysis of S. toyocaensis NRRL 15009 Mycelia

S. toyocaensis NRRL 15009 spore suspension (100 μL) was inoculated into SVM

and grown for 48 hours. SFM (50 mL, baffled, ground soygrits) was inoculated with 0.5

mL saturated SVM and grown 96 hours, unless specified otherwise. Culture was always

examined for A47934 production by biological assay vs. B. subtilis prior to use. Mycelia

(typically 5-7 grams) were harvested by centrifugation at 6,000 x g for 20 min at 4 ^{O}C,

washed with 0.85% NaCl and stored at –70 ^{O}C until use. All subsequent steps were

performed at 4 ^{O}C. Thawed mycelia were resuspended in 20 mL homogenization buffer

(50 mM HEPES pH 7.2, 50 mM KCl, 1 mM EDTA, 5% glycerol) and homogenised in a

ground glass homogeniser. The homogenate was centrifuged as before and resuspended

in 10 mL lysis buffer (homogenisation buffer including 1 mM PMSF and 0.1 mM DTT).

Assays for PKS and PS were performed on protein extracts prepared in the presence and

in the absence of both PMSF and DTT, should either of these reagents affect enzyme

activity. Cells were lysed by passage three times through a French Press pressure cell at

20,000 psi, and soluble protein was recovered by centrifugation at 10,000 x g for 15 min.

Extracts were assayed immediately for enzyme activity. Negative controls for enzyme

assays were made up by mixing the same reagents used in real assays with cell-free

extract that had been incubated at 100 $^\circ$C for 10 minutes and spun down to remove

insoluble material. Positive controls were simply pure reaction product (when available)

in reaction buffer. Protein determinations were done using the Bradford Assay (2).

3.3.3 Tyrosine β-hydroxylase Assays

All enzyme assay reactions (100 μL) contained 50 mM HEPES pH 7.2, 40 mM

potassium chloride, 10 mM ATP, 1 mM D,L-tyrosine, and 0.4 μCi [^{14}C]-D,L-tyrosine. In

addition, reactions contained one of the following "Cofactor packets" (CoP).

CoP1 added FAD$^+$ to 0.1 mM, FMN to 0.1 mM, and NADPH to 0.5 mM. CoP2 added

Cu^{2+} to 0.1 mM and ascorbate to 5 mM. CoP3 added Fe^{2+} to 0.1 mM and NADPH to 0.5

mM. CoP4 added FAD$^+$ to 0.1 mM, FMN to 0.1 mM, NADPH to 0.5 mM, Cu^{2+} to 0.1

mM, ascorbate to 5 mM, and Fe^{2+} to 0.1 mM Reactions were initiated by the addition of

20 μL S. toyocaensis NRRL 15009 cell free extract and incubated for either 2 or 16 hours

at room temperature. Samples were centrifuged to pellet sediment and 5 x 2 μL were

spotted onto Cellulose F TLC sheets (20 cm). These were run to within 2 cm from the

top of the TLC sheet in n-butanol:acetic acid:water (6:3:1), dried and exposed to Kodak

XOMAT film for 24 to 96 hours (all film exposures performed at –80 $^\circ$C).

Alkaline hydrolysis of covalently bound intermediates was performed as

described previously (4). Sample (30 μL) was treated with 5 μL 0.6 N potassium

hydroxide (or water in control reactions) for 60 min at room temperature and then

neutralised with 5 μL of 0.6 N hydrochloric acid (or water). Samples were then subject

to TLC as before and analysis by sodium dodecyl sulfate polyacrylamide gel electrophoresis (SDS-PAGE). Autoradiography was for 24 to 96 hours.

3.3.4 Polyketide Synthase Assays

Mycelia used to prepare cell-free extracts were grown for various lengths of time. Reactions (100 µL) contained 50 mM HEPES pH 7.2, 40 mM potassium chloride, 5 mM ammonium chloride, 1 mM NADPH, 0.2 mM acetyl-CoA, 0.2 mM malonyl-CoA, and 0.1 µCi of [^{14}C]-malonyl-CoA. Reactions were initiated by the addition of 20 µL *S. toyocaensis* NRRL 15009 cell free extract and incubated for either 2 or 16 hours at room temperature. Samples were centrifuged to pellet sediment and 5 x 2 µL were spotted onto Cellulose F TLC sheets (20 cm). These were run in *n*-butanol:acetic acid:water (6:3:1), dried and exposed to film for 24 to 96 hours.

3.3.5 Peptide Synthetase Assays

Reactions (100 µL) contained 80 mM Tris-Cl pH 8.0, 4 mM magnesium acetate, 4 mM sodium pyrophosphate, 2 mM amino acid substrate, 1 mM DTT, 1 mM sodium fluoride, 0.2 mM EDTA, 0.1 mM dATP, 0.1 mg/mL bovine serum albumin and 15 µCi of [^{32}P]-sodium pyrophosphate. Reactions were initiated by the addition of 20 µL *S. toyocaensis* NRRL 15009 cell free extract and incubated for 2 hours at room temperature. Reactions were stopped by the addition of 40 µL of cold 0.35 M sodium pyrophosphate, 10.5% perchloric acid and 3% charcoal, the products filtered through phosphocellulose filter paper, washed with 3 x 1 mL of water and dried. Filter paper was added to scintillation vials containing 3 mL scintillation fluid and counted for 3 minutes. To

compensate for the amount of (^{32}P)-dATP formed from other processes in the cell,

reactions were done in the presence and absence of the substrate amino acid, and the

difference was taken as adenylation activity.

3.3.6 D-alanyl-D-alanine Assays

Reactions (25 µL) contained 100 mM Tris-Cl pH 8.6, 20 mM magnesium

chloride, 10 mM potassium chloride, 6 mM ATP, 10 mM D-alanine, and 0.1 µCi of

[^{14}C]-D-alanine. Reactions were initiated by the addition of 5 µL of *S. toyocaensis*

NRRL 15009 cell free extract and incubated overnight at room temperature. Samples

were centrifuged to pellet sediment and 5 x 2 µL were spotted onto Cellulose F TLC

sheets (20 cm). These were run to 90% completion in *n*-butanol:acetic acid:water

(6:3:1), dried and exposed to Kodak film for 24 to 96 hours. Assays for the use of

alternative substrates were as above but included the test substrate(s) at a final

concentration of 10 mM (or solution saturation). Amino acid mixtures were as follows.

MixA contained D-alanine. The remaining mixtures contained mixtures of D and L

enantiomers. MixB contained glutamate and aspartate, MixC contained asparagine,

MixD contained histidine, arginine and lysine, MixE contained tryptophan, tyrosine and

phenylalanine, MixF contained proline, isoleucine, leucine, valine and methionine, and

MixG contained serine, threonine, cysteine and glycine.

3.4 Results and Discussion

3.4.1 Synthesis and Characterisation of βHT

Table 3.1 summarises the synthesis of βHT. BOB was fairly easily formed in good yield, however the critical second step proved exceptionally difficult to perform. Eventually it was accomplished by G.D. Wright to yield the benzyl ester of βHT in sufficient quantity to deprotect and characterise.

Table 3.1. Synthesis of βHT

Compound Made	Amount Made (g)	Yield (%)
Benzyloxybenzaldehyde	10	60
βHT benzyl ester	3.4	34
βHT	3.0	88

Proton NMR of the synthesised compound compared to that of tyrosine (Figure 3.16) confirmed that it was indeed βHT. The α-carbon proton was shifted slightly from 3.2 to 3.25 and was clearly split by a single proton into a doublet, unlike in tyrosine where it is split by both of the β-carbon protons into a triplet. Furthermore, in tyrosine the β-carbon protons are diastereotopic and are split by each other as well as by the adjacent α-carbon proton, giving the doublet of doublets centered around 2.6 ppm. In βHT this feature was replaced by a doublet at 4.5 ppm that represents the single proton at the β-carbon position and its significant deshielding by the hydroxyl group. As expected, the aromatic protons at 6.4 and 6.9 ppm were unaffected.

UV-visible spectral analysis showed it to have similar absorption properties as tyrosine (Figure 3.17). At pH 7.5, both compounds absorbed maximally at 272 nm while
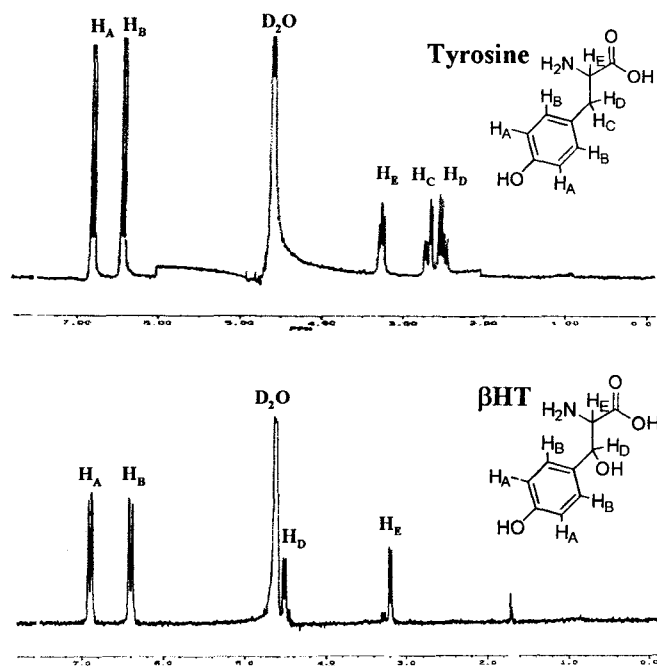
Figure 3.16. NMR Analysis of Tyrosine and βHT.
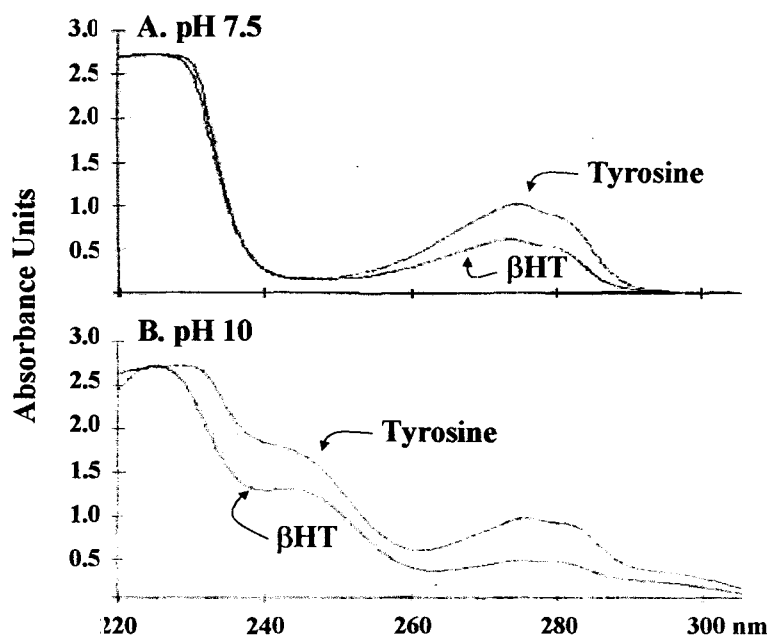
Figure 3.17. UV-Visible Light Absorption Analysis of Tyrosine and βHT. A. pH 7.5 B. pH 10.

at pH 10 maximal absorbance was at 245 nm. βHT had lower molar extinction

coefficients than tyrosine at all wavelengths tested.

Cellulose F TLC of various aromatic compounds in 2 different solvent systems is

summarised in Table 3.2. A single spot was observed in all lanes run with βHT,

indicating that neither of these systems resolved the diastereomers produced in the

synthesis. Better resolution was obtained in *n*-butanol:acetic acid:water (6:3:1) and this

system also ran faster than the 12:3:5 mixture, travelling 16.5 cm compared to 14.3 cm in

10 hours. In this time, tyrosine was separated from βHT by 1.8 cm.

Table 3.2. R_f Values of Various Compounds Analysed by TLC

Compound	Ratio of *n*-butanol:acetic acid:water	
	6:3:1	12:3:5
tyrosine	0.22	0.25
βHT	0.11	0.16
tyrosine, βHT	0.22, 0.11	0.27, 0.16
phenylalanine	0.45	0.50

Separation of βHT and tyrosine was also optimised by HPLC (Table 3.3) using

isocratic solvent systems. βHT eluted as a single peak, again indicating that no

distinction between diastereomers was made. βHT and tyrosine were more resolved

using 10% than 20% acetonitrile, however run time was 5 minutes longer per reaction.

Furthermore, A47934 did not elute in this system. Both systems could find application

depending on the requirements of the assay.

Table 3.3. Retention Times in Minutes of Various Compounds Analysed by HPLC

Compound	Concentration of Acetonitrile in 0.1% TFA	
	10%	20%
tyrosine	13.5	9.0
βHT	7.8	6.6
tyrosine, βHT	13.5, 7.8	9.0, 6.6
A47934	>60	45

Flowrate was 0.5 mL/min using isocratic solvent systems. Void volume was 2.5 mL.

3.4.2 Tyrosine β-hydroxylase Assays

Since the nature of the tyrosine hydroxylase enzyme predicted in A47934

biosynthesis was unknown, a variety of assays were employed that supplemented

different combinations of potentially required cofactors (see methods). None of the

reactions resulted in the production of any βHT as determined by TLC and HPLC

analysis (Figure 3.18). Variations in the length of time mycelia were grown, the method

of harvest and lysis, or the length of time the assays were incubated did not result in any
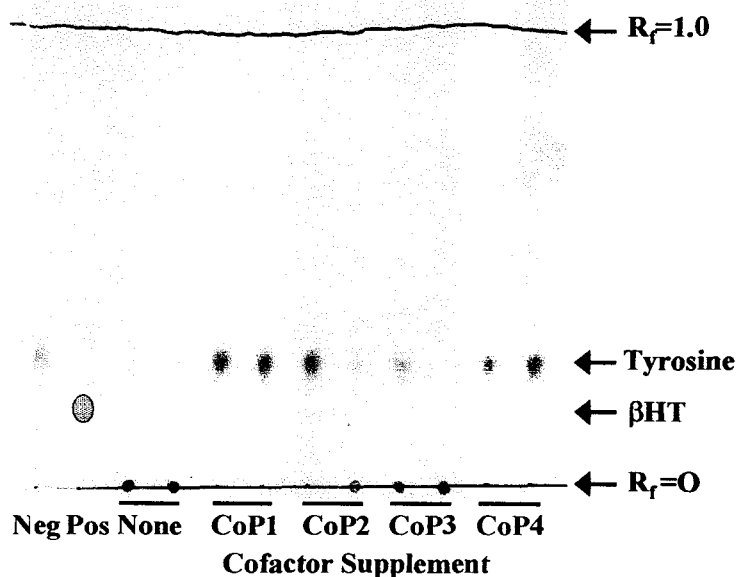
Figure 3.18. TLC Analysis of Tyrosine Monooxygenase Assays. CoP1, flavins and NADPH. CoP2, copper and ascorbate. CoP3, iron and NADPH. CoP4, all of the above.

detectable βHT formation. Insoluble products were consistently detected in reactions

containing no cofactors and the CoP3 mixture (targeted to P-450 hydroxylases) that were

not detected in the other mixtures (occasionally in CoP2 reactions). These products,

which formed dark spots at the origin of the TLC, were investigated as possible

covalently-bound enzyme intermediates which may have formed due to events

downstream of hydroxylation. SDS-PAGE analysis (Figure 3.19) did in fact indicate the

[14]C-labelling of several proteins in reactions with insoluble products, however these

products were poorly released by basic hydrolysis arguing against thioesterification as the

mode of attachment. Furthermore, TLC analysis of base-treated reactions did not reveal

the presence of any βHT released from these proteins (Figure 3.20). Trace amounts of

tyrosine were detected, and confirmed by cutting out the cellulose in the area

corresponding to tyrosine, adding scintillation fluid and counting radioactive decay (data

not shown). It therefore appeared that tyrosine β-hydroxylation, if in fact required in the

synthesis of A47934, was not detectable in cell-free extracts of *S. toyocaensis* NRRL

15009 and therefore not a good candidate for the reverse genetics approach.

3.4.3 Polyketide Synthase Assays

As no standard was available for the predicted reaction product of a PKS involved

in DHPG synthesis, and other pathways using the identical substrates were presumed to

function in normal metabolism, [^{14}C]-malonyl CoA–containing assays were set up using

mycelia grown to different stages of the growth cycle. It was hoped that a difference in

product pattern would be observed in cells making A47934 and thus indicate the activity
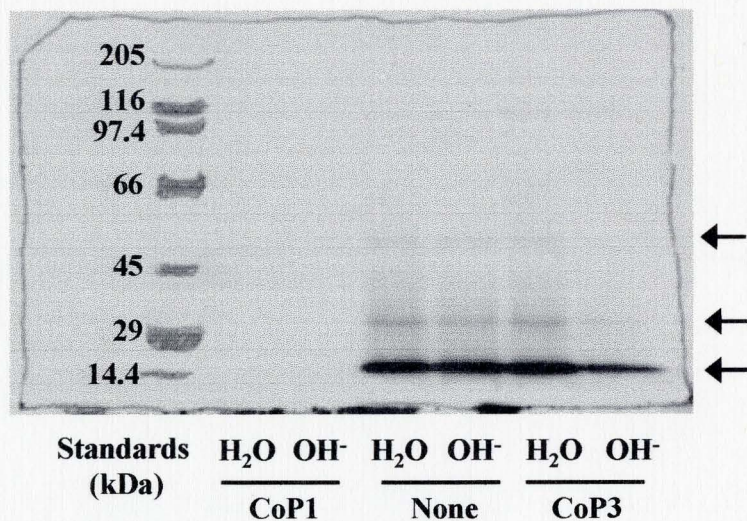
Figure 3.19. SDS-PAGE Analysis of Base-Hydrolysed Intermediates.
OH- refers to base-treated reactions, H2O refers to negative control
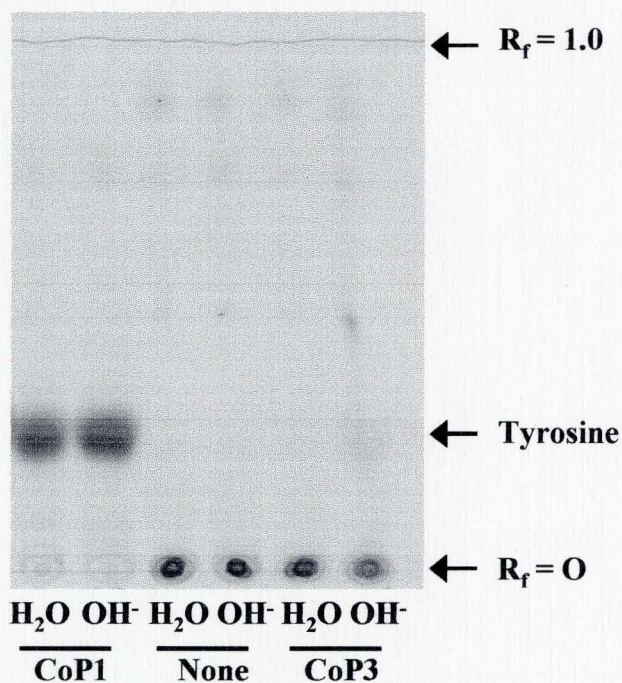
Figure 3.20. TLC Analysis of Base-Hydrolysed Intermediates.
OH- refers to base-treated reactions, H2O refers to negative control

of a pathway specific PKS. While several different products were resolved by the TLC

system employed, there was no difference in the reaction products generated by cell-free

extracts prepared from antibiotic producing mycelia (Figure 3.21). Oddly, all of the

products detected were also present in the negative control (which contains heat-

inactivated cell-extract, see Methods). These products were not detected in lanes

containing assay mixtures lacking any cell extracts. While it was possible that DHPA or

DHPG was being formed but was masked by another product with identical R_f, the

ambiguity of these results and the large time investment required to develop it into a

useful form weighed heavily against its use as a screen for an A47934 biosynthetic

enzyme.
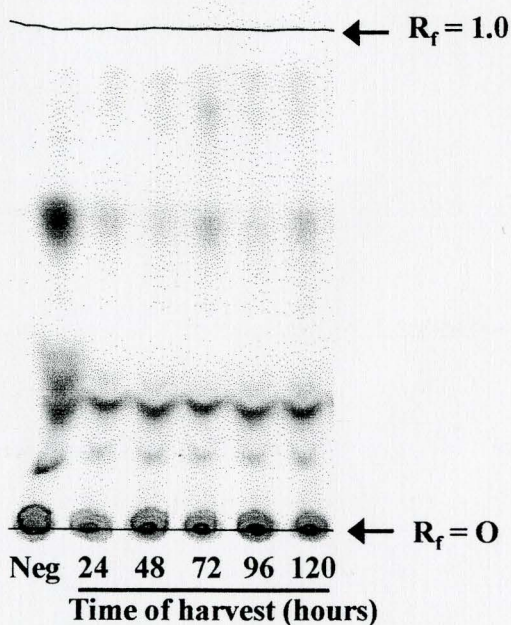
Figure 3.21. TLC Analysis of PKS Assays. Negative control
contains boiled cell extract.

3.4.4 Peptide Synthetase Assays

Phosphocellulose binding of (^{32}P)-dATP formed by microscopic exchange with PPi in an amino-acid dependent fashion was measured in assays using *S. toyocaensis* NRRL 15009 cell-free extracts. Adenylation reactions were performed using tyrosine, βHT and pHPG as amino acid substrates and compared to rates obtained in the absence of substrate (Figure 3.22). Mild activity was detected in reactions containing βHT, however the signal was not much higher than background. At the time this screen was developed, bioassay of the cultures used in this assay (and cultures subsequently prepared) indicated that no A47934 was being secreted in measurable yields. Thus this moderate level of activity may have reflected a downregulated A47934 production system in these cultures. At the time these studies were conducted, other avenues leading to the A47934 biosynthetic cluster that were not dependent on A47934 production in fermentation (see Chapter 5) were available and chosen in favour of this one.
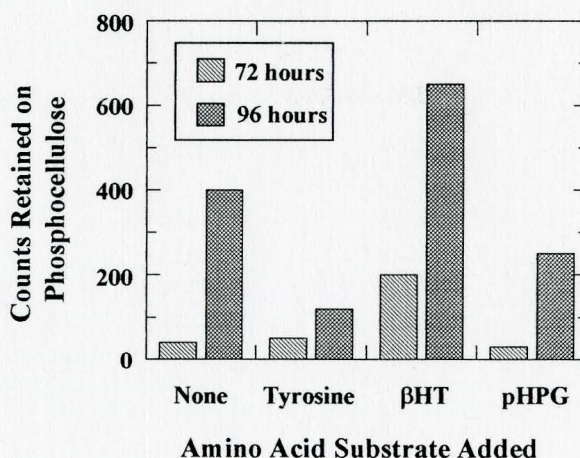
Figure 3.22. Phosphocellulose Binding Assays for Peptide Synthetase Activity. Hours refers to length of time cultures grown.

3.4.5   D-alanyl-D-alanine Assays

D-alanyl-D-alanine ligase activity was readily apparent in cell-free extracts of *S.*

toyocaensis NRRL 15009 (Figure 3.23), which was not unexpected as all gram-positive

organisms require a Ddl of some kind. To determine if this Ddl activity was in fact due

to a Ddl of altered specificity, several amino acids were assayed in specific groupings.

No additional products were observed using these amino acids, leading to four

possibilities. 1) The Ddl activity was due to a D-alanyl-D-alanine only ligase, and a

resistance ligase was not present (ie. a novel mode of resistance was employed. 2) A

resistance ligase was employed, but was present at very low levels as growth in late log
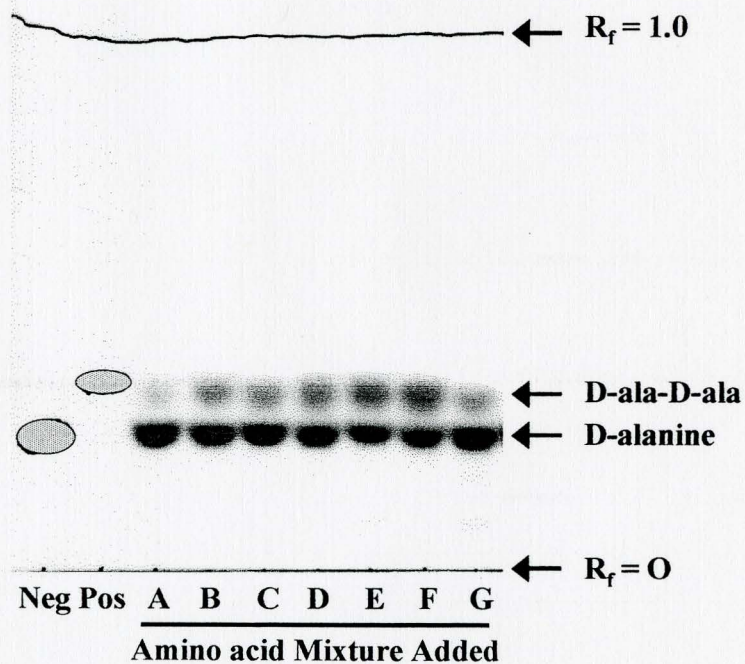
Figure 3.23. TLC Analysis of D-Alanyl-D-Alanine Ligase Assays.
A: A. B: D and E. C: N. D: H, R, and K. E: W,Y,and F. F: P,I,L,V and M.
G: S,T,C, and G.

phase is minimal. 3) A resistance ligase was employed, however it was not supplied with the correct alternative substrate. 4) The correct alternative substrate was supplied, however the product runs with an identical R_f to D-alanyl-D-alanine or D-alanine and was masked. Not knowing the nature of the alternative substrate, this problem was very difficult to troubleshoot and required considerable resources. Again, other avenues were available that appeared more promising, including the purification of chloroperoxidases (Chapter 4) and the identification of A47934 resistance genes using a degenerate PCR approach (Chapter 5).

3.5. Conclusions

Assays to detect three separate enzyme activities predicted to be required for A47934 biosynthesis in *S. toyocaensis* NRRL 15009, and one activity predicted to be required for resistance to A47934, were developed and used to screen cell-free extracts prepared from cells actively producing antibiotic. None of these assays detected any of the predicted activities, precluding them for use in the reverse genetics approach to cloning the A47934 biosynthetic cluster. The inability to detect these activities does not necessarily mean that they were not present, just that they were not apparent under the conditions used. While the assay for tyrosine hydroxylation was relatively thorough, screens for PKS, peptide synthetase and ligase activities could have been more fully developed and re-applied. This strategy was not undertaken for two reasons. 1) Strong chloroperoxidase activity was detected and pursued as described in Chapter 4. 2) Intrinsic difficulties in this approach, most notably inconsistent A47934 production in

109

fermentations, made other methods to identify the biosynthetic gene cluster more

favourable. These methods are fully discussed in Chapter 5.

3.6 References

1. **Bolhofer, W. A.** 1954. The preparation of hydroxyphenylserines from benzyloxybenzaldehydes and glycine. J Am Chem Soc. **76:**1322-1326.

2. **Bradford, M. M.** 1976. A rapid and sensitive method for the quantitation of microgram quantities of protein utilizing the principle of protein-dye binding. Anal Biochem. **72:**248-54.

3. **Bugg, T. D., S. Dutka-Malen, M. Arthur, P. Courvalin, and C. T. Walsh.** 1991. Identification of vancomycin resistance protein VanA as a D-alanine:D-alanine ligase of altered substrate specificity. Biochemistry. **30(8):**2017-21.

4. **Froshov, O., T. L. Zimmer, and S. G. Laland.** 1970. The nature of the enzyme bound intermediates in gramicidin S biosynthesis. FEBS Lett. **7(1):**68-71.

5. **Gunsalus, I. C., T. C. Pederson, and S. G. Sligar.** 1975. Oxygenase-catalyzed biological hydroxylations. Annu Rev Biochem. **44:**377-407.

6. **Harayama, S., M. Kok, and E. L. Neidle.** 1992. Functional and evolutionary relationships among diverse oxygenases. Annu Rev Microbiol. **46:**565-601.

7. **Hopwood, D. A., and D. H. Sherman.** 1990. Molecular genetics of polyketides and its comparison to fatty acid biosynthesis. Annu Rev Genet. **24:**37-66.

8. **Katz, L., and S. Donadio.** 1993. Polyketide synthesis: prospects for hybrid antibiotics. Annu Rev Microbiol. **47:**875-912.

9. **Krause, M., M. A. Marahiel, H. von Dohren, and H. Kleinkauf.** 1985. Molecular cloning of an ornithine-activating fragment of the gramicidin S synthetase 2 gene from *Bacillus brevis* and its expression in *Escherichia coli*. J Bacteriol. **162(3):**1120-5.

10. **Lehninger, A. L., D. L. Nelson, and M. M. Cox.** 1997. Principles of Biochemistry. Worth Publishers, New York.

11. **Martin, M. F., and P. Liras.** 1989. Organization and expression of genes involved in the biosynthesis of antibiotics and other secondary metabolites. Annu Rev Microbiol. **43:**173-206.

12. **McDaniel, R., S. Ebert-Khosla, D. A. Hopwood, and C. Khosla.** 1993. Engineered biosynthesis of novel polyketides: manipulation and analysis of an aromatic polyketide synthase with unproven catalytic specificities. J Am Chem Soc. **115:**11671-11675.

13. **Munro, A. W., and J. G. Lindsay.** 1996. Bacterial cytochromes P-450. Mol Microbiol. **20(6):**1115-25.

14. **Narhi, L. O., and A. J. Fulco.** 1986. Characterization of a catalytically self-sufficient 119,000-dalton cytochrome P-450 monooxygenase induced by barbiturates in *Bacillus megaterium.* J Biol Chem. **261(16):**7160-9.

15. **Narhi, L. O., and A. J. Fulco.** 1987. Identification and characterization of two functional domains in cytochrome P-450BM-3, a catalytically self-sufficient monooxygenase induced by barbiturates in *Bacillus megaterium.* J Biol Chem. **262(14):**6683-90.

16. **Nicas, T. I., and R. D. G. Cooper.** 1997. Vancomycin and Other Glycopeptides, p. 363-392. *In* W. R. Strohl (ed.), The Biotechnology of Antibiotics. M. Dekker, New York.

17. **Pavela-Vrancic, M., E. Pfeifer, H. van Liempt, H. J. Schafer, H. von Dohren, and H. Kleinkauf.** 1994. ATP binding in peptide synthetases: determination of contact sites of the adenine moiety by photoaffinity labeling of tyrocidine synthetase 1 with 2-azidoadenosine triphosphate. Biochemistry. **33(20):**6276-83.

18. **Stewart, L. C., and J. P. Klinman.** 1991. Cooperativity in the dopamine beta-monooxygenase reaction. Evidence for ascorbate regulation of enzyme activity. J Biol Chem. **266(18):**11537-43.

19. **Stewart, L. C., and J. P. Klinman.** 1988. Dopamine beta-hydroxylase of adrenal chromaffin granules: structure and function. Annu Rev Biochem. **57:**551-92.

20. **Tian, G., J. A. Berry, and J. P. Klinman.** 1994. Oxygen-18 kinetic isotope effects in the dopamine beta-monooxygenase reaction: evidence for a new chemical mechanism in non-heme metallomonooxygenases [published erratum appears in Biochemistry 1994 Dec 6;33(48):14650]. Biochemistry. **33(1):**226-34.

21. **Walsh, C. T.** 1977. Enzymatic Reaction Mechanisms. W.H. Freeman and Company, New York.

22. **Zmijewski jr., M. A., and B. Briggs.** 1989. Biosynthesis of vancomycin: Identification of TDP-glucose aglycosyl-vancomycin glycosyltransferase from *Amycolatopsis orientalis*. FEMS Microbiol Lett. **59:**129-133.

23. **Zmijewski jr., M. J., B. Briggs, R. Logan, and L. D. Boeck.** 1987. Biosynthetic studies on antibiotic A47934. Antimicrob Agents Chemother. **31**(10)**:**1497-501.

Chapter 4

Identification and Purification of
Two Haloperoxidases from *S. toyocaensis* NRRL 15009

Adapted from

4.1 Introduction

4.1.1 Biohalogenation

Three of the hydroxyphenyl rings in A47934 and two of the hydroxyphenyl rings in vancomycin are *meta*-chlorinated (Figure 4.1). Biological halogenation of organic substrates was once considered to be a rare occurrence, however it is now known to be very common in many different classes of organisms and there are thousands of halogenated metabolites known (11). Bromination is the most prevalent and is particularly abundant in marine organisms, while chlorination is the second most common and primarily found in terrestrial-derived metabolites (20). Iodination occurs less frequently and fluorination is very rare. Halogenation has been observed in many different classes of higher plants (6), algae (20), fungi (21), and bacteria (23), and is often associated with secondary metabolism. In bacteria, there is considerable structural
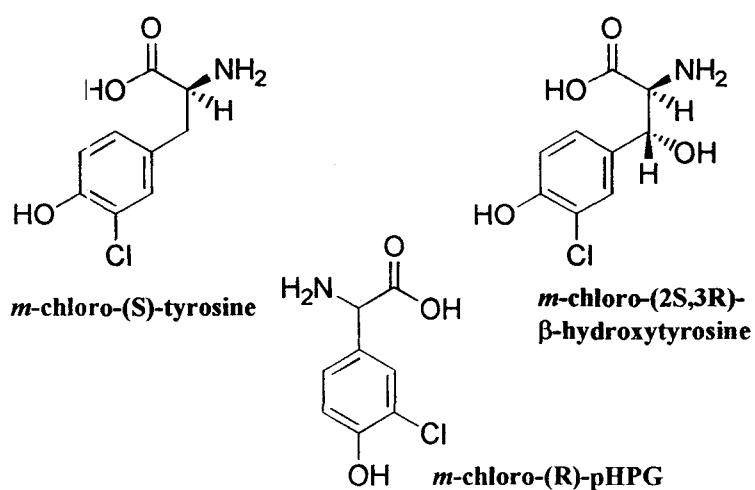
Figure 4.1. Chlorinated Amino Acids in A47934.

variety in the halometabolites produced, however the large majority are aromatic compounds. While the functions of halogenation are likely diverse, these groups have been shown to play important roles as metabolites engineered without their halide constituents are typically reduced in activity (26). Mono- and didechlorovancomycin have about 70 and 50% of the activity of vancomycin, respectively (13). The role of the chlorine atoms in GPAs is not known, however it has been suggested that they function in dimer formation, solubility or both.

4.1.2 Activities of Haloperoxidases

Organic halogenation reactions are oxidation reactions requiring the activity of a haloperoxidase, a diverse family of enzymes. The general reaction equation for haloperoxidation is:

$$A—H + H_2O_2 + X^- + H^+ \rightarrow A—X + 2\ H_2O$$
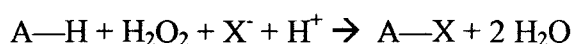
where AH is the organic substrate, X^- is a halide anion, and AX is the halogenated product. The reduction of peroxide to water drives the oxidation of the halide anion, generating the electrophilic species (X^+) that halogenates the organic substrate. The exact nature of the halogenating agent (X^+, HOX, Enz—OX) has not been determined (9).

In addition to halogenation, many of these enzymes are capable of two additional activities, catalase and peroxidase activity, despite the fact that they may not utilize them in their natural environment. In some of these multi-functional enzymes, however, it is the haloperoxidase activity that is not the relevant *in vivo* activity (7). Catalases perform a bimolecular dismutation of two molecules of hydrogen peroxide, in which one molecule reduces the other to generate water and oxygen:

$$2 \, H_2O_2 \rightarrow H_2O + O_2$$
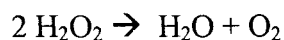
Enzymes that have evolved to perform this function are ubiquitous in aerobic organisms as peroxide is a common and dangerous by-product of oxidative metabolism. They are also one of the most efficient enzymes known, with catalytic efficiencies (k_{cat}/K_m) in the order of $10^7 \, M^{-1}s^{-1}$. (33). In peroxidases, reduction of peroxide is coupled to the one-electron oxidation of organic substrates, which are usually aromatic compounds that form stable radicals. These either disproportionate to regenerate one molecule of substrate and one molecule of oxidised product, or they can couple to form polymers:

$$2 \, AH + H_2O_2 \rightarrow 2 \, A\bullet + H_2O$$

$$2 \, A\bullet \rightarrow AH + A \; \text{ or } 2 \, A\bullet \rightarrow A—A$$
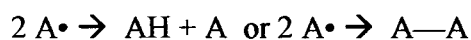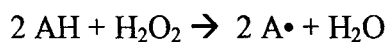
Similar to catalases, peroxidases are extremely efficient, however they differ in that they are much less ubiquitous, and have been found predominantly in plant metabolism (33).

4.1.3   Heme-Containing Haloperoxidases

Haloperoxidases can be classified into three major groups based on the type of cofactor present, either a heme (protoporphyrin IX) prosthetic group, a vanadium metal ion or no cofactor whatsoever. The heme haloperoxidases were the first discovered (19) and are the best characterised. Most can perform all three activities described above, and the catalytic cycle of the well-studied chloroperoxidase (CPO) from the marine fungus *Caldariomyces fumago* is presented in Figure 4.2 (5). All three pathways begin the same way, with H_2O_2 reduction to water coupled to the oxidation of ferric heme to the porphyrin radical cation $Fe^{IV}=O$. This is the same intermediate observed in the cytochrome P-450 pathway. The nomenclature in the peroxidase literature has

AH

$A\cdot + H^+$

II.Peroxidase

O

N—||—N
| Fe^{IV} |
N—|—N
      S
Cys   Compound II

$A\cdot + OH^-$

AH

N——N
| Fe^{III} |
N—|—N
      S
Cys

H_2O_2 H_2O

O

N—||—N
| Fe^{IV} |$\bullet +$
N—|—N
      S
Cys   Compound I

$H_2O + O_2$ I.Catalase H_2O_2

$AX + OH^-$

AH

X
 \
  O
N—|—N
| Fe^{III} |
N—|—N
      S
Cys

X^-

III.Chloroperoxidase
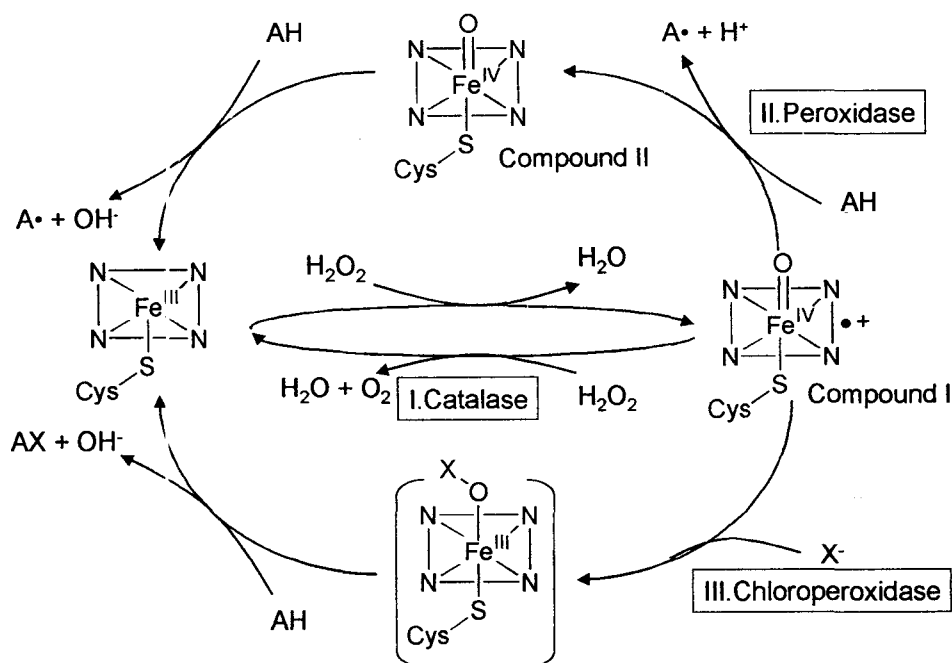
Figure 4.2. Catalytic Cycles of CPO Activities. Figure adapted from Ref. 5.

designated this intermediate Compound I, which is visible by spectral analysis and has a

green colour. In the catalase pathway, another molecule of peroxide is oxidised

producing oxygen and restoring ferric iron. The peroxidase cycle proceeds by two one-

electron oxidations of the organic substrate, generating the red coloured Compound II as

a reactive intermediate. In the chloroperoxidase route, chloride anion is oxidised to

generate an intermediate that is believed to resemble hypochlorite, in which the halogen

approaches the character of the X^+ electrophile in the formal reaction equation. This

reactive intermediate rapidly and specifically halogenates the organic substrate.

Evidence for this scheme has only been generated for CPO, however the other heme-

containing haloperoxidases are presumed to operate in the same fashion. CPO has

spectral properties nearly identical to cytochrome P-450 (15), with α and β bands fusing

and red-shifting upon dithionite reduction, and red-shifting of the Soret band upon carbon monoxide binding. These characteristics are diagnostic of a thiolate proximal ligand (the fifth ligand) to the heme iron, as has been confirmed by X-ray crystallographic studies (24). Most heme haloperoxidases have shown similar spectral properties, but at least one, a chloroperoxidase from the marine worm *Notomastus lobatus*, follows in the footsteps of the classical peroxidases by using an imidazole proximal ligand (10). Of those heme haloperoxidases identified in bacteria (*Pseudomonas aureofaciens, Streptomyces phaeochromogenes*), only bromination of organic substrates has been observed, despite the fact that several of these organisms manufacture only chlorinated metabolites (29, 30).

4.1.4 Vanadium-Containing Haloperoxidases

In heme-containing haloperoxidases, the heme iron provides electrons required to lyse the O—O peroxide bond, and subsequently recovers them from a halide anion. In vanadate-containing haloperoxidases, a vanadate ion (V^{5+}) co-ordinates to both peroxide oxygens and the halide ion simultaneously, functioning as an electron sink. In the proposed mechanism outlined in Figure 4.3, hydrogen peroxide displaces water in the trigonal bipyramidal coordination of hydrogen vanadate, forming the oxoperoxovanadate intermediate (18). Binding of halide ion to form a hexaco-ordinated intermediate results in electron transfer from the halide to the peroxide oxygens via the metal center. Oxidised halide (HOCl in the figure) is generated and directed towards the organic substrate. Both bromoperoxidase (*Corallina pilulifera*) and chloroperoxidase (*Curvularia inaequalis*) activities have been observed, as well as enzymes with additional

peroxidase and catalase activities (17, 25, 34). Thus far, no vanadium-containing

haloperoxidases have been isolated from a bacterium.
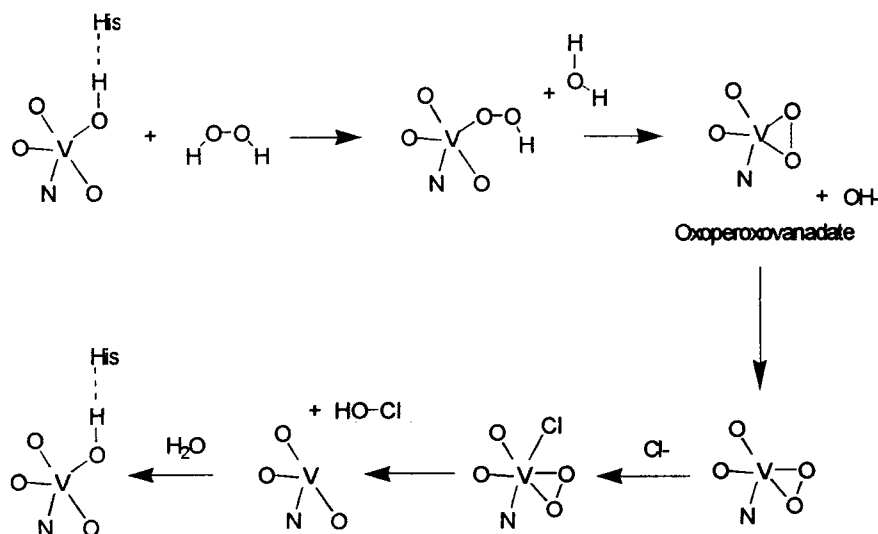
Figure 4.3. Proposed Mechanism of Vanadium-Containing Haloperoxidases.
Figure adapted from Ref. 18.

4.1.5 Metal-free Haloperoxidases

A third class of haloperoxidase lacks any cofactor and relies solely on a catalytic

triad composed of serine, histidine and aspartate (14, 22). In the proposed mechanism

(Figure 4.4), an acetate ester is formed with serine which is cleaved by hydrogen

peroxide to form peracetic acid in the active site (32). This strong oxidising agent is used

to oxidise the halide anion to the hypohalite, which can halogenate the organic substrate.

The halogenation step is thought to be non-enzymatic as there is a lack of a specific

halide binding site in these enzymes. These enzymes have only been found in bacteria to

date, and both chlorinating and brominating versions have been observed (31, 35). None

of these enzymes have been reported to have any catalase or peroxidase activities. A

chloroperoxidase from the producer of pyrrolenitrin, *Pseudomonas pyrrocinia*, was found

to chlorinate pyrrolenitrin intermediates, implicating it in the synthesis of the antifungal

agent (35). However high substrate K_m values (3), the non-specific nature of the

peracetic acid reaction mechanism and the fact that a gene replacement mutant was

unaffected in pyrrolenitrin formation (16) argue against a role for this enzyme in drug

synthesis.
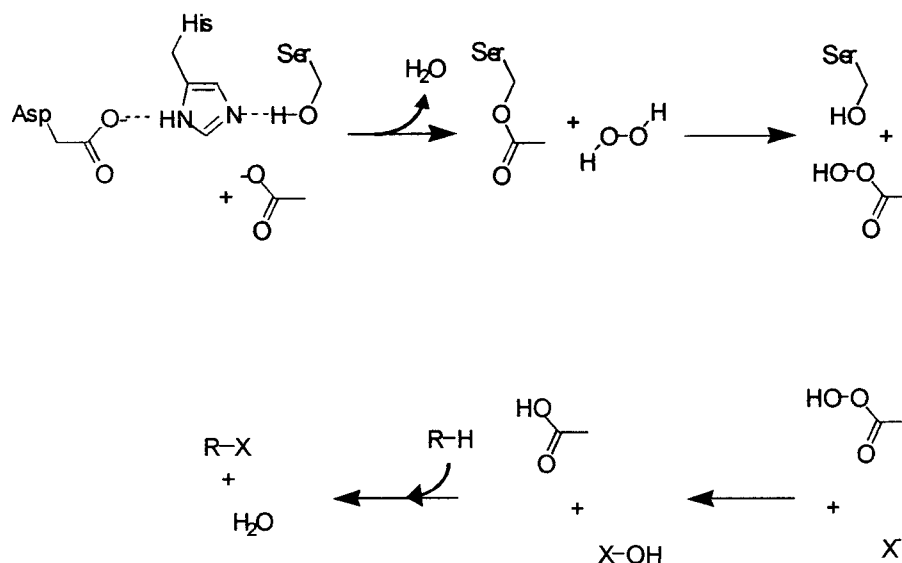
Figure 4.4. Proposed Mechanism of Non-metal Haloperoxidases.

4.1.6 Screening S. toyocaensis NRRL 15009 for Chloroperoxidase

The conventional screen for haloperoxidases for nearly 40 years utilises the β-

diketone monochlorodimedone (MCD) (Figure 4.5), which is not a natural substrate of

any known halogenating enzyme (12). Halogenation to form dichlorodimedone (DCD)

disrupts a conjugated bond system that absorbs at 290 nm, providing a convenient

spectrophotometric assay. All three classes of haloperoxidase have been detected using

MCD as a substrate, and it is almost always the means by which these enzymes are detected in cell-free extract. Peroxidase activity is similarly measured using an artificial substrate that has unique absorption properties. The compound *ortho*-dianisidine (Figure 4.5) is universally used to detect and measure peroxidase activity from all three classes of haloperoxidase (4). In this case, oxidation creates a conjugated bond system that absorbs at 460 nm. Catalase activity is easily measured by monitoring the disappearance of H_2O_2 which absorbs at 240 nm.
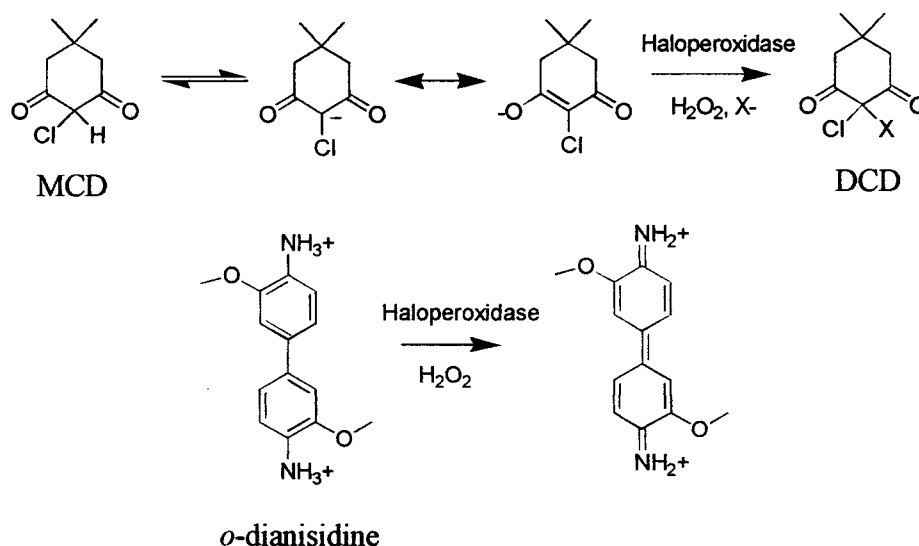
Figure 4.5. Substrates for Detection of Haloperoxidase Activities.

While the general acceptance of the substrates MCD and *o*-dianisidine by the various classes of haloperoxidases simplifies the task of identifying and purifying one of these enzymes in *S. toyocaensis* NRRL 15009 cell-free extracts, demonstrating activity specific to the A47934 pathway requires that the correct *in vivo* substrate be provided. As the timing of the chlorination events is unknown, we can only make educated guesses

at the probable substrates for this reaction. The reactive nature of the intermediates generated in the catalytic cycle of halogenases should require a fairly tight active site that is well-excluded from the polar solvent. If this is the case then smaller substrates such as the individual amino acid residues would be the logical substrates for these enzymes. However, it is also possible that the heptapeptide is the substrate, in which case it may be partially or fully cross-linked. These substrates are not available and difficult to synthesise.

This chapter describes the detection and purification of two halogen peroxidases from *S. toyocaensis* NRRL 15009, a heme bromoperoxidase/catalase (BPx) and a heme chloroperoxidase (CPx), and their partial characterisation. Their involvement with A47934 biosynthesis was assessed using a variety of potential substrates for chlorination.

4.2 Materials

MCD, *o*-dianisidine, tyrosine, tri-tyrosine, pHPG and the protein standards used in gel exclusion chromatography were all obtained from Sigma. Hydrogen peroxide, sodium acetate, potassium dihydrogen phosphate, ammonium sulfate, sodium dithionite, and sodium azide were purchased from BDH. Phenol was from Anachemia. Superbrite 0.1 mm glass beads were made by 3M. All column resins were purchased from Pharmacia. Centriprep 10 protein concentrators were from Amicon. Bio-sil C-18 HL 90-5S column (250 x 4.6 cm) was supplied by BioRad.

4.3 Methods

4.3.1 Culture Conditions

S. *toyocaensis* NRRL 15009 spore suspension (100 µL) was inoculated into SVM (50mL) and grown for 48 hours. SAM media was inoculated with 1% v/v saturated SVM and grown 72 hours. Culture was always examined for A47934 production by biological assay vs. *B. subtilis* prior to use. Mycelia were harvested by centrifugation at 6,000 x g for 20 min at 4 ^{O}C, washed with 0.5% NaCl (wt/vol), 5% glycerol (vol/vol) and stored at –80 ^{O}C until use. Enzymatic activity was preserved for at least one month in cells stored in this fashion.

4.3.2 Enzymatic Assays and Protein Determination

Haloperoxidase activity was monitored with a mixture (0.8 mL) of 48 µM monochlorodimedone (MCD), 8.8 mM H_2O_2, 100 mM NaBr and an appropriate amount of enzyme in 100 mM sodium acetate (NaOAc), pH adjusted to 5.0 with acetic acid, at room temperature. The decrease in absorbance at 290 nm ($\varepsilon = 1.99 \times 10^4 M^{-1}cm^{-1}$) upon bromination of the MCD enol was monitored over time on a Cary 3 UV-Vis spectrophotometer. One unit of bromoperoxidase is defined as the amount of enzyme required to form 1 µmol of bromochlorodimedone in one minute.

Organic peroxidase activity was assayed according to Clairborne and Fridovich (4). Reaction mixtures consisted of 48 µM *o*-dianisidine, 7.2 mM H_2O_2, in 50 mM potassium phosphate, pH 6.0 The formation of the oxidised product was monitored at 460 nm.

Catalase activity was determined by the decrease in absorbance of H_2O_2 at 240 nm ($\varepsilon = 43.6$ $M^{-1}cm^{-}$). Reactions were run in 100 mM NaOAc, pH 5.5, 10 mM H_2O_2.

Protein determination was done by the method of Bradford with bovine serum albumin as standard (2).

4.3.3 Purification of Haloperoxidases

All purification steps were performed at 4 ^{O}C. Cells from 6 L of growth medium (typically 100-120 g wet weight) were suspended in lysis buffer consisting of 50 mM HEPES, pH 7.5, 2 mM EDTA, 1 mM PMSF, 0.1 mM DTT, 5% glycerol and homogenised in a Biospec Beadbeater in the presence of 0.1 mm diameter acid-washed glass beads. The chamber was cooled to -5 ^{O}C and cell lysis was achieved following 15 cycles of 30 sec of breakage followed by 60 sec of cooling. The homogenate was centrifuged at 3,000 x g for 15 min, the supernatant collected, and the pellet re-extracted with lysis buffer. The combined supernatant was treated with ammonium sulphate and the fraction which precipitated between 20 and 70% was recovered by centrifugation. The pellet was taken up in a minimal amount of lysis buffer and dialyzed against 50 mM NaOAc, pH 5.5 to > 95% equilibration. The dialysate was centrifuged at 12,500 x g for 30 min, and the supernatant (acid soluble fraction) was loaded onto a DEAE Sepharose FF (3 x 10 cm) column equilibrated in 50 mM NaOAc, pH 5.5. Haloperoxidases were recovered using a gradient from 0-1 M NaCl over 8 bed volumes.

a) Catalase/bromoperoxidase (BPx): DEAE eluant fractions which demonstrated bromoperoxidase activity only were pooled and concentrated to less than 2 mL using a Centriprep 10. The concentrate was applied to a Superdex 200 column (62 cm x 1.6

cm) equilibrated with 50 mM HEPES pH 7.2. Haloperoxidase containing fractions were pooled and applied to a Mono Q (HR5-5) column equilibrated with 50 mM HEPES, pH 7.2. Haloperoxidase was recovered following elution with a linear gradient in NaCl from 0-0.5 M. The enzyme containing fractions were pooled and brought to 1.5 M in ammonium sulphate and applied to an Alkyl Superose (HR5-5) column equilibrated with 50 mM HEPES, pH 7.2, 1.5 M ammonium sulphate. Bromoperoxidase was recovered using a 1.5-0.75 M ammonium sulphate gradient. The purified enzyme was desalted into 50 mM HEPES, pH 7.2 by repeated cycles of concentration and dilution using a Centriprep10. The enzyme was stored at $4\,^{\circ}C$.

b) Chloroperoxidase (CPx): Fractions which showed activity with o-dianisidine and MCD following the DEAE column were pooled and purified to apparent homogeneity using the same sequence of chromatographic columns as for the catalase/bromoperoxidase but now fractions were pooled based on o-dianisidine oxidation activity.

4.3.4 *General Characterisation of Haloperoxidases*

The molecular weight of native haloperoxidases was determined by measuring retention by a Superdex 200 gel filtration column (1.0 x 30 cm). Injected sample (50 µg) was eluted at 0.4 mL/min in 50 mM HEPES, pH 7.2 and the retention volume (V_e) was correlated to molecular weight by a standard curve. The standard curve was generated using cytochrome C (10.4 kDa), carbonic anhydrase (29 kDa), bovine serum albumin (66 kDa), alcohol dehydrogenase, and β-amylase (200 kDa). Blue dextran (2000 kDa) was

used to determine the void volume (V_o). A linear fit of a plot of V_e/V_o gave a line with the equation $y = -0.5549x + 2.8059$ and a correlation coefficient of -0.96 (Figure 4.6).
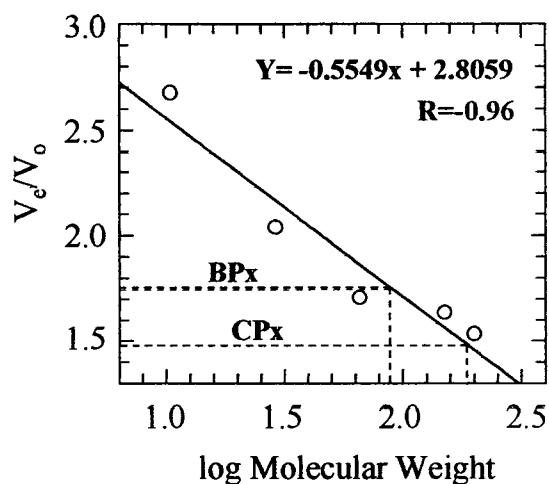
Figure 4.6. Gel Filtration Chromatography Standard Curve.

Amino-terminal sequencing was performed by Dr. W. Lane at Harvard Microchemistry Facility, while electrospray mass spectrometry was done by Dr. Lorne Taylor of the Department of Chemistry, Waterloo University.

Spectral analysis was done in 500 μL cuvettes in a Varian Cary 3E spectrophotometer. Protein samples (250 pmol for BPx, 700 pmol for CPx) were buffered in 50 mM HEPES pH 7.2 and scanned from 600 to 300 nm at 120 nm/min. Sodium dithionite was added to 100 mM final concentration and CO was bubbled in to solution saturation. Azide inactivation was performed by the addition of sodium azide to 1 μM.

Kinetic assays were performed as described above for the detection of enzyme

activities during purification, varying the concentration of the substrate in question, and

using 30 pmol (BPx) or 500 pmol (CPx) of enzyme. Insufficient amounts of enzyme were

available to measure rates in duplicate. To determine pH optima, a hybrid buffer system

of sodium citrate and sodium acetate was determined to have a minimal effect on the

enzyme, whereas HEPES, MES and phosphate buffers inactivated the enzyme.

4.3.5   Chlorination of A47934 Intermediates

Reactions (100 µL) contained 100 mM NaOAc, 100 mM sodium chloride, 10 mM

H_2O_2, 2 mM of test organic substrate, and either 30 pmol (BPx) or 500 pmol (CPx) and

were incubated 16 hours at room temperature. The pH of the acetate buffer was

determined by the optimum measured for MCD halogenation. Organic substrates tested

were tyrosine, phenol, pHPG, βHT and tyr-tyr-tyr (tri-L-tyrosine). Reactions were

injected onto a Bio-Sil C-18 Reverse Phase HPLC column and eluted at 0.5 mL/min with

1%, 10% or 21% acetonitrile in 0.1% TFA (depending on the organic substrate used).

Eluted peaks were monitored by measuring absorbance at 254 nm.

4.4   Results and Discussion

This section is divided into two parts, a and b, to discuss the purification and

characterisation of the two haloperoxidases separately.

4.4a.1   Purification of BPx from S. toyocaensis NRRL 15009

BPx was purified to >90% homogeneity from S. toyocaensis NRRL 15009 cell-

free extract in 6 steps (Figure 4.7), and was so poorly expressed that over 100 grams of

mycelia were required to obtain any amount of enzyme in reasonable yield. BPx was

purified on the basis of its ability to brominate MCD and its lack of peroxidase activity

(as determined by reactivity with o-dianisidine). Activity was not detectable until the
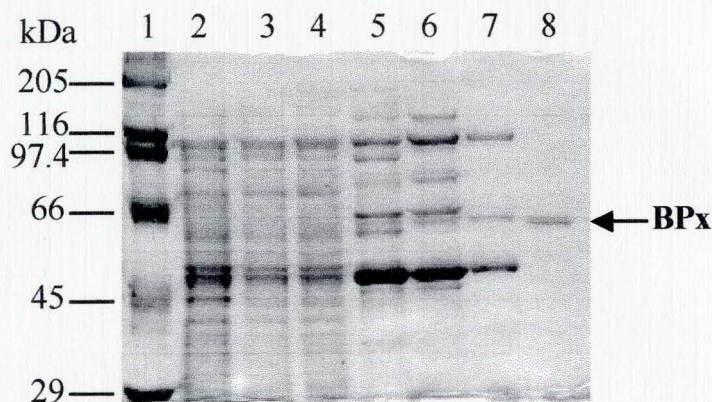
Figure 4.7. SDS-PAGE of Purified BPx. Gel (11% polyacrylamide) contained
protein standards (lane 1), cell lysate (lane 2), 20-70% saturation ammonium sulfate
fraction (lane 3), acid precipitate (lane 4), DEAE Sepharose pool (lane 5), Superdex S-200
pool (lane 6), Mono Q pool (lane 7), Alkyl Superose pool (lane 8).

completion of the third step, acid dialysis/precipitation, as has been previously described

in the purification of other haloperoxidases (28). It was not distinguishable from the

other haloperoxidase activity in S. toyocaensis NRRL 15009 crude extracts until

fractionation by a DEAE-sepharose ion exchange column (step 4), at which point it is

still contaminated with considerable amounts of CPx. These complications in activity

associated with BPx are reflected in the values listed for n-fold purification and percent

recovery in the purification table (Table 4.1). The apparent recovery of 2% is much

lower than its actual value due to the presence of CPx, while the n-fold purification (6.4)

is reduced by the inability to measure activity in the first two steps of the purification.

The table shows that only 0.12 mg of enzyme was recovered from over 4000 mg of

starting material, generated from 100-120 g of harvested *S. toyocaensis* NRRL 15009

mycelia. In the course of developing the protocol, hydroxyapatite resin, tyrosine agarose

and aminooctanol agarose were found to have minimal contributions to purification.

Table 4.1. Purification of BPx from *S. toyocaensis* NRRL 15009

Fraction	Protein (mg)	Specific Activity (mU/mg protein)	Total Activity[1] (U)	Recovery (%)	Purification (n-fold)
Cell lysate	4070	0	0	-	-
Ammonium sulphate (20-70%)	1080	0	0	-	-
Acid precipitation	931	0	0	-	-
DEAE Sepharose	38.7	32.4	1.25	100	-
Superdex S-200	11.8	48.1	0.57	45	1.5
Mono Q	2.2	107	0.24	19	3.3
Alkyl Superose	0.12	206	0.025	2	6.4

[1] 1 U was defined as 1 μmol MCD oxidised per minute.

4.4a.2 Partial Characterisation of BPx

A very small amount of BPx was purified with considerable effort, and thus

characterisation was targeted to the goal of determining involvement in A47934

biosynthesis. For those assays which did not destroy the enzyme sample, it was

recovered and reused.

In a gel filtration chromatography experiment performed with an analytical

Superdex 200 column, BPx eluted with a V_e/V_o ratio of 1.485, corresponding to a

molecular weight of approximately 185 kDa. Electrospray mass spectrometry gave a

monomer molecular mass of 53.89 ± 0.02 kDa (Figure 4.8), corresponding to a native

enzyme composed of 3.4 monomer units. As most enzymes function as either dimers or

tetramers, it is likely that BPx is a tetramer with anomalous chromatographic properties.
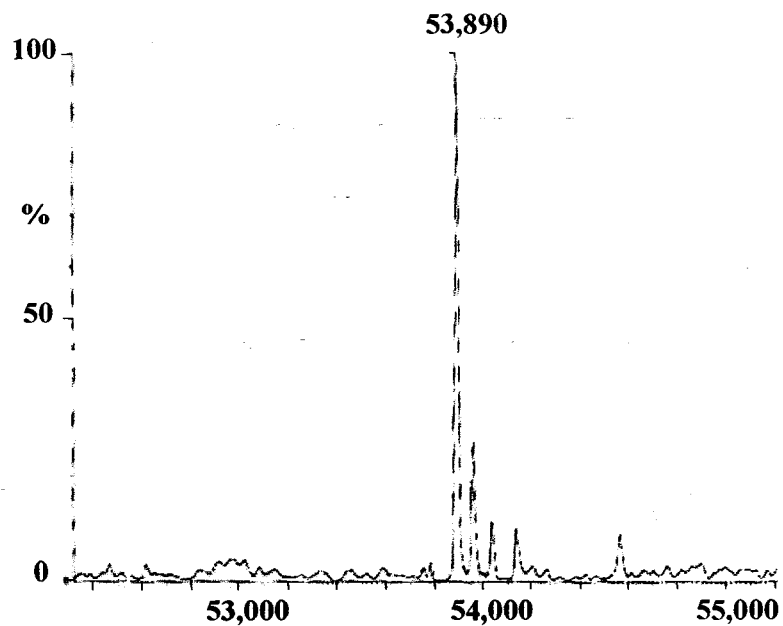
Figure 4.8. Electrospray-Mass Spectral Analysis of BPx.
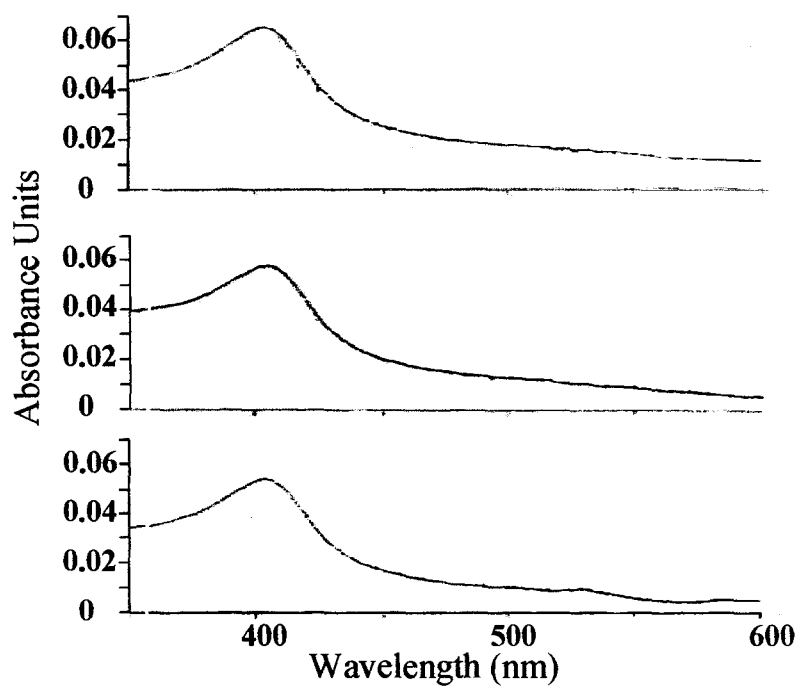
Figure 4.9. Spectral Analysis of BPx. A. Native enzyme B. Reduced with dithionite C. Reduced and treated with CO.

Azide inactivation of enzymatic activity and the presence of a broad Soret band at 405 nm in spectral scans indicated that BPx was in fact a heme-containing protein, however there were insufficient amounts of enzyme to observe the α and β bands typically present (Figure 4.9). Addition of sodium dithionite to produce the ferrous species had no effect on the spectrum, and CO did not bind. Thus it appears that fifth-ligand co-ordination to the heme is not a thiolate as in cytochrome P-450s and the well-characterised CPO from *Caldariomyces fumago* (5). Consistent with this, dithionite treatment had no effect on enzyme activity.

BPx had catalase activity in addition to bromoperoxidase activity (Table 4.2), with a K_m for H_2O_2 of 6.5 ± 1.1 mM and a V_{max} of 3.2 ± 0.17 mmol/min/mg protein at pH 5.5. This translates into a k_{cat} of $2.87 \pm 0.15 \times 10^3$ s^{-1} and a k_{cat}/K_m of 4.4×10^5 M^{-1}s^{-1}. These values seemed a little low (about 2 orders of magnitude) for a catalase which are one of the most efficient enzymes known.

Table 4.2. Enzymatic Properties of Purified BPx

Activity	Catalytic Parameters
catalase	K_m for H_2O_2 = 6.5 ± 1.1 mM
	V_{max} = 3.2 ± 0.2 mmol/min/mg protein (pH 5.5)
bromoperoxidase	K_m for Br$^-$ = 16 ± 7 mM
	V_{max} = 533 ± 62 nmol/min/mg protein (pH 5.0)
	pH optimum 5.0

BPx was not able to chlorinate, fluorinate or iodinate MCD, but could brominate it with a K_m for Br$^-$ of 16 ± 7 mM and a V_{max} of 533 ± 62 nmol/min/mg at pH 5.5. A pH profile using a hybrid buffer system demonstrated a pH optimum of 5.0 (Figure 4.10).
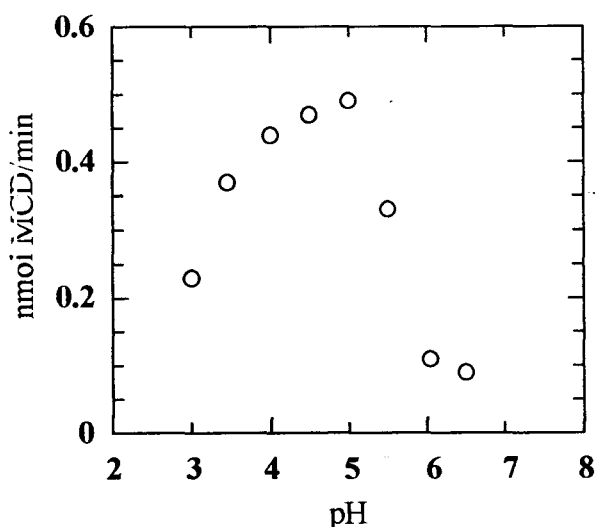
Figure 4.10. BPx MCD Halogenation pH Optimum.

N-terminal sequencing of BPx gave the sequence Thr-Gln-Gly-Pro-Leu-Thr-Thr-Glu-

Ala-Gly. A sequence search of the GeneBank and EMBL databases revealed that it was

100% identical with a catalase/bromoperoxidase, of predicted molecular mass 54, 092

kDa, cloned from the chloramphenicol producer *S. venezualae* (7). This enzyme is also

resistant to dithionite reduction, and is 49% similar to bovine catalase, a well-

characterised enzyme with a tyrosine-derived phenolate serving as a proximal ligand to

heme iron (8). This tyrosine is conserved in the *S. venezualae* enzyme and is likely

present in *S. toyocaensis* NRRL 15009 BPx. The gene encoding the *S.venezualae* BPx

was knocked out and found to be non-essential for chloramphenicol production, and in

light of the similarities to bovine catalase, likely fulfils a housekeeping function as a

scavenger of H_2O_2. This is also likely the case for *S. toyocaensis* NRRL 15009 BPx.

HPLC conditions were developed to obtain reasonable elution volumes for

potential *S. toyocaensis* NRRL 15009 haloperoxidase *in vivo* substrates using

acetonitrile/TFA solvent systems (Table 4.3). Chlorinated reaction products were not

available for use as standards, however the separation of aromatic compounds differing

by a single polar substituent had been demonstrated using similar conditions (Chapter 3).

Analysis of BPx reactions incubated 16 hours with various organic substrates yielded no

new peaks, which was not surprising given the results of the N-terminal sequencing

analysis.

Table 4.3. HPLC Separation of Various Haloperoxidase Substrates

Compound	Acetonitrile in TFA (%)	Retention Volume[1] (mL)
pHPG	1	5.4
βHT	1	7.9
tyrosine	10	18
phenol	10	35
tri-tyrosine	21	12.4

[1] Flowrate was 0.5 mL/min using an isocratic solvent system.
Column void volume was 3.4 mL

4.4b.1 Purification of CPx from S. toyocaensis NRRL 15009

CPx was identified in crude extracts by its ability to brominate MCD and its

peroxidative activity with *o*-dianisidine. It was more easily identified in crude extracts

and was recovered in nearly 100-fold better yield than BPx (Table 4.4). Again, percent

recovery and n-fold purification was affected by the removal of enzymes that competed

with CPx for substrates (catalase activity which depletes H_2O_2). Removing

bromoperoxidase activity had no effect on these values, however, as peroxidation of *o*-

dianisidine was used to measure CPx purification (as opposed to MCD). CPx appeared

as a single band when analysed by SDS-PAGE (Figure 4.11).

Table 4.4. Purification of CPx from *S. toyocaensis* NRRL 15009

Fraction	Protein (mg)	Specific Activity[1] (mU/mg protein)	Total Activity (U)	Recovery (%)	Purification (n-fold)
Cell lysate	7215	0	0	-	-
Ammonium sulfate (20-70%)	3850	0.0012	72	100	-
Acid precipitation	2810	0.008	22.5	31	0.67
DEAE Sepharose	62.4	0.128	8	11	10
Superdex S-200	16.28	0.300	4.89	6.8	25
Mono Q	8.36	0.364	3.04	4.2	30
Alkyl Superose	8.40	0.393	3.30	4.6	33

[1] Activity was measured by colorimetric oxidation of *o*-dianisidine.
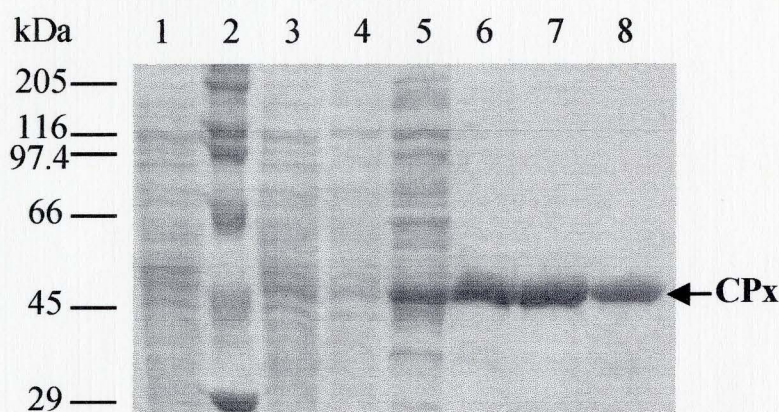
Figure 4.11. SDS-PAGE of Purified BPx. Gel (11% polyacrylamide) contained cell lysate (lane 1), protein standards (lane 2), 20-70% saturation ammonium sulphate fraction (lane 3), acid precipitate (lane 4), DEAE Sepharose pool (lane 5), Superdex S-200 pool (lane 6), Mono Q pool (lane 7), Alkyl Superose pool (lane 8).

4.4b.2   Characterisation of CPx

While 100-fold more CPx was recovered from enzyme preparations, 50-fold more enzyme was required in assays to get rates equivalent to those of BPx. Thus, characterisation was again limited and largely focussed on determining involvement in A47934 biosynthesis. Gel filtration chromatography using protein standards indicated

that CPx had a native molecular weight of 88 kDa, which corresponded to a dimer as the

ESI-MS gave a monomer mass of 42,882.

Like BPx, CPx was inactivated by azide and showed a broad Soret band, in this

case at 399 nm (Figure 4.12). Again, dithionite reduction and saturation with CO had no

effect on the spectral profile, indicating that the proximal ligand is not a cysteine thiolate.

CPx activity was ablated by reduction/CO treatment, however, and thus is distinct from

the phenolate-ligated heme of catalase and BPx. The only non-thiolate heme

chloroperoxidase is that from the marine worm *Notomastus lobatus*, which has been

shown to use an imidazole (10).
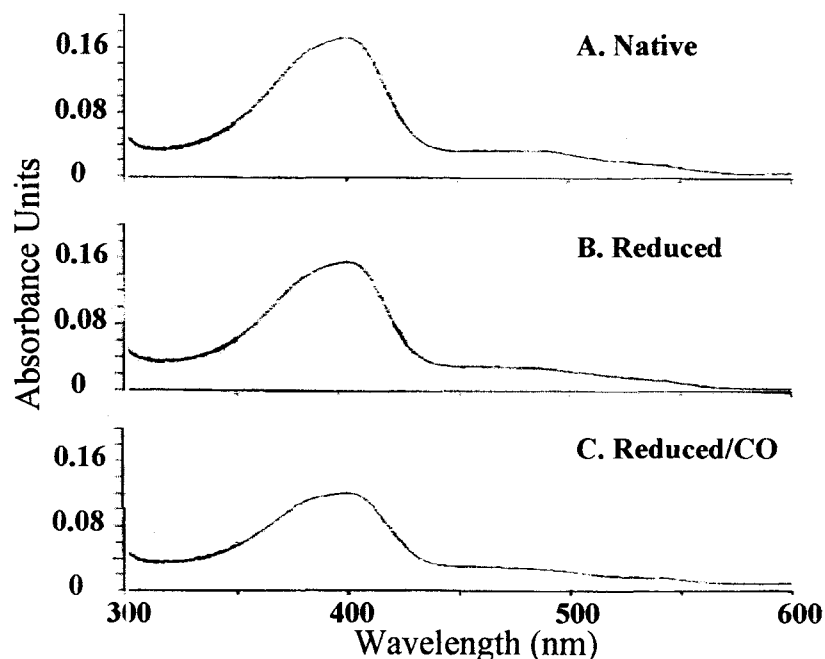
Figure 4.12. Spectral Analysis of CPx. A. Native enzyme B. Reduced with dithionite C. Reduced and treated with CO.

CPx lacked catalase activity but had peroxidase activity, as determined using the artificial substrate *o*-dianisidine (Table 4.5). The pH optimum for this activity was 4.0. Neither K_m nor V_{max} was determined. CPx was found to oxidise chloride in addition to bromide in MCD assays (and hence its designation). The K_m for Cl⁻, at about 60 mM was considerably lower than that for Br⁻, which could not be determined as rates continued to increase in a linear manner until 0.6 M. At equivalent concentrations, rates for Cl⁻ incorporation were slightly higher than for Br⁻. The Cl⁻ K_m is similar to the halide K_m values observed in other heme-containing haloperoxidases (1). As expected, the V_{max} for CPx was about 50 fold lower than that of BPx, and may reflect a greater percentage of inactive enzyme in the purified sample. The pH optimum for the chlorination of MCD was determined to be 4.5.

Table 4.5. Enzymatic Properties of Purified CPx

Activity	Catalytic Parameters
peroxidase	K_m/V_{max} not determined
	pH optimum 4.0
chloroperoxidase	K_m/V_{max} for Br⁻ = could not measure
	K_m for Cl⁻ = 57 ± 13 mM
	V_{max} (Cl⁻) = 22.5 ± 1.6 nmol/min/mg protein
	pH optimum 4.5

N-terminal sequencing gave the peptide sequence Met-Leu-Ser-Glu-Glu-Ser-Ala-Ala-Val-Leu-Arg, which did not match anything in the Genebank and EMBL databases. This was our primary candidate for an *S. toyocaensis* NRRL 15009 enzyme involved in A47934 biosynthesis, and reactions were set up to determine chlorination or peroxidation activity with tyrosine, βHT and tri-tyrosine. Disappointingly, no new peaks were

observed in HPLC runs of any of the reactions set up. Despite repeated attempts, no evidence for any kind of chemical transformation of these substrates was observed when incubated with CPx.

4.5 Conclusions

Two haloperoxidases, a catalase/bromoperoxidase and a chloroperoxidase, were purified, partially characterised and assayed for involvement in A47934 biosynthesis. The catalase/bromoperoxidase was determined to be very similar to a housekeeping enzyme in the chloramphenicol producer *S.venezualae*, and likely fulfils the same function in *S. toyoccensis* NRRL 15009. The chloroperoxidase was promising as it preferentially chlorinated MCD, had no catalase activity, could oxidise *o*-dianisidine, and was not similar to any other protein in its predicted N-terminal amino acid sequence. Unfortunately, *S. toyocaensis* NRRL 15009 chloroperoxidase was not found to be reactive in any way with the substrates provided, indicating that either it is not involved in A47934 biosynthesis or that the substrate for chlorination in this pathway is more complex. It has recently been suggested that all of the bacterial haloperoxidases discovered so far which have been linked to antibiotic biosynthesis are not in fact the enzymes responsible for halogenation in the synthesis of these antibiotics (27). A novel, as-yet-undiscovered class of haloperoxidase, with substrate and regio- specificity, must be the source of these halogenation reactions. Furthermore, the use of MCD, an artificial substrate which is used for its convenience and its general acceptance by

haloperoxidases, has been the reason that this class has remained undiscovered in these

antibiotic-producing organisms.

4.6 References

1. **Baden, D. G., and M. D. Corbett.** 1980. Bromoperoxidases from *Penicillus capitatus, Penicillus lamourouxii and Rhipocephalus phoenix*. Biochem J. **187**(1):205-11.

2. **Bradford, M. M.** 1976. A rapid and sensitive method for the quantitation of microgram quantities of protein utilising the principle of protein-dye binding. Anal Biochem. **72**:248-54.

3. **Burd, W., O. Yourkevich, A. J. Voskoboev, and K. H. van Pee.** 1995. Purification and properties of a non-haem chloroperoxidase from *Serratia marcescens*. FEMS Microbiol Lett. **129**(2-3):255-60.

4. **Claiborne, A., and I. Fridovich.** 1979. Purification of the o-dianisidine peroxidase from *Escherichia coli* B. Physicochemical characterization and analysis of its dual catalatic and peroxidatic activities. J Biol Chem. **254**(10):4245-52.

5. **Dawson, J. H., and M. Sono.** 1987. Cytochrome P-450 and chloroperoxidase: thiolate-ligated heme enzymes. Spectroscopic determination of their active site structures and mechanistic implications of thiolate ligation. Chem Rev. **87**:1255-76.

6. **Enguild, K. C., H. Egsgaard, and E. Larsen.** 1981. Determination of 4-chloroindole acetic acid methyl ester in *Viceae* species by gas chromatography-mass spectroscopy. Physiol Plant. **53**:79-81.

7. **Facey, S. J., F. Gross, L. C. Vining, K. Yang, and K. H. van Pee.** 1996. Cloning, sequencing and disruption of a bromoperoxidase-catalase gene in *Streptomyces venezuelae*: evidence that it is not required for chlorination in chloramphenicol biosynthesis. Microbiology. **142**(Pt 3):657-65.

8. **Fita, I., and M. G. Rossmann.** 1985. The active center of catalase. J Mol Biol. **185**(1):21-37.

9. **Franssen, M. C. R.** 1994. Halogenation and oxidation reactions with haloperoxidases. Biocatalysis. **10**:87-111.

10. **Franzen, S., M. P. Roach, Y. P. Chen, R. B. Dyer, W. H. Woodruff, and J. H. Dawson.** 1998. The unusual reactivities of *Amphrite ornata* and *Notomastus lobatus* chloroperoxidase do not arise from a histidine imidazole proximal haem iron ligand. J Am Chem Soc. **120:**1658-61.

11. **Gribble, G. W.** 1994. The natural production of chlorinated compounds. Environ Sci Technol. **28:**310A-319A.

12. **Hager, L. P., D. R. Morris, F. S. Brown, and H. Eberwein.** 1966. Chloroperoxidase. II. Utilization of halogen anions. J Biol Chem. **241**(8):1769-77.

13. **Harris, C. M., R. Kannan, H. Kopecka, and T. M. Harris.** 1985. The role of the chlorine substituents in the antibiotic vancomycin: preperation and characerization of mono and didechloro-vancomycin. J Am Chem Soc. **107:**6652-58.

14. **Hecht, H. J., H. Sobek, T. Haag, O. Pfeifer, and K. H. van Pee.** 1994. The metal-ion-free oxidoreductase from *Streptomyces aureofaciens* has an alpha/beta hydrolase fold. Nat Struct Biol. **1**(8):532-7.

15. **Hollenberg, P. F., and L. P. Hager.** 1973. The P-450 nature of the carbon monoxide complex of ferrous chloroperoxidase. J Biol Chem. **248**(7):2630-3.

16. **Kirner, S., K. Grimm, S. T. Lam, J. Ligon, and K.-H. van Pee.** 1995. Presented at the Fifth Int Symp Pseudomonas: Biotechnol Molec Biol, Tsukuba, Japan.

17. **Krenn, B. E., Y. Izumi, H. Yamada, and R. Wever.** 1989. A comparison of different (vanadium) bromoperoxidases: the bromoperoxidase of *Corallina pilulifera* is also a vanadium enzyme. Biochim Biophys Acta. **998:**63-68.

18. **Littlechild, J.** 1999. Haloperoxidases and their role in biotransformation reactions. Curr Opin Chem Biol. **3**(1):28-34.

19. **Morris, D. R., and L. P. Hager.** 1966. Chloroperoxidase. I. Isolation and properties of the crystalline glycoprotein. J Biol Chem. **241**(8):1763-8.

20. **Neidleman, S. L., and J. Geigert.** 1986. Biohalogenation: Principles, Basic Roles and Applications. Ellis Horwood, Chicester, U.K.

21. **Oxford, A. E., H. Raistrick, and P. Simonart.** 1939. Studies in the biochemistry of microorganisms LX. Griseofulvin, $C_{17}H_{17}O_6Cl$, a metabolic product of *Penicillum griseofulvin* Dierckx. Biochem J. **33:**240-48.

22. **Pelletier, I., J. Altenbuchner, and R. Mattes.** 1995. A catalytic triad is required by the non-heme haloperoxidases to perform halogenation. Biochim Biophys Acta. **1250**(2):149-57.

23. **Petty, M. A.** 1961. An introduction to the origin and biochemistry of microbial halometabolites. Bacteriol Rev. **25**:111-30.

24. **Poulos, T. L., B. C. Finzel, I. C. Gunsalus, G. C. Wagner, and J. Kraut.** 1985. The 2.6-A crystal structure of *Pseudomonas putida* cytochrome P-450. J Biol Chem. **260**(30):16122-30.

25. **Simons, B. H., P. Barnett, E. G. Vollenbroek, H. L. Dekker, A. O. Muijsers, A. Messerschmidt, and R. Wever.** 1995. Primary structure and characterization of the vanadium chloroperoxidase from the fungus *Curvularia inaequalis*. Eur J Biochem. **229**(2):566-74.

26. **Suzuki, T., H. Honda, and R. Katsumata.** 1972. Production of antibacterial compounds analogous to chloramphenicol by an n-paraffin-grown bacterium. Agr Biol Chem. **36**:2223-28.

27. **van Pee, K. H.** 1996. Biosynthesis of halogenated metabolites by bacteria. Annu Rev Microbiol. **50**:375-99.

28. **van Pee, K. H., and F. Lingens.** 1984. Detection of a bromoperoxidase in *Streptomyces phaeochromogenes*. FEBS Lett. **173**(1):5-8.

29. **van Pee, K. H., and F. Lingens.** 1985. Purification and molecular and catalytic properties of bromoperoxidase from *Streptomyces phaeochromogenes*. J Gen Microbiol. **131**(Pt 8):1911-6.

30. **van Pee, K. H., and F. Lingens.** 1985. Purification of bromoperoxidase from *Pseudomonas aureofaciens*. J Bacteriol. **161**(3):1171-5.

31. **van Pee, K. H., G. Sury, and F. Lingens.** 1987. Purification and properties of a nonheme bromoperoxidase from *Streptomyces aureofaciens*. Biol Chem Hoppe Seyler. **368**(9):1225-32.

32. **van Pee, K.-H., H. J. Hecht, A. Berkessel, T. Schrapel, and H. Laatsch.** 1994. German Patent No P44 30 327.0. Germany.

33. **Walsh, C. T.** 1977. Enzymatic Reaction Mechanisms. W.H. Freeman and Company, New York.

34.   **Wever, R., H. Plat, and E. de Boer.** 1985. Isolation procedure and some
      properties of the bromoperoxidase from the seaweed *Ascophyllum nodosum*.
      Biochim Biophys Acta. **830:**181-86.

35.   **Wiesner, W., K.-H. van Pee, and F. Lingens.** 1988. Purification and
      characterization of a novel bacterial non-heme chloroperoxidase from
      Pseudomonas pyrrocinia. J Biol Chem. **263**(27)**:**13725-732.

Chapter 5

Identification of *van*A/B-like Genes in *S. toyocaensis* NRRL 15009
and other GPA-producing Organisms

Adapted from

Marshall, C. G., G. Broadhead, B. K. Leskiw, and G. D. Wright. 1997. D-Ala-D-Ala
ligases from glycopeptide antibiotic-producing organisms are highly homologous to the
enterococcal vancomycin-resistance ligases VanA and VanB. Proc Natl Acad Sci U S A.
94(12):6480-3.

and

Marshall, C. G., I. A. Lessard, I. Park, and G. D. Wright. 1998. Glycopeptide
antibiotic resistance genes in glycopeptide-producing organisms. Antimicrob Agents
Chemother. **42**(9):2215-20

5.1 Introduction

In the course of conducting the studies summarised in the last two chapters, it became apparent that there were several difficulties in using the reverse genetics approach to identify the A47934 biosynthetic cluster in *S. toyocaensis* NRRL 15009. Cultures would often refuse to produce antibiotic despite being provided with optimal conditions. In some cases, the rate of growth or the kinetics of drug production was altered, making it difficult to ensure that the culture being assayed was actively producing antibiotic. Furthermore, enzymes involved in secondary metabolite production are notorious for low levels of expression and have proven very challenging to purify in useful yields (22). In the case of A47934 production, the substrates for the predicted activities were not well defined, as there was no information regarding the timing of the various chemical transformations. Assays for tyrosine hydroxylation, polyketide formation, amino acid adenylation, D-alanine-D-amino acid ligation and haloperoxidation had failed to reveal any clear indication of A47934 biosynthesis in *S. toyocaensis* NRRL 15009 cell-free extracts.

Another approach to identifying antibiotic biosynthesis and resistance genes is rooted in evolutionary genetics. The objective is the same as the reverse genetics approach – to generate an oligonucleotide probe for a biosynthesis or resistance gene that will allow identification of the entire (predicted) cluster of genes. However rather than purifying the corresponding enzyme, the probe is generated by comparing the amino acid sequences of similar enzymes in related organisms. By aligning these sequences, highly

conserved regions (usually dictated by function, and therefore likely conserved in the unknown sequence of the target enzyme) can be identified and serve as a template for the design of degenerate oligonucleotides. Often these regions are short, however, and not enough specificity can be incorporated into the probe. If two separate regions can be identified however, the technique can be taken a step further by using PCR amplification of the region in-between and a very specific, tight binding oligonucleotide probe can be constructed.

Synthesis of oligonucleotide probes by degenerate PCR has become a very popular technique in recent years for screening genome libraries (1, 7), and for good reason. While the reverse-genetics approach is a reliable method for the identification of genes in many situations, it can be difficult and laborious. More importantly, degenerate PCR has become a more powerful tool due to the immense amount of DNA sequencing that has occurred in the last decade, and which continues to increase at what is seemingly an exponential rate. The tremendous volume of data, in combination with the excellent databases and services associated with these databases, allows any researcher easy access to the nucleotide and amino acid sequences of countless gene families. So many sequences are available, that even highly specialised enzymes have multiple entries from multiple sources (bacterial, fungal, algal, higher plant, insect, etc). It is therefore relatively straightforward to compare the primary sequences encoded by these gene families and identify highly conserved regions. In some cases, enzymes of the same family with slightly different specificity can be distinguished based on primary sequence alone, allowing primer design that amplifies out only a specific sub-set of the gene family

(20). Primer design can also be fine-tuned based on the sequence of a gene (or its primary sequence) from an organism closely related to that in which genes are being probed. Many genes have been cloned in this manner, and as more sequences accumulate, degenerate PCR will continue to have an increasingly important role in gene cloning.

While there are clear advantages to the degenerate PCR approach, there are certain limitations as well. Obviously, there must be a sufficient number of genes in the target family already sequenced in order to be able to identify important regions likely to be conserved. In addition, not all gene families are as homologous as others, making it difficult to identify two highly conserved regions. Conversely, some gene families are closely related to others that function in independent pathways, making it difficult to design primers specific to the family. The conserved regions themselves can be problematic as well. Some amino acid codons are more degenerate than others, and a string of these amino acids can make primers so degenerate that they will bind at several locations in the chromosome. While this limitation also applies to the reverse-genetics approach, it is amplified in degenerate PCR as there are two distinct sites at which excess degeneracy can occur. This is less of a problem in organisms, such as Streptomyces, with DNA rich in guanosine (G) and cytosine (C). In these organisms, the third (or "wobble") position of codons is heavily biased towards these two nucleotides.

Of the predicted enzymes in the A47934 biosynthetic cluster, none of those specific to the pathway were part of a well-defined gene family. While peptide synthetases are well defined, organisms closely related to *S. toyocaensis* NRRL 15009

have been shown to utilise several of these enzymes in pathways independent of antibiotic biosynthesis (13). These organisms produce several secondary metabolites, such as siderophores, pigments, and sporulation factors, all of which could be synthesised by peptide synthetases. The modular nature of these genes also complicates matters, as degenerate primers specific for one domain in a given module would amplify that domain in every module in that peptide synthetase, as well as in every module of every other peptide synthetase in the genome. While dozens of PCR products could be cloned, substrate specificity cannot as yet be determined by primary sequence, and those affiliated with A47934 biosynthesis could not be distinguished. The same problem existed with using degenerate PCR to try and clone a portion of the putative PKS, which bears significant similarity in its conserved regions to FASs. Other enzyme activities like monooxygenase and haloperoxidase are catalysed by diverse classes of enzymes, and thus were poor candidates. Racemases, transaminases and dehydrogenases are common in primary metabolism and were not specific enough targets.

One well defined family which catalyses a very specific reaction is D-Ala-D-Ala ligase (Ddl) (6). Ddl genes have been cloned from many organisms, are specific to cell wall synthesis pathways and were the anticipated mode of resistance in GPA-producing organisms. The Ddl in *S. toyocaensis* NRRL 15009 was predicted to have altered specificity, synthesising D-Ala-D-X, where X is some unknown, perhaps discrediting it as a candidate for degenerate PCR. However, other ligases with altered specificity, including VanA, which uses D-lactate (D-lact), and VanC, which uses D-serine, aligned well with the strictly D-Ala ligases, and specific regions were highly conserved across all

classes of Ddl (6). Thus, a *ddl* gene became the target of a cloning strategy using a degenerate PCR approach, with the goals of 1) elucidating the mechanism of GPA resistance in GPA producing organisms and 2) identifying A47934 biosynthesis genes which may be flanking the GPA resistance gene(s).

This chapter describes the cloning of a partial *S. toyocaensis* NRRL 15009 *ddl* gene using degenerate PCR, and its use to construct and screen a sub-genomic library. The *Bam*HI fragment cloned from *S. toyocaensis* NRRL 15009 contained elements very similar to those found in the VanA/B phenotypes of *Enterococcus*. However the cluster was incomplete and further cloning was based on a partial *vanX* gene, also made by degenerate PCR. In the 8.1 kilobase pairs (kb) of chromosomal DNA cloned and analysed, several genes were discovered including homologues of *vanH*, *vanA* and *vanX* arranged in an identical manner as in VRE. Furthermore, a similar cluster was found on a 3.5 kb *Bam*HI fragment cloned from *A. orientalis* C329.2, the producer of vancomycin. Both Southern blotting and PCR experiments provided evidence for similar clusters in other GPA-producing organisms. Interestingly, some closely related, but non-GPA producing, organisms also had these genes. Unfortunately, no A47934 biosynthesis genes were found flanking the immediate regions in either *S. toyocaensis* NRRL 15009 or *A. orientalis* C329.2.

5.2 Materials

A. orientalis C329.2 was a gift from Dr. R. Baltz of Eli Lilly. *A. orientalis* 18098, *A. orientalis* subsp. *lurida* and *A. coloradensis* subsp. *labeda* were purchased from the

American Tissue Type Collection (ATCC). *Streptomyces griseochromatogenes, S. argenesis* and *S. gougerotii* chromosomal DNA samples were a gift from Dr. Astrid Petrich. *S. fradiae* was a gift from Dr. Julian Davies.

Proteinase K and RNase were from Boehringer Mannheim. Phenol was obtained from Anachemia. BSA and salmon sperm DNA were purchased from Sigma. SDS and agarose were from Bioshop. *Taq* polymerase, Klenow fragment, calf intestinal alkaline phosphatase (CIAP), T4 DNA ligase and all restriction endonucleases were purchased from MBI Fermentas. Nucleotides were purchased from NEB. [^{32}P]-dATP was made by DuPont. Nylon and nitrocellulose membranes were from Hybond. Hybridization tubes and incubator were made by TekStar.

Oligonucleotide primers were made by the MOBIX Central Facility at McMaster University. QuiexII kits were purchased from Qiagen. pGEMT kits and the plasmid vector pGEM-7Z were obtained from Promega, while competent *E.coli* SURE cells and the plasmid vector pBluescript II KS+ were from Stratagene. The nested deletion kit was obtained from Pharmacia.

The software used to analyse DNA sequences, including Editseq, Mapdraw, Megalign and Seqman was part of the DNAStar Package by Lasergene. Phylogenetic analysis was calculated by the Clustal W method (19) and was accessed at the url http://www2.ebi.ac.uk/clustalw/. The trees were generated with the program TreeView obtained at http://taxonomy.zoology.gla.ac.uk/rod/treeview.html. Homology searches were done using the Basic Local Alignment and Search Tool (BLAST) service provided by NCBI at http://www.ncbi.nlm.nih.gov/.

5.3 Methods

5.3.1 Media and Buffers

SET buffer contained 20 mM Tris pH 7.5, 75 mM NaCl, and 25 mM EDTA pH 8. TE buffer contained 10 mM Tris pH 8.0, 1 mM EDTA pH 8.0. TE-RNase contained TE + 50 µg/mL RNase. Proteinase K solution contained 20 mg/mL proteinase K in water. SDS solution contains 10% SDS in water. Buffered phenol was melted phenol extracted with 500 mM Tris pH 8.0 until neutral, at which time it was extracted twice more with 50 mM Tris pH 8.0. TAE contained 40 mM Tris-acetate pH 8.5, 2 mM Na_2EDTA. *Taq* buffer contained 10 mM Tris-HCl pH 8.8, 50 mM KCl, and 0.08% Nonidet P40. Klenow buffer contained 10 mM Tris-Cl, pH 7.5, 5 mM $MgCl_2$, 7.5 mM DTT. Hybridization buffer contained 250 mM Na_2HPO_4 pH 7.2, 3.5% SDS, 1 mM EDTA and 5 mg/mL bovine serum albumin (BSA). Low stringency buffer contained 40 mM Na_2HPO_4 pH 7.2, 5% SDS, 1 mM EDTA and 5 mg/mL BSA. High stringency buffer contained 40 mM Na_2HPO_4 pH 7.2, 1% SDS, and 1 mM EDTA. Luria broth (LB) contained 10 g tryptone, 5 g yeast extract and 10 g NaCl per litre.

Penassay Broth (PAB) was made from powder as described by the manufacturer. SMM contained 0.5 M sucrose, 10 µM maleic acid and 10 µM $MgCl_2$. SOC (500 mL) contained 10 g tryptone, 2.5 g yeast extract, 0.3 g NaCl, 0.1 g KCl, 1 g $MgCl_2 \bullet 6H_2O$, 0.6 g $MgSO_4$ and 1.8 g glucose.

5.3.2 Isolation of Genomic DNA from GPA-Producing and Related Organisms

The following procedure is given in detail, as adherence to these details is required for the procedure to work. Total DNA was isolated from GPA-producing and related organisms using a modified version of the Salting-Out Procedure, a method developed by Pospiech and Neumann in an unreleased new edition of the Streptomyces Laboratory Manual (8). Mycelia were grown at 30 °C, 275 rpm in baffled flasks to late log phase in SAM media supplemented with glycine to 0.5%. This corresponded with approximately 48 hours of growth after inoculation of media with either 1% vol/vol freshly saturated culture or 0.2% vol/vol spore suspension. Mycelia (1.0-1.2 g for every 50 mL of culture) were harvested by centrifugation (6,000 x g, 20 min, 4 °C) and washed with TE containing 10% glycerol before freezing in 1.0-1.2 g aliquots. Prior to lysis, cells were suspended in SET buffer, homogenised in a ground glass homogeniser and centrifuged as before. Mycelia (1.0-1.2 g) were suspended thoroughly in SET buffer to 10 mL in a clear glass Universal bottle, allowed to warm to 25 °C and 400 µL of lysozyme solution was added. Mixtures were triturated (mixed by pipetting) constantly for first 2 minutes and then allowed to react with only occasional swirling until noticeably viscous (5 to 30 minutes, depending on the strain. See Table 5.1). Proteinase K solution (280 µL) and SDS solution (1.2 mL) were added and mixed in by gentle inversion, and the mixture allowed to incubate at 55 °C for 2 hours with occasional gentle mixing by inversion. After cooling to RT, the mixture (extremely viscous) was extracted with 5 mL buffered phenol solution for 10 min, 5 mL of chloroform added and

extracted further for 10 min. All extractions were performed in resistant tubing sealed with an O-ring and taped down to a test tube rocker at a 45° angle to the tilt plane to minimise shearing. Tube capacity was never more than twice the sample volume. The aqueous phase was recovered by centrifugation at 6000 x g, 20 min at RT in a clear glass tube. Wide bore pipettes and slow, even pipetting were required to remove the aqueous phase without disturbing the interface. The aqueous phase was warmed to $55^{O}C$ and 5 M NaCl added to 1.25 M final. Solution was gently mixed and allowed to equilibrate 5 minutes, and then allowed to cool to $37^{O}C$ over a 10-minute period. The mixture was extracted with 10 mL of chloroform for 30 min at RT and the aqueous phase recovered as described above. This was transferred to a clear glass bottle and 0.6 volumes of isopropanol added. Gently mixing by inversion took several minutes, after which chromosomal DNA was readily spooled onto a sealed Pasteur pipette. At this juncture, multiple aliquots were pooled by spooling onto the same rod. DNA was rinsed in 70% ethanol 5 minutes, allowed to air dry to near completion and allowed to incubate overnight on the pipette in a solution of 1-2 mL TE-RNase buffer per gram of mycelia lysed. DNA was gently dislodged from rod and incubated several hours at $37^{O}C$ to dissolve. DNA required several days incubation at $4^{O}C$ to dissolve completely. Absorbance at 260 nm was not an accurate method of quantifying chromosomal DNA due to contaminant RNA. Samples were subject to electrophoreses through 0.5 % TAE-agarose along with known quantities of plasmid DNA and compared visually after ethidium bromide staining and UV-light illumination. Samples were stored at $4^{O}C$ and aliquots removed with wide-bore autoclaved tips only.

Table 5.1. Lysis Times of Various Actinomycetes

Organism	Lysis Time (min)
S. toyocaensis NRRL 15009	7
A. orientalis C329.2	10
A. orientalis 18098[1]	30
A. orientalis subsp. *hirida*	6
A. coloradensis subsp. *labeda*	15
S. coelicolor	12
S. lividans 1326	15
S. fradiae	10

[1]Culture not grown in glycine-supplemented media, which accelerates lysis.
Some batch-wise variation observed in lysis times.

5.3.3 Synthesis of Gene Fragments using Degenerate PCR

Degenerate PCR primers were designed by analysis of Clustal W-aligned primary

sequences encoded by the target gene family, either *ddl* or *vanX*. Analysis of *ddl* gene

products was greatly facilitated by a very thorough study conducted by the Courvalin

group (6). Regions that bore a minimum of 5 consecutive conserved amino acids were

considered. Forward and reverse primers were evaluated in their own categories based

on degeneracy of the amino acids using Streptomyces codon usage preferences (21).

Those with the least amount of degeneracy were selected and in the case when equal

amount of degeneracy were present, then the primers were selected based on the greater

length of amplification product generated (i.e. the primer closest to the end of the gene).

No primer pairs giving products less than 200 base pairs (bp) or greater than 1500 base

pairs were considered (Table 5.2). Primers were also evaluated for annealing

temperature using the equation:

$$T_n = 81.5 + 0.41(\%G+C) - (675/N) - \%mismatch \quad (2)$$

where %G+C is the percentage of the sum of guanosines and cytosines in the sequence

and N is the total length of the primer. Due to the degeneracy, a single T_m cannot be

calculated, so the (%G+C) of all of the primers was average. A zero percentage of

mismatch was assumed. Primers used had a minimum average T_m of $50\,^{O}C$.

Table 5.2. Degenerate PCR Primers Constructed

Primer Name	DNA Sequence (5' →3')	Consensus Primary Sequence	Target Protein	Enzymes Compared
ddl5'deg	GGIGAGGACGGI (T/A)(C/G)I(C/A)TI CAGGG	GEDGAMQG	Ddl	*E. coli* DdlA *E. coli* DdlB *E. faecium* VanA
ddl3'deg	GTGAAICC(G/C)G GIA(T/G)IGTGTT	NT(L/I)PGFT		*E. faecium* VanB
vanX5'deg	CA(T/C)TC(G/C)CG IGGI(T/A)C(C/G)(A/G)C(C/G)ATCGAC	HSRG(S/T)(A/T)ID	VanX	*E. coli* VanX *E. faecium* VanXA *E.faecium* VanXB
vanX3'deg	G(T/A)AGTGCCAC CA(T/C)T(T/C)	EWWHY		

The designation 5' and 3 correspond to forward and reverse primers, respectively.

All PCR reactions (100 μL) contained 500 ng of chromosomal DNA template, 1

μM of each primer, 1X *Taq* buffer, 0.4 mM of each dNTP, and 2 U of *Taq* polymerase.

In addition, reactions contained either 0, 2 or 4 mM $MgCl_2$ and either 0 or 5%

dimethylsulfoxide (DMSO) as outlined in Table 5.3. Reactions were cycled 35 times

with an initial annealing temperature of $50\,^{O}C$, however the latter was adjusted

empirically depending on the number of non-specific products generated and the relative

amount of the target fragment. Reactions were evaluated by TAE-agarose

electrophoresis of a portion of the sample. Reactions that gave a sufficient amount of the

desired product were separated by preparative TAE-agarose electrophoresis, the desired

product excised and purified using a QuiexII DNA purification kit. These were ligated to the pGEMT plasmid vector and transformed into a competent strain of *E. coli*. Some strains of *E. coli*, such as XL1-Blue, were not capable of hosting the actinomycete DNA, however the SURE strain was found to be a suitable host. Isolated clones found to contain the degenerate PCR product were sequenced on both strands using primer sites in the plasmid vector. Cycle sequencing was performed on an Applied Biosystems automated DNA sequencer by Dr. Brian Allore of the MOBIX central facility at McMaster. DNA sequences were analysed using the program EditSeq. Database searches were done using the NCBI service BLAST.

Table 5.3 Reaction Conditions for Various Degenerate PCR Products

Organism	Target Gene(s)	Primers	Product Length (bp)	Mg^{2+} (mM)	DMSO (%)	Annealing Temperature (^{O}C)
S. toyocaensis NRRL 15009	*ddl*	ddl5'deg ddl3'deg	600	2	5	50
S. toyocaensis NRRL 15009	*vanX*	vanX5'deg vanX3'deg	350	2	0	48
A. orientalis C329.2	*ddl-vanX*	ddl5'deg vanX3'deg	1300	2	5	50

Gene fragments were used as templates to make [^{32}P]-dATP labelled oligonucleotide probes for use in constructing and screening sub-genomic libraries of GPA-producing organisms. Template (200 ng) was mixed with 1 μL of each degenerate PCR primer, made to 40 μL, heat denatured and then rapidly chilled to 0 ^{O}C. To this, a mixture of 1X Klenow buffer, 1 mM of each of dGTP, dCTP, dTTP, 30 μCi of [^{32}P]-dATP and 10 U of the Klenow fragment was added to a final volume of 60 μL. After 1 hour at 37 ^{O}C, 8 μg of salmon sperm DNA was added and the mixture precipitated with

ammonium acetate and ethanol. The pellet was washed with 70% ethanol, dried and

suspended in 50 μL cdH$_2$O. A sample (2 μL) was assayed in a scintillation counter and

typically gave 0.5 x 10^6 cpm/μL.

5.3.4   Cloning of an 8.1 kb ddl-containing Fragment from S. toyocaensis NRRL 15009

S. toyocaensis NRRL 15009 chromosomal DNA (10 μg) was digested to

completion with a variety of different restriction endonucleases (in separate experiments)

in 100 μl reaction volumes. Restriction endonucleases all recognised hexamer DNA

sequences and varied in their G+C content. Digestion products were precipitated with

sodium acetate and ethanol, suspended in 10 μL, and run out at reduced current on a

TAE-agarose gel. Products were visualised by ethidium bromide staining and

photographed next to a ruler. Products were then transferred to a nylon membrane

(Hybond N+) by standard alkaline transfer methods (2).

Chromosomal fragments containing the *ddl* gene were identified by hybridisation

to a radiolabelled *ddl* gene probe in the following manner. The nylon blot was incubated

in hybridisation buffer for one hour at 65 ^{O}C and then replaced with fresh buffer (5 mL).

[^{32}P]-labelled *ddl* probe (2.5 x 10^6 cpm) was boiled with 200 μL of salmon sperm (4

mg/mL) for 10 min, rapidly chilled to 0 ^{O}C, and hybridised to the blot overnight at 65 ^{O}C

with constant mixing. The blot was washed twice with low stringency buffer (25 mL) for

10 min at 25 ^{O}C and then twice with high stringency buffer (25 mL) for 10 min at 65 ^{O}C.

The blot was exposed to Kodak film overnight at –80 ^{O}C, developed and the approximate

sizes of the *ddl*-containing digestion products were determined by aligning the labelled

bands with the standards in the photograph based on the distance travelled from the loading wells. A 3.6 kb *Bam*HI fragment was identified as a suitable candidate for cloning.

The following procedures for the construction and screening of a sub-genomic library are standard molecular biology techniques (2). A *Bam*HI digestion of chromosomal DNA was performed and reaction products separated out exactly as before. All fragments spanning 3.3 to 3.9 kb were excised, gel purified and ligated to pGEM-7Z (Stratagene) that had been treated with *Bam*HI and CIAP. Ligation products were transformed into *E. coli* SURE competent cells and plated on LB-ampicillin (100 μg/mL). Colonies (approximately 600) were transferred to nitrocellulose filters and treated with sodium hydroxide to lyse the cells. Released DNA was immobilised by UV light treatment and the filters were subject to pre-hybridisation, hybridisation and washing as before, however larger volumes were required for full immersion. Exposure to film allowed the identification of 2 clones carrying the *ddl*-containing *Bam*HI fragment. Isolation of recombinant DNA from the host and hybridisation of radiolabelled probe to a Southern blot confirmed the identity of positive clones.

Preliminary sequencing of the *Bam*HI fragment from the primer sites in the plasmid vector revealed that the *ddl* gene was incomplete at the 3' end. This necessitated construction of a subsequent sub-genomic library made from *Sac*I fragments cloned into the plasmid vector pBluescript II KS+, and the isolation of a 3.0 kb fragment that contained the *ddl* gene.

The discovery of an incomplete *vanX*-like gene 3' to the *ddl* required once again that more downstream sequence be cloned out of *S. toyocaensis* NRRL 15009. Degenerate PCR was used to clone a section of the *S. toyocaensis vanX* gene and this was used to isolate a 5.2 kb *Pst*I fragment in the same manner that the *Bam*HI and *Sac*I fragments were obtained. Upon analysis, no further upstream or downstream genetic information was required.

5.3.5 Cloning of a 3.5 kb ddl-containing Fragment from A. orientalis C329.2

Degenerate PCR was used to produce a gene fragment that spanned the *ddl* and *vanX* genes in the vancomycin producer *A. orientalis* C329.2. As in *S. toyocaensis* NRRL 15009, Southern Blotting was used to identify a 3.5 kb *Bam*HI fragment containing these genes, and this fragment was isolated from a sub-genomic library made in pGEM-7Z. Initial attempts to clone a 7.0 kb *Eco*RI fragment met with repeated failure, and even the shorter *Bam*HI fragment was poorly hosted by the SURE cells it was grown in. In order to obtain a sufficient amount of the *Bam*HI fragment for sequencing analysis, the recombinant had to be introduced and amplified in *E. coli* DH5α strain. Preliminary sequencing indicated that the entire genes were encoded on the *Bam*HI fragment.

5.3.6 Sequencing and Analysis of Large Gene Clusters

The 3.6 kb *Bam*HI fragment cloned from *S. toyocaensis* NRRL 15009 was sequenced by making nested deletions from one end using exonuclease III (Nested Deletion Kit). The *Sac*I and *Pst*I fragments were sequenced by the synthesis of specific primers, which was facilitated by the knowledge of the sequence in the region amplified

by degenerate PCR. The 3.5 kb *Bam*HI fragment from *A. orientalis* C329.2 was also

sequenced by primer walking. DNA cycle sequencing reactions were performed by Dr.

Brian Allore. Sequencing required good overlap due to the frequency of compressions

and general ambiguity in certain sections caused by the G/C rich nature of the DNA.

Primary sequencing data was carefully edited to minimise errors. The program SeqMan

was used to assemble individual sequence runs into one contiguous DNA sequence (a

contig). Match size was set to 12 residues with a minimum match percentage of 85%.

Consensus threshold was 75% (ie. a minimum of 3 out of 4 residues must agree). The

consensus sequence of the assembled contig was analysed by MapDraw for ORFs

allowing both ATG and GTG as start codons, and the usual TGA, TAG and TAA was

recognised as stop codons. One limitation of the software which resulted in

complications was the inability to recognise ORFs that were not completely defined on

the contig (ie. the 5' end or the 3' end was off the edge of the sequenced region of the

chromosome). All ORFs were analysed further by comparison of the primary amino acid

sequence encoded with all others registered in the non-redundant database using BLAST.

Those ORF primary sequences that registered significant homology (probability of

coincidence value less than 10^{-2}) with some other protein sequence were considered as

possible genes. The primary sequence was then aligned with the two or three most

similar sequences using the program MegAlign. Alignment was by the Clustal W

method, version 1.7, using the Blosum matrix with a gap penalty of 10 and a gap

extension of 0.05 (19). In addition to demonstrating phylogenetic relationships, this

proved useful for identifying frameshift errors in the sequencing. The final annotated

nucleotide clusters were entered into Genbank. Although the three fragments cloned

from *S. toyocaensis* NRRL 15009 are contiguous, the *Pst*I fragment was registered under

its own accession number AF039028, while the remainder has the accession number

U82965. The *A. orientalis* C329.2 gene cluster has the accession number U83170.

5.3.7 Detection of van Genes in Chromosomal DNA Preparations of Various GPA-Producing Organisms

Southern blotting of restriction endonuclease-digested chromosomal DNA from

various GPA-producing organisms was performed essentially as done using *S.*

toyocaensis DNA, except that *Bam*HI was the only enzyme used. The probe for the blot

was made using the *A. orientalis* C329.2 *Bam*HI fragment as template in a Klenow

reaction primed using the *ddl* degenerate primers (ddl5'deg and ddl3'deg).

5.3.8 PCR Screen for van Genes in Various GPA-Producing Organisms and Closely Related GPA Non-Producers

To determine the prevalence of the *vanHAX* gene cluster motif in a variety of

organisms, a *vanH* forward primer (vanH5') was designed to be used in conjunction with

the vanX3'deg reverse primer. This forward primer was designed based on alignments of

the *vanH* gene from *S. toyocaensis* NRRL 15009, *A. orientalis* C329.2, and the recently

discovered *S. coelicolor van* gene clusters (Cosmid SC66T3). The sequence (5'-

TGCACGACTACCGGCTGA-3') is near the middle of the gene and is not a formally a

degenerate primer as there is no sequence variation. PCR reactions (100 μL) contained

500 ng chromosomal DNA, 1 μM vanH5' primer, 1 μM vanX3' primer, 1X *Taq* buffer, 2

or 4 mM MgCl$_2$, 5% DMSO, 0.4 mM of each dNTP, and 2 U *Taq* polymerase. Reactions

were incubated at 94 $^{\circ}$C, 55 $^{\circ}$C and 72 $^{\circ}$C for 1.5 minutes at each temperature for 40

cycles. Reaction products were separated out on a 1% TAE-agarose gel.

5.3.9 Expression of A. orientalis C329.2 van Genes in B. subtilis DB104

The *van* genes of *A. orientalis* C329.2 were cloned downstream of the

constitutive promoter *vegII* in the *E. coli/B. subtilis* shuttle vector pRB374 (4) using Vent

PCR. The forward primer was designed to incorporate a *Bacillus* Shine-Delgarno

sequence 9 bp upstream of the *vanH*$_{Aov}$ start codon. Both primers incorporated restriction

endonuclease sites to facilitate cloning behind the *vegII* promoter. Reactions (100 μL)

contained pGEMC329vn3.5 (500 ng), 1 μM forward primer (5'-

CCCAAGCTTAAGGAGTGTCGGGCATGACCTACAGCGAACCAGCG- 3'), 1 μM

reverse primer (5'- CGGGATCCCTACTCGATGGGAAAATCCAA -3'), 1X Vent

buffer, 5% DMSO, 0.4 mM each dNTP, 2 mM additional MgSO$_4$ and 2 U Vent DNA

polymerase. Reactions were cycled 25 times at 94, 52, and 72 $^{\circ}$C for 0.5, 0.5 and 3.0 min

respectively. The amplified 2.7 kb product was purified with a QuiexII kit and digested

with *Hind*III and *Bam*HI by standard methods. Digestion products were separated in

TAE-agarose (1%) and the large fragment purified by QuiexII. This was ligated by

standard methods to similarly digested pRB374. Ligation products were transformed into

E. coli JM109 cells, plated onto LB-ampicillin and clones containing the *Bam*HI

fragment identified by RFLP (Restriction Fragment Length Polymorphism) of mini-lysate

plasmid DNA. Purified pRBC329vn2.7 was transformed into *B. subtilis* DB104 using a

previously described electroporation method (9). Cells were grown from a fresh

overnight culture to an O.D.$_{600}$ of 0.5 in PAB (100 mL) and harvested at 4 ^{O}C. After

three washings with cold SMM, cells were suspended in 0.9 mL SMM and kept on ice.

Cell aliquots (200 μL) were allowed to warm to RT for 1 min before addition of DNA (4

μg, supercoiled, in no more than 10 μL of salt-free water). Samples (50 μL) of this

mixture were added to 0.1 cm gap cuvettes and electroporated at various capacitance,

voltage and resistance. Immediately after electroporation, 1 mL of SMM:SOC (1:1) was

added and cells allowed to recover for 2 hours at 37 ^{O}C. The entire sample was gently

spread onto PAB-kanamycin (25μg/ml) to select for recombinants. Optimal

transformation occurred using a capacitance of 3.0 μF, a voltage of 2.5 kV and a

resistance of 400 ohms (time constant was 1.1 ms), which produced 52 colonies of

DB104/pRBC329vn2.7. One colony was selected for assay of vancomycin resistance.

Resistance to vancomycin of DB104/pRBC329vn2.7 and the control

DB104/pRB374 was determined by growth in liquid culture and on agar in the presence

of various quantities of vancomycin. Liquid cultures (3 mL) of LB-kanamycin containing

various amounts of vancomycin (ranging from 0 to 50 μg/mL) were inoculated with 1%

vol/vol freshly saturated culture and grown for 12 hours. Agar cultures were spread on

LB-kanamycin, and various amounts of vancomycin (ranging from 0 to 5 μg/mL) applied

to cotton disks laid on the surface. These were grown for 16 hours. In addition, the same

experiments were done supplementing the media with D-lactate to 10 mM final

concentration.

5.4 Results and Discussion

5.4.1 Isolation of Genomic DNA from GPA-Producing and Related Organisms

Several different methods of chromosomal DNA isolation from *S. toyocaensis* NRRL 15009 were attempted before the Salting-Out Procedure was employed. Using the procedure in its unmodified version gave chromosomal DNA in low yield and of poor quality. Homogenisation and washing of the mycelia in buffers containing EDTA was essential to remove nucleases prior to lysis, and a phenol step greatly improved the quality of the preparation. Yields from *S. toyocaensis* NRRL 15009 (approx. 0.1 mg/g mycelia) were still about an order of magnitude lower than those obtained from other actinomycetes. Genomic DNA samples took days to dissolve, required warming and wide bore tips for dispensing, and took a long time (and warming) before dissolving into reaction mixtures such as restriction digests. Samples were viscous even at high dilutions, and difficult to aliquot evenly.

5.4.2 Synthesis of Gene Fragments using Degenerate PCR

The 600 bp *ddl* gene fragment cloned from *S. toyocaensis* NRRL 15009 would only amplify in the presence of 5% DMSO, and slightly preferred 2 mM over 4 mM MgCl$_2$ in the reaction. The *vanX* gene fragment, on the other hand, required 2 mM MgCl$_2$ and somewhat less non-specific reaction products were produced in 0% DMSO than in 5%. The 1.3 kb fragment spanning these genes in *A. orientalis* C329.2 had very specific requirements of 2 mM MgCl$_2$ and 5% DMSO. Thus, there was little rationale to the conditions required to obtain amplification, and optimisation was always required.

5.4.3 Cloning of an 8.1 kb ddl-containing Fragment from S. toyocaensis NRRL 15009

Hybridisation of the restriction endonuclease digestion products of *S. toyocaensis*

NRRL 15009 chromosomal DNA with the *ddl* gene probe revealed that most of the

enzymes used did not cut (Figure 5.1, A). Many of the enzymes initially selected

recognised A-T rich sequences, in the hope that large fragments could be obtained. A 3.6

kb *Bam*HI fragment was the only option at this juncture. A second *Bam*HI band of

approximately 0.7 kb appeared to hybridise to the probe. At the time, it was interpreted

as a distinct ligase of lesser homology as the sequence obtained for the 600 bp *ddl* gene

probe did not contain any *Bam*HI sites. Upon cloning of the 3.5 kb fragment, however, it

was discovered that the enzyme did in fact cut internal to the gene and the 3' end was

missing. As the probe fragment was generated by *Taq* PCR, it presumably mutated
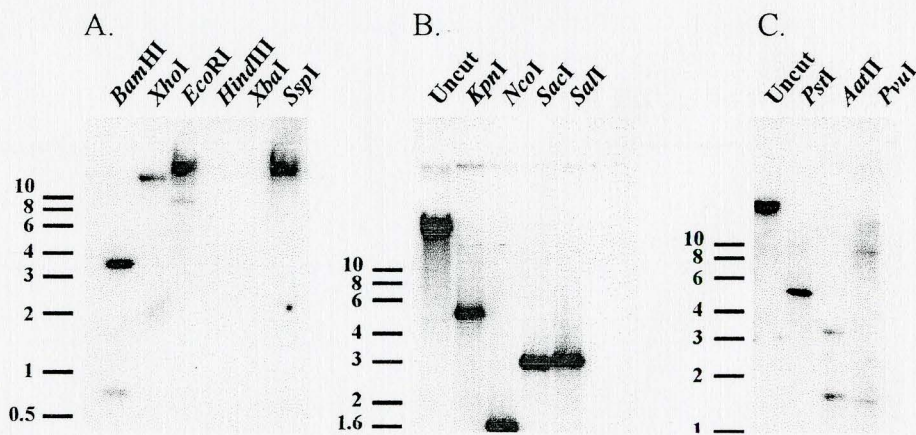
Figure 5.1. Southern Blot Analysis of *S. toyocaensis* Chromosomal DNA Digestion Products. Blots were probed using ^{32}P-labelled gene fragments amplified by degenerate PCR. See Methods.

during amplification. A second blot (Figure 5.1, B) was generated and a 3.0 kb *Sac*I fragment cloned. Analysis of this fragment indicated a *vanX* downstream of the *ddl* that was also missing its 3' end. Thus a 5.2 kb *Pst*I (Figure 5.1, C) fragment that hybridised to a *vanX* gene probe (made similarly to the *ddl* probe by degenerate PCR) was identified and cloned. In this manner, 8.1 kb of the *S. toyocaensis* NRRL 15009 chromosome was isolated and analysed.

What was discovered was unexpected and remarkable. In total, eight distinct genes were identified by comparing the primary sequences encoded by ORFs with those in the non-redundant protein database (Table 5.4). As had been suggested by the sequencing data generated from the 600 bp *ddl* probe, *S. toyocaensis* NRRL 15009 contained a ddl similar to the VanA/B class of VRE. It was not until the entire *ddl* gene and its surrounding DNA had been sequenced, however, that the level of similarity was revealed. The protein encoded by the *S. toyocaensis ddl*, named DdlM, was more homologous to the VanA/B enzymes than any other ddl for which the primary sequence was known (Table 5.5). In addition, *ddlM* was flanked by *vanH* and *vanX* genes (named *vanH$_{St}$* and *vanX$_{St}$*) that encoded proteins with similar levels of homology to their respective VRE enzymes. The genes were found in an identical arrangement as in VRE (Figure 5.4), with *vanH$_{St}$* at the 5' end followed by *ddlM* and then *vanX$_{St}$*. As in the VRE clusters, the 5' end of *ddlM* was nested in the 3' end of *vanH$_{St}$*. None of the other *van* genes usually associated with VRE (namely *vanR, vanS, vanW, vanY* and *vanZ*) were found. A gene encoding a D-Ala-D-Ala adding enzyme (*murF$_{St}$*) and a gene involved in assembling glycine bridges in peptidoglycan cross-links (*femA$_{St}$*) were upstream of the

van cluster, while a protein of unknown function (*orf1*), a cold shock protein (*csp1*) and a

putative transcriptional regulator (*tr1*) were encoded downstream. Unfortunately, none

of these genes are expected to be involved in A47934 biosynthesis.

Table 5.4. Genes Present on 8.1 kb *S. toyocaensis* Chromosomal Fragment

Gene	Location on 8.1 kb Chromosome Fragment	Length (bp)	Percent G/C
femA$_{St}$ (partial)	0→294	294	71
murF$_{St}$	307←1638	1332	73
vanH$_{St}$	1766→2758	993	65
ddlM	2746→3768	1023	65
vanX$_{St}$	3800→4408	609	66
orf1	4604→6190	1587	69
csp1	6280←6483	204	64
tr1(partial)	8051→8131	81	62
total	0 — 8131	8131	68

Table 5.5. Proteins Encoded by Genes on 8.1 kb Fragment

Protein	Primary Sequence	Reading Frame	Most Homologous protein(s)[1]	Percent Similarity[2]
FemA$_{St}$ (partial)	...RRGH.	1 (for)	*S. coelicolor* SCH24.26c	57
			Treponema pallidum FemA	39
MurF$_{St}$	MIPL... AGLA.	2 (rev)	*M. tuberculosis* MurF	40
			E. coli MurF	31
VanH$_{St}$	MTHS... AWPD.	2 (for)	*E. faecium* VanH	54
			E. faecalis VanHB	52
DdlM	MARL... VSSL.	1 (for)	*E. faecium* VanA	63
			E. faecalis VanB	68
VanX$_{St}$	MTDG... FPIM.	2 (for)	*E. faecium* VanX	64
			E. faecalis VanXB	65
Product of orf1	MTVF... IDA.	2 (for)	*M. tuberculosis* RV2752c	51
			Corynebacterium glutamicum 69.1 kDa protein	47
Csp1	MATG... INLA	2 (rev)	*S. coelicolor* SCOF	87
			S. clavuligerus CSP7.0	77
Tr1 (partial)	MQVP...	2 (for)	*S. coelicolor* SCH35.02	78
			M. tuberculosis RV0081	63

[1]As determined by BLAST analysis as of May, 1999.
[2]As determined by Clustal W alignment.

The immediate implication of finding a *van*-like cluster was that *S. toyocaensis* NRRL 15009 employed a similar mechanism of GPA resistance as VanA/B VRE, differing perhaps in the mechanism of regulation as no *vanR* or *vanS* genes were nearby. The presence of a VanH (D-lactate dehydrogenase) and the similarity of DdlM to the VanA/B ddl suggest that this ligase uses D-lactate to form depsipeptide, rather than dipeptide as had been anticipated. The presence of a VanX suggested that resistance was induced and that D-Ala-D-Ala was incorporated prior to induction. This result also suggested that VRE may have acquired its resistance genes from a GPA-producing organism. However, as only one GPA producer had been examined, it seemed premature to draw such an inference without determining the prevalence of this gene cluster in GPA-producing organisms.

5.4.4 Cloning of a 3.5 kb ddl-containing Fragment from A. orientalis C329.2

A 3.5 kb *Bam*HI fragment was cloned from *A. orientalis* C329.2, the organism which produces vancomycin, using a degenerate PCR probe designed to span adjacent *ddl* and *vanX* gene homologues. This fragment was also found to contain the *van* gene homologues *vanH_{Aov}*, *ddlN* and *vanX_{Aov}* (Table 5.6 and 5.7). These genes encoded enzymes that were very similar to their respective *S. toyocaensis* NRRL 15009 counterparts (69-73%), and about equally similar to the VRE proteins (56-62%). They also were arranged exactly as the *S. toyocaensis* NRRL 15009 and VRE genes (Figure 5.4). No additional genes were found flanking the *A. orientalis* C329.2 *van* genes, although only an additional 800 bp of DNA was sequenced.

Table 5.6. Genes Present on 3.5 kb *A. orientalis* C329.2 Chromosomal Fragment

Gene	Location on 3.5 kb Chromosome Fragment	Length (bp)	Percent G/C
vanH$_{Aov}$	534→1580	1047	60
ddlN	1568→2614	1047	66
vanX$_{Aov}$	2604→3212	609	65
total	1 – 3470	3470	65

Table 5.7. Proteins Encoded by Genes on 3.5 kb Fragment

Protein	Primary Sequence	Reading Frame	Most Homologous proteins[1]	Percent Similarity[2]
VanH$_{Aov}$	MTYS...VWVG.	3 (for)	*S. toyocaensis* VanH$_{St}$	69
			E. faecium VanH	61
			E. faecalis VanHB	56
DdlN	MGRL...TNEG.	2 (for)	*S. toyocaensis* DdlM	73
			E. faecium VanA	59
			E. faecalis VanB	62
VanX$_{Aov}$	MRDD...FPIE.	3 (for)	*S. toyocaensis* VanX$_{st}$	73
			E. faecium VanX	61
			E. faecalis VanXB	61

[1] As determined by BLAST analysis as of May, 1999.
[2] As determined by Clustal W alignment.

These findings further supported the implication that VRE resistance genes may

be derived from GPA-producing organisms. Again, however, only two GPA producing

organisms had been tested.

5.4.5 Detection of van Genes in a Variety of GPA-Producing and Related Non-Producing Crganisms

In order to determine the prevalence of the *van* gene cluster in a rapid and

convenient manner, Southern blotting and degenerate primer PCR was performed on

chromosomal DNA preparations from a variety of different organisms. Using a *ddl* probe

constructed from the *ddlN* gene (Figure 5.2), homologues of *vanA* were detected in

*Bam*HI-digested chromosomal DNA from *Amycolatopsis* strains that produce the GPAs

chloro-eremomycin (*A. orientalis* 18098), ristocetin (*A. orientalis* subsp. *lurida*), and

both teicoplanin and avoparcin (*A. coloradensis* subsp. *labeda*).
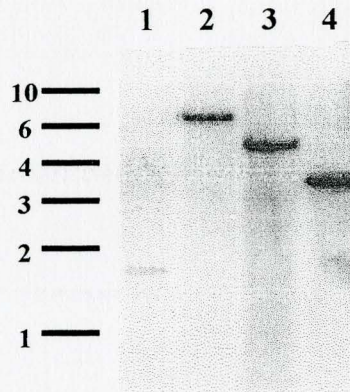
Figure 5.2. Detection of van Genes in Various GPA-Producing Organisms. *Bam*HI **digestion products of** *A. orientalis* **18098 (lane 1),** *A. orientalis* **subsp.** *lurida* **(lane 2),** *A. coloradensis* **subsp.** *labeda* **(lane3) and** *A. orientalis* **C329.2 (lane 4).**

Degenerate PCR using a forward primer that binds in the *vanH* gene and a reverse

primer that binds in the *vanX* gene produced the predicted 2.2 kb products in reactions

containing chromosomal DNA from all of these organisms (Figure 5.3). This indicated

that not only were the genes present in the chromosome, they were present in the same

arrangement as in *S. toyocaensis* NRRL 15009 and VRE. Therefore, from this limited

study, it appeared that the *van* gene cluster was well-conserved and also well-distributed

amongst GPA-producing organisms, and could very well have been the original source of

the resistance genes employed by clinically relevant VRE. The average G/C content of

these genes in *S. toyocaensis* NRRL 15009 (65%) and *A. orientalis* C329.2 (64%) was

much higher than in VRE (44% in *vanA* and 49% in *vanB*), indicating that the genes have

not been transferred recently. Alternatively, perhaps recent transfer into VRE has

occurred from an intermediate organism that gradually lowered the G/C content.
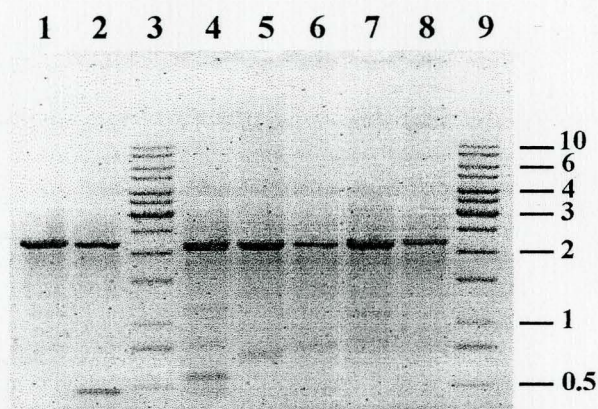
Figure 5.3. PCR Screen of Various Organisms for *van* Gene Cluster.
Reactions contained chromosomal DNA from *S. lividans* (lane 1), *S. coelicolor* (lane 2),
A. orientalis 18098 (lane 4), *A. orientalis* subsp. *lurida* (lane 5), *A. coloradensis* subsp.
labeda (lane 6), *A. orientalis* C329.2 (lane 7), and *S. toyocaensis* NRRL 15009 (lane 8).
DNA standards were in lanes 3 and 9.

Table 5.8 Organisms Screened for *van* Gene Cluster

Organism	GPA Produced	PCR Screen
S. toyocaensis NRRL 15009	A47934	Positive
A. orientalis C329.2	Vancomycin	Positive
A. orientalis 18098	Chloro-eremomycin	Positive
A. orientalis subsp. *lurida*	Ristocetin	Positive
A. coloradensis subsp. *labeda*	Teicoplanin	Positive
	Avoparcin	
S. fradiae	None	Negative
S. griseochromatogenes	None	Negative
S. argenensis	None	Negative
S. gourgerotii	None	Negative
S. coelicolor	None	Positive
S. lividans 1326	None	Positive

In similar PCR screening reactions using template DNA from a variety of

Streptomyces. that are known not to produce GPAs, most of the reactions (*S. fradiae, S.*

griseochromatogenes, S. argenesis, S. gougerotii) resulted in no amplification product

(Table 5.8). However, two non-producing organisms, *S. coelicolor* and *S. lividans*,

screened positive for the *van* gene cluster. That the DNA from these two organisms

produced the same result is not surprising, as it has been suggested that they are actually

the same organism (11). However, it was unexpected that they harboured this cluster

given that they are both very well characterised organisms and are known not to

manufacture any GPA. As part of an on-going genome sequencing project, several *van*-

like genes were reported on the *S. coelicolor* Cosmid SC66T3 in June of 1999 (Table

5.8) (14). This cosmid contained homologues of *vanH*, *vanA* and *vanX*, with high

primary sequence homology to the *A. orientalis* C329.2 and *S. toyocaensis* NRRL 15009

genes. Again, the genes were found in an identical arrangement as the VRE VanA/B

clusters (Figure 5.4), however none of the other *van* genes were present. A *femA*
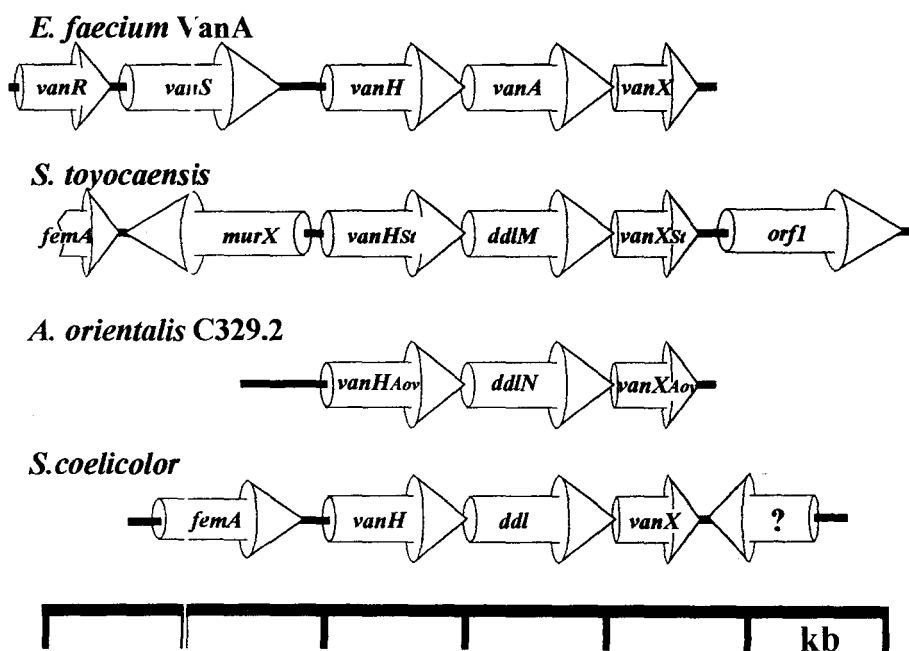
Figure 5.4. Genetic Arrangement of *van* Genes From Various Sources.

homologue (distinct from the one designated SCH24.26c which was originally detected

when the *S. toyocaensis* NRRL 15009 genes were first sequenced) was upstream of the

vanH homologue, however no *murF* or *orf1* homologues were present. Clearly this

cluster is related to those observed in the GPA-producers, and may have been acquired as

a means of competing with these organisms in their natural environment. Alternatively,

the phenotype conferred by the cluster (conversion of PG termini to depsipeptide) may

serve some other function in these organisms.

Table 5.9 *van* Genes Found on *S. coelicolor* Cosmid SC66T3

Gene Homologue or Description	Location on Cosmid SC66T3	Length (bp)	Percent G/C	Most Homologous Protein(s)[1]	Percent Homology[2]
unknown	391→1383	993	72	None	N.A.
femA	1574→2767	1194	70	$FemA_{St}$	87
vanH	2862→3875	1014	63	$VanH_{Aov}$	68
				$VanH_{St}$	67
vanA	3886→4926	1041	67	DdlM	78
				DdlN	69
vanX	4923→5531	609	68	$VanX_{St}$	77
				$VanX_{Aov}$	72
unknown	5581←6393	813	74	M.tuberculosis protein	28

[1]As determined by BLAST analysis as of August, 1999.
[2]As determined by Clustal W alignment.

5.4.6 *Phylogenetic Relationships of VanH, VanA and VanX Homologues*

BLAST analyses had indicated that the enzymes encoded by the *S. toyocaensis*

NRRL 15009 and *A. orientalis* C329.2 *van* genes were close relatives of the clinically

important VRE enzymes in all three classes. To evaluate the significance of the

similarity between these the enzymes from these two very different sources, and to place

the relationship in context with all enzymes that bear homology to the VRE enzymes,

phylogenetic trees were constructed using ClustalW alignments. Proteins were chosen on

the basis of homology to the enzymes found in the VanA phenotype of VRE, as

determined using BLAST analysis.

Several D-lactate dehydrogenase primary sequences are available as many

bacteria utilise the enzyme in anaerobic respiration. A number of these enzymes bear

significant homology to VanH, and an alignment of 14 of these primary sequences

reveals clear evolutionary relationships (Figure 5.5). The VRE enzymes VanH, VanHB,

and VanHD form a closely related family, and are more proximal to the actinomycete

family (VanH homologues from *S. toyocaensis* NRRL 15009, *A. orientalis* C329.2 and *S.*
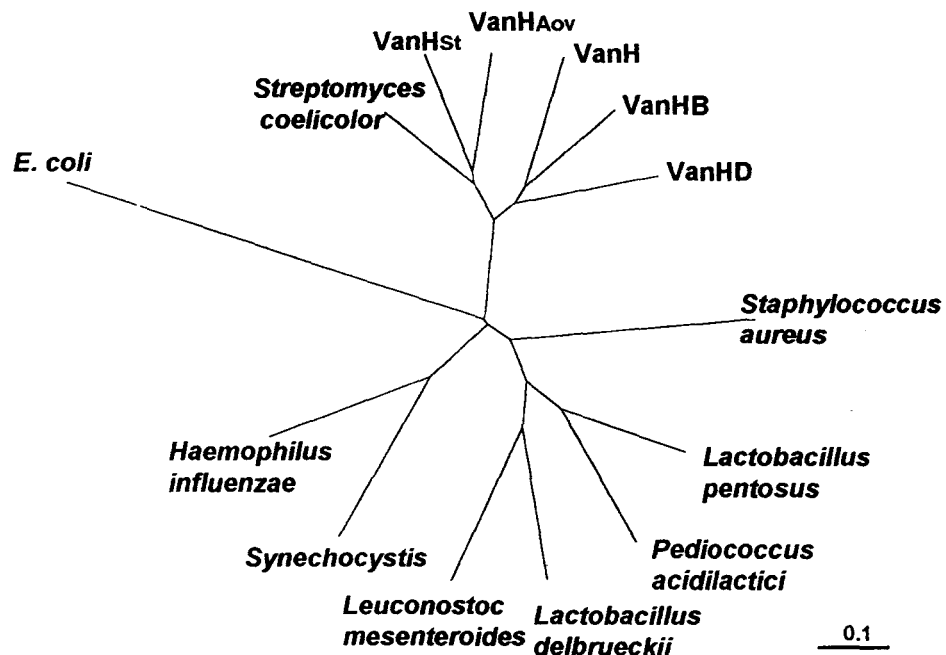
Figure 5.5. Phylogenetic Relationship of VanH Homologues. Alignments
performed using the Clustal W Method.

coelicolor) than to ary other group by a significant margin. The lactic acid bacteria also

form a cluster, while the rest of the enzymes are fairly diverse.

The ddl enzyme family is also well populated as all bacteria use PG for their cell

wall. An alignment of 20 of these sequences produces a tree with a very distinct branch

for the VRE and acti lomycete enzymes (Figure 5.6). The sequences of some VanC

enzymes (D-Ala-D-Ser synthesising ligases) are also available, and are present on this

branch, however they are further away from the VanA, VanB and VanD enzymes than

the actinomycete enzymes. Also further from the VRE enzymes are the ddls of the lactic

acid bacteria which naturally manufacture D-Ala-D-lact. This demonstrates the strong

relationship between actinomycete ddls and depsipeptide-forming VRE, and provides
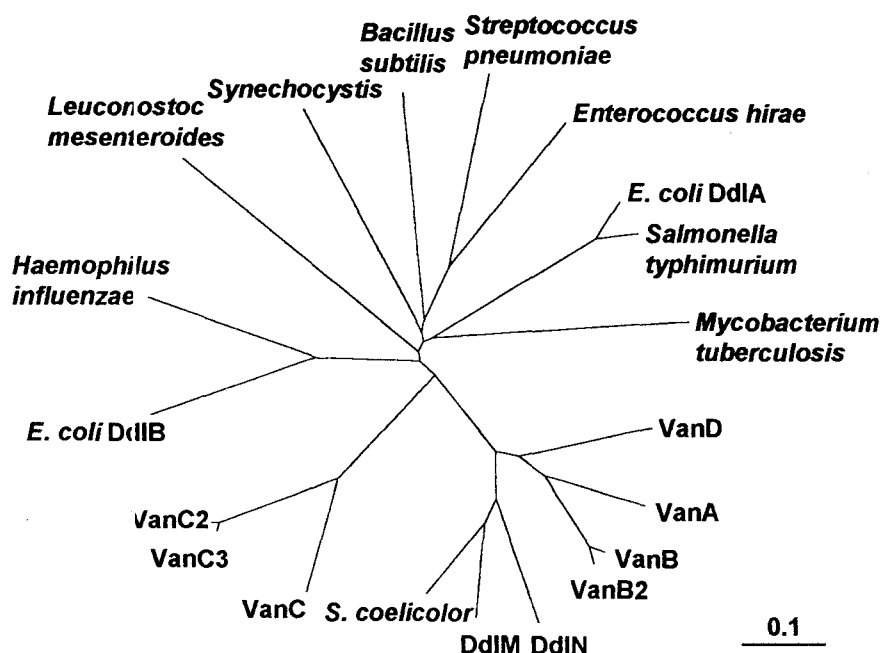
Figure 5.6. Phylogenetic Relationship of VanA Homologues. Alignments performed using the Clustal W Method.

further evidence for an actinomcyete origin of clinical resistance.

As the di-peptidase activity of VanX is not a common requirement in most organisms, not as many enzymes are available for comparison to this VRE enzyme. The alignment of 10 of the most similar of these enzymes generated a tree with parallel themes as the other two (Figure 5.7). The VRE enzymes clustered tightly, as did the actinomycete enzymes, and the two groups were closely related compared to those from other organisms.
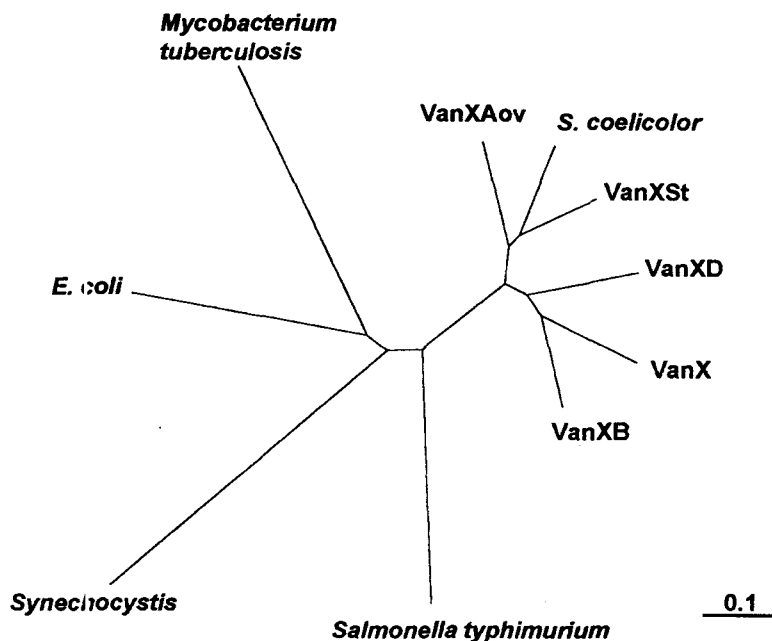
Figure 5.7. Phylogenetic Relationship of VanX Homologues. Alignments performed using the Clustal W Method.

In summary, phylogenetic analysis of these three classes of enzymes reinforced the close relationship between *van* gene products derived from GPA-producing actinomycetes and clinically important, D-Ala-D-lact forming VRE.

5.4.7 Analysis of the Region Upstream of Actinomycete vanH Genes

The region upstream of the vanH genes from *S. toyocaensis* NRRL 15009, *A.*

orientalis C329.2, and *S. coelicolor* was aligned using the Clustal W method and found

to contain three highly conserved regions (Figure 5.8). These regions may be important

in the regulation of the *van* gene operon. Streptomyces promoters are highly diverse,

however, making it difficult to positively identify any of these regions as specific

promoter elements. The sequence encompassing all three regions was too short to

register any significant hits using the BLAST search tool.
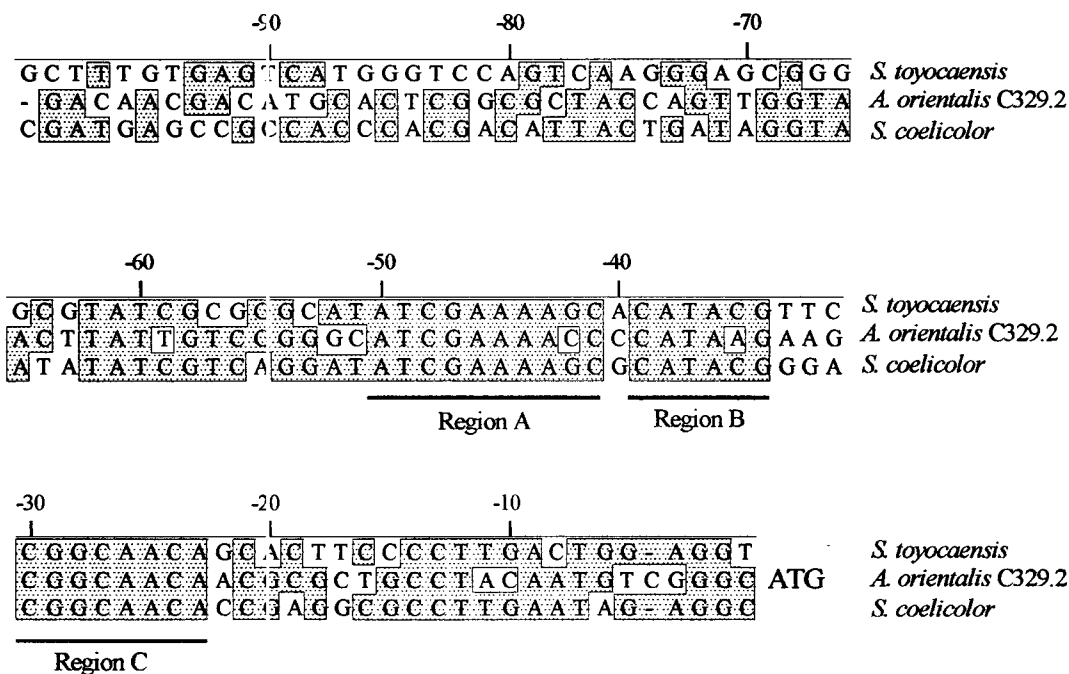
Figure 5.8. Alignment of the DNA Region Upstream of *vanH*. Alignments performed
using the Clustal W Method. Residues matching the consensus sequence are boxed and shaded.

5.4.8 Expression of A. orientalis C329.2 van Genes in Bacillus

The 3.5 kb *Bam*HI fragment from *A. orientalis* C329.2 was cloned downstream

of the *vegII* promoter in the shuttle vector pRB374 and transformed into *B. subtilis*

DB104. The primers used to sub-clone the fragment incorporated a Shine-Delgarno

sequence upstream of the *vanH$_{Aov}$* start codon. DB104 holding this construct did not

have increased resistance to vancomycin relative to DB104 holding pRB374 vector only,

even when supplemented with D-lactate. It was clear from the primary sequence of the

van genes that they function to synthesise D-Ala-D-lact, which is incorporated into PG to

confer resistance to GPAs. Expression of protein in heterologous hosts is frequently

impeded by problems relating to codon usage and protein folding, and was likely the

problem here. This problem was also encountered with the VanA gene cluster, which

conferred resistance when transferred into *E. faecalis* and *B. thuringiensis*, but not in *B.*

subtilis (3).

5.4.9 Predicted Function of Actinomycete-Derived Van Enzymes

As key catalytic residues have been identified in the various classes of Van

enzymes, information regarding the function of the *S. toyocaensis* NRRL 15009 and *A.*

orientalis C329.2 enzymes can be obtained by examining their primary sequence. These

are discussed in greater depth in later chapters and are only made note of here. Both

VanH$_{St}$ and VanH$_{Aov}$ possessed the conserved R235, E264 and H296 that function in

substrate binding and acid catalysis in *L. pentosus* D-LDH (17, 18), for which the crystal

structure has been solved (16).

The strictly dipeptide forming DdlB of *E. coli* has also been solved using X-ray studies, and residues important in ATP binding (K97, K144), Mg^{2+} binding (D257, E270), D-Ala$_1$ binding (E15, R255), and D-Ala$_2$ COO$^-$ binding (S281) (15) were conserved in the VanA/B and GPA-producer ddls. However, key residues in substrate specificity (K215 and Y216) (12), in what has been termed the ω- loop region, are not conserved in the depsipeptide-forming VanA/B enzymes. This ω- loop of the VanA/B ligases was well conserved in the ddls of the GPA-producers.

VRE VanX has been well studied by both structural (5) and mutagenesis (10) methods. The primary sequence of VanX was well conserved in the GPA-producers, and residues involved in Zn^{2+} binding (D123, H116, H184, and E181), substrate binding (S114, D142) and catalysis (R71, D68) were all present.

5.5 Conclusions

Using the degenerate PCR approach, several GPA-resistance genes were cloned out of the A47934 producer *S. toyocaensis* NRRL 15009 and the vancomycin producer *A. orientalis* C329.2. These genes were found to be very similar in primary sequence and arrangement as the genes found in VanA and VanB VRE phenotypes, and were found in a number of different GPA producing organisms, suggesting that these soil microbes may have been the source of the *van* gene cluster found in clinical isolates of enterococci. The much increased G/C content of the genes from the soil microbes argued against recent direct transfer to VRE, and an intermediate host may have been involved. This

sort of genetic promiscuity was evidenced by the presence of the cluster in non-GPA producing actinomycetes such as *S. lividans* and *S. coelicolor*. Phylogenetic analysis confirmed the close relationship of the gene products from VRE and actinomycetes. Primary sequence analysis indicated that the GPA-producer enzymes function similarly to the VRE enzymes, and thus could serve as models in drug development studies where using the VRE enzyme may not be feasible. Unfortunately, none of the genes flanking the GPA-resistance genes in *S. toyocaensis* NRRL 15009 were putative A47934 biosynthesis genes. If the cluster was proximal to the GPA biosynthetic cluster, it was at least 2 kb removed from it. At this juncture, other avenues were becoming available for identifying the genes required for A47934 synthesis, as will be discussed further in Chapter 9. The discovery of VanA/B homologues with similar ω-loop regions provided a unique opportunity to study these enzymes in novel ways as neither VanA nor VanB had formed crystals for use in X-ray studies.

5.6 References

1. **Agata, Y., E. Matsuda, and A. Shimizu.** 1998. Rapid and efficient cloning of cDNAs encoding Kruppel-like zinc finger proteins by degenerate PCR. Gene. **213**(1-2):55-64.

2. **Ausubel, F. M., R. Brent, R. E. Kingston, D. D. Moore, J. G. Seidman, J. A. Smith, and K. Struhl (ed.).** 1995. Current Protocols in Molecular Biology. John Wiley and Sons, Inc., New York.

3. **Brisson-Noel, A., S. Dutka-Malen, C. Molinas, R. Leclercq, and P. Courvalin.** 1990. Cloning and heterospecific expression of the resistance determinant vanA encoding high-level resistance to glycopeptides in *Enterococcus faecium* BM4147. Antimicrob Agents Chemother. **34**(5):924-7.

4. **Bruckner, R.** 1992. A series of shuttle vectors for *Bacillus subtilis* and *Escherichia coli*. Gene. **122**(1):187-92.

5. **Bussiere, D. E., S. D. Pratt, L. Katz, J. M. Severin, T. Holzman, and C. H. Park.** 1998. The structure of VanX reveals a novel amino-dipeptidase involved in mediating transposon-based vancomycin resistance. Mol Cell. **2**(1):75-84.

6. **Evers, S., B. Casadewall, M. Charles, S. Dutka-Malen, M. Galimand, and P. Courvalin.** 1996. Evolution of structure and substrate specificity in D-alanine:D-alanine ligases and related enzymes. J Mol Evol. **42**(6):706-12.

7. **Hommes, N. G., D. J. Arp, and L. A. Sayavedra-Soto.** 1995. Generation of polymerase chain reaction-specific probes for library screening using single degenerate primers. Genet Anal. **12**(1):53-6.

8. **Hopwood, D. A., M. J. Bibb, K. F. Chater, T. Keiser, C. J. Bruton, H. M. Keiser, D. J. Lydiate, C. P. Smithe, and J. M. Ward.** 1985. Genetic Manipulations of *Streptomyces*. John Innes Foundation, Norwich.

9. **Kusaoke, H., H. Yoshitaka, K. Yasuhiro, and H. Kimoto.** 1989. Optimum conditions for electric pulse-mediated gene transfer to *Bacillus subtilis* cells. Agric Biol Chem. **53**(9):2441-46.

10. **Lessard, I. A., and C. T. Walsh.** 1999. Mutational analysis of active-site residues of the enterococcal D-ala-D- Ala dipeptidase VanX and comparison with *Escherichia coli* D-ala-D-Ala ligase and D-ala-D-Ala carboxypeptidase VanY. Chem Biol. **6**(3):177-87.

11. **Nodwell, D. J.** 1999. Personal Communication.

12. **Park, I. S., C. H. Lin, and C. T. Walsh.** 1996. Gain of D-alanyl-D-lactate or D-lactyl-D-alanine synthetase activities in three active-site mutants of the *Escherichia coli* D-alanyl-D-alanine ligase B. Biochemistry. **35**(32):10464-71.

13. **Pelzer, S., W. Reichert, M. Huppert, D. Heckmann, and W. Wohlleben.** 1997. Cloning and analysis of a peptide synthetase gene of the balhimycin producer *Amycolatopsis mediterranei* DSM5908 and development of a gene disruption/replacement system. J Biotechnol. **56**(2):115-28.

14. **Redenbach, M., H. M. Kieser, D. Denapaite, A. Eichner, J. Cullum, H. Kinashi, and D. A. Hopwood.** 1996. A set of ordered cosmids and a detailed

genetic and physical map for the 8 Mb *Streptomyces coelicolor* A3(2) chromosome. Mol Microbiol. **21**(1):77-96.

15. **Shi, Y., and C. T. Walsh.** 1995. Active site mapping of *Escherichia coli* D-Ala-D-Ala ligase by structure- based mutagenesis. Biochemistry. **34**(9):2768-76.

16. **Stoll, V. S., M. S. Kimber, and E. F. Pai.** 1996. Insights into substrate binding by D-2-ketoacid dehydrogenases from the structure of *Lactobacillus pentosus* D-lactate dehydrogenase. Structure. **4**(4):437-47.

17. **Taguchi, H., and T. Ohta.** 1993. Histidine 296 is essential for the catalysis in *Lactobacillus plantarum* D-lactate dehydrogenase. J Biol Chem. **268**(24):18030-4.

18. **Taguchi, H., T. Ohta, and H. Matsuzawa.** 1997. Involvement of Glu-264 and Arg-235 in the essential interaction between the catalytic imidazole and substrate for the D-lactate dehydrogenase catalysis. J Biochem (Tokyo). **122**(4):802-9.

19. **Thompson, J. D., D. G. Higgins, and T. J. Gibson.** 1994. CLUSTAL W: improving the sensitivity of progressive multiple sequence alignment through sequence weighting, position-specific gap penalties and weight matrix choice. Nucleic Acids Res. **22**(22):4673-80.

20. **Turgay, K., and M. A. Marahiel.** 1994. A general approach for identifying and cloning peptide synthetase genes. Pept Res. **7**(5):238-41.

21. **Wright, F., and M. J. Bibb.** 1992. Codon usage in the G+C-rich Streptomyces genome. Gene. **113**(1):55-65.

22. **Zmijewski jr., M. A., and B. Briggs.** 1989. Biosynthesis of vancomycin: Identification of TDP-glucose aglycosyl-vancomycin glycosyltransferase from *Amycolatopsis orientalis*. FEMS Microbiol Lett. **59**:129-133.

Chapter 6

Identification and Purification of D-alanyl-D-alanine Ligases
from *S. toyocaensis* NRRL 15009

Adapted from

Marshall, C. G., and G. D. Wright. 1997. The glycopeptide antibiotic producer
Streptomyces toyocaensis NRRL 15009 has both D-alanyl-D-alanine and D-alanyl-D-
lactate ligases. FEMS Microbiol Lett. **157**(2):295-9.

6.1 Introduction

At the time that the *S. toyocaensis* NRRL 15009 and *A. orientalis* C329.2 Ddls

were cloned, these enzymes were the only D-Ala-D-lact ligases with a VanA/B-like ω-

loop region. This was very exciting as the *Enterococcus* enzymes had not formed

crystals that could diffract X-rays with sufficient resolution, and an understanding of the

mechanism of these enzymes could not be complete without knowledge of the structure

of key residues in the active site.

Most of what we know today about the mechanism of Ddls comes from extensive

studies done on *E. coli* DdlB. This enzyme was crystallised and solved by X-ray

crystallography in a complex with ADP and the inhibitor phosphinophosphate (4). This

compound is formed by the enzyme-catalysed reaction of a D-Ala-D-Ala phosphinate

derivative (D-Ala[PO_2-CH_2]D-Ala) and ATP, and it mimics the tetrahedral intermediate

formed by attack of D-Ala$_2$ on the acyl phospate of D-Ala$_1$ (Figure 6.1). The

phophinophosphate binds so tightly to the enzyme (dissociation time scale of days), that

it acts as a time-dependent inactivator. Its presence in the solved structure facilitates

identification of residues involved in the binding of natural substrates and in catalysis.

Residues can be classified to some extent based on function, including binding of ATP,

Mg^{2+}, D-Ala$_1$ and D-Ala$_2$, as well as charge stabilisation and acid/base catalysis. It is

important to note that the reaction has two major steps, D-Ala$_1$ phosphorylation followed

by nucleophilic attack by D-Ala$_2$ resulting in peptide bond formation. It is the tetrahedral

intermediate in the second step which the phosphinophosphate inhibitor mimics, and it is

in the second step where Ddls that prefer to use D-lactate are likely to have different

mechanistic requirements.
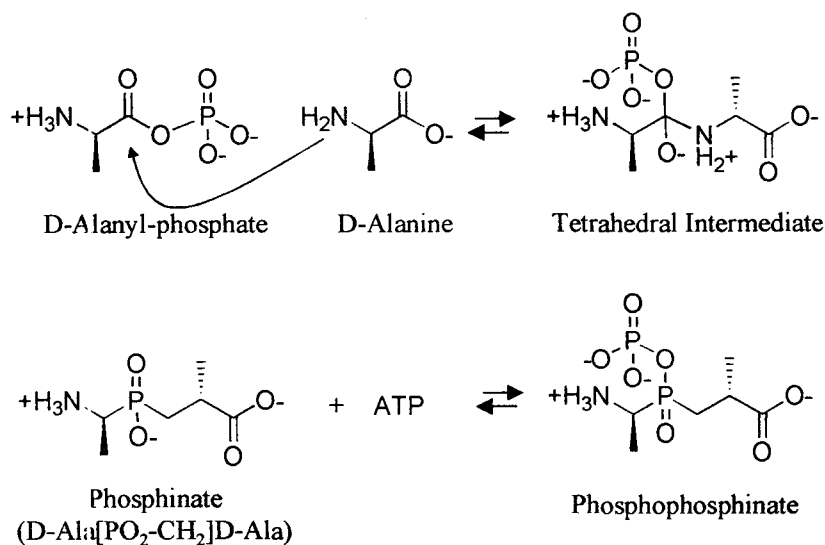
Figure 6.1. Formation of the Inhibitor Phosphinophosphate.

Figure 6.2 shows some of the residues involved in phosphinophosphate binding

(and therefore intermediate binding) in a general representation of the active site of DdlB.

The functions of these residues suggested by the structure were confirmed or refuted by

mutagenesis, providing strong evidence for their role in the catalytic mechanism (11).

K97 and K144 function in ATP binding, E270 and D257 in Mg^{2+} binding, E15 and R255

in D-Ala$_1$ binding and S281 in D-Ala$_2$ carboxylate binding. All of these residues are

conserved in VanA/B and the GPA-producer Ddls, and likely play similar roles in the D-

lactate-utilising class of enzymes. K215 and Y216 are also important residues, and are

found on the α-helix H9 which forms an ω-loop in the 3-dimensional structure. This

loop is protease sensitive in the absence of ADP and phosphinate (12), and is thought to

swing in and over the bound substrates, protecting the active site from the bulk solvent.

K215 appears to play a role in co-ordination of transferring γ-phosphate and was proven
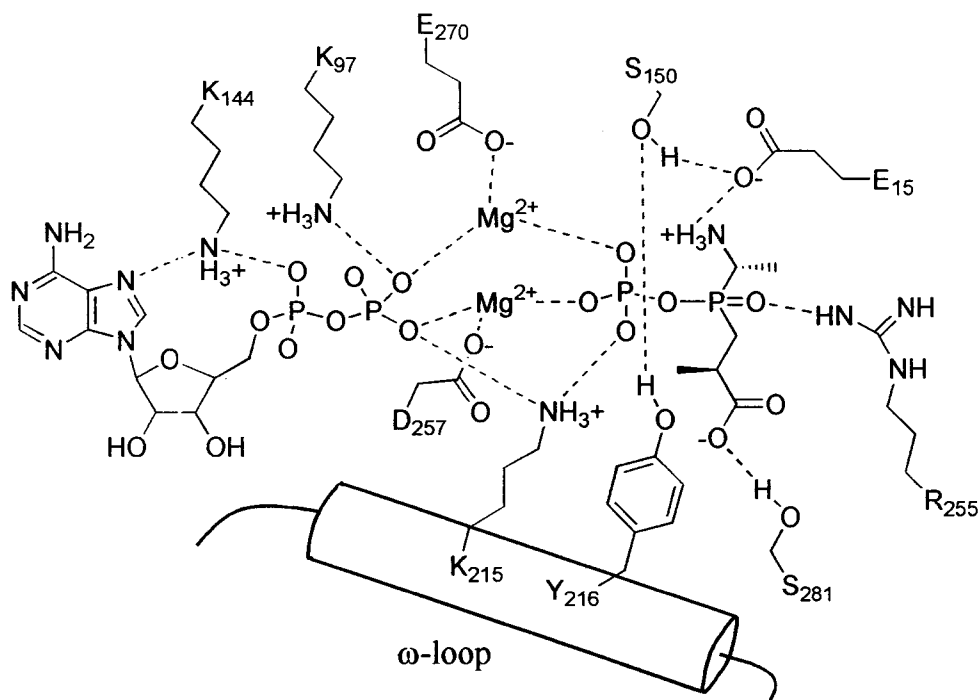
Figure 6.2. Representation of the Active Site of DdlB with Bound ADP and Phosphinophosphate. Figure adapted from Ref. 11.

essential by mutagenesis. Y216 was originally suspected to function as a general base,

removing a proton from the amino group of the incoming D-Ala$_2$ to drive nucleophilic

attack on the acyl phosphate. Mutagenesis studies, however, argue against this role and

suggest that this residue may be important in substrate specificity. In D-Ala-D-lact

ligases from the naturally resistant lactobacilli, this position is always occupied by a

phenylalanine (Figure 6.3), and D-Ala-D-Ala ligases can be made into D-Ala-D-lact

ligases (and vise-versa) by toggling between these two amino acids (10). Importantly,

the VanA/B class of enzymes have a completely different amino acid sequence on the

region that aligns with the DdlB ω-loop. K215 is not conserved at all, and neither

tyrosine nor phenylalanine align with the 216 position. It is therefore impossible to

extend what is known about the DdlB mechanism (which is admittedly still incomplete)

to the VanA/B Ddls as a model for the active site cannot be unambiguously developed.

Figure 6.3 clearly shows that the primary sequence of the DdlM/N ω-loop region is very

similar to that of the VanA/B enzymes. Together they form a distinct class of ω-loop,

designated as group II to distinguish them from the DdlB-like group I loops.

Figure 6.3. Comparison of the ω-loop from Various Ddls. Y216 is indicated
with an asterisk. ω-loops are classified into I. DdlB-like and II. VanA/B-like.

As *ddlM* was cloned well before *ddlN*, expression studies focused on this gene

first. This chapter describes the different attempts to express this gene at high levels in

heterologous hosts with the goal of establishing biochemical similarity to the VanA/B

enzymes and the development of protein crystals that diffract to high resolution. DdlM was produced in *E. coli* BL21(DE3), *B. subtilis* BR1157, *S. lividans* 1326 and in *E. coli* JM109 as a fusion with Maltose Binding Protein, however none of these systems produced sufficient quantities of *wild-type* protein. Ultimately, DdlM was purified from its natural source, *S. toyocaensis* NRRL 15009, and partially characterised. In the process, a second Ddl was detected in this organism, and was similarly purified and characterised.

6.2 Materials

D,L -amino acids, D-lactate, maltose and malachite green were purchased from Sigma. Ammonium molybdate, trisodium citrate, potassium dihydrogen orthophosphate, Triton X-100, β-mercaptoethanol (β-ME), and all media components were from BDH. Antibiotics were obtained from Bioshop. Polyethyleneglycol (PEG) 1000 was made by NBS Biologicals. ATP and lysosyme were purchased from Boehringer Mannheim. [^{14}C]-D-Ala was from ICN Biomedicals while [^{14}C]-D-lact was from American Radiolabeled Chemicals. Isopropyl-β-D-thiogalactopyranoside (IPTG) was obtained from ChemBridge. All columns were from Pharmacia, except those made with Affigel (Bio-Rad) and amylose (NEB). All restriction endonucleases were purchased from MBI Fermentas. Vent polymerase, the pMal-C2 system (including Factor Xa), and *E. coli* JM109 cells were from NEB. Polyvinylidene fluoride (PVDF) membranes was from Bio-Rad. The pET system was purchased from Novagen. The plasmid pRB374 was a

gift from R. Brückner. The plasmid pFD666 was a gift from Dr. A. Petrich. *S. lividans* 1326 was from Dr. D. Hopwood. *B. subtilis* BR1157 was a gift from Dr. Stüber.

6.3 Methods

6.3.1 Media and Buffers

Yeast Extract-Malt Extract (YEME) medium, P buffer, lysosyme solution, and R2YE were made according to the *Streptomyces* Laboratory Manual (5). Malachite green colour reagent was made by mixing 3 parts of 0.045% (wt/vol) malachite green hydrochloride in water with 1 part 4.2% (wt/vol) ammonium molybdate in 4 N HCl for a minimum of 20 minutes prior to use. Citrate solution consisted of 34% (wt/vol) trisodium citrate in water.

6.3.2 Thin-layer Chromatographic Assays of Ligases

The activities of *S. toyocaensis* NRRL 15009 ligases were monitored during purification using radiolabelled substrate TLC assays. Dipeptide ligase assays (10uL) contained 100 mM Tris 8.6, 20 mM $MgCl_2$, 10 mM KCl, 10 mM ATP, 2.5 mM D-Ala, 0.04 μCi [^{14}C]-D-Ala, and 40% v/v protein sample (0.5 -5.0 μg). Depsipeptide ligase assays were as above but included 2.5 mM D-Lact and utilised [^{14}C]-D-Lact as the radioactive label. Reactions were incubated 2 hours at 37 ^{O}C and 5 x 1.2 μL was spotted onto a Kodak cellulose TLC plate. Products were eluted in *n*-butanol-acetic acid-water (12:3:5), dried, and exposed to film overnight.

6.3.3 Boil-lysis and SDS-PAGE

Boil-lysis and SDS-PAGE were used as a preliminary test of gene expression in recombinant hosts. Cells were grown to a state of maximal gene expression (3 hours

after IPTG-mediated gene induction or mid to late log phase in constitutive systems), at which point 1.5 mL was removed and cells sedimented by centrifugation.

For gram-positive organisms: Pellets were suspended in 85 μL of solution A (50 mM Tris, 20 mM EDTA, pH 8.0). Addition of 10 μL solution B (85 mM Tris, pH 8.0, 4 mg/mL lysosyme) was followed by a 10 min incubation at RT. Solution C (50 mM Tris, 40 mM EDTA, 5% Triton X-100) was added (10 μL) and the mixture boiled for 1 min. Samples were rapidly chilled on ice for 5 min and spun at 14, 000 x g for 15 min at 4°C. Supernatants were mixed with 1 volume of SDS-PAGE loading buffer and electrophoresed through 11% SDS-PAGE gels.

For gram-negative organisms: Pellets were suspended in 50 μL TE buffer, to which 50 μL SDS-PAGE buffer was added. Cells were boiled 15 minutes and spun at 14,000 x g for 5 min. Supernatants were ready for electrophoresis.

6.3.4 Cell Lysis

All steps were performed at 4°C. Cells were suspended in a minimum volume of 50mM HEPES buffer pH 7.5, 300 mM NaCl, 2 mM EDTA, 1 mM DTT and 1 mM PMSF and lysed by passage 3 times through a French pressure cell at 20,000 psi. Upon centrifugation at 10, 000 rpm for 10 min, the sedimented debris was extracted with a minimal amount of lysis buffer, and the pooled supernatants were diluted with buffer to less than 150mM NaCl.

6.3.5   Column Chromatography of DdlM Expressed in Heterologous Hosts

The cell-free extract was subject to gel exclusion chromatography or anion

exchange chromatography prior to assay. Column buffers consisted of 50 mM HEPES

pH 7.5, 1 mM EDTA, 0.1 mM DTT and a variable amount of NaCl.

A Superdex 200 gel exclusion column (2.6 x 114 cm), equilibrated with 100 mM

NaCl in column buffer, was used to separate applied protein samples (< 6 mL) at 0.5

mL/min. Eluant fractions were screened for D-Ala-D-lact formation by TLC assay.

Ion exchange chromatography was performed on a Q-Sepharose column (3.0 x 10

cm) equilibrated in 150 mM NaCl in column buffer. Proteins were eluted with a linear

gradient from 150 to 500 mM NaCl over 4 column volumes at 3 mL/min, and assayed for

D-Ala-D-lact formation.

6.3.6   Expression of DdlM in E. coli BL21(DE3)

The *ddlM* gene was amplified from the *Sac*I chromosomal fragment (described in

the last chapter) by Vent PCR using primers with engineered restriction endonuclease

sites. Reactions (100 μL) contained pBlutoyoddl3.0 (500 ng), 1 μM forward primer (5'-

GAGATATACATATGGCCAGACTGAAGATCGG-3'), 1 μM reverse primer (5'-

TGACATAAGCTTCAGAGCGAGGAGACGGTGA-3'), 1X Vent buffer, 5% DMSO,

0.4 mM each dNTP, 2 mM additional $MgSO_4$ and 2 U Vent DNA polymerase. Reactions

were cycled 35 times at 94, 52, and 72°C for 1.5 minutes at each temperature. The

amplified 1.1 kb product was purified with a QuiexII kit and digested with *Nde*I and

*Hind*III. Digestion products were separated in TAE-agarose (1%) and the large fragment

purified by QuiexII. This was ligated to similarly endonuclease-digested pET22b

plasmid vector, and transformed into *E. coli* BL21(DE3) strain. Recombinants

containing the *ddlM* gene were identified by RFLP of mini-lysate plasmid preparations.

The gene was sequenced entirely using plasmid primer binding sites and a single internal

primer. Three mutations were detected, two of which were silent. The third mutation

was near the 5' end of the gene, just upstream of a unique *Aat*II site, and was eliminated

by replacement with the 5' end of another recombinant which possessed the wild-type

sequence. *E. coli* BL21(DE3)/pETDdlM was grown in LB-ampicillin (0.5 L) at 250

rpm, 37°C to mid-log phase and gene expression induced by the addition of IPTG to 1

mM final concentration. Cells (1.3-1.5 g) were harvested (5,000 x g, 10 min at 4°C) after

3 hours of induction, washed with 0.85% NaCl and stored frozen as a pellet at -80°C.

6.3.7 Expression of DdlM in B. subtilis BR1157

The *ddlM* gene was removed from the pET22b vector using the restriction

endonucleases *Xba*I and *Kpn*I and cloned into similarly digested plasmid vector pRB374

(1). Ligation products were transformed into *E. coli* JM109 and positive clones

identified. Purified pRBDdlM was transformed into *B. subtilis* BR1157 using a

previously described electroporation method (6). Optimal transformation occurred using

2.0 kV for 0.4 ms, which produced 6 colonies. Recombinant colonies were grown and 1

mL of culture assayed for the presence of DdlM by boil-lysis/SDS-PAGE. All positive

clones contained a band at 37 kDa (predicted molecular mass of DdlM) that was not

present in *wild-type* BR1157. One clone (BR1157/pRBDdlM) was grown in PAB-

kanamycin (0.5 L) to late-log phase (A_{600}=1.1) at 250 rpm, 37°C. Cells were harvested,

washed and frozen as usual.

6.3.8 Expression of DdlM in S. lividans 1326

Expression vectors that function in *Streptomyces* are fairly limited in number and diversity. The *E. coli/Streptomyces* shuttle vector pFD666 (3) was available and possessed a reasonably useful multiple cloning site (MCS), however it did not provide a promoter for gene expression. To express *ddlM* in *S. lividans* 1326, the entire 3.0 kb *Sac*I fragment was cloned in with the hope that the DNA region upstream of *vanH* would serve as a functional promoter as it does in *S. toyocaensis* NRRL 15009. In order to make this clone, the *Sac*I fragment was first cloned into pET22b to acquire some of the MCS. The fragment was then excised using *Xba*I and *Hind*III and the 3.0 kb fragment ligated to similarly digested pFD666. Ligation products were transformed into *E. coli* and positive clones identified by RFLP of mini-lysate plasmid DNA preparations. A positive clone was identified, designated 666toyoddl3.0 and transformed into *S. lividans* protoplasts.

S.lividans protoplasts were prepared as described by Hopwood (5). YEME (25 mL) supplemented with glycine to 0.5% was inoculated with 0.1 mL spore suspension and grown at 30°C, 275 rpm to late-log phase (about 40 hours, monitored O.D.$_{600}$). Cells were sedimented by centrifugation (often required dilution with sterile water), and washed twice with 10.3% sucrose. Cells were suspended in 4 mL lysosyme solution, incubated 30 min at 30°C, triturated three times with a 5 mL pipette and incubated a further 15 min. P buffer was added, and the sample filtered through a filter tube (the same kind used to make spore suspensions, see Chapter 2). Protoplasts were gently sedimented and suspended in fresh P buffer (1 mL). Aliquots (0.1 mL) were frozen and

stored at -80°C. To transform, cells were thawed rapidly by running under warm water and washed with 5 mL P buffer. The cell pellet was suspended in the drop remaining after decanting (by tapping) and supercoiled DNA (0.1 mg in no more than 5 µL water) was added and immediately mixed. As quickly as possible, P buffer containing 25% PEG 1000 (200 µL) was added and the sample mixed by pipetting. The mixture was plated on R2YE media dried in a laminar flow hood to 85% the original mass (not including petri plate), and grown at 30°C. The following day, neomycin was overlaid in 1-2 mL water to a final concentration of 10 µg/mL, and cultures allowed to grow for 2-3 days. Several colonies (10) were observed and one selected (designated *S. lividans*/666toyodll3.0). SAM-neo (100 mL) was inoculated with a 1% vol/vol of saturated culture and grown to late log phase (about 50 hours). Harvested mycelia (1.8 g) were disrupted in a ground glass homogeniser and washed in 0.85% NaCl prior to freezing.

6.3.9 Expression of DdlM-MBP in E. coli JM109

The *ddlM* gene was excised from pETDdlM using *Nde*I and *Hind*III and ligated to similarly digested pMalC2. This placed it downstream of the gene encoding the maltose binding protein (MBP) in the correct reading frame to produce a fusion protein. Ligation products were transformed into *E. coli* JM109 and a positive clone identified by RFLP as before. *E. coli* JM109/pMalDdlM was grown in LB-ampicillin (1.0 L) to mid-log phase and induced with addition of IPTG to 1.0 mM for 3 hours at 30°C. Harvested cells (1.8 g) were washed and stored at -80°C. SDS-PAGE of boil-lysates indicated clear induction of an 80 kDa protein (the expected mass of the fusion of the 45 kDa MBP and

DdlM). Cells were lysed by French pressing and the clarified lysate applied to an amylose column (0.5 x 20 cm) equilibrated in 20 mM Tris-Cl pH 7.4, 200 mM NaCl, 10 mM β-ME. Proteins were eluted as a single peak in buffer containing 10 mM maltose. The fusion protein was de-salted, concentrated and cleaved as described by the manufacturer. Reactions (1 mL) contained 20 mM Tris-Cl pH 8.0, 2 mM $CaCl_2$, 82 mM NaCl, 1.0 mg fusion protein and 10 µg Factor Xa, and were incubated for 8 hours at RT or 48 hours at 4^OC. Reaction products were separated by ion exchange chromatography on a MonoQ (0.5 x 5 cm) equilibrated in column buffer. Proteins were eluted with a linear gradient of 0 to 200 mM NaCl in column buffer and analysed by SDS-PAGE.

6.3.10 Enzyme Purification from S. toyocaensis NRRL 15009

S.toyocaensis NRRL 15009 was inoculated into SAM media (0.5 L) lacking antibiotic (D-Ala-D-Ala ligase) or containing 5 µg/mL A47934 (D-Ala-D-Lact ligase) using 1% vol/vol of saturated SVM culture and grown to mid-log phase (approximately 40 hours). After washing with 0.85% NaCl, 5% glycerol, cells (approximately 5.5 g) were stored for up to one month at -80°C. Cells were lysed by French press and the clarified lysate immediately applied to a Q Sepharose column (3 x 10 cm). Proteins were eluted in buffer from 150 mM to 500 mM NaCl over 4 column volumes. Fractions containing >10% the activity of the most active fraction were pooled and concentrated using an Amicon centriprep 10 to approximately 1.0 mL. This concentrate was loaded and run through a 120 mL Superdex S-200 equilibrated in 50 mM HEPES pH 7.5, 100 mM NaCl. Active fractions were pooled and loaded directly onto a MonoQ column (0.5 x 5 cm). Protein was eluted in buffer from 100 mM to 400 mM NaCl over 60 column

volumes. Active fractions were pooled and ammonium sulphate (AS) was added to 1.7

M. This was applied to a Phenyl Superose column (0.5 x 5.0 cm) and eluted in buffer

from 1.7 to 0 M AS over 100 column volumes. This was sufficient to purify the D-Ala-

D-Ala ligase to homogeneity. The D-Ala-D-Lact ligase extract was desalted and applied

in less than a bed volume to a 1.0 mL D-Ala-D-Ala agarose (made by coupling D-Ala-D-

Ala to BioRad Affigel 15) column, and gently eluted in buffer from 0 mM to 200 mM

NaCl.

6.3.11 Kinetic Assays of D-Alanine Ligases

Kinetic assays (50uL) were carried out using the Malachite Green P_i Detection

Assay (7). Inorganic phosphate standards ranged from 5 nmol to 50 nmol in 0.05 mL

final volumes. Colour reagent was added to 0.8 mL final volume, 0.1 mL citrate solution

added and A_{660} measured in a Varian Cary 3E spectrometer. All ligase assays contained

50 mM HEPES buffer pH 8.6, 10 mM $MgCl_2$, 10 mM KCl, and were incubated at 37 ^{O}C.

A) Dipeptide ligase assays also contained ATP and D-Ala at various concentrations and

0.5 μg enzyme. B) Depsipeptide ligase assays also contained 5 mM D-Ala, ATP and D-

Lact at various concentrations, and 1.0 μg of enzyme. Depsipeptide formation rates were

calculated by subtracting the rate of reaction measured in the presence of 5 mM D-Ala

alone from all measured rates. C) ATP K_m and V_{max} were determined using reactions

containing kinetically saturating amounts of D-alanine, no D-lactate, and various

concentrations of ATP and 0.5 μg of enzyme.

Data were fit to the equation:

$$v = V_{max}[S] / ([S] + K_m)$$

by non-linear least squares methods using the program Grafit ver. 3.01 (8). D-Ala-D-

Ala ligase kinetic analysis is potentially complex, as there are three substrates, two of

which are the same. However, in DdlB and many other ligases the K_m of D-Ala$_1$ is much

lower than that of D-Ala$_2$ and easy to distinguish kinetically. All of the reported D-

alanine K_m values were for D-Ala$_2$.

6.3.12   Miscellaneous

TLC assays of DdlM and the *S. toyocaensis* NRRL 15009 Ddl using alternative

substrates were done as described for D-Ala in Section 6.3.2, but included the alternative

substrate at 2.5 mM (or solution saturation). D- and L- forms of every proteinaceous

amino acid were tested as well as D-lactate.

DdlM (30 pmol) was prepared for ESI-MS by desalting and concentrating to 30 μL.

Analysis was performed by Dr. Lorne Taylor of the Department of Chemistry, Waterloo

University. N-terminal sequencing of DdlM transferred to a PVDF membrane was done

by the Biotechnology Service Centre, Dept. of Clinical Biochemistry at the University of

Toronto.

6.4   Results

6.4.1   Expression of DdlM in Heterologous Hosts

The *ddlM* gene expressed to high levels in *E. coli* BL21(DE3) as

determined by boil-lysis and SDS-PAGE. However, it was noticed in the early stages of

purification that DdlM had unusual properties in this host. Activity was associated with

the void volume of the gel exclusion columns, indicating that DdlM was forming

multimers of very large mass (> 600, 000 kDa). It was also eluting from anion exchange

resins at very low ion concentrations, which was unexpected as the highly homologous

VanA enzyme binds strongly to these resins (2). The activity of this DdlM was also

unusual, in that it could form a product that had an R_f identical to D-Ala-D-lact in the

absence of any D-Ala (Figure 6.4). The only substrates present in these reactions were

ATP and D-lactate. This behaviour was not common in any known ligase, and would

later be revealed as a activity not demonstrated in *wild-type* DdlM. As this DdlM had

these atypical properties, it was suspected that it was not folded properly, forming large

aggregates and not representative of *wild-type* DdlM.

◀ $R_f = 1.0$

◀ D-lact

◀ D-Ala-D-Ala/D-Ala-D-lact
◀ D-Ala

◀ $R_f = 0$

1 2 3 4 5
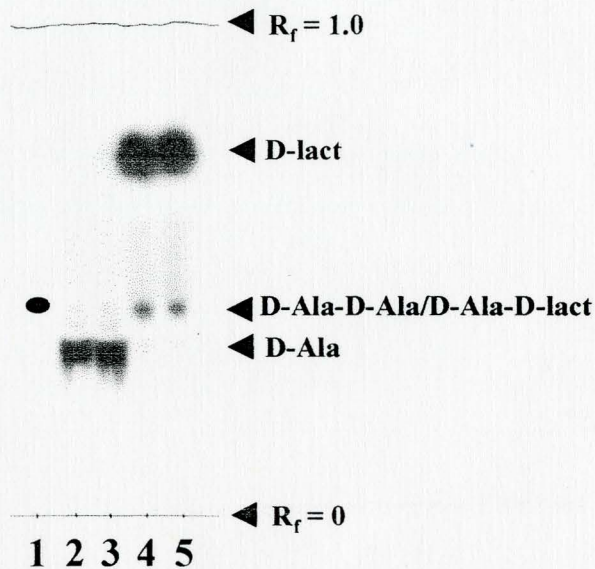
Figure 6.4. Activity of Heterologously Expressed DdlM. Reactions
contained D-Ala only (lane 2), D-Ala and D-lact with [^{14}C]-D-Ala (lane 3), D-Ala and D-
lact with [^{14}C]-D-lact (lane 4), and D-lact only (lane 5).

DdlM expression from the *vegII* promoter in *B. subtilis* BR1157 initially appeared

promising due to the appearance of a distinct band of 36 kDa observed in boil-lysates of

transformed clones. Unfortunately, no D-Ala-D-lact forming activity was ever observed in extracts made from this expression system, despite partial purification attempts.

The *ddlM* gene was cloned into *S. lividans* 1326 under the control of its own upstream genetic elements as no shuttle vectors with strong promoters upstream of a MCS were available. Due to the close relationship of this host to the native environment of the gene, it seemed reasonable that these elements would be recognised as part of global stationary phase gene expression pathways. DdlM activity was detected in this expression system at low levels, however the chromatographic behaviour of this enzyme form was similar to that observed in *E. coli* BL21(DE3) cells, suggesting that it was not *wild-type* either.

As DdlM expressed in *E. coli* had catalytic activity with D-lactate (albeit unusual in character), this form of the enzyme was related to the *wild-type* form. The *ddlM* gene was cloned downstream of the *malE* gene and expressed in *E. coli* with the hope that folding of DdlM fused to Maltose Binding Protein would more closely resemble that of the native enzyme. The fusion product expressed in a soluble form to high levels as determined by boil lysis and SDS-PAGE. However, D-lactate activity assays of the fusion protein indicated that it possessed the same unusual characteristics as other heterologously expressed forms. Factor Xa-cleavage of DdlM from the fusion and its subsequent chromatographic analysis demonstrated the same unusual properties observed before. In addition to this, DdlM was inactivated by the reaction conditions required for sufficient cleavage.

In summary, all attempts to express *ddlM* in a heterologous host resulted in either

poor expression or expression of a form of the enzyme that did not resemble *wild-type*

DdlM, or both.

6.4.2 Purification of D-Alanine Ligases from S. toyocaensis NRRL 15009

Initial assay for DdlM activity from *S. toyocaensis* NRRL 15009 crude extracts

were performed with the objective of defining *wild-type* chromatographic properties and

product formation. Very low levels of DdlM were detected in cultures grown to late log

phase, and no activity was present in mid-log phase mycelia. Addition of A47934 to the

culture medium (5 μg/mL) greatly increased levels of DdlM activity in mid- to late-log

phase cultures and allowed partial purification (Table 6.1). Five purification steps were

applied to produce 0.12 mg of protein from 5.5 grams of cells, although the effectiveness

of the last step (D-Ala-D-Ala Agarose) was negligible. DdlM from *S. toyocaensis* NRRL

15009 did not elute from the void volume of gel exclusion columns or from low-salt

washes of anion exchange columns, and had chromatographic properties similar to VanA.

This form of DdlM also did not form products from only D-lactate and ATP, requiring

the presence of D-alanine to produce a spot corresponding to D-Ala-D-lact on TLC

sheets. A protein of apparent molecular mass 37 kDa was associated with active

fractions and predicted to be DdlM. DdlM was not purified to homogeneity as at least

five other proteins were present in the final sample as determined by SDS-PAGE analysis

(Figure 6.5, A).

Table 6.1. Purification of DdlM from *S. toyocaensis* NRRL 15009

Protein Sample	Protein (mg)	Specific Activity (U/mg protein)	Total Activity[1] (U)	Recovery (%)	Purification (n-fold)
Clarified Lysate	148.0	-	-	-	-
Q Sepharose	51.9	1.26	65.4	-	-
Superdex 200	17.4	1.37	23.8	36.4	1.09
Mono Q	4.16	4.28	17.8	27.2	3.40
Phenyl Superose	0.05	79.1	4.11	6.28	62.8
D-Ala-D-Ala Agarose	0.12	34.4	4.13	6.31	27.3

[1] 1 U was defined as 1 nmol ATP hydrolysed per minute.
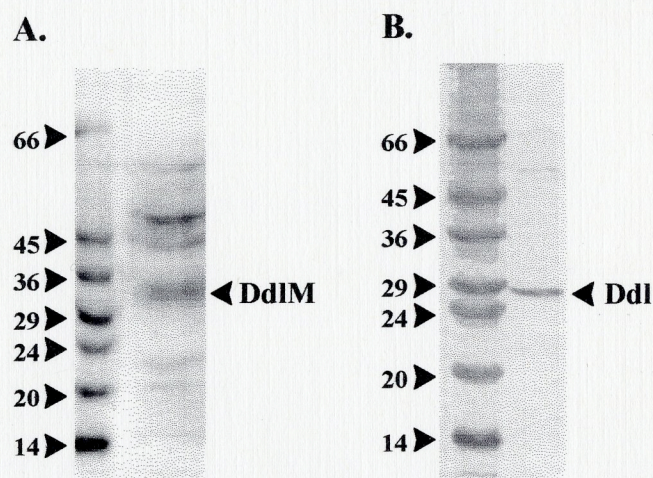
Figure 6.5. SDS-PAGE of Purified *S. toyocaensis* NRRL 15009 Ddls. Gels (11% polyacrylamide) show A. Partially purified DdlM sample. B. Purified 29 kDa Ddl.

In mid-log phase cultures grown in the absence of A47934, no D-Ala-D-lact forming activity was detected, however D-Ala-D-Ala formation was observed. This activity was purified in four steps (Table 6.2), yielding 0.05 mg from 5.5 g of cells. Activity was found to correspond to a protein of apparent molecular mass 29 kDa by SDS-PAGE analysis (Figure 6.5, B).

Table 6.2. Purification of D-Ala-D-Ala Ligase from *S. toyocaensis* NRRL 15009

Protein Sample	Protein (mg)	Specific Activity (U/mg protein)	Total Activity[1] (U)	Recovery (%)	Purification (n-fold)
Clarified Lysate	160	-	-	-	-
Q Sepharose	50.2	64.2	3220	-	
Superdex 200	14.7	75.15	1100	34.2	1.17
Mono Q	1.89	143	270	8.4	2.22
Phenyl Superose	0.05	504	20	0.71	7.84

[1] 1 U was defined as 1 nmol ATP hydrolysed per minute.

6.4.3 Characterisation of S. toyocaensis NRRL 15009 D-Ala Ligases

As only small amounts of enzyme were recovered from each preparation, characterisation studies were fairly limited. The quality of the samples (particularly DdlM) was low and interfered with some assays. For both DdlM and the 29 kDa Ddl, neither ES-MS nor N-terminal sequencing produced any conclusive data.

To determine its preferred substrate for ligation to D-alanine, DdlM was incubated with ATP, radiolabelled D-alanine and a variety of amino acids (D- and L-) or D-lactate. Products formed were assessed by TLC/autoradiography. DdlM was found to use D-alanine, D-lactate, D-phenylalanine and D-methionine (Figure 6.6, A). This substrate specificity profile was found to be identical to that of the VanA enzyme (2), and was consistent with a role for DdlM in PG alteration as a mode of GPA resistance. The 29 kDa Ddl, on the other hand, did not react with any substrate other than D-alanine, making D-alanyl-D-alanine exclusively even in the presence of D-lactate (Figure 6.6, B). These observations suggested a role for this enzyme in cell-wall biosynthesis independent of GPA-resistance pathways.

A.

1 2 3 4   ◄ $R_f = 1.0$

D-lact►

D-Ala►

◄ $R_f = 0$

B.

1 2 3   ◄ $R_f = 1.0$

D-lact►

D-Ala►

◄ $R_f = 0$
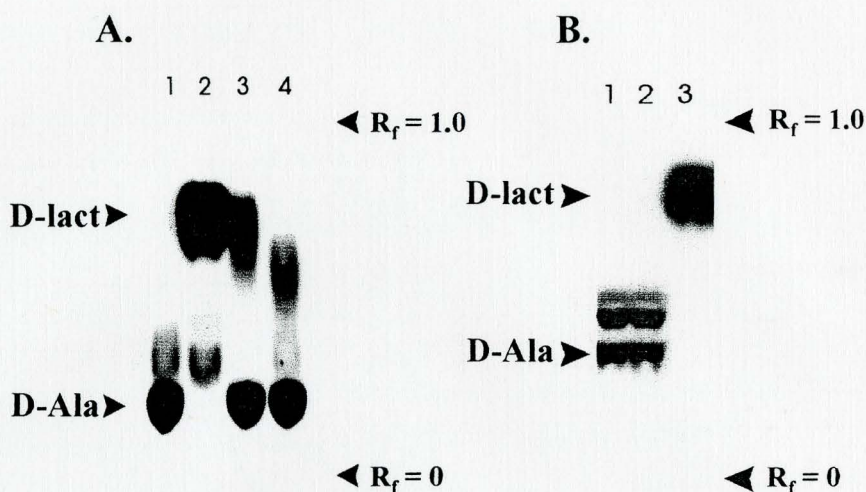
Figure 6.5. Substrate Utilisation by _S. toyocaensis_ NRRL 15009 Ddls. **A.**
TLC/autoradiogram of DdlM reactions containing D-Ala only (lane 1), D-Ala and D-lact with
[^{14}C]-D-lact (lane 2), D-Ala and D-Phe with [^{14}C]-D-Ala (lane 3), and D-Ala and D-Met with
[^{14}C]-D-Ala (lane 4). B. TLC/autoradiogram of Ddl reactions containing D-Ala only (lane 1),
D-ala and D-lact with [^{14}C]-D-Ala (lane 2), and D-ala and D-lact with [^{14}C]-D-lact (lane 3).

Kinetic analysis of DdlM is reported in Table 6.3. Both K_m and V_{max} were

reported for this enzyme using D-alanine and D-lactate (D-Ala$_2$ and D-lact, respectively)

as a substrate for ligation to D-alanine (D-Ala$_1$). It should be noted, however, that V_{max}

values were calculated using protein determinations done on a partially purified DdlM

sample, and were therefore expected to be lower than the true values. While DdlM had a

33-fold higher V_{max} using D-Ala$_2$, the K_m for D-Ala$_2$ was 150 times higher than that for

D-lact, resulting in a 4.3 fold greater efficiency for the formation of depsipeptide. The

K_m values obtained for DdlM are quite similar to those for the VanA enzyme, which has

values of 195 mM and 0.9 mM for D-Ala$_2$ and D-lact, respectively (9). Ddl had a K_m for

D-Ala$_2$ of 2.7 ± 0.25 mM which was comparable to that for DdlM's D-lact and _E. coli_

DdlB's D-Ala$_2$ (1.1 mM). Its V_{max} for dipeptide formation was much higher than DdlM's

depsipeptide maximal rate, making it an order of magnitude more efficient of an enzyme.

Table 6.3. Kinetic Parameters of *S. toyocaensis* NRRL 15009 Ddls

Enzyme	Substrate	K_m (mM)	V_{max} (U/mg)[1]	V_{max}/K_m (Umg^{-1}M^{-1})
DdlM	D-Ala$_2$	166 ± 27	720 ± 62	4.34 x 10^3
	D-lact	1.08 ± 0.10	21.8 ± 0.4	1.85 x 10^4
Ddl	D-Ala$_2$	2.72 ± 0.25	406 ± 14	1.49 x 10^5
	ATP	0.581 ± 0.068	711 ± 33	1.37 x 10^6

[1] 1 U was defined as 1 nmol ATP hydrolysed per minute.

This data, combined with the observation that DdlM activity is completely absent

from mid-log phase culture extract unless A47934 is present in growth media, strongly

supported the role of DdlM in GPA resistance predicted by the genetic studies of the

previous chapter. *S. toyocaensis* NRRL 15009 Ddl was present in extracts regardless of

the presence of A47934 in culture, and its exclusive formation of D-Ala-D-Ala indicated

that this enzyme was the cornerstone ligase in the PG biosynthesis pathway. Its presence

further supported the role of a VanX enzyme in *S. toyocaensis* NRRL 15009, which

would be required to affect the transition from PG terminating in D-alanine to PG

terminating in D-lactate.

6.5 Conclusions

S. toyocaensis NRRL 15009 DdlM did not express in *E. coli, B. subtilis or S.

lividans* in a *wild-type* form, but rather in a (presumably) mis-folded form that had

unusual chromatographic properties as well as unusual catalytic activity with D-lactate.

Expression as a fusion protein with MBP did not remedy the problem. DdlM was

detected in *wild-type* form in *S. toyocaensis* NRRL 15009, however only in small amounts in late-log phase mycelia. The level of DdlM was greatly increased if mid-log phase mycelia grown in the presence of A47934 were used to make extracts. DdlM was partially purified and found to have similar substrate utilisation properties and kinetic parameters as the *Enterococcal* VanA/B enzymes. This would suggest that DdlM or enzymes like DdlM would serve as good models for these enzymes which have been difficult to study. In addition to DdlM, a 29 kDa Ddl was also purified from *S. toyocaensis* NRRL 15009 extracts and found to have properties similar to Ddls that function in normal PG biosynthesis, such as DdlB. Its expression was independent of the presence of A47934, which is consistent with the need for a VanX enzyme in the conversion of mycelia from GPA sensitive to GPA resistant. Unfortunately, there was insufficient quantities of both *S. toyocaensis* NRRL 15009 Ddls to allow detailed study of mechanism.

It is interesting that *S. toyocaensis* NRRL 15009 maintains a D-Ala-D-Ala ligase given that this organism produces a GPA. Why not manufacture and incorporate D-Ala-D-lact constitutively? It is possible that PG made from D-Ala-lact is inferior in some way that confers an evolutionary disadvantage (although it is not likely a structural disadvantage, given the time frame that the ester must remain intact). Alternatively, this may be a relatively new adaptation, and there has not been sufficient time for the organism to lose the old system. This would require that GPA biosynthesis was a new adaptation too, unless there are multiple resistance mechanisms. A third possibility is that conversion of cell wall to D-Ala-D-lact in late log phase serves some other purpose,

perhaps part of the series of global changes that occur as the cells enter into stationary

phase. This might correlate with the existence of these genes in organisms (*S. coelicolor*,

S. lividans) which do not produce GPAs.

6.6 References

1. **Bruckner, R.** 1992. A series of shuttle vectors for *Bacillus subtilis* and *Escherichia coli*. Gene. **122**(1):187-92.

2. **Bugg, T. D., S. Dutka-Malen, M. Arthur, P. Courvalin, and C. T. Walsh.** 1991. Identification of vancomycin resistance protein VanA as a D-alanine:D-alanine ligase of altered substrate specificity. Biochemistry. **30**(8):2017-21.

3. **Denis, F., and R. Brzezinski.** 1992. A versatile shuttle cosmid vector for use in *Escherichia coli* and actinomycetes. Gene. **111**(1):115-8.

4. **Fan, C., P. C. Moews, C. T. Walsh, and J. R. Knox.** 1994. Vancomycin resistance: structure of D-alanine:D-alanine ligase at 2.3 A resolution. Science. **266**(5184):439-43.

5. **Hopwood, D. A., M. J. Bibb, K. F. Chater, T. Keiser, C. J. Bruton, H. M. Keiser, D. J. Lydiate, C. P. Smithe, and J. M. Ward.** 1985. Genetic Manipulations of Streptomyces. John Innes Foundation, Norwich.

6. **Kusaoke, H., H. Yoshitaka, K. Yasuhiro, and H. Kimoto.** 1989. Optimum conditions for electric pulse-mediated gene transfer to *Bacillus subtilis* cells. Agric Biol Chem. **53**(9):2441-46.

7. **Lanzetta, P. A., L. J. Alvarez, P. S. Reinach, and O. A. Candia.** 1979. An improved assay for nanomole amounts of inorganic phosphate. Anal Biochem. **100**(1):95-7.

8. **Leatherbarrow, R. J.** 1992. Grafit, 3.0 ed. Erithacus Software Ltd., Staines, U.K.

9. **Lessard, I. A. D.** 1997. Personal communication, VanA Kinetic Parameters.

10. **Park, I. S., C. H. Lin, and C. T. Walsh.** 1996. Gain of D-alanyl-D-lactate or D-lactyl-D-alanine synthetase activities in three active-site mutants of the *Escherichia coli* D-alanyl-D-alanine ligase B. Biochemistry. **35**(32):10464-71.

11. **Shi, Y., and C. T. Walsh.** 1995. Active site mapping of *Escherichia coli* D-Ala-D-Ala ligase by structure- based mutagenesis. Biochemistry. **34**(9)**:**2768-76.

12. **Wright, G. D., and C. T. Walsh.** 1993. Identification of a common protease-sensitive region in D-alanyl-D- alanine and D-alanyl-D-lactate ligases and photoaffinity labeling with 8-azido ATP. Protein Sci. **2**(10)**:**1765-9.

Chapter 7

Purification and Characterisation of the
D-Alanyl-D-Lactate Ligase DdlN from *A. orientalis* C329.2

Adapted from

7.1 Introduction

As efforts to express the *ddlM* gene to high levels met with no success, *ddlN* was the next logical choice. As neither *vanD* nor the *S. coelicolor vanA*-homologue had yet been discovered, DdlN was also the only available alternative. The goals of studying DdlN were identical to those stated in the previous section relating to DdlM. Biochemical evidence was required to support the primary sequence homology evidence that a Ddl from a GPA-producing organism could serve as a model for studying the clinically important VanA/B enzymes.

Substrate specificity and steady-state kinetic parameters were used to examine DdlM for functional homology to VanA, however there are other aspects of catalysis which can be analysed to establish a close relationship between enzymes. As VanA is capable of producing two distinct products, dipeptide and depsipeptide, factors that determine the flux of substrate to these two products is also a characteristic that can be used in drawing comparisons. Another tool is enzyme inhibition using specific molecules. In the last section, the use of a phosphinate compound in developing a model for the active site of DdlB was discussed. These molecules are also useful in their ability to inhibit the steady-state kinetic properties of enzymes. As they mimic the substrates used in catalysis, they can bind to the enzyme active site and sequester enzyme from the pathway that results in product formation. In this regard they behave as reversible competitive inhibitors. However, upon phosphorylation in the active site, these molecules closely mimic the tetrahedral intermediate of the second catalytic step, and become bound so tightly that they essentially inactivate the enzyme. This process is

relatively slow and produces biphasic product curves (initial rates are a reflection of phosphinate binding, final rates are zero and are the result of phosphinophosphate binding). By measuring the degree of inhibition of phosphinate itself, and the rate at which phosphorylation (i.e. time-dependent inactivation) occurs, enzyme active sites can be compared for their ability to bind and process these inhibitors, respectively. For depsipeptide ligases, the effects of phosphonate inhibitors (Figure 7.1), which more closely resemble depsipeptide intermediates, can be compared to the phosphinate-mediated effects.

Phosphinate
(D-Ala[PO$_2$-CH$_2$]D-Ala)

Phosphonate
(D-Ala[PO$_2$-O]D-Ala)
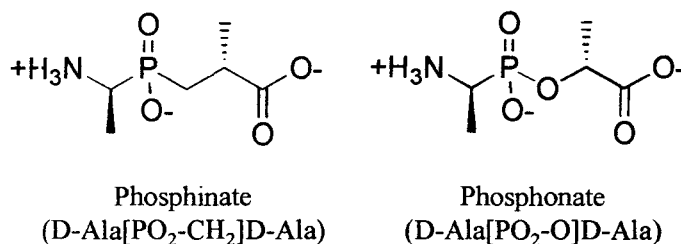
Figure 7.1. Slow-Binding Inhibitors Used to Study DdlN. Also known as time-dependent inactivators, but the phosphorylated forms of these molecules are not true inactivators as they do eventually dissociate.

This chapter describes the expression of *ddlN* to moderate levels in *E. coli* BL21(DE3) and the subsequent purification of DdlN. This enzyme was characterised with respect to substrate utilisation, steady-state kinetic parameters, product partitioning and catalytic inhibition, and its properties compared to the enzymes VanA and DdlB. DdlN was also purified in large amounts for X-ray crystal screens.

7.2 Materials

Phosphoenolpyruvate (PEP), NADH, MES, CHES, cycloserine and all amino acids and hydroxy acids were purchased from Sigma. Pyruvate kinase / lactate dehydrogenase and Tris were from Boehringer Mannheim. All columns were from Pharmacia and all restriction enzymes were obtained from MBI Fermentas. Vent was from New England Biolabs. The phosphinate and phosphonate inhibitors were a gift from P.A. Bartlett.

7.3 Methods

7.3.1 DdlN Detection Assays

DdlN was assayed during purification using both inorganic phosphate (P_i) detection and [^{14}C]-D-lactate incorporation into depsipeptide. [^{14}C]-incorporation assays (25 μL) contained 100mM Tris pH 8.0, 20 mM $MgCl_2$, 10 mM KCl, 6 mM ATP, 2.5 mM D-Ala, 2.5 mM D-lact, 0.1 μCi [^{14}C]-D-lact and 1-2 ug enzyme. Reactions were incubated 1 hour at 37 ^{O}C and 4-5 μL spotted onto Kodak Cellulose TLC plates. Products were eluted in n-butanol:acetic acid:water (12:3:5), dried and exposed to film. P_i detection assays (50 μL) contained 100 mM HEPES pH 8.0, 20 mM $MgCl_2$, 20 mM KCl, 6 mM ATP, 1 mM D-Ala 10 mM D-lactate and varying amounts of enzyme. Reactions were incubated 10-20 min at 37°C and inorganic phosphate was detected by binding to molybdate/Malachite Green (6).

7.3.2 Construction of pETDdlN

The *ddlN* gene was cloned behind the T7 promoter of pET22b by engineering restriction sites at its 5' and 3' ends. This was accomplished using Vent PCR of a clone containing the entire van gene cluster from *A. orientalis* C329.2. PCR reactions (50uL) contained 250 ng pGEMC329vn3.5, 10 mM KCl 20 mM Tris-HCl pH 8.8, 10 mM AS, 4 mM MgSO$_4$, 0.1% Triton X-100, 5% DMSO, 0.4 mM dNTPs, 1 unit Vent polymerase and 1 μM of each of the following primers: 5'- GCTCTAGACATATGGGTAGGCTG AAAATCGGAATTCTG - 3' and 5'- CCCAAGCTTTCATCCCTCATTCGTCACGC CCG - 3'. Reactions were cycled 25 times through 94 $^{\circ}$C, 50 $^{\circ}$C and 72 $^{\circ}$C for 0.5 min, 0.5 min and 1.0 min, respectively. 2 μg of product of approximately 1.1 kb was isolated and digested to completion with *Nde*I and *Hind*III. This was ligated to similarly digested pET22b vector and transformed into competent *E.coli* BL21(DE3). Clones containing the *ddlN* gene were identified by RFLP of small-scale plasmid isolates. The fidelity of amplification was confirmed by DNA sequencing performed by Dr. B. Allore on an ABI automated cycle sequencer.

7.3.3 DdlN Purification

E.coli BL21(DE3) containing the plasmid pETDdlN was grown in 1.0 L quantity to mid-log phase and T7 polymerase was induced with 1mM IPTG for 3 hours. All the following steps were performed at 4 $^{\circ}$C. Cells (1.9 g) were suspended in 100mM HEPES pH 7.5, 300 mM NaCl, 5 mM MgCl$_2$, 1 mM EDTA, 5 mM DTT, 1 mM PMSF and passed twice through a French Press pressure cell at 20, 000 psi. The lysate was clarified

by centrifugation at 12,000 x g, and AS was added to 20%. Precipitated proteins were

removed by centrifugation at 12,000 x g and AS added to 50%. Precipitated proteins

were removed and suspended in a minimum volume of column buffer containing 200mM

NaCl. Column buffer contained 50 mM HEPES pH 7.5, 5 mM $MgCl_2$, 1 mM EDTA, and

0.1 mM DTT. Proteins were loaded onto a Superdex S-200 column (2.6 x 114 cm) and

eluted at 0.5 mL/min. Active fractions were pooled, concentrated/desalted to 10 mL in

column buffer containing 100 mM NaCl and loaded onto a Q Sepharose column (1.0 x

13 cm). Proteins were eluted with a linear gradient of 100 mM NaCl to 500 mM NaCl in

column buffer over 10 column volumes. Active fractions were pooled,

concentrated/desalted to 1 mL in column buffer containing 100 mM NaCl and AS was

added to 1.5 M. The sample was loaded onto a Phenyl Superose column (0.5 x 5 cm) and

eluted with a linear gradient of 1.5 M to 0 M AS in column buffer over 60 column

volumes. Active fractions were pooled and concentrated/desalted to 0.5 mL in column

buffer containing 100 mM NaCl. Total protein concentration was determined by

Bradford Assay and sample purity was evaluated by SDS-PAGE.

7.3.4 Characterization of DdlN

    To determine DdlN substrate specificity, various substrates were incubated with

DdlN and [^{14}C]-D-Ala and products analyzed by TLC-autoradiography. Reactions (25

μL) contained 100mM Tris pH 8.0, 20 mM $MgCl_2$, 10 mM KCl, 6 mM ATP, 2.5 mM D-

alanine, 10 mM varied substrate, 0.1 μCi [^{14}C]-D-alanine, 2 μM DdlN and were allowed

to proceed for 16 hours at room temperature.

Kinetic analysis of DdlN was done using a continuous spectrophotometric assay in which ADP production was coupled to pyruvate kinase- (PK) and lactate dehydrogenase- (LDH) dependent consumption of NADH (3). Reactions (1 mL) contained 50 mM HEPES pH 7.5, 40 mM KCl, 10 mM MgCl$_2$, 0.6 mg PEP, 0.2 mg NADH, 20 µg of PK/LDH, 10 µg of DdlN, saturating amounts of the fixed substrate and differing amounts of the variable substrate. To measure D-Ala-D-lact formation, 5 mM D-Ala was included in reaction mixtures and the rate obtained using 0 mM D-lact was taken as the baseline rate. NADH oxidation was monitored at 340 nm over several minutes and linear slopes measured.

Data were fit to the equation [1] by non-linear least squares methods using the program Grafit ver. 3.01 (7).

$$v = V_{max}[S] / ([S] + K_m)$$ [1]

The effect of pH on DdlN product partitioning was determined in a manner similar to that described for VanA (9). Reactions contained a composite buffer containing MES, HEPES, Tris, and CHES (50 mM each), 20 mM MgCl$_2$, 10 mM KCl, 6 mM ATP, 10 mM D-Ala, 5 mM D-hydroxybutyrate, 0.1 µCi [^{14}C]-D-Ala, 2 µM DdlN and were allowed to proceed for 16 hours at room temperature. A portion of each reaction (5 µL) was spotted onto Kodak Cellulose TLC plates. Products were eluted in n-butanol:acetic acid:water (12:3:5), dried and exposed to film. Products were quantified by exposing to a phosphoimaging screen and spot intensities integrated.

7.3.5 Inhibitor Assays

Inhibition of DdlN by cycloserine, phosphinate and phosphonate was measured by measuring the kinetic parameters of D-Ala-D-Ala formation at various concentrations of inhibitor. Data (initial steady-state rates) collected were analysed by fitting to equation 2, 3, or 4 for competitive, uncompetitive inhibition, or noncompetitive mixed, respectively. Inhibition constants for phosphinate and phosphonate inhibitors were calculated under the assumption that these inhibitors bound to the E•ATP•D-Ala$_1$ form of the enzyme, as depicted in Figure 7.2. While an excellent argument is made for the binding of these types of inhibitors to E•ATP (5), data could not be fit to the corresponding equations due to the difficulty in measuring inhibition of rates at D-Ala concentrations near the K_m of D-Ala$_1$. Calculation of the true K_i values for these inhibitors with DdlN was not required for comparison to VanA or DdlB values as these have been calculated both ways for these enzymes (5).

$$v = V_{max}S / [K_{m2}(1 + I/K_{is}) + S]$$ [2]

$$v = V_{max}S / [K_{m2} + S(1 + I/K_{ii})]$$ [3]

$$v = V_{max}S / [K_{m2}(1 + I/K_{is}) + S(1 + I/K_{ii})]$$ [4]

Parameters obtained from the best fit are reported with standard errors to the fit. Replots of slope and/or intercept of double reciprocal plots were linear.

Analysis of the time-dependent inactivation of DdlN by phosphinate and phosphonate in the presence of ATP was based on a review by Morrison and Walsh (8). Reactions contained 6 mM ATP (5 x K_m), 90 mM D-Ala (0.5 x K_m) and 10 to 45 μM

A.

$$
\text{E•ATP} \underset{K_{m1}}{\overset{\text{D-Ala}}{\rightleftarrows}} \text{E•ATP•D-Ala}_1 \underset{K_{m2}}{\overset{\text{D-Ala}}{\rightleftarrows}} \text{E•ATP •D-Ala}_1 \text{•D-Ala}_2 \overset{k_{cat}}{\longrightarrow} \begin{array}{l} \text{D-Ala-D-Ala} + \\ \text{E + ATP + P}_i \end{array}
$$

$$K_{is} \updownarrow\ I$$

E•ATP•D-Ala$_1$•I

B.

$$
V = \frac{V_{max}\ [\text{D-Ala}]^2}{K_{m1}K_{m2} + K_{m2}\,[\text{D-Ala}]\left[1 + \frac{[I]}{K_{is}}\right] + [\text{D-Ala}]^2}
$$

$$
V = \frac{V_{max}\ [\text{D-Ala}]}{K_{m2}\left[1 + \frac{[I]}{K_{is}}\right] + [\text{D-Ala}]}
$$

when $K_{m1} \ll K_{m2}$
and $[\text{D-Ala}] = K_{m2}$
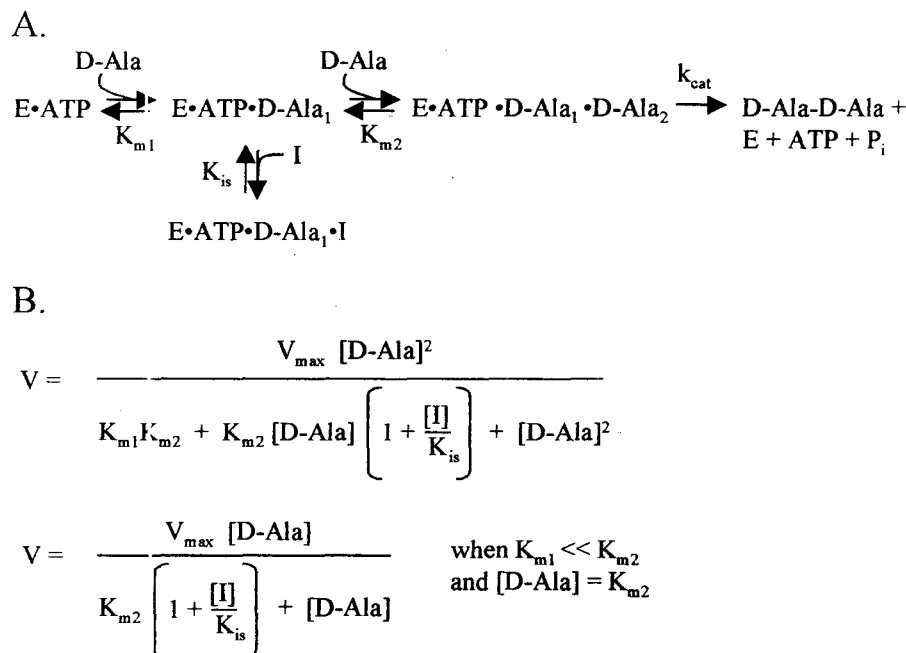
Figure 7.2. Kinetic Analysis for the Inhibition of DdlN. **A. Reaction pathway for inhibitor binding. B. Equation that describes the observed inhibition pattern.**

(phosphinate) or 30 to 100 µM (phosphonate) inhibitor. From the biphasic curves obtained, initial rate and final rate were measured (final rates were zero at all concentrations of inhibitor used). In addition, an estimate for the observed rate of inactivation (k_{obsd}) was obtained by taking the reciprocal of the x co-ordinate (time) of the point of intersection of the asymptotes to the measured rates. Eight to nine points were taken from the curve at equal time distributions and fit to equation 5 that describes product formation versus time in the presence of a slow-binding, irreversible inhibitor. Data were fit to the equation by non-linear least squares methods using the program Grafit ver. 3.01 (7). From each inhibitor concentration a value of k_{obsd} was obtained which is related to inhibitor concentration by equation 6. A reciprocal plot of k_{obsd} versus

inhibitor concentration was fit by linear regression to give a line with a y-intercept of $1/k_3$. k_3 is the rate constant for inhibitor phosphorylation (represented as EI $\rightarrow$ EI') described by equation 7, and is commonly called k_{inact}.

$$P = (V_O [1 - e^{(-k't)}]) / k' \qquad [5]$$

$$k' = k_{obsd} = k_3(I / [K_i(1 + S/K_s) + I]) \qquad [6]$$

$$\overset{k_1 \quad k_3}{E + I \leftrightarrow EI \rightarrow EI'} \qquad [7]$$
$$\underset{k_2}{}$$

The rate at which phosphinate-inactivated DdlN could regain activity once removed from inhibitor was determined as described for the *S. typhimurium* Ddl (4). DdlN (400 μg) was incubated overnight at 4 °C with or without 500 μM phosphinate in 100 mM HEPES pH 7.5, 10 mM MgCl$_2$, 10 mM KCl, 2 mM ATP in a total volume of 0.1 mL. Reactions were passed over a fast desalt column at 5 mL/min in 50 mM HEPES pH 7.5, 50 mM NaCl. DdlN containing fractions (2 x 0.5 mL) were pooled and stored at 4 °C. At the specified time points, 25 μL of the sample was used to assay activity as described above using 185 mM D-Ala and 6 mM ATP and the coupled assay system.

7.3.6 Purification of DdlN for X-Ray Crystallography Crystal Trials

Purification of large quantities of highly pure DdlN was necessary for crystal screening procedures and required a specific purification protocol. LB medium (20 L) supplemented with ampicillin to 50 μg/mL was prepared in a 45 L New Brunswick Scientific Fermentor and was inoculated by the addition of 1% (vol/vol) of a freshly saturated culture. Cells were grown to an optical density of 1.1 at 600 nm at 37 °C with an impeller speed of 200 rpm and air infusion at 15 L per minute. Cells were induced

with IPTG added to 1 mM for 3 hours to an optical density of 1.3. Cells were harvested

in a continuous flow centrifuge to yield 60-65 g (wet weight). These were washed in

0.85 % NaCl, frozen in 12-14 g aliquots and stored at –80 $^\circ$C. All subsequent steps were

performed at 4 $^\circ$C. Aliquots were suspended in 50 mL of lysis buffer (100 mM HEPES

pH 7.5, 300 mM NaCl, 5 mM MgCl$_2$, 1 mM EDTA, 5 mM DTT, 1 mM PMSF) and

passed three times through a French Press set to 20, 000 psi. Lysate was clarified by a 15

minute spin at 15, 000 x g, the pellet re-extracted with lysis buffer and the combined

supernatants diluted 1.5 fold with column buffer (50 mM HEPES pH 7.5, 5 mM MgCl$_2$, 1

mM EDTA, 0.1 mM DTT). The sample was applied to a Q Sepharose column (3 x 10

cm) at 3 mL/min and proteins eluted with a linear gradient from 200 to 400 mM NaCl in

column buffer over 3 column volumes. Fractions (6 mL) were screened for DdlN by P$_i$

release assay and SDS-PAGE. DdlN containing fractions were pooled and AS slowly

added to 700 mM final concentration (20% solution saturation). Sample was allowed to

equilibrate and applied to a Phenyl Superose column (3 x 7 cm) equilibrated in 700 mM

AS in column buffer at 3 mL/min. Proteins were eluted using a linear gradient from 700

to 500 mM AS in column buffer over 6 column volumes. DdlN containing fractions (6

mL) were pooled and concentrated to 2.5-3.0 mL. This was loaded onto a Superdex 200

(2.6 x 114 cm) equilibrated in 100 mM NaCl in column buffer at 0.45 mL/min using a

minimum length of tubing between sample and column bed. Ddl-containing fractions (4

mL) were pooled and assayed for total protein content (usually about 30 mg) by Bradford

Assay. Aliquots (5 mg) were applied to a MonoQ column (0.5 x 5.0 cm) in 200 mM

NaCl in column buffer at 1 mL/min. Proteins were eluted with a linear gradient from 200

to 400 mM NaCl over 30 column volumes. DdlN-containing fractions (1 mL) were identified by SDS-PAGE and pooled. The pure sample was concentrated and diluted repeatedly to desalt the sample to a final concentration of 10 mg/mL in 5 mM HEPES, pH 7.5, 0.1 mM DTT and no more than 1 mM NaCl. Yield was typically 20 mg from 12-14 g of cells.

7.4 Results and Discussion

7.4.1 Purification of DdlN from E. coli BL21(DE3)

Unlike *ddlM*, *ddlN* expressed to high levels in an apparently *wild-type* form using the pET expression system (Novagen). D-Ala-D-lact forming activity was not found in the void volume of gel exclusion columns nor was it eluted from anion exchange columns with low ionic strength buffer. Furthermore, no products were detected when the only substrates present in DdlN reactions were ATP and D-lactate. Table 7.1 shows that DdlN was purified in four steps to yield 0.4 mg from 1.9 g of cells. While this was still low compared to typical yields of protein expressed by this system, it allowed for a much more detailed study than was possible with DdlM. SDS-PAGE of the purified sample (Figure 7.3) indicated that DdlN had an apparent mass of 38 kDa and was at least 95% pure.

Table 7.1. Purification of DdlN from *E. coli* BL21(DE3)

Protein Sample	Protein (mg)	Specific Activity[1] (U/mg protein)	Total Activity (U)	Recovery (%)	Purification (n-fold)
Clarified lysate	124	6.82	843	-	-
AS (20-50% saturation)	67.6	11.5	780	92.5	1.7
Superdex 200	11.6	71.4	825	97.9	10.5
Q Sepharose	2.8	265	742	88	38.9
Phenyl Superose	0.4	748	299	35.5	110

[1] 1 U was defined as 1 nmol ATP hydrolysed per minute
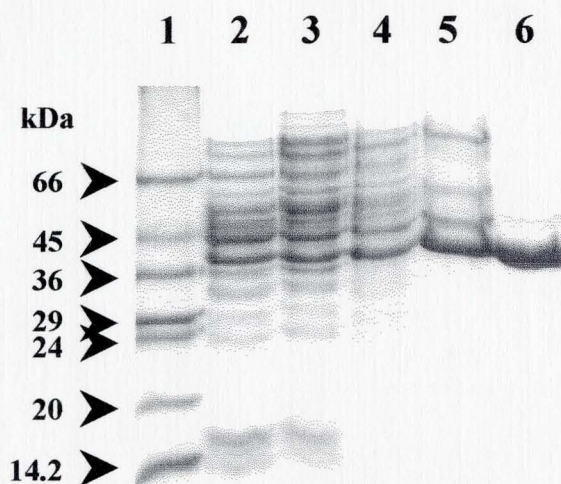
Figure 7.3. SDS-PAGE of DdlN Purification Samples. Gel (11% polyacrylamide) contained molecular weight standards (lane 1), clarified lysate (lane 2), 20-50% AS saturation fraction (lane 3), Superdex S-200 pool (lane 4), Mono Q pool (lane 5), Phenyl Superose pool (lane 6).

7.4.2 Substrate Utilisation by DdlN

DdlN was assayed using a variety of substrates including several that are known to by utilized by VanA for ligation to D-Ala$_1$ (2). All twenty proteinaceous amino acids were tested (both D- and L- isomers) as well as several different hydroxy acids. In addition to synthesis of D-Ala-D-Ala and D-Ala-D-lact, DdlN could form D-Ala-D-Met, D-Ala-D-Phe, D-Ala-D-hydroxybutyrate (D-Hbut) and D-Ala-D-hydroxyvalerate (D-

Hval) (Figure 7.4). This profile matched VanA well, which also uses Met, Phe, Hbut, and Hval. Of these compounds, DdlB uses only D-Ala, although D-Ala-D-lact is formed at barely detectable levels at very low pH. The profile shared by DdlN and VanA indicates an interesting combination of promiscuity and specificity, as the active site will accept a bulky amino acid like phenylalanine in place of $D-Ala_2$/D-lact and yet will not accept serine or tyrosine.
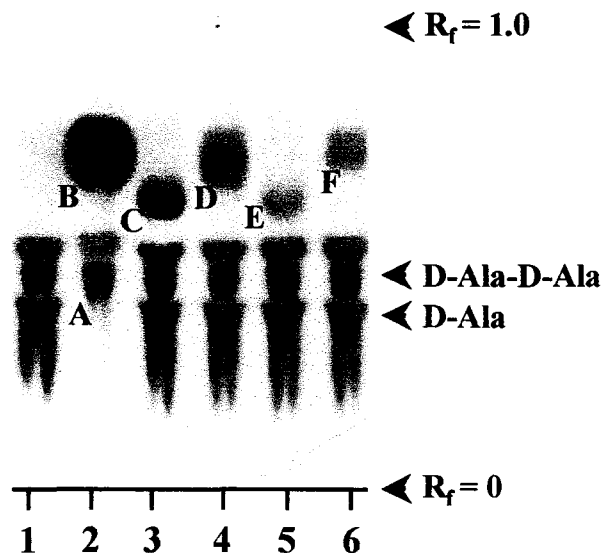
Figure 7.4. Substrate Specificity of DdlN. Autoradiogram from TLC analysis of DdlN substrate specificity. All reaction mixtures contained 2.5 mM D-Ala and 1 mM ATP, and the radiolabel was [^{14}C]-D-Ala except where noted. D-ala (lane 1), D-lact with [^{14}C]-D-lact label (lane 2), D,L-Met (lane 3), D,L-Phe (lane 4), D-hydroxybutyrate (lane 5), D-hydroxyvalerate (lane 6). Letters indicate the following: A, D-Ala-D-lact; B, D-lact; C, D-Ala-D-Met; D, D-Ala-D-Phe; E, D-Ala-D-Hbut; F, D-Ala-D-Hval.

7.4.3 Kinetic Parameters of DdlN

The steady-state kinetic parameters of DdlN were calculated using D-Ala, D-lact and D-Hbut as substrates (Table 7.2). The K_m values for $D-Ala_1$, $D-Ala_2$, D-lact and D-Hbut were very similar to those for VanA (2). DdlN k_{cat} values for D-Ala-D-Ala

formation (5.3 s^{-1}) and D-Ala-D-lact formation (0.91 s^{-1}) were also comparable to the

VanA values. As expected, the K_m for D-Ala$_1$ was considerably lower than D-Ala$_2$ (270-

fold), and nearly 2-fold higher than that of D-lact. While this relationship is consistent

with what is observed in VanA, the K_m of D-Ala$_1$ in DdlB is 1000-fold lower than that of

D-Ala$_2$, and is 330-fold and 750-fold lower than the D-Ala$_1$ K_m values of DdlN and

VanA, respectively. Thus it appears that the D-Ala-D-lact Ddls have sacrificed D-Ala$_1$

binding in remodelling their active sites for depsipeptide synthesis. DdlN and VanA are

also about 100-fold less efficient than DdlB.

While DdlN used D-Hbut better than D-Ala$_2$, it was an order of magnitude less

efficient than its use of D-lact, and is not likely an *in vivo* substrate. DdlN's ATP K_m

seemed unusually high at 1.2 mM.

Table 7.2 Kinetic Parameters of DdlN and VanA

Enzyme	Substrate	k_{cat} (s^{-1})	K_m (mM)	k_{cat}/K_m (s^{-1}/M^{-1})
DdlN	D-Ala$_1$	0.7 ± 0.1	0.69 ± 0.19	6.1 x 10^1
	D-Ala$_2$	5.3 ± 0.2	185 ± 8	2.9 x 10^1
	D-lact	0.91 ± 0.02	0.4 ± 0.1	2.3 x 10^3
	D-Hbut	0.53 ± 0.03	2.5 ± 0.3	2.1 x 10^2
	ATP[2]	1.2 ± 0.1	1.2 ± 0.2	9.8 x 10^2
VanA[1]	D-Ala$_1$	-	3.4	-
	D-Ala$_2$	15.7	195	8.1 x 10^1
	D-lact	0.75	0.9	8.3 x 10^2
	D-Hbut	1.8	0.6	3.0 x 10^3
	ATP	-	0.12	-
DdlB	D-Ala$_1$	-	0.0012	
	D-Ala$_2$	31.2	1.13	2.7 x 10^4
	ATP	-	0.049	

[1]Data obtained from reference 2.
[2]Measured in the presence of 1 mM D-Ala, 10 mM D-lact.
Hbut - hydroxybutyrate.

7.4.4 Partitioning of Dipeptide and Depsipeptide Ligase Activities of DdlN

In a series of experiments in which both D-Ala and D-Hbut were available to

DdlN in buffers of various pH, DdlN was observed to prefer depsipeptide synthesis at

lower pH and dipeptide synthesis at higher pH (Figure 7.5). D-Hbut was used rather than

D-lact as D-Ala-D-Hbut has a different R_f by TLC than D-Ala-D-Ala. This behaviour

was also observed in VanA and depsipeptide-forming mutants of DdlB (9), and may

reflect a need for α-amino deprotonation of D-Ala$_2$ for efficient catalysis. Thus one of

the strategies depsipeptide ligases may have evolved to select for hydroxy acid ligation to

D-Ala$_1$ is the absence of a mechanism for ammonium deprotonation.
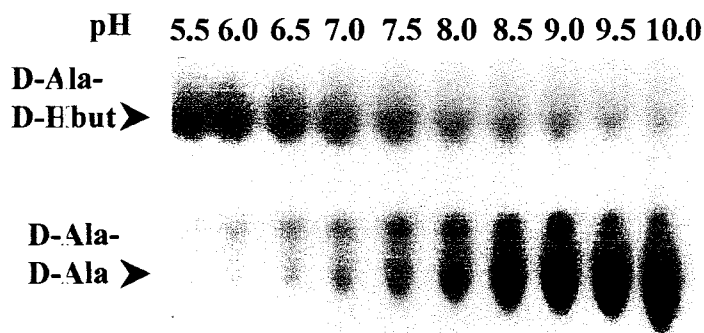
Figure 7.5. pH Dependence of Partitioning of the Syntheses of Peptide and Depsipeptide by DdlN. Autoradiogram of a TLC separation of the products of reaction mixtures containing [^{14}C]-D-Ala, unlabeled D-Ala and D-Hbut.

While the data presented in Figure 7.5 gives the impression that DdlN dipeptide

synthesis was competitive with depsipeptide at neutral pH, it should be noted that 1)

twice as much D-Ala was present as D-Hbut and 2) the efficiency of D-Ala-D-lact

synthesis is much higher than that of D-Ala-D-Hbut. Thus at neutral pH and with

equivalent amounts of substrate, D-Ala-D-lact formation would by far predominate that

of D-Ala-D-Ala.

7.4.5 Inhibition of DdlN

DdlN was inhibited by a number of compounds in a manner similar to VanA

(Table 7.3). The D-alanine analogue D-cycloserine was competitive with D-Ala$_2$ binding

with a K_{is} only 3 fold higher than that for VanA (1). DdlN was also inhibited by

phosphinate (D-Ala[PO$_2$-CH$_2$]D-Ala) and phosphonate (D-Ala[PO$_2$-O]D-lact)

compounds which have been found to bind tightly to other Ddls such as DdlB (Figure

7.6). DdlN K_{is} values for these compounds were approximatly half those observed when

Table 7.3 Inhibition of DdlN

Enzyme	Inhibitor	Pattern	K_i (μM)	k_{inact} (min^{-1})	k_{regain} (hours^{-1})
DdlN	D-cycloserine	C	K_{is}= 2300 ± 400	-	-
	phosphinate	C	K_{is} = 27 ± 3	0.7	4.4 x 10^{-3}
	phosphonate	NC	K_{ii} = 82 ± 18	1.2	-
			K_{is} = 190 ± 46		
VanA[1]	D-cycloserine	C	K_{is}= 730	-	-
	phosphinate	C	K_{is} = 60	4.9	-
	phosphonate	C	K_{is} = 130	-	-
DdlB[1]	phosphinate	C	K_{is} = 4	62	-
	phosphonate	C	K_{is} = 18	-	-

[1]Data obtained from reference 5.
Inhibition pattern was determined by Lineweaver-Burk plots and was either competitive (C) or mixed-type
non-competitive (NC), with respect to D-Ala$_2$. K_i values given do not take into consideration competition
with D-Ala$_1$.

VanA is similarly inhibited. It was unusual to observe a K_{ii} for phosphonate inhibition of

DdlN, as these molecules presumably bind only the form of the enzyme that binds D-

Ala$_1$, and should therefore be exclusively competitive. As was the case for VanA, the

phosphonate was a poorer inhibitor than the phosphinate, although this is not what one

would predict based on the preferred substrates for these enzymes. This may indicate

that in the depsipeptide ligase active site, D-Ala$_1$ binding facilitates subsequent D-lact

binding. Neither of these inhibitors were as potent on DdlN or VanA as they are on

DdlB, suggesting that the active sites of these enzymes are less complimentary to these

molecules than that of DdlB.
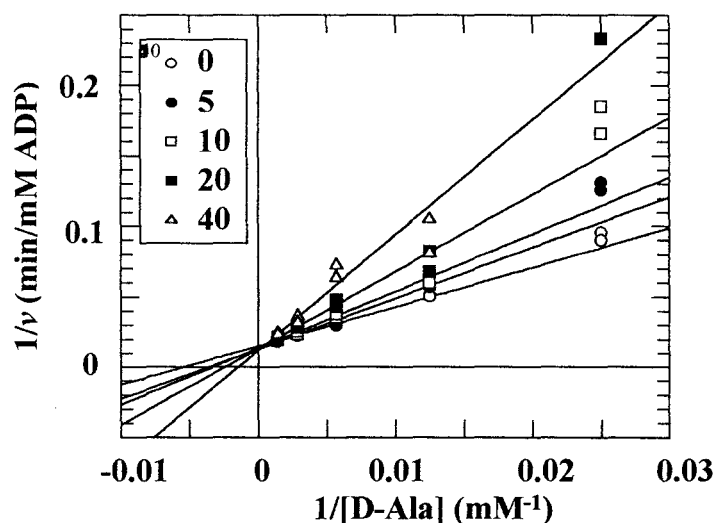
Figure 7.6. Effect of phosphinate on DdlN Kinetic Utilisation of D-Ala.
Lineweaver-Burk plots of D-Ala utilisation by DdlN at various concentrations of D,D-phosphinate, given in the legend in μM.

Both the phosphinate and phosphonate inhibitors were observed to function as

time-dependent inactivators of DdlN if reactions were allowed to proceed long enough

(Figure 7.7, A). This behaviour is also observed with DdlB and VanA and reflects

conversion of the inhibitor to the tightly-binding phosphorylated form. The rate at which

inactivation was observed to occur (k_{obsd}) was measured at various concentrations of

inhibitor, and the rate of phosphorylation (k_{inact}) determined from a reciprocal plot

(Figure 7.7, B). Phosphinate was phosphorylated by DdlN at a slightly lower rate than

phosphonate, and was 7-fold slower than VanA. This indicated that, while DdlN was

slightly better than VanA at binding these compounds, it was not nearly as good at

phosphorylating them. DdlB is by far superior in this respect to both enzymes, with a

k_{inact} 12-fold higher than VanA, and 90-fold higher than DdlN.

A.

B.
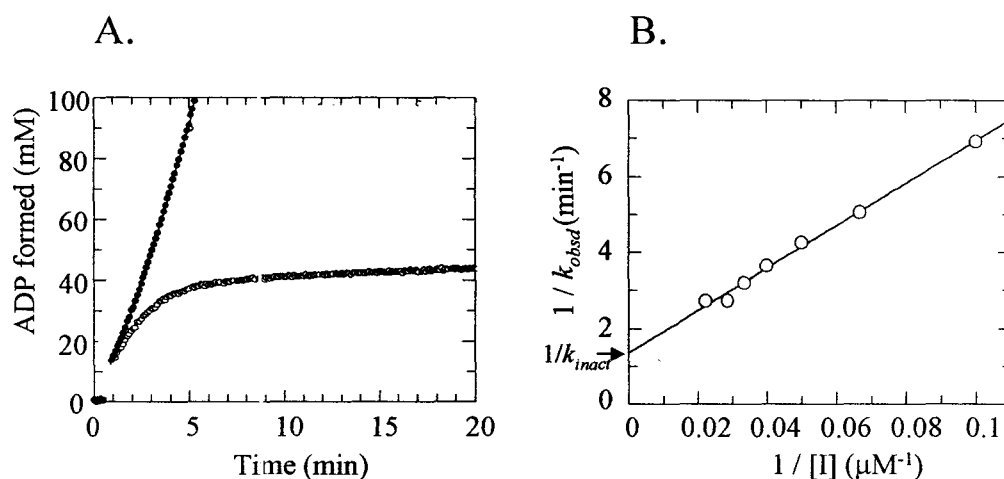
Figure 7.7. Time-dependent inactivation of DdlN by phosphinate. **A. Time course of ADP formation in the presence of 0 µM phosphinate (●) and 25 µM phosphinate (○); B. Effect of phosphinate on the observed rate of inactivation, k_{obsd}.**

Phosphinate-inactivated DdlN had a very low k_{regain} once removed from bulk

inhibitor, requiring 158 hours at 4 °C to recover half its D-Ala-D-lact ligase activity

(Figure 7.8). In a similar experiment, it took 8.2 hours for the Ddl from *S. typhimurium*

to recover (4). This Ddl was competitively inhibited by phosphinate with a K_{is} of 1.2

µM. It therefore appears that, while dipeptide Ddls like DdlB and the *S. typhimurium*

Ddl bind to and phosphorylate phosphinate much better than DdlN, DdlN is much more

tightly associated with the phosphorylated form of the inhibitor than these enzymes.
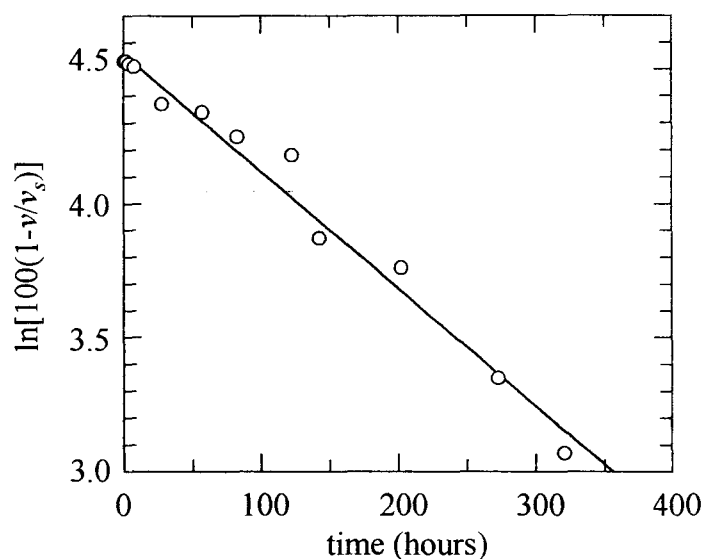
Figure 7.8. Regain of activity of phosphinate inhibited DdlN. The
initial time point (t=0) was taken as the moment of sample injection onto
desalting column. At each time point, rate (*v*) was measured and compared to
final velocity (*v$_s$*).

While it is difficult to extract any mechanistic information from these inhibitor

studies, they are useful in drawing comparisons between enzymes, and reinforce the

functional similarity between DdlN and VanA. They also support the classification of

these enzymes as a family of ligase distinct from the strictly dipeptide-forming ligase

DdlB.

7.4.6 DdlN X-Ray Crystallography

Close to 100 mg of DdlN has been purified and sent in concentrated, desalted

form to the laboratory of Dr. J. Knox at the University of Connecticut for X-ray crystal

screens. Unfortunately, efforts have not yet yielded any crystals that diffract with

sufficient resolution.

7.5 Conclusions

DdlN was purified from *E. coli* BL21(DE3) cells with good yield and purity. The enzyme was characterised with respect to substrate specificity, steady-state kinetic parameters, product partitioning and susceptibility to D-Ala-D-Ala ligase inhibitors. DdlN was found to be very similar to the enterococcal enzyme VanA in all of these categories. As all of these studies had been conducted on VanA previously, no new information was obtained about the mechanism of D-Ala-D-lact ligases with a group II ω-loop. However, functional homology between DdlN and VanA was established and supports use of DdlN as a model for VanA in structural studies. DdlN was purified in large quantities in a highly pure form for crystal screens, however crystals capable of diffracting X-rays with high resolution have not yet been obtained. These studies are ongoing.

7.6 References

1. **Bugg, T. D., S. Dutka-Malen, M. Arthur, P. Courvalin, and C. T. Walsh.** 1991. Identification of vancomycin resistance protein VanA as a D-alanine:D-alanine ligase of altered substrate specificity. Biochemistry. **30**(8):2017-21.

2. **Bugg, T. D., G. D. Wright, S. Dutka-Malen, M. Arthur, P. Courvalin, and C. T. Walsh.** 1991. Molecular basis for vancomycin resistance in *Enterococcus faecium* BM4147: biosynthesis of a depsipeptide peptidoglycan precursor by vancomycin resistance proteins VanH and VanA. Biochemistry. **30**(43):10408-15.

3. **Daub, E., L. E. Zawadzke, D. Botstein, and C. T. Walsh.** 1988. Isolation, cloning, and sequencing of the *Salmonella typhimurium* ddlA gene with purification and characterization of its product, D-alanine:D- alanine ligase (ADP forming). Biochemistry. **27**(10):3701-8.

4. **Duncan, K., and C. T. Walsh.** 1988. ATP-dependent inactivation and slow binding inhibition of *Salmonella typhimurium* D-alanine:D-alanine ligase (ADP) by (aminoalkyl)phosphinate and aminophosphonate analogues of D-alanine. Biochemistry. **27**(10)**:**3709-14.

5. **Ellsworth, B. A., N. J. Tom, and P. A. Bartlett.** 1996. Synthesis and evaluation of inhibitors of bacterial D-alanine:D-alanine ligases. Chem Biol. **3**(1)**:**37-44.

6. **Lanzetta, P. A., L. J. Alvarez, P. S. Reinach, and O. A. Candia.** 1979. An improved assay for nanomole amounts of inorganic phosphate. Anal Biochem. **100**(1)**:**95-7.

7. **Leatherbarrow, R. J.** 1992. Grafit, 3.0 ed. Erithacus Software Ltd., Staines, U.K.

8. **Morrison, J. F., and C. T. Walsh.** 1988. The behavior and significance of slow-binding enzyme inhibitors. Adv Enzymol Relat Areas Mol Biol. **61:**201-301.

9. **Park, I. S., C. H. Lin, and C. T. Walsh.** 1996. Gain of D-alanyl-D-lactate or D-lactyl-D-alanine synthetase activities in three active-site mutants of the *Escherichia coli* D-alanyl-D-alanine ligase B. Biochemistry. **35**(32)**:**10464-71.

Chapter 8

Molecular Mechanism of
S. toyocaensis NRRL 15009 VanHst

Published as

8.0 Prologue

This chapter is being presented in a sandwich format, as in addition to conducting

nearly all of the described experiments myself, I was also responsible for the composition

of the primary drafts of the corresponding publication in the journal *Biochemistry*. I wish

to acknowledge the significant contributions of Michaela Zolli, who assisted in the

purification of the VanHst enzyme as well as who was responsible for all of the VanHst-

related information in Table 8.2. I also wish to acknowledge the important role that

Professor G. Wright performed in editing and writing the discussion relating to the pH

study. I would also like to include the assistance of Lisa Kush in formatting the

publication.

I have re-formatted the publication for its inclusion in this thesis, however the

content has not been modified, including the introduction which in some places may re-

iterate material discussed in previous sections. The introduction also fails to place the

work in the context of this thesis, which I will now address.

The VanA/B ligases are undoubtedly the most sought after targets in the *van*-

mediated mechanism of GPA resistance as their function is central to this mode of

resistance. As discussed in Chapter 1, however, the action of all three of the *van* gene

products which function to alter PG are required for *Enterococci* to transform themselves

into an immune state. Therefore, all three classes of enzymes, VanH, VanA/B and VanX

are equally important targets when considering drug design, although other factors such

as toxicity and bio-availability may come into play further down the development

pathway. At the time that the experiments contained within this chapter were being

designed, *Enterococcal* VanH, like VanA and VanB, was refusing to form crystals of use in X-ray crystallography. Therefore, the discovery of a VanH homologue, VanHst, was a unique opportunity to study an enzyme which could serve as a model for VanH. This chapter describes the study of VanHst and its comparison to both VanH and the D-lactate dehydrogenase (D-LDH) from *Lactobacillus pentosus*, for which the crystal structure was solved and which served as the paradigm for this enzyme class in much the same way that DdlB did for Ddls.

8.1 Introduction

Bacterial resistance to the glycopeptide antibiotics, which include the clinically important compounds vancomycin and teicoplanin, has had a profound effect on the current and future use of these drugs for the treatment of serious infections caused by Gram-positive bacteria. The major problem at this juncture is the rise of VRE which has emerged over the past decade as a serious source of hospital acquired infection. High level glycopeptide resistance in VRE requires the biosynthesis of peptidoglycan terminating in D-Alanine-D-Lactate (D-Ala-D-Lac) rather than the virtually ubiquitous D-Ala-D-Ala (1, 17). This inducible shift in peptidoglycan structure involves the expression of a unique D-Ala-D-Lac biosynthetic pathway which requires three novel enzymes: VanA/B, a D-Ala-D-Lac synthetase, VanX, a D-Ala-D-Ala specific hydrolase, and VanH, an α-ketoacid reductase which supplies sufficient levels of D-Lac.

This specialised D-Ala-D-Lac synthesis mechanism appears to originate in the bacteria which produce glycopeptide antibiotics where we have recently found a gene cluster consisting of *vanH*, *vanA*, *vanX* homologues in the identical arrangement as the genes found on transposable elements in VRE (9). The VanA equivalents, DdlM from *Streptomyces toyocaensis* NRRL 15009 which produces the 'aglyco'-glycopeptide A47934, and DdlN from *Amycolatopsis orientalis* C329.2 which produces vancomycin, have been characterised and shown to be bona fide D-Ala-D-Lac ligases with enzymatic properties which closely mirror the VanA and VanB ligases from VRE (8, 10, 11). The *S. toyocaensis* NRRL 15009 VanX homologue, VanXst, has recently been purified and

characterised as well and it has the expected D-Ala-D-Ala peptidase activity (7). Both the VanA and VanX homologues found in glycopeptide producing organisms have the predicted catalytic activities, but there are differences when compared to the enzymes from VRE. For example, VanXst has 10 fold higher k_{cat}/K_m for D-Ala-D-Ala than VanX from *Enterococcus faecium* (7), and DdlN from *A. orientalis* C329.2 shows a restricted substrate specificity in terms of the flexibility of the D-α-hydroxyacid tolerated in the C-terminal position than the VRE enzyme VanA (10).

In contrast to the VanA and VanX enzymes, there has been relatively little detailed work describing the α-ketoacid reductase VanH from any system. The VanH enzymes from VRE and antibiotic producing bacteria show significant amino acid sequence homology to the D-lactate dehydrogenase (D-LDH) family of enzymes (2, 9). A recent three-dimensional structure of the D-LDH from *Lactobacillus plantarum* (since renamed *Lactobacillus pentosus*) (12) provides a point of reference for mechanistic analysis not only for this particular enzyme, but also for the VanH enzymes which share primary sequence homology, and presumably, structural similarity with D-LDH. In principle, a compound which inhibits any of the Van enzymes could find use as a potentiator of glycopeptides in the clinic where resistance is an issue. Inhibitor design requires a thorough understanding of enzyme mechanism and structure. We have initiated mechanistic work on the Van enzymes from glycopeptide antibiotic producing bacteria as these enzymes provide not only an opportunity for study of important antibiotic resistance determinants but provide additional access to proteins which may be more amenable for structural analysis than the enzymes from VRE. We report herein the

characterisation of the mechanism of VanHst through steady state kinetics and site directed mutagenesis. These studies now provide the appropriate background for future function and structure research within the VanH family of enzymes.

8.2 Materials

NADH, NADPH, NADP$^+$, sodium pyruvate, lithium D-lactate, sodium oxamate, α-ketobutyrate, α-ketocaproate, α-ketoisocaproate, α-ketoisovalerate, and henylpyruvate were purchased from Sigma. NAD$^+$ (free acid) was purchased from Boehringer Mannheim.

8.3 Methods

8.3.1 Overexpression of VanHst in Escherichia coli

The *vanHst* gene was amplified employing Vent polymerase using the genomic library clone pBlutoyddl3.0 as template (9). Reactions contained 100 ng template, 10 mM KCl, 20 mM Tris-HCl pH 8.8, 10 mM AS, 0.1 % Triton X-100, 4 mM MgSO$_4$, 5.0 % (v/v) DMSO, 0.4 mM dNTPs, 1 μM of each of 5'-GCTCTAGACATATGACCCAC AGCGAGAAGG-3' and 5'-TGACATAAGCTTAGTCTGG CCATGCTGATTCC-3', and 2 units Vent polymerase. Amplification reactions consisted of 25 cycles of 94 °C, 50 °C and 72 °C for 1, 1.5 and 1.5 minutes, respectively. The approximately 1.0 kb product was digested with *Nde* I and *Hind* III, purified and ligated to similarly treated pET22b (Novagen) by standard methods. A recombinant clone (pETVanHst) was identified and completely sequenced to ensure no mutations occurred during

amplification. DNA sequencing was performed by Dr. Brian Allore using an ABI

automated sequencer at the MOBIX central facility at McMaster University.

8.3.2 Purification of VanHst

E. coli BL21(DE3)/pETVanHst (1 L) was grown at 37 °C, 250 rpm to mid-log

phase in Luria Broth supplemented with ampicillin to 50 µg/ml. Protein expression was

induced by the addition of isopropyl β-D-thiogalactopyranoside to 1 mM and cells were

harvested following additional growth for 3 hours. Harvesting and washing yielded 2.5

grams (wet weight) of cells which were suspended in 20 mL of lysis buffer containing

100 mM HEPES pH 7.5, 300 mM NaCl, 1 mM EDTA, 1 mM dithiothreitol, 1 mM

phenylmethylsulfonyl fluoride, and passed twice through a French pressure cell at 20,000

psi. The extract was clarified by centrifugation at 10000 x g and soluble proteins were

subsequently fractionated by the addition of AS to 20% and 50% saturation, respectively.

Following recovery of the insoluble fraction by centrifugation at 10, 000 x g for 10

minutes, this pellet was suspended in a minimum of column buffer consisting of 50 mM

HEPES pH 7.5, 1 mM EDTA, 0.1 mM dithiothreitol and applied to a Superdex S200

(Pharmacia) gel exclusion resin (2.6 x 114 cm) equilibrated with 50 mM NaCl in column

buffer. Eluant fractions were screened by both sodium dodecyl sulfate polyacrylamide

gel electrophoresis (SDS-PAGE) and enzymatic assay for the presence of VanHst.

Active fractions were pooled and applied to a MonoQ column (0.5 x 6.0 cm, Pharmacia)

equilibrated in column buffer. Proteins were eluted with a linear gradient from 100 mM

to 400 mM NaCl in column buffer over 50 column volumes. VanHst-containing

fractions were pooled and AS was added to a final concentration of 1.0 M. This sample

was applied to a Phenyl Superose column (0.5 x 6.5 cm, Pharmacia) equilibrated with 1.0 M AS in column buffer. Proteins were eluted with a linear gradient from 1.0 M to 0 M AS in column buffer over 50 column volumes. VanHst-containing fractions were pooled, de-salted and concentrated with Millipore concentrators to 0.5 mg/mL. VanHst site mutants were purified in an identical fashion. In all cases, SDS-PAGE revealed a single Coomassie blue stained band migrating with an apparent mass of 36 kDa.

8.3.3 Assays

Protein concentration was determined by Bradford assay (3) using a Bio-Rad kit. Sample purity was determined by SDS-PAGE. During purification, VanHst enzyme activity was assayed by monitoring the decrease of NADH concentration in 1 mL reactions containing 100 mM sodium phosphate pH 5.6, 100 μM NADH, and 10 mM pyruvate at 37 ^{O}C. NADH was detected by measuring absorbance at 340 nm, at which its molar extinction coefficient is 6,220 $M^{-1}cm^{-1}$. Kinetic assays of VanHst contained 100 mM sodium phosphate buffer pH 5.6, saturating quantities of the non-varied substrate and 27.7 pmol of enzyme, unless otherwise specified.

Data were analysed by nonlinear least squares methods using Grafit 3.0 (6). Kinetic parameters for purified VanHst were determined by fitting to equation (1). Inhibition experiments were analysed by fitting to equations (2), (3) or (4) for competitive, non-competitive-mixed, or uncompetitive inhibition respectively. Parameters obtained from the best fit are reported with standard errors to the fit.

$$v = V_{max}S/(K_m + S) \qquad (1)$$

$$v = V_{max}S/(K_m(1 + I/K_{is}) + S) \qquad (2)$$

$$v = V_{max}S/(K_m + S(1 + I/K_{ii}))$$ (3)

$$v = V_{max}S/(K_m(1 + I/K_{is}) + S(1 + I/K_{ii}))$$ (4)

Replots of slope and/or intercept of double reciprocal plots were linear.

The dependence of kinetic parameters on pH was performed in the following buffers each at 100 mM sodium acetate pH 4.0-5.5, sodium citrate pH 5.5-7.0, HEPES pH 7.0-8.5, and TAPS pH 8.5-9.5. Data were fit to equations (5) or (6) as indicated above.

$$Y = Lim_1 + Lim_2 \times 10^{(pH-pKa)}/10^{(pH-pKa)} + 1$$ (5)

$$Y = Lim \times 10^{(pH-pKa)}/10^{(pH-pKa)} + 1$$ (6)

Where Y is the varied parameter (k_{cat} or k_{cat}/K_m), Lim is the limiting value of the kinetic parameter, pH is the log of the hydrogen ion concentration and pKa is the log of the ionization constant of the titrated group.

The stereochemistry of the VanHst reaction product was determined as follows. VanHst reaction (1 mL) contained 25 mM pyruvate, 25 mM NADH, either 0 or 8 :g VanHst in 100 mM HEPES pH 7.0 and was incubated 16 hours at room temperature. Reactions were passed through a 0.45 μM filter and used as substrates for the D-Ala-D-Lac ligase DdlN. Reactions (50 μL final volume) contained 10 mM MgCl$_2$, 10 mM KCl, 5 mM ATP, 5 mM D-alanine, 20μg DdlN and 25μL of VanHst reaction products in HEPES pH 7.0 and were incubated for 5 min at 37 ^{O}C. DdlN was purified and assayed by phosphate release activity as previously described (10).

8.3.4 Site-directed Mutagenesis

Point mutations were introduced into *vanHst* using Stratagene's Quickchange

mutagenesis kit. Thermocycled reactions were performed as described by the

manufacturer's protocol with the exception that dimethylsulfoxide was added to 5.0 %

(v/v). The primers used to construct Arg237Gln were 5'-GGTCATCAACACCGGACA

GGG TGGGCTCATCG-3' and 5'-CGATGAGCCCACCCTGTCCGGTGTTGATGACC

-3'. The primers used to construct Glu266Ala were 5'-CGTCGAAGGCGCGGAGGG

CATCTTCTACG-3' and 5'-CGTAGAAGATGCCCT-CCGCGCCTTCGACG-3'. The

primers used to construct His298Ala were 5'-GCGCATCACTCCGGCCACCGCCT

ACTACACG-3' and 5'-CGTGTAGTAGGCGGTGGCCGGAGTGATGAGC-3'.

Construction of each mutant was confirmed by complete sequencing of the gene.

8.4 Results and Discussion

8.4.1 Overexpression and Purification of VanHst

The *vanHst* gene was amplified using Vent polymerase PCR from a clone

obtained from a library of *S. toyocaensis* NRRL 15009 genomic DNA which we had

constructed previously (9). The amplified gene was cloned downstream of the T7

promoter in the expression vector pET22b, placing it under control of the bacteriophage

T7 polymerase. Induction of mid-log cultures of *E. coli* BL21(DE3) for 3 hours at 37 ^{O}C

with isopropyl β-D-thiogalactopyranoside resulted in good expression of VanHst in a

soluble form, as determined by SDS-PAGE analysis. Table 8.1 summarises the four-step

protocol developed to purify VanHst from soluble protein extracts of *E. coli*, yielding 3.1

mg of pure enzyme from 2.5 g of cells. While VanHst could be detected in fractions by

assaying for pyruvate-coupled NADH oxidation, endogenous *E. coli* D-LDHs were

frequently contaminating during chromatographic separation and SDS-PAGE was

required to identify VanHst enriched fractions. Contaminating D-LDHs were removed by

the Mono Q column and are responsible for the apparent poor recovery and purification

at this step.

Table 8.1. Purification of VanHst from *E. coli* BL21(DE3)/pETVanHst

Sample	Protein (mg)	Activity (nmole/sec)	Specific Activity (nmole/sec/mg)	Recovery (%)	Purification (n-fold)
Clarified lysate	319	19.3	60.5	100	-
AS (20-50% saturation)	215	12.1	56.4	63	0.9
Sephacryl S200	27	8.45	313	44	5.2
Mono Q	10.9	3.23	296	17	4.9
Phenyl Superose	3.1	2.50	806	13	13.3

8.4.2 Characterisation of Steady State Kinetic Parameters

Table 8.2 compares the steady state kinetic parameters of purified VanHst with

that of the enterococcal enzyme VanH (4). VanHst has nearly 17-fold greater affinity for

pyruvate (K_m = 0.09 mM) than does VanH. This increase in apparent affinity is not

paralleled in a decrease in catalytic rate, as VanHst's turnover number of 12 s^{-1} is only

3.3 fold less than that of VanH. VanHst has an overall efficiency of 1.3 x 10^5 $M^{-1}s^{-1}$,

nearly an order of magnitude better than the value of 2.7 x 10^4 $M^{-1}s^{-1}$ calculated for

VanH. VanHst was also evaluated for its ability to reduce alternative substrates

structurally similar to pyruvate. None of the substrates tested were preferred by VanHst

over pyruvate with respect to K_m nor catalytic turnover. Compared to VanH, VanHst had

lower K_m values for α-ketobutyrate and α-ketocaproate, however these reductions were matched by near proportional decreases in k_{cat}, resulting in similar efficiencies of the two enzymes for these substrates. VanHst is dramatically less capable of reducing α-ketoisocaproate and α-ketoisovalerate, with no detectable activity at concentrations of these compounds nearing solution saturation. While not efficiently utilised, these compounds are reduced with measurable rates in the presence of VanH.

Table 8.2. Characterisation of Steady State Parameters of VanHst

Substrate	*S. toyocaensis* VanHst			*E. faecium* VanH[1]		
	k_{cat} (sec^{-1})	K_m (mM)	k_{cat}/K_m (M^{-1}sec^{-1})	k_{cat} (sec^{-1})	K_m (mM)	k_{cat}/K_m (M^{-1}sec^{-1})
Pyruvate	12±0.3	0.09±0.01	1.3 x 10^5	40	1.5	2.7 x 10^4
α-ketobutyrate	5.7±0.2	0.71±0.1	8.0 x 10^3	35	2.6	1.3 x 10^4
α-ketocaproate	1.4±0.1	2.9±0.5	4.8 x 10^2	2.4	20	1.2 x 10^2
α-ketoisocaproate		>100		5.2	31	1.7 x 10^2
α-ketoisovalerate		>100		5.2	150	3.5 x 10^1
Phenylpyruvate		>100		<2		
NADH	13±0.3	0.010±0.001	1.3 x 10^6		0.021	
NADPH	16±0.8	0.011±0.001	1.5 x 10^6		0.002	

[1] Data from reference 4.

Table 8.2 also shows the lack of selectivity of VanHst in its choice of nicotinamide cofactor, using NADH and NADPH with equal efficiency. This contrasts with VanH from *E. faecium* which has a NADPH K_m of 2 µM, a full order of magnitude lower than that of NADH (4). This is also consistent with the observation that, unlike VanH (4), VanHst does not bind to 2',5'-ADP agarose, a hallmark of many NADP$^+$-dependent enzymes (not shown).

8.4.3 Stereochemistry of the VanHst Reaction Product

The predicted D-specific stereochemistry of the VanHst reaction product was confirmed by utilising the stereospecific incorporation of D-lactate into the depsipeptide D-alanine-D-lactate by the DdlN ligase of *A. orientalis* C329.2. DdlN was observed to release inorganic phosphate from ATP at a rate of 0.08 nmole/s when reaction products from VanHst were added. No rate was observed when the substrates of the VanHst reaction or when L-lactate was added at concentrations greater than those of the VanHst reaction products.

8.4.4 Inhibition of VanHst by Oxamate

Oxamate (1) is a pyruvate isostere and is known to be a competitive inhibitor of D-LDHs (13).

$$H_2N \overset{O}{\underset{O}{\parallel}} O-$$
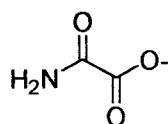
1

Oxamate is also a competitive inhibitor of pyruvate for VanHst with K_{is} of 28 ± 3 µM, 3.2 fold lower than the K_m for pyruvate (90 µM). This is in contrast to the relationship of these two parameters in the D-LDH of *L. plantarum*, in which the K_i (5 mM) for oxamate is a full order of magnitude larger than the pyruvate K_m (0.5 mM) (13). We also determined the effect of oxamate on VanHst NADH oxidation. The double reciprocal plot gave rise to parallel lines characteristic of uncompetitive inhibition with K_{ii} of 0.36 ± 0.03 mM (Figure 8.1). This is consistent with exclusive affinity for oxamate to the NADH•VanHst binary complex and is suggestive of an ordered BiBi kinetic mechanism.
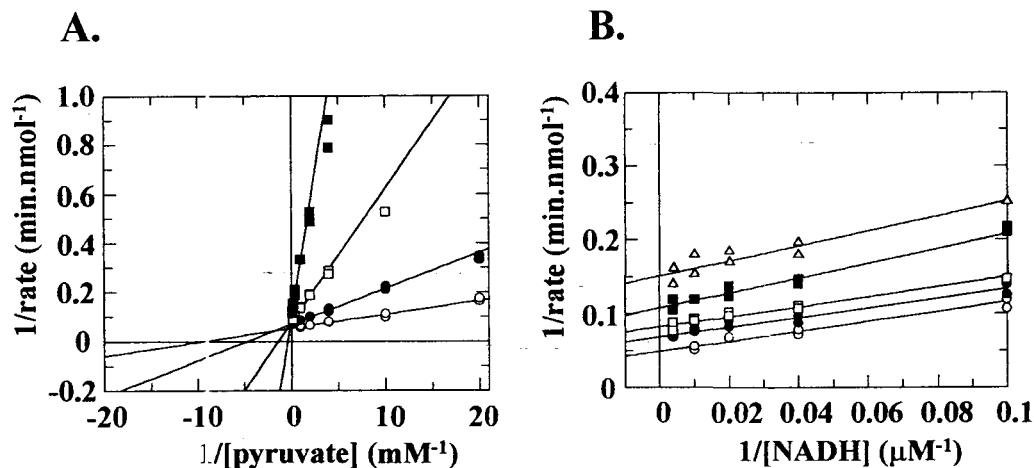
Figure 8.1. Inhibition of VanHst by oxamate. (A) Double reciprocal plot of the effect of increasing oxamate concentrations on the steady-state rate with varying pyruvate. Oxamate concentrations were 0 mM (O), 0.1 mM (●), 0.5 mM (□), and 2.5 mM (■). (B) Double reciprocal plot of the effect of increasing oxamate concentrations on the steady-state rate with varying NADH. Oxamate concentrations were 0 mM (O), 0.1 mM (●), 0.2 mM (□), and 0.4 mM (■).

8.4.5 Product Inhibition Studies on VanHst

The kinetic mechanism of VanHst was further elaborated using the reaction products D-lactate and NAD^+ as inhibitors of the reduction of pyruvate. The inhibition patterns observed when VanHst activity was assayed in the presence of products are summarised in Table 8.3. NAD^+ was a competitive inhibitor of NADH, indicating that both these molecules bind the same enzyme form (Figure 8.2). No other competitive inhibition patterns were observed. Both NAD and D-lactate were mixed-type noncompetitive inhibitors of pyruvate at subsaturating concentrations of the non-varied substrate. D-lactate also served as a mixed-type inhibitor of NADH oxidation. However this inhibition pattern converts to uncompetitive as pyruvate concentration is increased to

saturating levels (Figure 8.3). These patterns of inhibition are consistent with VanHst utilising an ordered BiBi kinetic reaction mechanism where NADH binds first and pyruvate binds second. After hydride transfer occurs in the ternary complex, product release is also ordered with lactate leaving first followed by NAD^+ (Scheme 1).
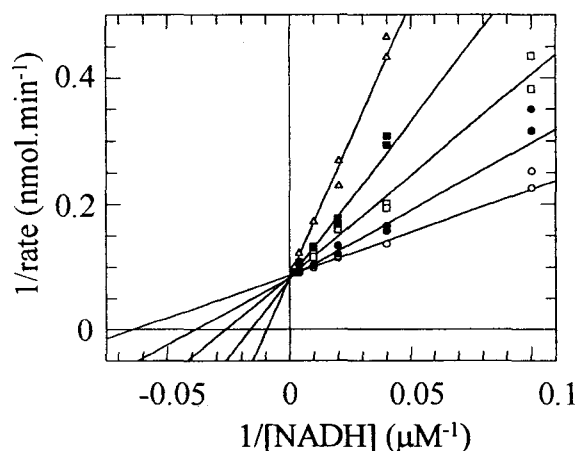

Figure 8.2. Inhibition of VanHst by NAD^+. Double reciprocal plot of the effect of increasing NAD^+ concentrations on the steady-state rate with varying NADH. NAD^+ concentrations were 0 mM (O), 1.0 mM (●), 2.5 mM (□), 5.0 mM (■), and 10 mM (Δ).

Table 8.3. Product Inhibition Patterns for VanHst

| Product Inhibitor | NADH varied | | | | Pyruvate varied | |
| | Unsaturated with pyruvate | | Saturated with pyruvate | | Unsaturated with NADH | |
	Pattern	K_i (mM)	Pattern	K_i (mM)	Pattern	K_i (mM)
D-Lactate	NC	$K_{ii} = 8.8 \pm 1.9$	UC	$K_{ii} = 5.5 \pm 0.2$	NC	$K_{ii} = 3.9 \pm 0.3$
		$K_{is} = 7.4 \pm 0.1$				$K_{is} = 3.8 \pm 0.6$
NAD^+	C	$K_{is} = 2.1 \pm 0.1$	n.d.		NC	$K_{ii} = 3.3 \pm 0.8$
						$K_{is} = 5.3 \pm 0.4$

NC - mixed-type noncompetitive inhibition, UC - uncompetitive inhibition,
C - competitive inhibition, n.d. – not determined
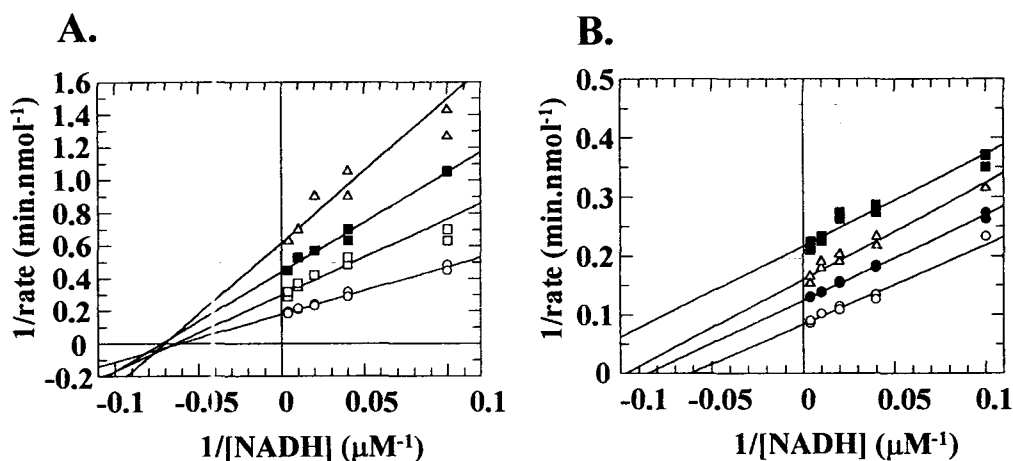
Figure 8.3. D-Lactate Inhibition Patterns for VanHst. (A) Double reciprocal plot of the effect of increasing D-lactate concentrations on the steady-state conversion of NADH at 0.05 mM pyruvate. D-Lactate concentrations were 0 mM (○), 0.1 mM (●), 5.0 mM (□), 10 mM (■), and 20 mM (△). (B) Double reciprocal plot of the effect of increasing D-lactate concentrations on the steady-state conversion of NADH at 0.2 mM pyruvate. D-Lactate concentrations were 0 mM (○), 0.1 mM (●), 5.0 mM (□), 10 mM (■), and 20 mM (△).
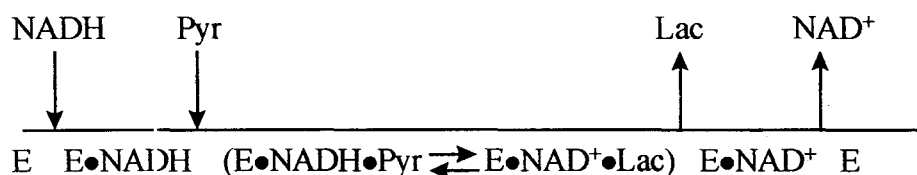
Scheme 1

8.4.6 Site-directed Mutagenesis of VanHst

Mutagenesis studies conducted with the D-LDHs of *Lactobacillus plantarum* and *Lactobacillus bulgaricus* have identified key amino acids involved in substrate binding and catalysis (5, 13, 14). These results have suggested a mechanism of hydride transfer

(Figure 8.4) where a conserved Arg interacts with both the keto and carboxylate groups of pyruvate, positioning the substrate and polarising the α-keto group. An invariant His acts as a catalytic base and a conserved Glu interacts with the protonated His. The recently determined 3D-structure of the D-LDH of *L. plantarum* has confirmed the presence of the residues Arg235, Glu264, and His296, which were predicted to be important by mutagenesis, in the active site region (12).
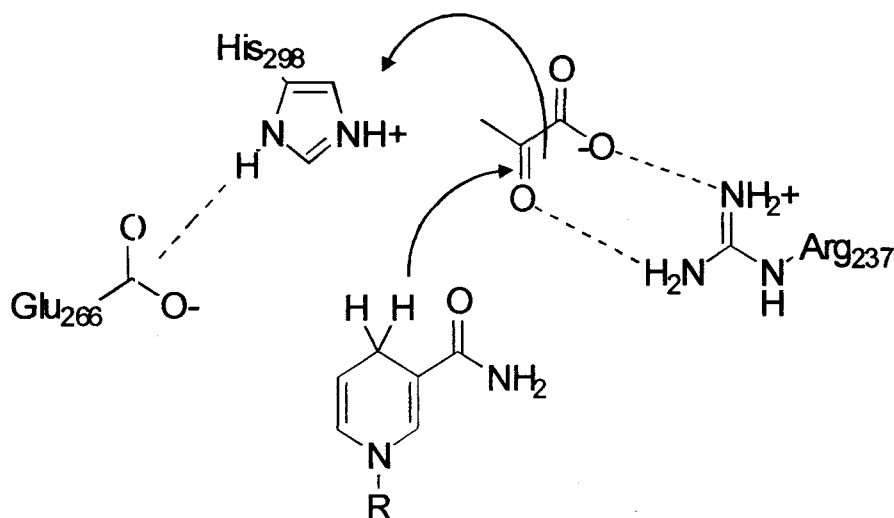
Figure 8.4. Predicted Molecular Mechanism of D-LDHs. Numbering of residues is based upon the VanHst sequence.

Clustal W alignment (16) of the amino acid sequence of VanHst with these and other D-LDHs indicated that residues Arg237, Glu266 and His298 of VanHst may be similarly important in enzyme function (Figure 8.5), a hypothesis which we explored by site directed mutagenesis. Each of the VanHst mutants, Arg237Gln, Glu266Ala, and His298Ala, were expressed in *E. coli* BL21(DE3) and purified to homogeneity and their steady state parameters determined (Table 8.4).

S. toyocaensis	T	G	R_{237}	G	G	....	E	G	E_{266}	E	G	....	T	P	H_{298}	T	A		
E. faecium	T	G	R_{231}	G	P	....	E	G	E_{260}	E	E	....	T	P	H_{292}	T	A		
Synechocystis	T	S	R_{235}	G	H	....	E	E	E_{264}	E	E	....	T	A	H_{296}	Q	G		
L. plantarum	F	A	R_{235}	G	T	....	E	Y	E_{264}	T	K	....	T	P	H_{296}	T	A		

Figure 8.5. Primary Sequence Alignment of Various D-lactate Dehydrogenases.
Alignment calculated by the CLUSTAL W method (16). The conserved residues mutated in this study are boxed.

Table 8.4. Characterisation of Steady State Parameters of VanHst Mutants

VanHst	Pyruvate			NADH		
	k_{cat} (s^{-1})	K_m (mM)	k_{cat}/K_m $(M^{-1}sec^{-1})$	k_{cat} (s^{-1})	K_m (μM)	k_{cat}/K_m $(M^{-1}sec^{-1})$
wild-type	12±0.3	0.094±0.01	1.3×10^5	13±0.3	10±1	1.3×10^6
Arg237Gln	0.40±0.01	5.5±0.2	7.3×10^1	0.4±0.02	7.2±0.9	5.6×10^4
Glu266Ala	8.3±0.2	2.6±0.1	2.3×10^4	9.5±0.2	8.3±0.7	1.1×10^6
His298Ala	0.02±0.001	1.5±0.4	1.3×10^1	ND	ND	

Arg237Gln had essentially wild type affinity for NADH, as assessed by modest changes in K_m but had a 30 fold reduction in k_{cat} and a nearly 60 fold increase in pyruvate K_m, reflecting a decreased capacity in both catalytic rate and in α-ketoacid substrate binding. This 1780 fold decrease in k_{cat}/K_m is comparable in direction, but not magnitude, to that found in the Arg235Gln mutant of *L. plantarum* D-LDH which resulted in a 1.5×10^5 fold decrease in k_{cat}/K_m (13). Nevertheless, these results are consistent with a role in substrate binding and catalysis for VanHst Arg237 as predicted by the mechanism in Figure 8.4.

The His298Ala mutant showed a 10^4 fold drop in k_{cat}/K_m, primarily as a result of a 600 fold reduction in k_{cat} to 0.02 s^{-1}, while pyruvate K_m increased 16 fold. The poor

activity precluded accurate measurement of the NADH dependence. This is comparable to the magnitude of k_{cat}/K_m decrease in the His296Tyr mutant in the *L. plantarum* D-LDH, though in this case, there is negligible effect on K_m (1.4 fold drop) (14). Thus His298 of VanHst plays an important function in catalysis consistent with a role as an active site acid which provides a proton to the product hydroxyl (Figure 8.4).

The Glu266 equivalent in the *L. plantarum* D-LDH crystal structure (Glu264) is positioned within hydrogen bonding distance of the catalytic His (12). In VanHst, a Glu266Ala mutation has only a modest effect on k_{cat} (1.5-fold decrease at pH 5.6); however, K_m for pyruvate was increased 10-fold (Table 8.4). The NADH K_m was relatively unchanged. The corresponding Glu264Gly mutation in *L. bulgaricus* (5) and Glu264Gln mutation in *L. plantarum* (15) D-LDHs have been prepared and these show respectively 62 and 1740-fold decreases in k_{cat}/K_m for pyruvate. The Glu264Asp mutation in *L. plantarum* has also been prepared and shows a 40-fold decrease in pyruvate k_{cat}/K_m (15). Further analysis of the pH dependence of *L. bulgaricus* Glu254Gly mutant revealed a 2 pH unit shift towards acidic pH in a single k_{cat}-dependent pKa (5). This observation was attributed to Glu264 modulation of the ionisation of the catalytic His, a hypothesis which is consistent with the proximity of these residues in the *L. plantarum* D-LDH crystal structure (12). However, in the *L. plantarum* Glu264Gln and Glu264Asp mutants, there was generally little change in the pH dependence of kinetic parameters, though their magnitudes were significantly decreased as indicated above (15).

Wild-type VanHst shows a k_{cat}-dependence on pH with both acidic and basic pKas (Figure 8.6, A). However, the data do not fit a bell-shaped pH dependence curve, and it would appear that the loss in activity on the acidic arm of the curve (pH < 5) may be a result of several equilibria. The pH data on the basic side of pH 5 could be fit to curve describing a single ionisation with pKa of 8.1 ± 0.1. The pH dependence of k_{cat}/K_m resulted in a bell shaped curve with pKas of 4.6 ± 0.1 and 9.7 ± 0.1 (Figure 8.6, B). Analysis of the Glu266Ala mutant revealed that the general shapes of the pH-dependence curves were similar to wild type enzyme. However, the pKa determined from the k_{cat} plot was slightly more acidic at 7.7 ± 0.1. In the case of the k_{cat}/K_m-dependence on pH, the acidic pKa remained unchanged at 4.7 ± 0.1, while the basic pKa was lowered by almost 2 pH units to 7.9 ± 0.1. Thus these results are consistent with an important role
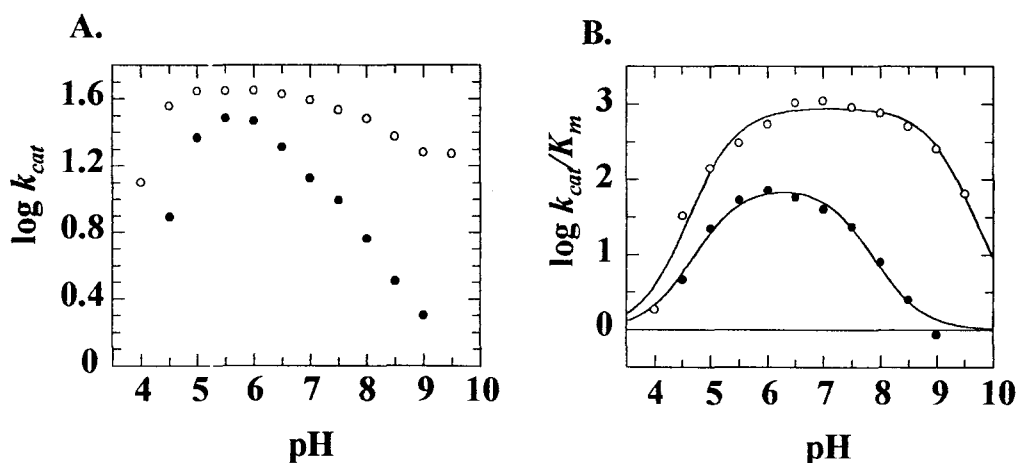
Figure 8.6. Comparison of the pH Dependence of the Steady-State Rate Pyruvate Conversion Parameters of VanHst Wild-type and Glu266Ala Mutant. Effect of pH on the enzyme turnover number, k_{cat} (A) and specificity, k_{cat}/K_m (B). Key: wild type (O), Glu266Ala (●).

for Glu266 in the productive interaction of pyruvate with the VanHst·NADH complex and to catalysis. The positioning of the His-Glu pair in the *L. plantarum* D-LDH structure demonstrates a close interaction between these residues and our pH-dependence results are consistent with a similar arrangement in VanHst. These results also imply that Glu266 helps to maintain His264 in a protonated state through a broad range of pHs. This information is therefore exploitable in drug design for VanH from enterococci.

8.5 Conclusions

VanH is one of three enzymes absolutely required for high level glycopeptide resistance in VRE and antibiotic producing organisms. These studies using the VanHst enzyme from an glycopeptide antibiotic producing organism provide the appropriate foundation for exploitation of VanH as a drug target and furthermore demonstrate the value in studying resistance mechanisms in streptomycetes. This analysis of the mechanism of VanHst indicates that compounds which share structural similarity between both substrates and which could take advantage of interactions with active site Arg and His protonated side chains have the potential to act as potent VanH inhibitors and could serve as the starting point for compounds which rescue vancomycin activity in VRE.

8.6 References

1.   **Arthur, M., and P. Courvalin.** 1993. Genetics and mechanisms of glycopeptide resistance in enterococci. Antimicrob Agents Chemother. **37**(8):1563-71.

2.   **Arthur, M., C. Molinas, S. Dutka-Malen, and P. Courvalin.** 1991. Structural relationship between the vancomycin resistance protein VanH and 2-hydroxycarboxylic acid dehydrogenases. Gene. **103**(1):133-4.

3.   **Bradford, M. M.** 1976. A rapid and sensitive method for the quantitation of microgram quantities of protein utilizing the principle of protein-dye binding. Anal Biochem. **72**:248-54.

4.   **Bugg, T. D., G. D. Wright, S. Dutka-Malen, M. Arthur, P. Courvalin, and C. T. Walsh.** 1991. Molecular basis for vancomycin resistance in *Enterococcus faecium* BM4147: biosynthesis of a depsipeptide peptidoglycan precursor by vancomycin resistance proteins VanH and VanA. Biochemistry. **30**(43):10408-15.

5.   **Kochhar, S., N. Chuard, and H. Hottinger.** 1992. Glutamate 264 modulates the pH dependence of the NAD(+)-dependent D- lactate dehydrogenase. J Biol Chem. **267**(28):20298-301.

6.   **Leatherbarrow, R. J.** 1992. Grafit, 3.0 ed. Erithacus Software Ltd., Staines, U.K.

7.   **Lessard, I. A., S. D. Pratt, D. G. McCafferty, D. E. Bussiere, C. Hutchins, B. L. Wanner, L. Katz, and C. T. Walsh.** 1998. Homologs of the vancomycin resistance D-Ala-D-Ala dipeptidase VanX in *Streptomyces toyocaensis, Escherichia coli* and *Synechocystis*: attributes of catalytic efficiency, stereoselectivity and regulation with implications for function. Chem Biol. **5**(9):489-504.

8.   **Marshall, C. G., G. Broadhead, B. K. Leskiw, and G. D. Wright.** 1997. D-Ala-D-Ala ligases from glycopeptide antibiotic-producing organisms are highly homologous to the enterococcal vancomycin-resistance ligases VanA and VanB. Proc Natl Acad Sci U S A. **94**(12):6480-3.

9.   **Marshall, C. G., I. A. Lessard, I. Park, and G. D. Wright.** 1998. Glycopeptide antibiotic resistance genes in glycopeptide-producing organisms. Antimicrob Agents Chemother. **42**(9):2215-20.

10.   **Marshall, C. G., and G. D. Wright.** 1998. DdlN from vancomycin-producing *Amycolatopsis orientalis* C329.2 is a VanA homologue with D-alanyl-D-lactate ligase activity. J Bacteriol. **180**(21):5792-5.

11.   **Marshall, C. G., and G. D. Wright.** 1997. The glycopeptide antibiotic producer *Streptomyces toyocaensis* NRRL 15009 has both D-alanyl-D-alanine and D-alanyl-D-lactate ligases. FEMS Microbiol Lett. **157**(2):295-9.

12.   **Stoll, V. S., M. S. Kimber, and E. F. Pai.** 1996. Insights into substrate binding by D-2-ketoacid dehydrogenases from the structure of *Lactobacillus pentosus* D-lactate dehydrogenase. Structure. **4**(4):437-47.

13.   **Taguchi, H., and T. Ohta.** 1994. Essential role of arginine 235 in the substrate-binding of *Lactobacillus plantarum* D-lactate dehydrogenase. J Biochem (Tokyo). **115**(5):930-6.

14.   **Taguchi, H., and T. Ohta.** 1993. Histidine 296 is essential for the catalysis in *Lactobacillus plantarum* D-lactate dehydrogenase. J Biol Chem. **268**(24):18030-4.

15.   **Taguchi, H., T. Ohta, and H. Matsuzawa.** 1997. Involvement of Glu-264 and Arg-235 in the essential interaction between the catalytic imidazole and substrate for the D-lactate dehydrogenase catalysis. J Biochem (Tokyo). **122**(4):802-9.

16.   **Thompson, J. D., D. G. Higgins, and T. J. Gibson.** 1994. CLUSTAL W: improving the sensitivity of progressive multiple sequence alignment through sequence weighting, position-specific gap penalties and weight matrix choice. Nucleic Acids Res. **22**(22):4673-80.

17.   **Walsh, C. T., S. L. Fisher, I. S. Park, M. Prahalad, and Z. Wu.** 1996. Bacterial resistance to vancomycin: five genes and one missing hydrogen bond tell the story. Chem Biol. **3**(1):21-8.

Chapter 9

Identification and Isolation of Large Chromosomal DNA Fragments
containing GPA-Biosynthesis Genes
from *S. toyocaensis* NRRL 15009

9.1 Introduction

Despite the fascinating and lucrative discovery of the *van* gene homologues in the

S. toyocaensis NRRL 15009 chromosome, the primary objective of the thesis remained

the study of A47934 biosynthesis by this organism. The experience gained in creating

sub-genomic libraries and cloning the *van* genes into various expression systems

facilitated the more challenging task of creating a complete library of the *S. toyocaensis*

NRRL 15009 chromosome, which spans a predicted 8,000 kilobases. As an entire cluster

of adjacent genes was the target for discovery, a library containing large fragments of

intact chromosome was necessary. These types of libraries are routinely created using

cosmid technology, made possible by the detailed study of λ-phage replication (2).

During λ-phage rolling circle replication , the phage form concatamers of their

chromosomal DNA (48.5 kb) separated by *cos* sites (3). These sites are recognised by

enzymes of the Ter system which are responsible for packaging the chromosome into the

phage head. The Nu1-A enzyme attaches the region adjacent to the *cos* site to the mouth

of the head opening and the DNA fills the phage head by an unknown mechanism until

the next *cos* site in the concatamer is encountered. At this time the Ter nuclease cleaves

the DNA at the *cos* sites to generate single stranded cohesive termini (hence the name *cos*

site). Cleavage releases the packaged DNA from the concatamer and allows the tail to be

added. The fully assembled phage particle is then ready to infect an appropriate bacterial

host. The *cos* sites are both necessary and sufficient for packaging, allowing the

replacement of the bulk of the chromosome with foreign DNA. Specialised plasmid

vectors, called cosmids, can be linearised such that ligation to foreign DNA results in

concatamers of the foreign DNA separated by *cos* sites. Provided that the cumulative length of foreign DNA and plasmid vector separated by *cos* sites is 47-51 kb, the Ter system will package the DNA into phage heads as it would its native substrate (the λ genome). Once transfected into a host cell, the cosmid circularises and is propagated from its origin of replication. This was the strategy used to package 35-40 kb fragments of *S. toyocaensis* NRRL 15009 chromosomal DNA into λ-phage heads and their subsequent transfection into *E. coli*. The number of clones that must be screened (N) in order to find a target gene with a specified probability (P) is given by equation 1 (1).

$$N = \ln(1\text{-P}) / \ln[1\text{-}(I/G)] \hspace{2cm} [1]$$

where I is the size of the average cloned fragment and G is the size of the target genome. For a cosmid library (I = 35 kb) of *S. toyocaensis* NRRL 15009 (G = 8,000 kb), the number of clones required to screen to have a 99.9% chance of identifying a target gene was 1575.

Construction of the library, while technically difficult, was relatively straightforward in that it was simply a matter of following procedures that were already developed. Obtaining an oligonucleotide probe that was specific for the A47934 biosynthesis gene cluster was, of course, the more challenging task and was the focus of the work done in chapters 3, 4 and 5. None of the work described in these chapters resulted in the identification of a gene or oligonucleotide which could be used to specifically identify the biosynthetic gene cluster.

Other groups working in the field of GPA biosynthesis, however, had made progress while the data described in chapters 5 to 8 was being generated. Three separate,

but related, GPA biosynthesis gene clusters were identified and cloned. All three of these

gene clusters were identified from chromosomal libraries using an oligonucleotide based

on the primary sequence of the only GPA biosynthetic enzyme purified, TDP-

glucose:aglycosyl vancomycin glucosyltransferase. No glycosyltransferases are

predicted in the biosynthesis of A47934 as it is the only aglycone GPA.

The first two GPA biosynthesis gene clusters were published together in March of

1997 (6), one from the vancomycin producer *A. orientalis* C329.2 and the other from the

A82846B producer *A. orientalis* A82846 (Figure 9.1). Both were 5.7 kb in size, and both

contained very similar glycosyltransferases and genes which encoded hypothetical

hydroxylases (based on primary sequence homology searches of Genbank and EMBL

databases). Unfortunately, there was no biochemical or genetic evidence that any of

these hydroxylases had a role in GPA biosynthesis, limiting their usefulness for screening

for the A47934 biosynthesis cluster.
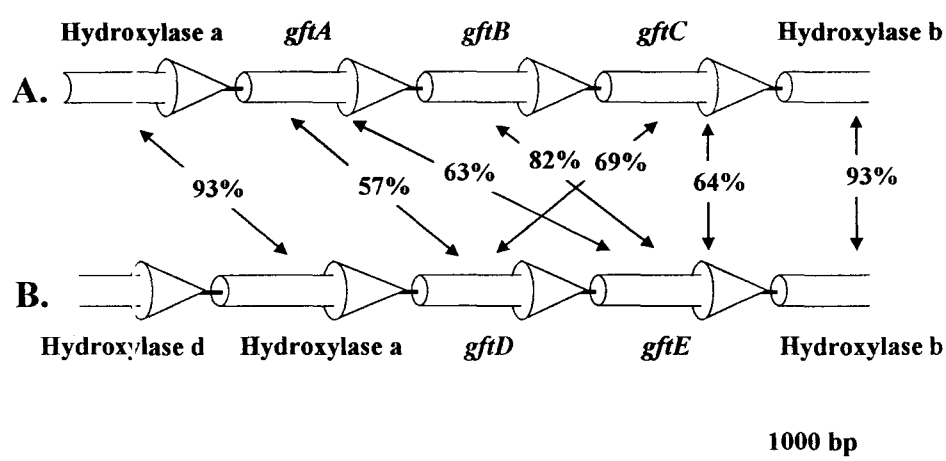
Figure 9.1. GPA Biosynthesis Genes. Chromosomal fragments containing glycosyltransferase genes and putative hydroxylase genes from *A. orientalis* A82846*UV37B* (A) and from *A. orientalis* C329.2 (B). Values indicate the percentage of identical amino acids. Figure adapted from Ref. 6.

The third GPA-biosynthesis gene cluster published was 72 kb from the chloro-

eremomycin (cl-erernomycin) producer *A. orientalis* 18098 (Figure 9.2) (9). This

extensive region of DNA contained glycosyltransferase genes similar to those found on

the other two gene clusters, as well as genes that encode enzymes predicted to

manufacture sugars (4-epi-vancosamine production), perform oxidative reactions

(potential role in cross-linking or amino acid biosynthesis), halogenate organic substrates

(role in chlorination), and other functions which had no clearly defined role in GPA

assembly. Notably there were three large peptide synthetases encoded, with a total of 7
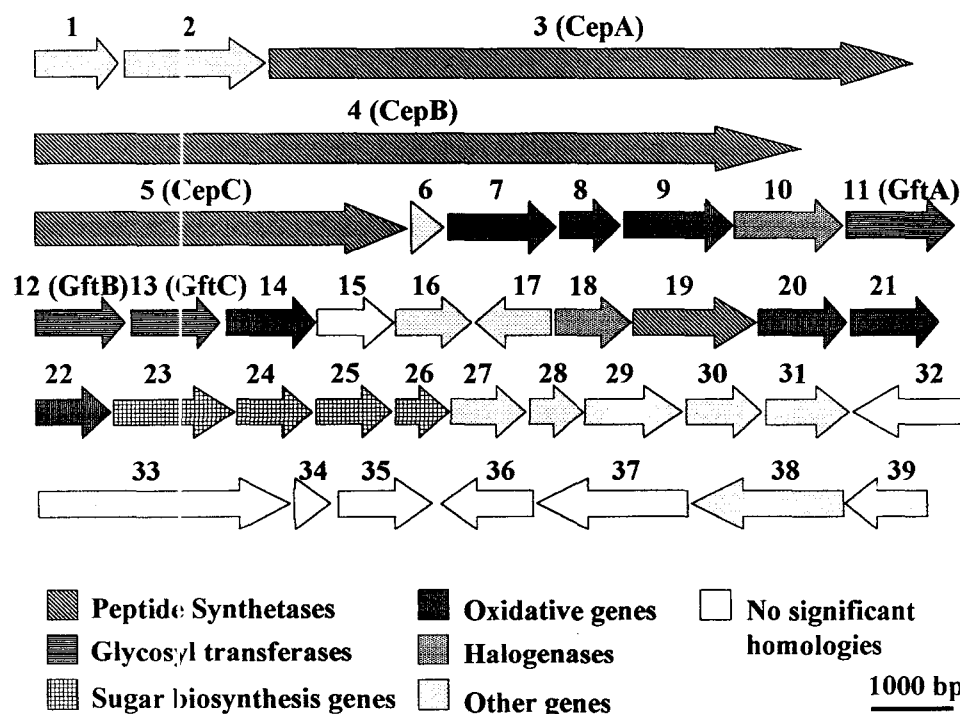
Figure 9.2. Chloro-eremomycin Biosynthesis Gene Cluster. 72 kb fragment from *A. orientalis* 18098 containing a number of genes predicted in GPA biosynthesis. Numbers indicate ORF assignments. Figure adapted from Ref. 9.

modules (Figure 9.3). These modules contained, in addition to the obligatory

adenylation, thiolation and condensation domains, three epimerisation domains, in

modules 2, 4, and 5. A thioesterase region was located near the C-terminus of CepC, the

third peptide synthetase which is predicted to activate and attach the final amino acid

(DHPG) to the GPA heptapeptide chain. This amino acid is highly conserved across

GPAs, and is present in A47934. As none of the sugar biosynthesis or attachment

enzymes were predicted to function in A47934 assembly, and the substrates of the

oxidation and halogenation enzymes encoded on the cl-eremomycin cluster were

undefined, the peptide synthetase genes were the only genes which may be useful in

screening for the corresponding cluster in *S. toyocaensis* NRRL 15009. As peptide
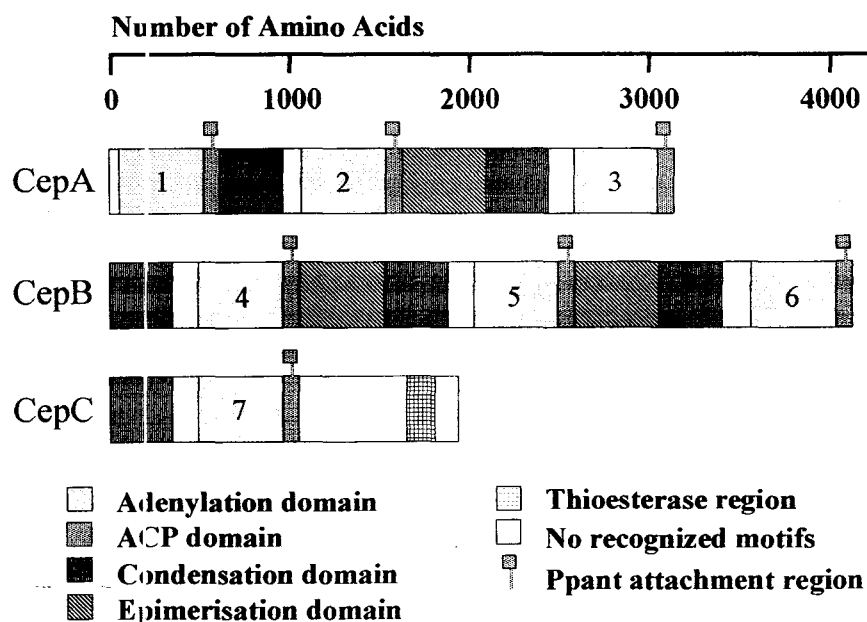
Figure 9.3. Chloro-eremomycin Peptide Synthetases. CepA, CepB and CepC, containing a total of 7 modules for each amino acid in cl-eremomycin. Numbers indicate the sequence of the amino acid activating domains on each peptide synthetase. Figure adapted from Ref. 9.

synthetase genes are modular, and the modules are fairly well conserved despite differences in substrate binding of their protein products, a probe to one module would potentially hybridise to every module of every peptide synthetase gene in the chromosome. The thioesterase region, however, should be unique to each peptide synthetase in the chromosome, and should result in less "hits" when used in a screen for novel GPA-producing peptide synthetases.

For these reasons the thioesterase region of the *cepC* gene was chosen as the gene fragment for use in screening for the A47934 biosynthesis gene cluster. This chapter describes the construction of a cosmid library of *S. toyocaensis* NRRL 15009 chromosomal DNA, the use of the thioesterase region of the cl-eremomycin *cepC* gene to identify 2 clones, and their subsequent preparation for complete sequencing.

9.2 Materials

CIAP, polynucleotide kinase (PNK), T4 DNA ligase, and all restriction endonucleases were purchased from MBI Fermentas. Vent polymerase, dNTPs, pUC18 and the Genome Priming System (GPS) were from New England Biolabs. pWE15, Gigapack III XL packaging extract and *E. coli* SURE cells were obtained from Stratagene. *E. coli* NovaBlue cells were from Novagen. All antibiotics were purchased from Bioshop. IPTC was from ChemBridge. The *cepC* gene from *A. orientalis* 18098 was a gift from Dr. Cathryn Shaw-Reid of Professor C.T. Walsh's group. Quiaprep Spin Plasmid Purification kits were from Quiagen. 5-bromo-4-chloro-3-indolyl-β-D-

galactopyranoside (X-gal) was purchased from Vector Biosystems. Pulsed Field Gel

Electrophoresis (PFGE) apparatus was manufactured by Bio-Rad.

9.3 Methods

9.3.1 Media and Buffers

Many of the media and buffers used in this chapter are described in Section 5.3.1.

STE buffer contained TE buffer + 10 mM NaCl. 2TY broth contained 10 g tryptone, 10

g yeast extract, and 5 g NaCl per litre. TBE (10X) contained 108 g Tris base, 55 g boric

acid, 40 mL 0.5 M EDTA, pH 8.0. SSC (20X) contained 3 M NaCl, 0.3 M tri-sodium

citrate, pH adjusted to 7.0 with HCl. To make terrific broth, 100 mL of a sterile solution

of 0.17 M KH_2PO_4, 0.72 M K_2HPO_4 was added to 900 mL of base broth (12 g bacto-

tryptone, 24 g bacto-yeast extract, 4.0 mL glycerol in 0.9 L final volume).

9.3.2 Construction of Cosmid Library from S. toyocaensis NRRL 15009 Chromosomal DNA

S. toyocaensis NRRL 15009 chromosomal DNA was isolated as described in

Section 5.3.2. It was essential that sample was completely dissolved before use, which

often required up to a week incubation at 4 °C. Chromosomal DNA could not be reliably

quantified by measuring absorbance at 260 nm, therefore quantity was assessed by

electrophoresis of various dilutions through 1% TAE-agarose and comparison of

ethidium bromide/UV-light visualised band intensity to known quantities of standard

DNA. Values determined in this manner were usually an order of magnitude less than

those obtained by the absorbance method.

In all cases when DNA larger than 10 kb was handled, wide-bore pipette tips were used. All steps requiring mixing of large DNA fragments with other reagents (including water) were done by alternating cycles of warming and gentle tapping or tilting. Mixing often required up to 10 minutes to ensure a (somewhat) homogeneous solution. Particular attention was paid when making master mix solutions for *Sau*3aI partial digestions. Precipitated DNA required a long time and cycles of warming and tapping to dissolve. Buffers or water used to solvate these pellets had to be slightly alkaline.

DNA was partially digested with *Sau*3aI and 35-40 kb fragments isolated for cloning into an appropriate cosmid vector. In order to determine the amount of *Sau*3aI required to digest 1 μg of DNA such that an optimal amount of 35-40 kb fragments were produced, a series of reactions were set up. Reactions (100 μL) contained 1 μg of chromosomal DNA, 1X *Sau*3aI buffer, 1X BSA, and various amounts of *Sau*3aI. Reactions were pre-warmed 5 min before the addition of enzyme and allowed to react for 20 min at 37 °C. Reactions were terminated by the addition of 300 μL of TE and 400 μL of Tris-HCl buffered phenol:chloroform (1:1). Aqueous phases were recovered and digestion products precipitated with sodium acetate pH 4.2/ethanol, washed with 70% ethanol, air-dried and suspended gently in 15 μL TE. Fragment lengths were analysed by 0.6% TAE-agarose electrophoresis and comparison to standards of appropriate length (*Bam*HI-digested λ-DNA spanning 8 to 50 kb). From this analysis, reactions containing 30 mU of *Sau*3aI contained the largest quantity of fragments in the desired size range. To obtain enough *Sau*3aI-digested DNA for cloning into a cosmid vector, two reactions (500 μL) containing 5 μg of DNA and 150 mU of *Sau*3aI were set up and reacted exactly

as before. Termination was with 500 μL of the phenol:chloroform solution, and the precipitated DNA was suspended in a total volume of 200 μL STE buffer. The sample was immediately loaded onto a 12 mL sucrose gradient from 10 to 40% sucrose in 20 mM Tris-HCl pH 7.5, 1 M NaCl, 5 mM EDTA and centrifuged at 30, 000 rpm, 17 hours at 4 °C in a Beckman SW-41 rotor. Fractions (750 μL) were precipitated by the addition of NaCl to a final concentration of 1.25 M and 0.6 volumes of isopropanol. Due to the high sucrose content, precipitation required a 1-2 hour incubation at –20 °C and centrifugation for 60 minutes at 14, 000 x g. Pellets were washed twice with 70% ethanol, dried and suspended in 20 μL 1.0 mM Tris-HCl pH 8.0. Fractions were analysed by electrophoresis of a sample (5 μL) through 0.6% TAE-agarose containing the appropriate standards. Fractions containing Sau3aI fragments of the desired size were pooled and concentrated under vacuum to 10 μL and approximately 0.15 μg/μL. This was stored at 4 °C until use for ligation to cosmid vector.

The cosmid vector pWE15 was prepared for ligation as described by the manufacturer (8). pWE15 (10 μg) was digested with 50 U BamHI by standard methods in a 100 μL reaction. The reaction was extracted with buffered phenol:chloroform (1:1) and precipitated with sodium acetate/ethanol. The pellet was washed and dried as usual and dissolved in 80 μL ddH$_2$O. The linearised cosmid was dephosphorylated by treatment with CIAP by standard methods in a 160 μL reaction. The enzyme was inactivated and the products extracted and precipitated as before. BamHI-digested, dephosphorylated pWE15 was suspended in 13 μL of ddH$_2$O (to 0.5 μg/μL), stored at –

20 °C, and tested as follows. Ligations (5 μL) contained 100 ng digested, dephosphorylated cosmid, 1X T4 DNA ligase buffer, 100 cohesive end units T4 DNA ligase and 0 or 1 U PNK. After 16 hours at 17 °C, reactions were transformed into competent *E. coli* SURE cells and spread onto LB-ampicillin plates. The reaction containing PNK yielded 500 colonies, while the reaction without PNK yielded 20.

*Sau*3aI-digested, size fractionated chromosomal DNA fragments were ligated to *Bam*HI-digested, dephosphorylated pWE15 as follows. Reaction (20 μL) contained 1.5 μg chromosomal DNA, 3.0 μg cosmid DNA, 1X T4 DNA Ligase buffer, and 140 cohesive end units of T4 DNA Ligase. After 16 hours at 4 °C, 4 μL was used for packaging into λ-phage. Packaging was performed as described in the manual for Stratagene's Gigapack III XL packaging extract kit (7), with the following details. Thawed extracts required pulse centrifugation before use. Packaging occurred for 105 min. After chloroform extraction, the entire sample (500 μL) was transferred (carefully avoiding the chloroform) to a fresh tube and stored at 4 °C. To titre the library, dilutions of packaged ligation were transfected into *E. coli* SURE cells and plated onto LB-ampicillin plates as directed by the manufacturer (7), except that 2TY was used in place of LB to grow out the cells. The lowest dilution which resulted in a high transfection efficiency (15-fold) was selected for large-scale transfection of the library. A portion of the packaged ligation (100 μL) was diluted 15-fold and transfected accordingly into *E. coli* SURE cells in 10 separate tubes. Cells were spread on 10 LB-ampicillin plates and grown overnight. Colonies (approximately 2250) were suspended in 2 x 2 mL LB per

plate, pooled, glycerol added to 20% and dispensed into 50 x 1 mL aliquots. These were

stored at –80 °C until needed. A titre of one of these stocks gave 10^5 colonies/μL.

9.3.3   Construction of GPA-Specific Probes and Library Screening

The partial gene fragment encoding hypothetical hydroxylase b from the putative

vancomycin biosynthesis gene cluster was cloned by Vent PCR amplification of the

fragment from the A. orientalis C329.2 chromosome. Reactions (100 μL) contained 500

ng chromosomal DNA, 1 μM of the forward primer (5'-GCTCTAGACATATGTCGA

CCACTTCCCGGT-3'), 1 μM of the reverse primer (5'-TGACATAAGCTTAAGATC

TGGTCGAACGACGTGC-3'), 1X Vent buffer, 0.4 mM each dNTP, 5% DMSO, 2 mM

exogenous $MgSO_4$, and 1 U Vent polymerase. Reactions were incubated at 94, 50 and 72

°C for 1, 1.5, and 1.5 min respectively, for 28 cycles. A 0.65 kb fragment was isolated,

digested with NdeI and HindIII and ligated to similarly treated pET22b. Ligation

products were transformed into E. coli BL21 cells and a positive clone (E.coli

BL21/pEThydb) identified by standard methods.

The cepC gene from the putative chloro-eremomycin biosynthesis gene cluster

was assayed for its ability to hybridise to S. toyocaensis NRRL 15009 chromosomal

DNA by Southern blotting. Chromosomal DNA (5 μg) was digested with a variety of

restriction endonucleases (in separate tubes) in 100 μL reactions and concentrated to 20

μL by precipitation. Digestion products were loaded onto a 6 cm thick 1% agarose gel

made in 0.5X TBE and separated by PFGE. Samples were run for 10 hours at 6 V/cm

with a switch time ramped from 1 to 6 seconds at 14 °C in 0.5X TBE buffer. The gel

was stained with ethidium bromide and photographed next to a ruler. The gel was

prepared for transfer by standard methods (1), with a 30 minute depurination step at RT.

Transfer to nylon was in 20X SSC using a capillary stack for 24 hours. The blot was

washed in 2X SSC and exposed to UV-light (120 mJ) to cross-link DNA to the nylon

matrix. [^{32}P]-dATP labelled *cepC* was made using Klenow polymerase as described in

Section 5.3.3. The primers used in the reaction, 5'-CTTCGATCTCGAGCATATGAT

CGG-3' and 5'-GTCGAAAAGCTTCGTCATCGTTGTGTCC-3' specifically hybridise

to the 1.6 kb thioesterase region. This probe was hybridised to the blot and washed as

described in Section 5.3.4, except that high stringency washes were done at 55 ^{O}C. The

blot was exposed to Kodak film for 24 hours.

For library screening, approximately 2250 colonies were plated onto 6 plates.

These were transferred to nitrocellulose filters, lysed and released DNA crosslinked to

the membrane by standard methods. Filters were hybridised to *cepC*, washed and

exposed to film in an identical manner as the *cepC* Southern blotting experiment. Four

colonies were identified, their cosmid DNA prepared as described in the Gigapack III XL

manual (7), and the presence of the *cepC* gene homologue confirmed by Southern

blotting (exactly as described before for chromosomal DNA). Two of these were positive

for the *cepC* gene. In an identical Southern blotting experiment using the partial gene

fragment encoding *A. orientalis* C329.2 hydroxylase b, no hybridisation was observed.

The two clones (pWECepC1 and pWECepC4) were mapped using a variety of different

restriction endonucleases and RFLP.

9.3.4 Preparation of cepC-Containing Cosmid Clones for Sequencing

pWECepC1 and pWECepC4 were used as target DNA for the Genome Priming

System, which randomly inserts a selectable transposon into the target to facilitate

sequencing. The procedure was carried out as described in the manual provided by the

manufacturer (4), with the following details. The donor DNA carrying chloramphenicol

resistance was used as the target did not confer this phenotype. *E. coli* Nova-blue

competent cells (guaranteed 10^8 colony forming units/µg 3.0 kb plasmid DNA) were

transformed with 2 µL of the GPS reaction according to the manufacturer of the cells (5).

Of the 500 µL volume of transformed cells, 1 µL was spread on LB-ampicillin and both

10 and 100 µL volumes were spread on LB containing ampicillin and chloramphenicol.

Transposon-inserted cosmid DNA was prepared from 1.5 mL cultures grown in Terrific

Broth according to the protocol given in the Gigapack III XL instruction manual (7).

These were suspended in 15 µL of ddH$_2$O and 5 µL used in *Bam*HI RFLP mapping

experiments.

pWECepC1 and pWECepC4 were also partially digested with *Sau*3aI to give 1-

1.2 kb fragments for sub-cloning into a sequencing vector. Cosmid DNA (1 µg) was

digested in 50 µL reactions containing various amounts of *Sau*3aI for 20 min at 37 $^\circ$C.

Reactions were terminated and concentrated in a manner similar to the chromosomal

*Sau*3aI partial digests. The amount of *Sau*3aI that gave the greatest amount of 1 kb

fragments under these conditions was 3.5 U. Reactions (4 x 50 µL) were set up to

prepare sufficient amounts of 1 kb *Sau*3aI fragments for cloning. Digestion products

were pooled and 1 kb products isolated by QuiexII gel purification. These were ligated to

BamHI-digested, dephosphorylated pUC18 plasmid vector (purchased from MBI

Fermentas) and ligation products transformed into *E. coli* NovaBlue competent cells and

spread onto 4 LB-ampicillin plates containing X-gal and IPTG as directed by the

manufacturer of the cells (5). Plasmid DNA was isolated from 1.5 mL cultures of white

colonies grown in Terrific Broth using Quiagen Spin Miniprep Kits.

9.3.5 Cosmid Sequencing and Analysis

All sequencing was done by Dr. Brian Allore of the MOBIX Central facility using

DNA cycle sequencing and an ABI automated sequencer. Transposon inserted cosmid

clones were sequenced using Primer N and Primer S, included with the GPS kit. pUC18-

hosted DNA was sequenced using the M13 forward and reverse primers. DNA was

analysed using Lasergene's DNAStar software. Genetic and primary sequence homology

was established by comparison to sequences present in GenBank using NCBI's BLAST.

9.4 Results and Discussion

9.4.1 Construction of Cosmid Library from S. toyocaensis NRRL 15009 Chromosomal DNA

S. toyocaensis NRRL 15009 chromosomal DNA was partially digested with

*Sau*3aI and digestion products separated by sucrose gradient size fractionation (Figure

9.4). Fragments of length 35-40 kb were isolated and ligated to the cosmid vector

pWE15, which had been digested with *Bam*HI and dephosphorylated. Ligation products

were packaged into λ-phage and dilutions of the packaging reaction were transfected into

E. coli SURE cells (Table 9.1). While a 20-fold dilution gave the highest efficiency of

recombinant clones, 10-fold was nearly as efficient and much easier to process, and as

such was used to transfect the library.

Fraction
Number 7 8 M 9 10 11 12 13 14 15 16
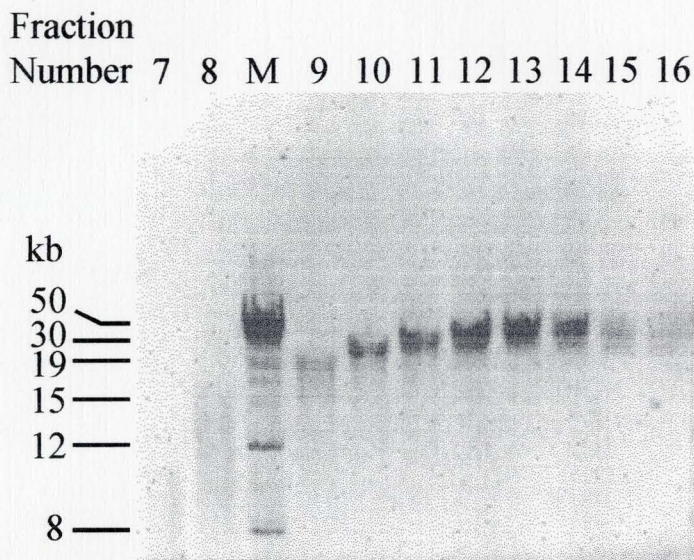
**Figure 9.4. Sucrose Gradient Fractions of *Sau*3aI-digested *S. toyocaensis*
NRRL 15009 Chromosomal DNA.** Fraction number increases with sucrose
concentration. M, mass standards.

Table 9.1 *E. coli* SURE Transfection Titration

| Dilution[1] (n-fold)	Number of Colonies	Expected Number of Colonies[2]	Efficiency (%)
20	51	51	100
10	89	102	87
4	83	255	33
2	62	510	12
0	65	1020	6.4

[1]Final volume 20 μL.
[2]Based on highest efficiency dilution.

Approximately 2250 recombinant clones were obtained, each harbouring an *S.*

toyocaensis NRRL 15009 chromosomal fragment of 35-40 kb. Thus approximately 80

megabases of the chromosome, about 10-fold greater than the predicted size of the

genome, were contained in the library. As only 1575 clones were predicted to be

required to have a 99.9% chance of finding a target gene in *S. toyocaensis* NRRL 15009,

the chromosome was well represented by this library.

9.4.2 Screening of the Cosmid Library Using Genes Associated with GPA Biosynthesis

The thioesterase region of the *cepC* gene from the cl-eremomycin biosynthetic

cluster was assayed for its ability to bind specifically to *S. toyocaensis* NRRL 15009

chromosomal DNA restriction endonuclease digestion products. In the Southern blot

presented in Figure 9.5, lanes that were missing a band were observed to be devoid of

DNA in the corresponding agarose gel, due to the fact that undigested or poorly digested

chromosomal DNA did not enter the gel. In those lanes in which digestion was more

complete, a clearly dominant band was present accompanied by some fainter bands (lanes

2 and 3). This pattern was paralleled in the lane containing digested *A. orientalis* 18098
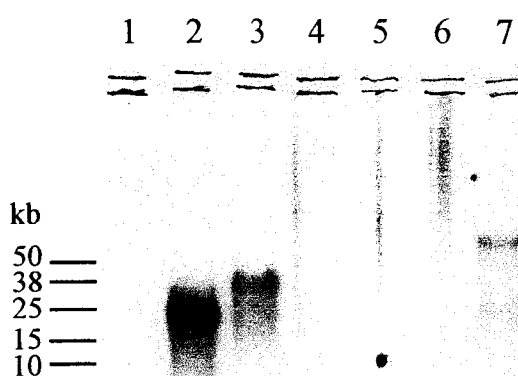
**Figure 9.5. Southern Blot of *S. toyocaensis* NRRL 15009 Total DNA
Hybridised with Cl-eremomycin *cepC* gene.** Lanes contained *S. toyocaensis*
NRRL 15009 DNA digested with no enzyme (1), *Bgl*II (2), *Eco*RI (3), *Hind*III (4), *Ssp*I
(5), *Xba*I (6) or *A. orientalis* 18098 DNA digested with *Hind*III (7).

DNA from which the *cepC* gene was cloned (lane 7). Thus it appeared that not only did this thioesterase region hybridise to *S. toyocaensis* NRRL 15009 chromosomal DNA under the conditions tested, it did so in a specific manner. This was important given the potential for this probe to bind to several peptide synthetase modules in the chromosome.

This portion of the *cepC* gene was used to screen the *S. toyocaensis* NRRL 15009 cosmid library using stringency conditions identical to those applied to the Southern blot. Four clones were obtained, two of which were confirmed to contain a *cepC* homologue by Southern blotting. The cosmids were isolated from these clones, designated pWECepC1 and pWECepC4 and mapped using a variety of restriction endonucleases (Figure 9.6). Digestion products given by *Bam*HI show these two clones to be distinct, however they do carry similar regions of DNA (not including the pWE vector backbone, represented by a 9.5 kb band). From the mapping experiment, it appears that these two clones share about 10-12 kb of chromosomal DNA. Thus, these two *cepC*-containing clones contain a total of approximately 65 kb of the *S. toyocaensis* NRRL 15009 chromosome.

The four clones that were originally obtained from the library screen were assayed by Southern blot for hybridisation to the gene encoding Hydroxylase b from the vancomycin biosynthesis gene cluster, as well as the *ddlM* gene. Neither of these genes hybridised to any of the library clones (data not shown). If these genes are proximal to the A47934 biosynthetic gene cluster, the fact that they were not contained on these clones suggests they may be some distance from the *cepC* homologue.
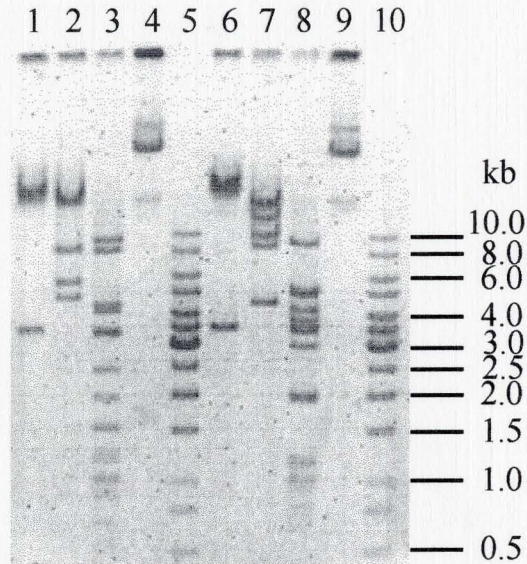
Figure 9.6. Map of *S. toyocaensis* NRRL 15009 Cosmid Clones with *cepC*-like Genes. Lanes contained pWECepC1 digested with *Hind*III (1) *Eco*RI (2) *Bam*HI (3), and no enzyme (4); pWECepC4 digested with *Hind*III (6) *Eco*RI (7) *Bam*HI (8), and no enzyme (9); mass standards (5 and 10).

9.4.3 Preparation of cepC-Containing Cosmid Clones for Sequencing

In order to sequence the chromosomal fragments contained on pWECepC1 and pWECepC4, the Genome Priming System (GPS) was used. This system uses a mixture of transposases to incorporate a transposon randomly into target DNA (Figure 9.7). The reaction products are transformed into *E. coli* and selected for using a resistance marker on the transposon. Using primer binding sites at the edges of the inserted DNA (designated N and S), the clones can be sequenced at a variety of locations, eventually building one long contiguous consensus sequence. By sequencing twice the amount of DNA that was contained in the clone (i.e. 100 kb per clone), most of the contig would be
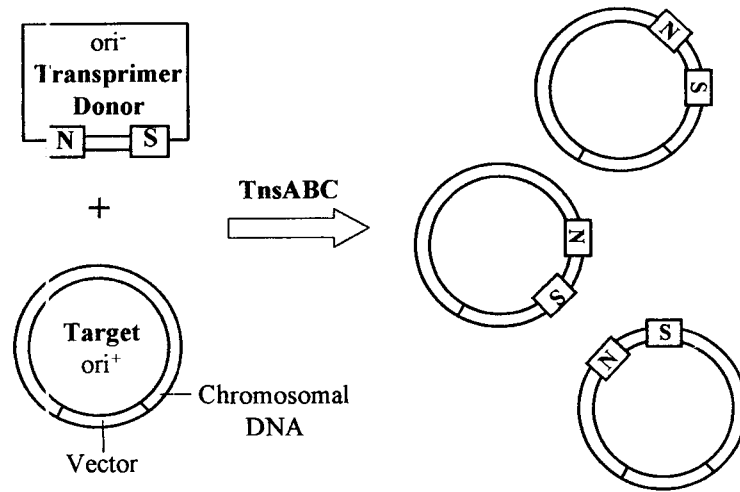
Figure 9.7. Mechanism of Genome Priming Kit. N and S are primer binding sites for Primer N and Primer S, respectively. TnsABC, mixture of transposases A, B and C. Figure adapted from Ref. 4.

assembled, requiring only minor amounts of primer walking to fill in the gaps. Using the protocol included with the kit, the insertion efficiency expected (ratio of colonies that possess both plasmid-conferred and transposon-conferred resistance to colonies that possess only plasmid-conferred resistance) is about 1%. It was therefore unexpected to obtain insertion efficiencies of 50% and 30% for pWECepC1 and pWECepC4, respectively. Subsequent sequencing from the N primer site revealed that many of the clones had multiple insertions, as well as "hot-spots" (regions of target DNA with a higher incidence of insertion). Furthermore, the large size of these clones resulted in mini-lysate cosmid preparations of generally lower yields and poorer quality than conventional preparations. The G/C rich nature of the DNA combined with the preparation complications resulted in lower quality and length of sequencing data. Thus, this method was put aside despite the preparation of over two hundred mini-lysates.

As an alternative, the cosmid clones were partially digested with *Sau*3aI to produce an optimal amount of 1-1.2 kb fragments (Figure 9.8). These were cloned into pUC18 for sequencing from the M13 forward and reverse primers. It was necessary to
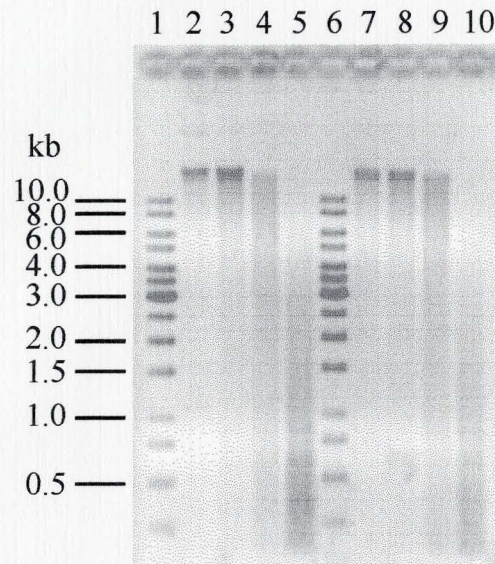
Figure 9.8. *Sau*3aI **partial digestions of Cosmid Clones.** Lanes contained pWECepC1 digested with 0 mU (1), 1 mU (2), 2 mU (3), and 4 mU *Sau*3aI (4); pWECepC4 digested with 0 mU (6), 1 mU (7), 2 mU (8), and 4 mU *Sau*3aI (9), and mass standards (5).

use high quality *Bam*HI, dephosphorylated vector in ligation reaction to facilitate blue/white screening of recombinant clones. Again, over two-hundred mini-lysates were prepared in good yield and of high quality. The data obtained from these clones was much cleaner and more pronounced, however upon sequencing the first few dozen, a problem with randomness became apparent. Two distinct patterns emerged, namely 1) certain regions were appearing at a significantly higher frequency than others (up to 20% of the clones sequenced) and 2) vector sequences were appearing at a higher frequency than expected (up to 50%). Of the sequences obtained, all of them had internal *Sau*3aI

sites, indicating that the problem was not due to complete digestion by *Sau*3aI. The problem was not alleviated by changing the host cell strain from NovaBlue to SURE cells. It seems likely that extensive secondary structure, a common feature in G/C rich DNA, may have created extensive bias in *Sau*3aI sites available to the enzyme during the partial digest. This was supported by the observation of distinct bands forming in *Sau*3aI partial digests that proceeded to near completion (as is the case in the generation of 1 kb fragments).

9.4.4 Analysis of Sequenced DNA

Due to the problems incurred with the sequencing of pWECepC1 and pWECepC4, very few intact genes have been identified. However, primary sequence homologies have been established using BLAST searches of gene fragments. Gene fragments encoding peptide synthetases and glycosyltransferases with strong homology to those found in the *A. orientalis* C329.2 vancomycin biosynthesis gene cluster and the *A. orientalis* 18098 cl-eremomycin biosynthesis gene cluster have been detected. Given that A47934 has no sugar residues attached, the presence of glycosyltransferases is intriguing. In addition, two-component regulatory genes with strong primary sequence homology to those found in *S. coelicolor* have also been found. This latter find is particularly interesting as the genes in *S. coelicolor* are proximal to the *van* gene cluster found in this organism. While it is still far too early to make any definitive statements, there do not appear to be any genes suspected in amino acid biosynthesis on the cloned *S. toyocaensis* NRRL 15009 gene cluster. None of the *van* resistance genes have been detected either.

9.5 Conclusions

Two cosmid clones, each harbouring approximately 35 kb of *S. toyocaensis*
NRRL 15009 chromosomal DNA were isolated using the thioesterase region of *cepC*
from the cl-eremomycin biosynthesis gene cluster. From restriction endonuclease
mapping experiments, these two clones have approximately 10-12 kb overlap, and should
therefore yield close to 65 kb of *S. toyocaensis* NRRL 15009 chromosome. Sequencing
of the DNA has been problematic, however preliminary information indicates that a
number of the genes contained on these cosmids are closely related to the other three
GPA biosynthesis gene clusters already cloned. Interestingly, the *S. toyocaensis* NRRL
15009 gene cluster appears to have glycosyltransferases, for which it should have no
need. It also possesses a two-component regulatory system not present on any other
GPA-biosynthesis cluster, but which has been observed in proximity to the *van* cluster in
S. coelicolor. This system is a potential link between GPA biosynthesis and resistance in
GPA producing organisms.

9.6 References

1. **Ausubel, F. M., R. Brent, R. E. Kingston, D. D. Moore, J. G. Seidman, J. A. Smith, and K. Struhl (ed.).** 1995. Current Protocols in Molecular Biology. John Wiley and Sons, Inc., New York.

2. **Hendricks, R. W. (ed.).** 1983. Lambda II. Cold Spring Harbour, New York.

3. **Maloy, S. R., J. E. Cronan jr., and D. Freifelder.** 1994. Microbial Genetics, 2nd ed. Jones and Bartlett Publishers, Boston.

4.   **NewEnglandBiolabs.** 1999. GPS-1 Genome Priming System Instruction Manual Version 2.

5.   **Novagen.** 1998. Competent Cells Instruction Manual TB009 9/98.

6.   **Solenberg, P. J., P. Matsushima, D. R. Stack, S. C. Wilkie, R. C. Thompson, and R. H. Baltz.** 1997. Production of hybrid glycopeptide antibiotics in vitro and in *Streptomyces toyocaensis*. Chem Biol. **4**(3):195-202.

7.   **Stratagene.** 1997. Gigapack III Gold Packaging Extract, Gigapack III Plus Packaging Extract, and Gigapack III XL Packaging Extract Instruction Manual Revision #027002a.

8.   **Stratagene.** 1999. pWE15 Cosmid Vector Kit Instruction Manual Revision #018001c.

9.   **van Wageningen, A. M., P. N. Kirkpatrick, D. H. Williams, B. R. Harris, J. K. Kershaw, N. J. Lennard, M. Jones, S. J. Jones, and P. J. Solenberg.** 1998. Sequencing and analysis of genes involved in the biosynthesis of a vancomycin group antibiotic. Chem Biol. **5**(3):155-62.

Chapter 10

Recent Developments and General Conclusions

10.1 Introduction

As mentioned in the previous chapter, three GPA biosynthesis gene clusters have been identified in recent years. Very recently, some of the genes from the balhimycin biosynthetic gene cluster have been cloned from *A. mediterranei* DSM5908 (3). A picture of the mechanism of GPA assembly is beginning to emerge from these landmark achievements. Apart from advances in understanding GPA biosynthesis, some developments relating to resistance have emerged during course of conducting the studies described in this thesis. GPA resistance has been detected in strains of *B. circulans* (1), and tolerance has been detected in *S. pneumoniae* by a previously unobserved mechanism (2). This chapter discusses each of these developments in turn, and discusses what we currently know and do not know about GPA biosynthesis and resistance. The work presented in this thesis is also discussed in the context of current knowledge in this field.

10.2 Recent Developments

10.2.1 GPA Biosynthesis

The GPA biosynthesis genes cloned from *A. orientalis* strains producing A82846 and vancomycin contained 3 and 2 glycosyltransferases, respectively, corresponding well to the 3 and 2 sugars present on the GPAs produced by these organisms (4). Of the 5 enzymes, only GftE and GftE', both of which attach glucose to the peptide core, were assayed catalytically (GftE' contains a single point mutation of Pro to Ser and is believed to be essentially identical to *wild-type*). These enzymes were found to utilise UDP-glucose as well as TDP-glucose as substrates (Table 10.1). Of various (activated) sugars

tested, only glucose and xylose were substrates for these enzymes. GftE' (from the

vancomycin producer) was also assayed for specificity with respect to aglycone

heptapeptide substrate, and found to accept not only aglycosyl vancomycin (presumably

its natural substrate), but also A47934 and A41030A (A47934 lacking the sulphate). It

would appear that this enzyme is indifferent to the identity of residues 1 and 3 in the

heptapeptide. The efficiency of incorporation was not measured in any of these substrate

specificity studies, however, making it difficult to say how promiscuous these enzymes

actually are. When expressed from a strong constitutive promoter in *S. toyocaensis*

NRRL 15009, GftE' was capable of modifying A47934 to produce a HPLC peak with

area approximately 50% that of A47934. While these experiments addressed the

Table 10.1 *In vitro* Glycosylation Reactions of GftE' and GftB.

Heptapeptide	NDP-sugar	GftE'	GftB
Aglycosylvancomycin	TDP-D-glucose	+	+
	UDP-D-glucose	+	+
	UDP-D-xylose	+	+
	UDP-D-galactose	-	-
	UDP-D-mannose	-	-
	UDP-N-acetylglucosamine	-	-
	UDP-galacturonic acid	-	-
A41030A	TDP-D-glucose	+	(+)
	UDP-D-glucose	+	NT
A47934	TDP-D-glucose	+	-
	UDP-D-glucose	+	NT

Symbols: +, 25-75% conversion to product; (+), < 2% conversion to product;
-, no conversion observed; NT, not tested. Data obtained from Ref. 4.

potential for creating hybrid antibiotics, little was learned about the mechanism of

substrate binding and catalysis. A detailed analysis of the active site of one of these

glycosyltransferases is essential to engineering these enzymes beyond limited substrate

utilisation and mediocre product yield. No information was obtained regarding substrate utilisation or catalysis by the enzymes encoded by the hydroxylase genes.

While some enzymatic studies were conducted with the A82846 and vancomycin gene products, none were done with any of the gene products encoded on the 72 kb cluster cloned from the cl-eremomycin producer (5). All of the gene assignments were based on primary sequence homology to enzymes of known function. Regardless, many inferences could be, and were, made from this type of analysis. Cl-eremomycin (Figure 10.1) is a heptapeptide like all GPAs. Residues 1, 2, 4, and 5 have the *R*-configuration (corresponding to a D-amino acid). The core has 2 sugars attached to residue 4 and 1 sugar attached to residue 6. Residue 1 is N-methylated, residues 2 and 6 are both chlorinated and β-hydroxylated, and there are three separate oxidative cross-links, between residues 2 and 4, residues 4 and 6, and residues 5 and 7. All of these features
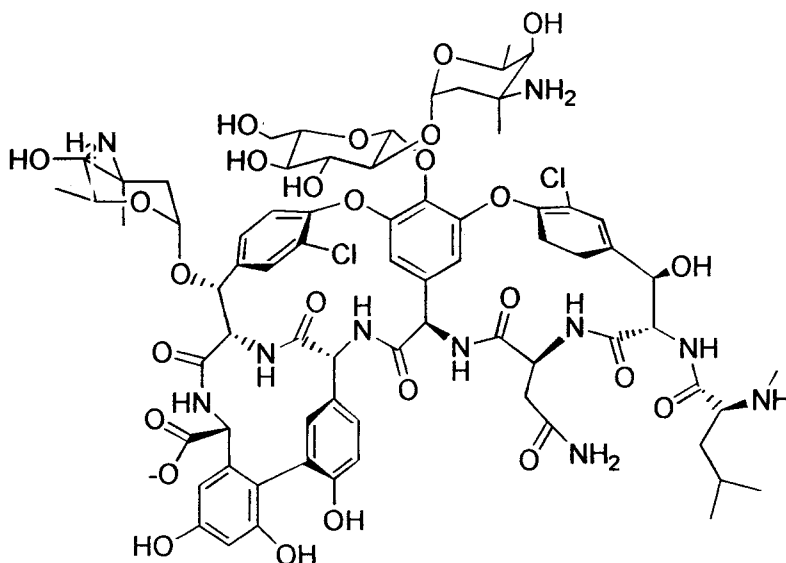

Figure 10.1. Structure of Chloro-eremomycin.

matched nicely with the set of genes discovered (Figure 10.2). The three peptide synthetases encoded contained a total of 7 adenylation modules, with epimerization domains in modules 2, 4, and 5. Thus only residue 1 is incorporated in the *R*-configuration. Three glycosyltransferases, two of which had strong primary sequence homology to those found in the vancomycin biosynthetic gene cluster, corresponded to the one glucose and 2 4-*epi*-vancosamine sugars that must be attached to the peptide core. Four sugar biosynthesis genes were contained in the cluster. Based on primary sequence homology to enzymes in the daunosamine and mycarose biosynthetic pathway, a scheme for the synthesis of 4-epi-vancosamine was inferred (Figure 10.3), although the scheme begins with a precursor of an ambiguous origin. Four heme proteins, with similarity to P-450-monooxygenases, and 2 non-heme oxidative enzymes were also encoded, and the authors suggest a role in the 2 β-carbon hydroxylations and 3 peroxidative couplings found in the final product. Two non-heme haloperoxidases were similarly implicated in the 2 chlorination reactions. Therefore, with the exception of N-methylation of residue 1, all of the activities required to make the final form of the GPA from the amino acid precursors were predicted by genes encoded on this cluster. However, for all of the information that was inferred by these gene product homology studies, many elements of synthesis were not addressed. The nature of the amino acid substrates cannot be determined by amino acid sequence alignments, so although it was reasonable to assume that the modules are co-linear with the residues in the heptapeptide (as they are in every other peptide synthetase), no information regarding the timing of modification could be
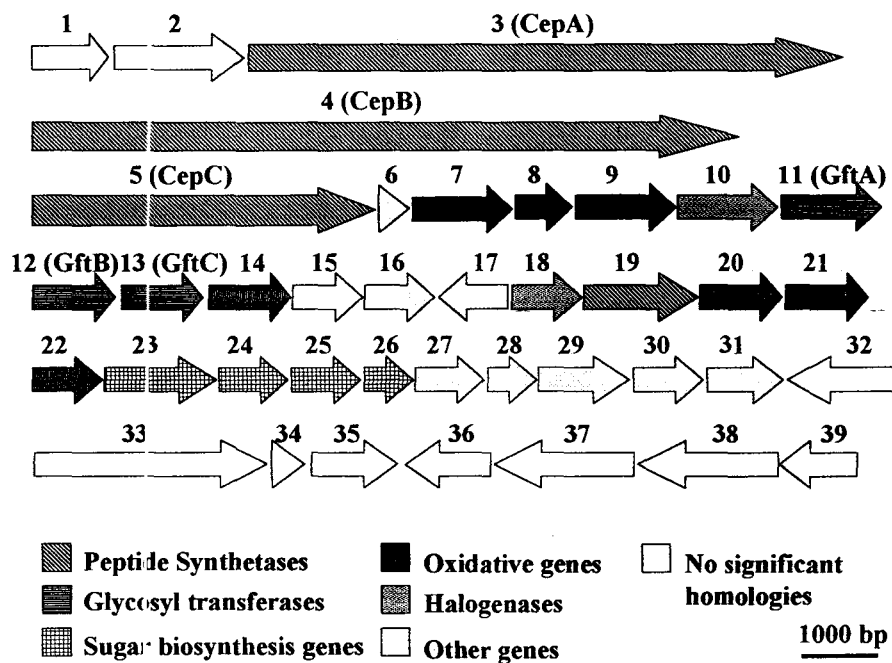
Figure 10.2. Chloro-eremomycin Biosynthesis Gene Cluster. 72 kb fragment from *A. orientalis* 18098 containing a number of genes predicted in GPA biosynthesis. Numbers indicate ORF assignments. Figure adapted from Ref. 5.
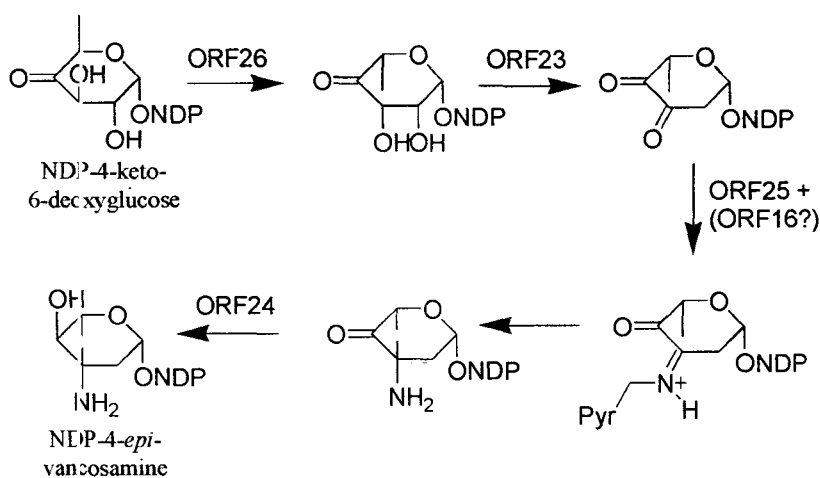
Figure 10.3. Proposed Scheme of NDP-4-*epi*-vancosamine Synthesis. Figure adapted from Ref. 5.

obtained. If indeed these chlorinating and hydroxylating enzymes perform the reactions assigned by the authors, what are their substrates – individual amino acids or peptide? Is the peptide free or enzyme-bound? Why are there eight oxidative enzymes when there are only 7 oxidative processes in making the GPA from the precursor amino acids? Is one of them involved in precursor biosynthesis? None of the enzymes predicted to function in amino acid biosynthesis were definitively found on the cluster. Conversely, there were several genes found on the cluster with activities not predicted in GPA assembly. What is their function, if any? Thus, in addition to the fact that none of the enzymes encoded on this cluster were assayed to confirm or clarify their role in GPA biosynthesis, many aspects of this process were not addressed by the manner of analysis used (namely, functional assignment based on primary sequence homology). This is not to say that the study was anything less than monumental in the field, only that many elements of this complex process remained largely uncharacterised. No follow-up work has been published by this group or any other group on the activities of the gene products encoded on this cluster.

Very recently, part of the gene cluster encoding enzymes required in balhimycin biosynthesis was cloned (3). Balhimycin is very similar to vancomycin, differing in that it lacks the vancosaminyl group attached to glucose and has a dehydrovancosaminyl group attached to residue 6 (Figure 10.4). The 9.8 kb cluster contained 7 intact genes very similar in primary sequence and identical in arrangement to genes found on the cl-

eremomycin cluster (Figure 10.5). OxyA, OxyB and OxyC were similar to P-450

monooxygenases,

Figure 10.4. Structure of Balhimycin.

Oxidative genes

Halogenases

Glycosyl transferases

Figure 10.5. Balhimycin Biosynthesis Gene Cluster Fragment. ORF
numbers refer to gene homologues from the cl-eremomycin biosynthesis gene cluster.

corresponding to the enzymes encoded by ORFs 7, 8 and 9 of the cl-eremomycin cluster,

while *bhaA* encoded a non-heme haloperoxidase that corresponded to ORF 10.

Accordingly, the three glycosyltransferases *bgftA*, *bgftB* and *bgftC* matched ORFs 11, 12

and 13, which was the identical arrangement observed in the vancomycin-producer's

gene cluster as well. It is therefore apparent that genetic organisation is highly conserved

in GPA producers. This group also performed a genetic knockout of bgtfB and of

oxyB/oxyC. The glycosyltransferase knockout mutant produced GPAs devoid of sugars,

as expected, providing the first biochemical evidence that these genes were required in

GPA biosynthesis. Interestingly, the oxyB/oxyC knockout produced two linear

heptapeptides, SP1134 and SP969. HPLC-mass spectrometry, fragmentation studies and

amino acid analysis were used to characterise these compounds. The predicted structure

of the more abundant SP969 (Figure 10.6) revealed that none of the cross-links normally

observed are present, implicating this gene product in this process. Also missing was

residue 7, however the authors believed that the missing residue was present in SP1134,

and that SP969 was a degradation product of SP1134. The fact that these compounds

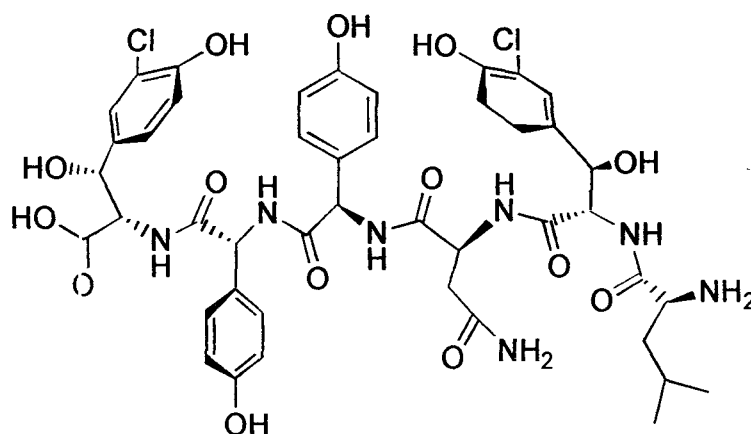were missing their sugars and their leucine N-methyl suggested that the addition of these

Figure 10.6. Predicted structure of SP969.

functionalities was dependent on peptide cross-linking. In contrast, chlorination and β-hydroxylation were not affected, and therefore may occur prior to cross-linking. The activities of the *oxyA* and *bhaA* gene products were not studied. This work clearly addressed some of the timing questions left unanswered from the study of the cl-eremomycin gene cluster. More studies of a similar nature, in combination with *in-vitro* analysis of purified enzymes, are required to fully elucidate the processes occurring after peptide assembly. As before, none of the genes predicted in synthesising the unusual amino acids of the heptapeptide have been identified, and this process remains a complete black box.

10.2.2   Resistance to GPAs

Of the recent reports relating to GPA resistance, two are especially notable. One described a familiar mechanism of resistance but in a new location, and thus addresses the issue of resistance dissemination and prevalence. The other describes what appears to be a new mode of GPA tolerance, which differs from GPA resistance in that cells cannot grow in the presence of antibiotic (and yet do not die, hence they are tolerant).

A 9.2 kb chromosomal fragment from the gram-positive organism *Bacillus circulans* VR0709 was reported to contain *van*-like genes with high primary sequence homology and identical arrangement as in VanA *E. faecium* (1). The genes discovered were *vanR, vanS, vanH, vanA, vanX, vanY* and *vanZ*, in that order, and genetic and amino acid identities were 93-96% and 87-95%, respectively. The *van* cluster was flanked by 10 bp inverted repeats (IRs), however these IRs were not related to those found in the transposon *Tn1546* affiliated with the VanA genes, nor were the resolvase or

transposase genes found upstream of *vanR*. Thus, while this cluster is clearly related to the Enterococcal VanA gene cluster, it does not appear that direct transfer has occurred. The source for this gene cluster remains ambiguous.

The bactericidal activity (leading to cell death, as opposed to bacteristatic, leading to cessation of growth) of cell wall inhibiting antibiotics was studied in *S. pneumoniae* in a recent report in the journal *Nature* (2). This organism uses autolysin proteins, such as LytA, to degrade its cell wall when it detects, by some unknown mechanism, the cessation of PG synthesis. The activity of these proteins is thought to be strongly negatively regulated as they are constitutively produced and potentially suicidal. Implicated in the regulatory pathway is a two-component signal transduction system, consisting of a histidine kinase/phosphatase (VncS) and a DNA-binding response regulator (VncR), which is thought to function as a gene expression repressor. In this model, VncR is constitutively phosphorylated by non-specific kinases, and thus is always "on" (Figure 10.7). In the presence of antibiotic, however, VncS dephosphorylates VncR, inactivating it and allowing expression of genes required for autolysis. In this report, a penicillin-resistant, vancomycin tolerant clinical isolate of *S. pneumoniae* was discovered, and upon further analysis, it was found to contain mutations in VncS that prevented it from dephosphorylating VncR. Experimentally-formed mutants of VncS had the same phenotype as the clinical isolate, however mutations in VncR were not tolerant – consistent with the need of phosphorylated VncR to repress autolysis. Unusually, under conditions that would induce autolysis, the VncS mutant strain possessed levels of LytA equivalent to *wild-type*, indicating that this protein is not down-

regulated as would be expected in the constitutively repressed system. Thus, this system

must repress some other component required in autolysis (for example, a LytA

translocation system). VncS/VncR showed reasonable identity to the VanS/VanR

enzymes (38%), but no homologues of *vanH*, *vanA* or *vanX* were found in the *S.*

pneumoniae genome, and clearly this system is distinct from that observed in

Enterococcus. The authors suggest that this mode of tolerance may be the fore-runner to

a new mode of resistance, however given that this mechanism in no way depletes the

GPA's ability to bind to PG, this does not seem to be a likely scenario. Given the

prevalence and mortality associated with *S. pneumoniae*, however, tolerance itself is

cause for concern.
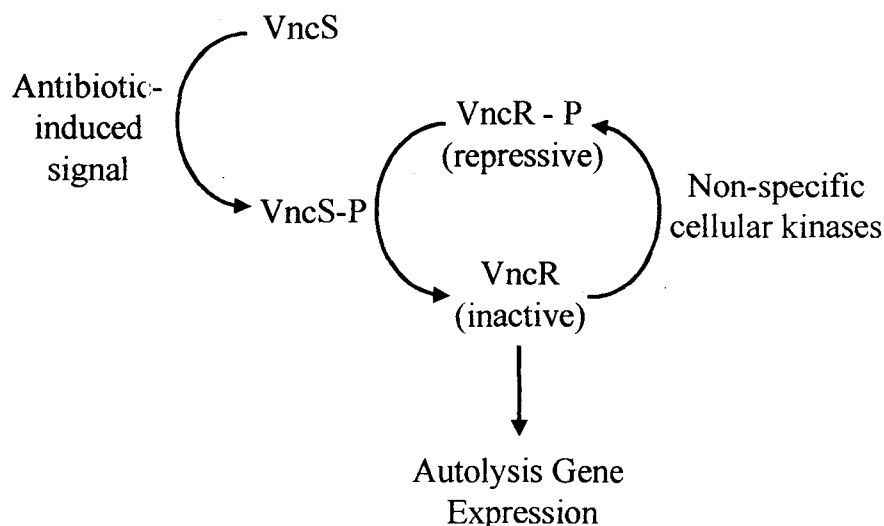
Figure 10.7. Proposed mechanism of Autolysis Gene Regulation in *S. pneumoniae*.

10.3 Summary and General Conclusions

The primary objective of this thesis was to advance our understanding of GPA biosynthesis and resistance in producing organisms. The initial strategy was to identify and purify an enzyme predicted to play a role in one of these processes, and design an oligonucleotide probe based on a partial amino acid sequence. Chapter 2 described the development of *S. toyocaensis* NRRL 15009 culture conditions that would favour the presence of such an enzyme, while chapters 3 and 4 described several unsuccessful attempts to identify an enzyme with a clear role in either biosynthesis or resistance. A new strategy was adopted using degenerate PCR to amplify and clone gene fragments potentially involved in GPA resistance. This method proved to be quite successful in identifying a region of the chromosome containing a *van* gene cluster – genes very similar to those found in clinically important VRE – not only in *S. toyocaensis* NRRL 15009 but also in *A. orientalis* C329.2 and several other GPA producing organisms. In addition to identifying the mode of GPA resistance in producing organisms, this find implicated these organisms as the source of the genes found in VanA, VanB and VanD-type VRE, and also provided a new source of enzymes for detailed analysis leading to drug development. As only the *vanH, vanA* and *vanX* genes were present, the question of regulation, normally addressed by the *vanR* and *vanS* gene products, was raised and remains as an intriguing problem that may tie in to global stationary phase gene expression in these organisms. Also absent from the chromosomal fragments containing the *van* genes were any genes implicated in GPA biosynthesis, forcing us to look to other means for identifying this gene cluster. However, with the *van* genes in hand, we were

presented with the unique opportunity to study the Van enzymes in a way that nobody else could. The VRE enzymes have resisted analysis required to provide an intimate understanding of their catalytic mechanism, and there is an urgent need for therapy for VRE infection. The work described in chapters 6 and 7 focussed on the development of the D-Ala-D-Ala ligases DdlM and DdlN as a model system for VanA and VanB. The dehydrogenase VanH is another target for drug development, and studies of the *S. toyocaensis* NRRL 15009 homologue VanHst was the subject of chapter 8. While the study of DdlN and VanHst have established their usefulness as models for the corresponding VRE enzymes, we have yet to learn novel insights into the mechanisms of these enzymes from these model systems. Chapter 9 was a return to the quest for the GPA biosynthesis genes, and describes the isolation of two cosmid library clones believed to contain some of these genes. The clones were identified using a probe constructed from the thioesterase region of the cl-eremomycin peptide synthetase gene, and therefore do not represent the first set of this class of genes. The three GPA biosynthesis gene clusters cloned to date have been isolated using a glycosyltransferase gene probe, which was not predicted to exist in *S. toyocaensis* NRRL 15009. While no clear information is available regarding the *S. toyocaensis* NRRL 15009 gene cluster at this time, there appears to be several peptide synthetase genes, a glycosyltransferase gene, and a two component regulatory system. This latter feature was not reported on any of the other three published GPA biosynthesis gene clusters, and will hopefully provide some insights into the regulation of GPA biosynthesis and resistance in GPA producing organisms.

Has the primary goal of this thesis been achieved? At this juncture, it is difficult to tell if the genes contained on the two cosmid clones will provide any new information regarding GPA biosynthesis. There is certainly some evidence that this work could shed some light on how this process is regulated, which has definite application in the commercial production of these important compounds. Similarly, it is not known if the studies conducted on DdlN or VanHst will contribute to our understanding of the mechanism of the corresponding VRE enzymes, however the potential to make advances which previously may have not been possible now exists. The one category in which definitive advances have resulted from this body of work is in our understanding of GPA resistance in producing organisms. The presence of the *van* genes *vanH*, *vanA* and *vanX* in every GPA-producer examined strongly supports this mode of resistance in these microbes. The high primary sequence homology and identical genetic arrangement implicates these genes as the source of the gene clusters found in clinical isolates of VRE. Thus we now know it is possible, if not likely, that an organism can obtain a set of genes that confer a phenotype through a complex process from an organism that exists in an entirely different microenvironment. The pathway by which this transfer has occurred, and likely continues to occur, is completely unknown.

10.4 Future Directions

There are several issues raised by the work contained in this thesis that remain unresolved, four of which are outstanding. 1) The two cosmid clones containing putative A47934 biosynthesis genes remain to sequenced and annotated. Based on preliminary

data, there is likely to be some novel information contained on this chromosomal fragment. 2) The regulation of A47934 biosynthesis and resistance in GPA producers remains a mystery, and may be similar to that observed in *E. faecium* or may be part of some global stationary phase gene expression regulon. 3) The Van enzymes from GPA producing organisms serve as suitable models for mechanistic studies of the VRE enzymes, and given the clinical importance of these enzymes, every effort should be made to solve these mechanisms. The physical properties of the model enzymes may prove invaluable in obtaining information that may not be available using the real targets. 4) If VRE did indeed acquire the *van* genes from a GPA producing organism, the transfer was neither recent nor direct. The pathway by which this transfer occurred is not known, and may provide insights into the ecology of genetic transfer in the microbial community. This is a fascinating avenue of research, and an understanding of this process could contribute to our knowledge of the transfer of all kinds of phenotypic determinants, including other forms of antibiotic resistance.

10.5 References

1.   **Ligozzi, M., G. Lo Cascio, and R. Fontana.** 1998. vanA gene cluster in a vancomycin-resistant clinical isolate of *Bacillus circulans*. Antimicrob Agents Chemother. **42(8):**2055-9.

2.   **Novak, R., B. Henriques, E. Charpentier, S. Normark, and E. Tuomanen.** 1999. Emergence of vancomycin tolerance in *Streptococcus pneumoniae* [see comments]. Nature. **399(6736):**590-3.

3.   **Pelzer, S., R. Sussmuth, D. Heckmann, J. Recktenwald, P. Huber, G. Jung, and W. Wohlleben.** 1999. Identification and analysis of the balhimycin biosynthetic gene cluster and its use for manipulating glycopeptide biosynthesis in

Amycolatopsis mediterranei DSM5908. Antimicrob Agents Chemother. **43**(7):1565-73.

4.   **Solenberg, P. J., P. Matsushima, D. R. Stack, S. C. Wilkie, R. C. Thompson, and R. H. Baltz.** 1997. Production of hybrid glycopeptide antibiotics in vitro and in *Streptomyces toyocaensis*. Chem Biol. **4**(3):195-202.

5.   **van Wageningen, A. M., P. N. Kirkpatrick, D. H. Williams, B. R. Harris, J. K. Kershaw, N. J. Lennard, M. Jones, S. J. Jones, and P. J. Solenberg.** 1998. Sequencing and analysis of genes involved in the biosynthesis of a vancomycin group antibiotic. Chem Biol. **5**(3):155-62.